REPORT DOCUMENTATION PAGE	Form Approved OMB No. 0704-0188

1. AGENCY USE ONLY *(Leave blank)*	2. REPORT DATE	3. REPORT TYPE AND DATES COVERED
	17.Sep.99	DISSERTATION

4. TITLE AND SUBTITLE
STUDIES OF OLEFIN DIMERIZATION, OLIGOMERIZATION, AND POLYMERIZATION CATALYZED BY CATIONIC (A-DIIMINE) NI(II) COMPLEXES (UNDER THE DIRECTION OF PROFESSOR

5. FUNDING NUMBERS

6. AUTHOR(S)
CAPT SVEJDA STEVEN A

7. PERFORMING ORGANIZATION NAME(S) AND ADDRESS(ES)
UNIVERSITY OF NORTH CAROLINA

8. PERFORMING ORGANIZATION REPORT NUMBER

9. SPONSORING/MONITORING AGENCY NAME(S) AND ADDRESS(ES)
THE DEPARTMENT OF THE AIR FORCE
AFIT/CIA, BLDG 125
2950 P STREET
WPAFB OH 45433

10. SPONSORING/MONITORING AGENCY REPORT NUMBER
FY99-312

11. SUPPLEMENTARY NOTES

12a. DISTRIBUTION AVAILABILITY STATEMENT
Unlimited distribution
In Accordance With AFI 35-205/AFIT Sup 1

12b. DISTRIBUTION CODE

DISTRIBUTION STATEMENT A
Approved for Public Release
Distribution Unlimited

13. ABSTRACT *(Maximum 200 words)*

19991108 108

14. SUBJECT TERMS	15. NUMBER OF PAGES 214
	16. PRICE CODE

17. SECURITY CLASSIFICATION OF REPORT	18. SECURITY CLASSIFICATION OF THIS PAGE	19. SECURITY CLASSIFICATION OF ABSTRACT	20. LIMITATION OF ABSTRACT

Studies of Olefin Dimerization, Oligomerization, and Polymerization Catalyzed by Cationic (α-Diimine)Ni(II) Complexes

Steven A. Svejda

A dissertation submitted to the faculty of the University of North Carolina at Chapel Hill in partial fulfillment of the requirements for the degree of Doctor of Philosophy in the Department of Chemistry

Chapel Hill

1999

Approved by:

Maurice Brookhart
Advisor

Reader

Reader

ABSTRACT

STEVEN A. SVEJDA: Studies of Olefin Dimerization, Oligomerization, and Polymerization Catalyzed by Cationic (α-Diimine)Ni(II) Complexes
(Under the direction of Professor Maurice Brookhart)

The polymerization of olefins by transition metal catalysts is an area of tremendous commercial significance and academic interest. Over the past twenty years, substantial improvements have been made in the design and industrial employment of these catalysts, especially with the development of early transition-metal metallocenes. The development of cationic (α-diimine)nickel(II) and palladium(II) complexes which catalyze the polymerization of both ethylene and α-olefins to high polymers represents a major advance in the field of olefin polymerization catalysis. Through simple variations of the α-diimine ligand structure and reaction conditions, the polymer molecular weights, molecular weight distributions, and microstructures can be easily controlled. The work in this dissertation focuses on olefin dimerization, oligomerization, and polymerization reactions catalyzed by (α-diimine)Ni(II) complexes, with the general goal of gaining an increased understanding of the mechanism of olefin polymerization by these nickel systems.

Chapter Two is a study of the effects of monomer concentration, reaction temperature, aluminum cocatalyst, and electron-donating or -withdrawing diimine ligand substituents on the (α-diimine)Ni(II)-catalyzed oligomerization of ethylene and the dimerization of propylene.

Chapters Three and Five are an account of detailed investigation of the effects of reaction conditions and diimine ligand structure on the properties of polyethylene and poly(α-olefin)s produced by (α-diimine)Ni(II) complexes. The effects of these variables on catalyst productivities, as well as polymer molecular weights and microstructures are presented.

A study of the dynamics of α-diimine compounds incorporating fluorinated substituents is presented in Chapter Four. The dynamic behavior of palladium complexes of one diimine is also investigated and presented.

The synthesis of a class of well-defined nickel complexes of the general formula [(α-diimine)NiMe(S)]$^+$[BAr'$_4$]$^-$ (S = solvent, Ar' = 3,5-(CF$_3$)$_2$C$_6$H$_3$) for use as mechanistic probes of nickel-catalyzed olefin polymerization reactions is described in Chapter 6. Low-temperature spectroscopic studies of the mechanism of olefin chain growth using these catalysts are presented.

Further investigation of the synthesis and reactivity of well-defined nickel complexes, with an emphasis on the preparation of β-agostic nickel complexes, is discussed in Chapter 7. Preliminary experiments to explore the mechanism of chain isomerization that occurs during the nickel-catalyzed polymerization of olefins are included.

ACKNOWLEDGEMENTS

First and foremost, I thank my advisor, Professor Maurice Brookhart, for accepting me into his research group, and allowing me to work on some terrific research projects. I am very fortunate to have had the opportunity to work on such a wide diversity of exciting projects in his laboratory. In addition to the excellent research opportunities, he has taught me new ways to think more critically and analytically about chemical problems, and his depth of knowledge about all aspects of the field is truly remarkable. In this same vein, I also thank my former research advisor, Professor Michael E. Wright, for providing me with invaluable training, laboratory skills, and enthusiasm for chemical research. These things played a major role in enabling me to successfully carry out some challenging organometallic chemistry at UNC, especially after spending six years away from the bench.

All of the work that comes out of any research group is a team effort, and the work described in this thesis is no exception. I thank all of the Brookhart group members, past and present, for all of their assistance in helping me to get through this program in the short amount of time I was given. Daily discussions, sharing compounds and NMR time, pitching in to maintain the supplies and equipment, and even something as simple as trading stories over a cup of coffee are the not-so-little things that maintain good morale and can really make or break research projects. The Brookhart lab has been a great place for me over the past few years, and I owe a lot to the enormously talented folks in the group who have it such a fun place to do chemical research.

Several people have contributed directly to the work presented in this dissertation. Dr. Derek P. Gates and Scott Shultz performed DSC analyses on the polyethylene samples prepared in Chapter 3. Derek also ran GPC analyses on the polyolefin samples prepared in Chapter 5. Derek Gates and Dr. Enrique Oñate synthesized some of the catalysts and corresponding polymers reported in Chapter 3;

their specific contribution to that work will be acknowledged in that chapter. Two of Enrique's catalysts were used to make some of the poly(α-olefin)s reported in Chapter 5. Lissa Nelson and Carole Urbston (DuPont) facilitated GPC analysis of numerous polyethylene samples at DuPont. Dr. Chi-Duen Poon and Dr. David Harris provided constant, invaluable assistance with NMR work of all descriptions, and this, as well as many other successful research efforts completed in the Brookhart laboratory, owe their success to the fine NMR facility at UNC. Dr. David S. Frohnapfel assisted with some of the NMR spectra reported in Chapter 2. Steve Gross assisted with the DMA experiment in Chapter 3.

I thank the United States Air Force Institute of Technology Civilian Institutions program (AFIT/CI) for sponsoring me in this degree program. I am also grateful to DuPont and the National Science Foundation for generous financial support of this research.

Most importantly, I thank my wife Alexia for her endless support. Yet another move, another job change, another house to buy and sell, and all of the other inconveniences related to moving every three years have been difficult for her at times, but she always manages to make lemonade out of the lemons. She is the most patient, optimistic, and understanding person I have ever met, and I am tremendously grateful to her for all of the sacrifices she has made for me over the past three years.

TABLE OF CONTENTS

LIST OF TABLES

LIST OF SCHEMES

LIST OF FIGURES

LIST OF ABBREVIATIONS

δ	chemical shift
ΔG	change in free energy
‡	denotes transition state
An	acenaphthyl; 1,8-naphth-diyl
Ar'	3,5-$(CF_3)_2C_6F_3$
atm	atmospheres
Bu	butyl
COSY	correlated spectroscopy
DMA	dynamic mechanical analysis
DSC	differential scanning calorimetry
eq	equivalents
Et	ethyl
g	grams
GC	gas chromatography
GLC	gas-liquid chromatography
GPC	gel permeation chromatography
h	hours
Hz	hertz
J	coupling constant
kcal	kilocalories
M	molar
MAO	methylaluminoxane

Me	methyl
mL	milliliters
MMAO	modified methylaluminoxane
M_n	number average molecular weight
mol	moles
M_w	weight average molecular weight
M_w/M_n	molecular weight distribution
NMR	nuclear magnetic resonance
P	polymer chain
PDI	polydispersity index
ppm	parts per million
Pr	propyl
s	seconds
SHOP	Shell Higher Olefin Process
soln	solution
T_g	glass transition temperature
T_m	melt transition temperature
TO	turnovers
TOF	turnover frequency
TON	turnover number

CHAPTER 1

Introduction to Late Transition Metal-Catalyzed Dimerization, Oligomerization, and Polymerization of Olefins

Transition Metal-Catalyzed Polymerization of Ethylene and α-Olefins

Polyethylene and polypropylene are two of the most important products of the chemical industry. In 1996, worldwide production of these polymers was roughly 60 million tons.[1] High-density polyethylene (HDPE), linear low-density polyethylene (LLDPE), and polypropylene make up the bulk of the overall production of these materials. These polymers are formed using catalysts based on early transition metals such as titanium, zirconium, and chromium, which are activated by aluminum alkyl cocatalysts.

Olefin polymerization catalysts have undergone several generations of improvements since the initial discoveries of Ziegler[2] and Natta[3] in the 1950s. The most notable improvement on the original heterogeneous titanium catalysts was the development of single-site metallocene complexes. These homogeneous, well-defined early metal complexes allowed for precise control of the resulting polymer stereochemistry and molecular weight distributions.[4-14] Improvements to the aluminum cocatalysts were also made, and by far the most important of these was the discovery of methylaluminoxane (MAO).[15,16] MAO is the product of partial hydrolysis of trimethylaluminum, and use of MAO as the cocatalyst in early transition metal-catalyzed olefin polymerizations resulted in dramatic improvements in catalyst productivity. In addition, MAO was found to generate active catalysts that could polymerize α-olefin monomers.

Late Transition Metal Catalysts

Early metal olefin catalysts are highly effective in the polymerization of nonpolar monomers such as ethylene and propylene, but these complexes are oxophilic and therefore ineffective in polymerizing olefins containing functional groups such as esters, ethers, and ketones. In addition, many such functional groups are incompatible with the aluminum alkyl cocatalysts that are needed to activate metallocene complexes. Since late transition-metal complexes are more electron rich than early metal complexes, they are less oxophilic and consequently more functional group-tolerant than their early metal counterparts. Unfortunately, the high electron density of late metals as compared to early metals makes β-hydride elimination and subsequent chain transfer dominant processes in late metal complexes. A wealth of experimental evidence demonstrates that late metal complexes, most commonly those of nickel and palladium, are typically olefin dimerization[17] or oligomerization[18] catalysts due to rapid chain transfer relative to chain propagation.

Several important industrial processes based upon the dimerization or oligomerization of olefins have been developed. The IFP Dimersol® process uses a cationic nickel salt to nonselectively dimerize propylene, butene, or ethylene.[19-21] The propylene dimers are particularly useful, and find utility as gasoline additives (octane boosters). Butene dimers and propylene/butene codimers are converted into alcohols, which are in turn converted into phthalates that are used as plasticizers. Ethylene dimerization to form butene is not currently an economically viable process, since the price of butene is lower than that of ethylene.

The oligomerization of ethylene to linear α-olefins is also an important industrial process. The most notable of these is the Shell Higher Olefin Process (SHOP).[22] The first step of the SHOP process is ethylene oligomerization. The oligomerization is catalyzed by neutral nickel complexes bearing P,O-chelating ligands (Figure 1.1), and these catalyst systems have been extensively researched by Keim and coworkers.[23-32] These complexes generate a Shultz-Flory (statistical)

distribution of linear α-olefin oligomers in the range of C_4-C_{30+}. The selectivity for linear olefins is about 99%, and 96-98% α-olefin products are obtained.

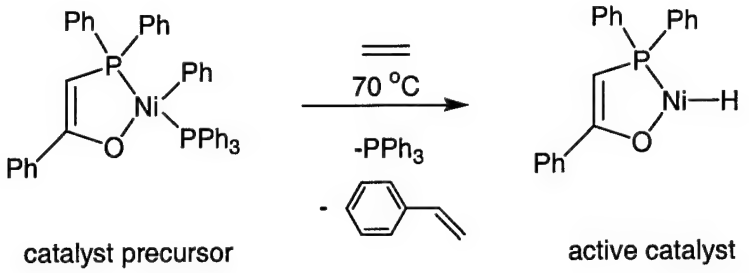

Figure 1.1. A typical SHOP catalyst.

Throughout the 1980s, modifications to the basic chelate complex shown in Figure 1.1 were made in an attempt to obtain higher molecular weight materials. A general finding was that as the ligand steric bulk about the nickel atom was increased, the molecular weights of the ethylene oligomer products also increased. Ostoja Starzewski and Witte reported that ethylene could be polymerized to molecular weights in excess of 10^6 g/mol (M_n) using bis(ylide)nickel complexes,[33,34] and that variations in the steric bulk of the ligands could be used to vary the molecular weight of the polyethylene products in a controlled manner. Klabunde and Ittel further improved upon these results by incorporating weakly bound nitrogen donor ligands in the place of phosphine ligands.[35,36]

While many successful efforts to create nickel-based complexes that could polymerize ethylene were reported, none of these catalyst systems were capable of polymerizing α-olefins. In 1985, Möhring and Fink[37] reported the oligomerization of α-olefins using a nickel aminobis(imino)phosphorane complex that was first reported by Keim (Scheme 1.1).[38] The reaction products are methyl-branched oligomers, and overall 2,ω-enchainment of the α-olefin monomer is observed. The unusual mode of enchainment was believed to be the result of a series of β-hydride elimination/reinsertion steps which resulted in the nickel center migrating to the end of the chain. The highest molecular weights of the materials obtained were relatively low ($M_n \approx 1000$).

Scheme 1.1. Oligomerization of α-olefins as described by Möhring and Fink.[37]

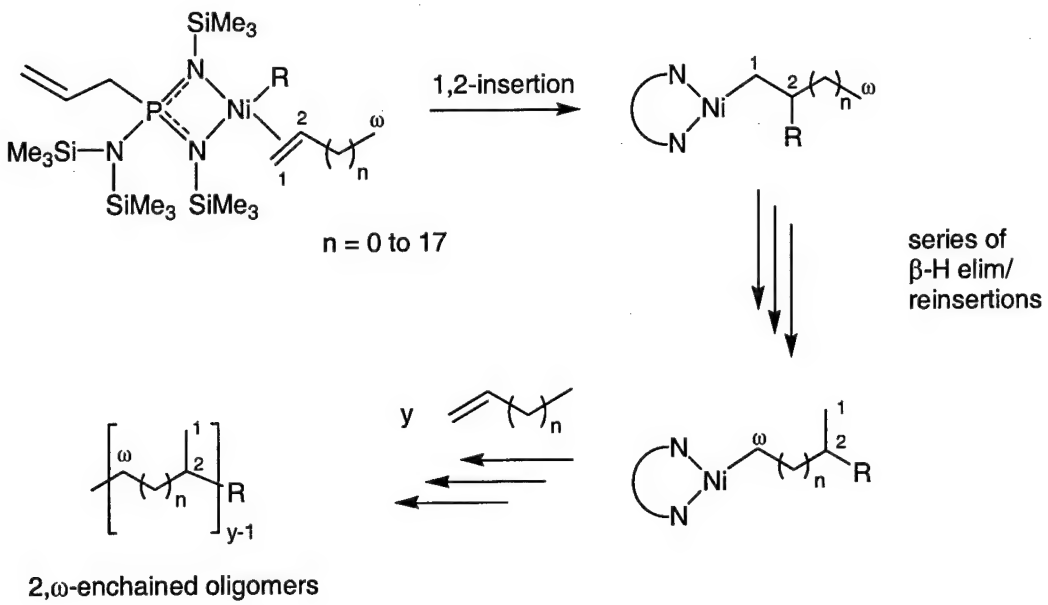

Cationic (α-Diimine)Ni(II) and -Pd(II) Catalysts

In 1995, Brookhart et. al. reported that cationic nickel and palladium complexes bearing sterically bulky α-diimine ligands could polymerize both ethylene and α-olefins to high polymer (Scheme 1.2).[39] The nickel complexes polymerize ethylene with activities that are comparable to those of metallocenes, and the polymers can reach molecular weights of M_n>500,000. The microstructure of the polyethylene formed by the nickel complexes varies from strictly linear to highly branched, and the degree of branching can be easily controlled through simple variations in the reaction temperature, monomer concentration, and the ligand structure. The raw polymers thus have properties ranging from those of hard thermoplastics to soft, rubbery gums, depending upon the degree of branching found in the polymer chain. The palladium complexes produce polyethylenes that are amorphous and highly branched (>100 branches/1000 carbons), regardless of the reaction conditions.

Scheme 1.2. Polymerization of ethylene and α-olefins by sterically bulky nickel and palladium diimine complexes.[39]

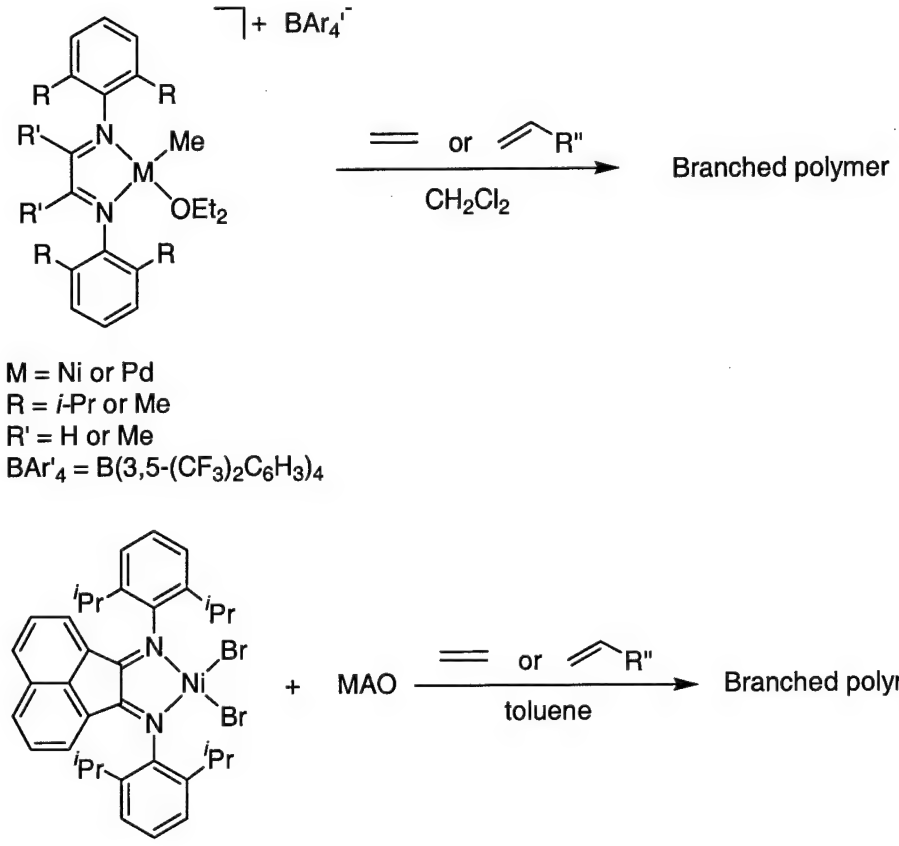

Sterically bulky nickel and palladium diimine complexes polymerize α-olefins such as propylene and 1-hexene to high molecular weight polymers. The complexes enchain these olefins in a fashion that results in *fewer* branches in the polymer products than would be expected from an enchainment process consisting of only 1,2-insertions. For example, simple 1,2-enchainment of propylene leads to 333 methyl branches per 1000 carbons; some of the nickel and palladium diimine complexes produce polypropylenes with branching frequencies as low as 160 methyl branches per 1000 carbons.[40]

At low temperatures (e.g. $T < 0$ °C) and low monomer concentrations, nickel complexes bearing sterically bulky diimine ligands polymerize α-olefins in a living fashion.[41-43] Propylene, 1-hexene, and 1-octadecene have been homopolymerized at -10 °C with these nickel systems to yield high molecular weight polymers with polydispersities near 1.1. Diblock copolymers of propylene and 1-

hexene, as well as elastomeric A-B-A triblock copolymers of 1-octadecene (A block) and propylene (B block) can be prepared using these nickel complexes.[41,42] Multiblock copolymers of ethylene and 1-hexene having elastomeric properties have also been prepared.[41,42]

Copolymerization of ethylene or propylene with polar monomers such as methyl acrylate, *tert*-butyl acrylate, methyl vinyl ketone, or the fluorinated monomer FOA (FOA = $H_2C{=}CHC(O)OCH_2(CF_2)_6CF_3$) has also been accomplished using palladium diimine catalysts,[44,45] which demonstrates these late metal systems have some degree of functional group compatibility. As is the case with homopolymers formed by these palladium catalysts, the ethylene/acrylate copolymers are amorphous and highly branched, and contain about 100 branches/1000 carbons. The polar groups are found at the end of branches attached to the main polymer chain. The carbonyl groups of the polar monomers chelate strongly to the metal center, and thus polymerization activities are considerably lower as compared to the turnover frequencies observed in ethylene and α-olefin homopolymerizations.

Nickel and palladium diimine complexes polymerize cyclopentene via an addition mechanism (Scheme 1.3).[46] Cyclopentene is enchained in a cis-1,3-fashion with chain-end stereochemical control. Molecular weights as high as 250,000 (M_w) can be achieved. The polycyclopentenes are melt processible, and have end-of-melting points in the range of 240 to 330 °C. A β-agostic resting state complex is observed during the course of these polymerizations by low-temperature NMR spectroscopy.

Scheme 1.3. Addition polymerization of cyclopentene by nickel diimine complexes.[46]

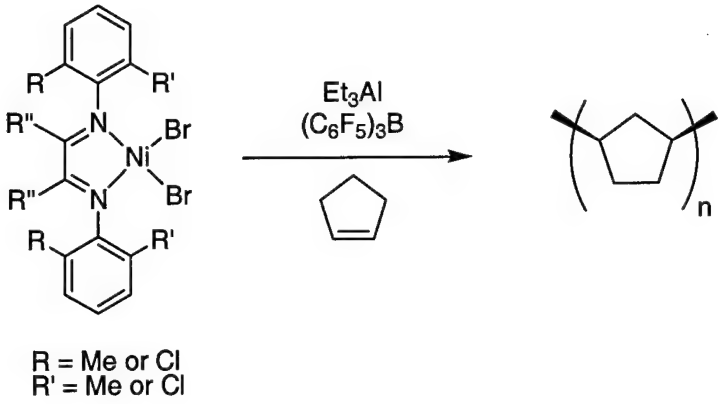

Removal of the bulky ortho aryl substituents on the diimine phenyl rings results in nickel complexes that are highly active in the oligomerization of ethylene to linear α-olefins (Scheme 1.4).[47] Selectivity for α-olefin oligomer products is high (>90%), and only linear products are observed by gas chromatography. A Schulz-Flory distribution of oligomers is produced, and this distribution can be varied by changing the reaction temperature and ethylene pressure. Turnover frequencies in excess of 100,000 h^{-1} are observed under some conditions.

Scheme 1.4. Oligomerization of ethylene by sterically non-bulky nickel diimine complexes.[47]

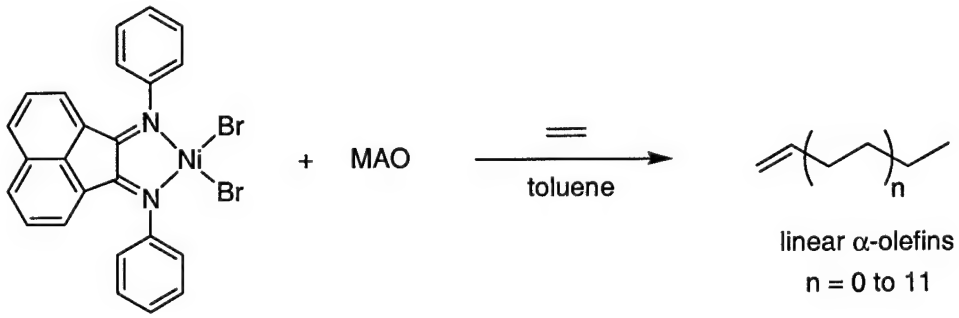

There are three key features of the nickel and palladium diimine complexes (Scheme 1.2) that result in their ability to form high polymer: (1) the sterically bulky α-diimine ligand, (2) a weakly-associated counterion, and (3) a readily-available, vacant coordination site on the metal. As was observed with the modified SHOP systems described above, the incorporation of a sterically

demanding ligand into the catalyst system is imperative if polymer is to be produced. The diimine aryl rings lie orthogonal to the plane formed by the diazadiene ligand backbone, which positions the bulky ortho aryl substituents above and below the axial sites of the metal in these square-planar complexes. Chain transfer in these systems appears to proceed via associative displacement of the growing polymer chain by olefin monomer. Since the axial sites of the metal center are effectively blocked by the steric bulk of the ligand ortho aryl substituents, chain transfer is greatly retarded, and high molecular weight polymers can be formed.

The importance of a non-coordinating counterion such as tetrakis(3,5-bis(trifluoromethyl)phenyl)-borane is two-fold: (1) the non-coordinating nature of such a ligand ensures that the open coordination site on the metal remains available for olefin coordination, and (2) the high solubility of this ion makes the metal complex soluble in a wide variety of organic solvents. The solubility factor is especially important in mechanistic studies, as some of these studies are conducted at extremely low temperatures (see Chapters 6 and 7).

The polymerization mechanism is the subject of ongoing studies in the Brookhart group. Many details of the palladium-catalyzed polymerizations have been uncovered thus far, and these findings are described in the following chapters. For the sake of brevity, the various mechanistic schemes are listed within each chapter, and the reader is referred to the introductions at the beginning of the following chapters for illustrations and further discussion of the proposed polymerization mechanism. Furthermore, the background and introductory information that is pertinent to the subject(s) of each chapter is located at the beginning of each, and therefore no further details of this chemistry will be outlined here.

Research Goals and Achievements

The overreaching goal of this research was to further develop our understanding of (α-diimine)Ni(II) olefin oligomerization and polymerization catalysts. While we have significantly advanced our knowledge of the mechanism of olefin polymerization catalyzed by (α-diimine)Pd(II)

complexes,[40,44,45,48,49] relatively little is known about the nickel analogues. This dissertation focuses on studies of the nickel complexes, but within this area, the work presented in the following chapters is quite broad in scope.

Chapter 2 is a detailed, systematic investigation of sterically unhindered (α-diimine)Ni(II) complexes in the oligomerization of ethylene to linear α-olefins (Scheme 1.5), and expands upon preliminary work carried out in the Brookhart group.[47] Addition of electron donor or acceptor groups to the diimine ligand was used to adjust the electronics of the catalytic system, and the effects of these electronic variations on the ethylene oligomer product distribution, selectivity for α-olefins, and catalytic efficiency. The effects of ethylene concentration, reaction temperature, and the nature of the aluminum cocatalyst on these product variables were also investigated. These sterically unhindered nickel complexes *dimerize* propylene (Scheme 1.5), and a full account of the effects of ligand electronics, reaction temperature, propylene concentration, and the nature of the aluminum cocatalyst on propylene dimer product distribution is presented in Chapter 2. The sum of this work has been published in *Organometallics*.[50]

Scheme 1.5. Ethylene oligomerization and propylene dimerization catalyzed by sterically unhindered (α-diimine)Ni(II) catalysts.

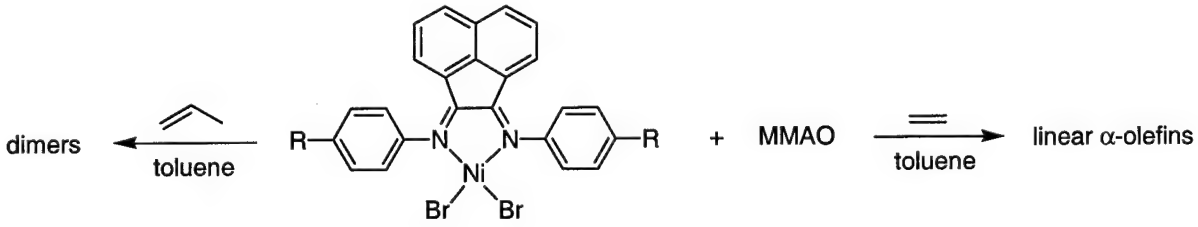

A detailed study of ethylene polymerization by nickel complexes bearing electrophilic α-diimine ligands is presented in Chapter 3. This work is the product of a team effort, and a detailed account of the contributions of each author is described at the beginning of Chapter 3. In this chapter, of the effects of reaction temperature, ethylene pressure, and the nature of the α-diimine ligand on ethylene

polymerization reactions are presented. This chapter is adapted from a paper that will soon be submitted for publication in *Macromolecules*.

The electrophilic α-diimine ligands synthesized in the course of the work described in Chapter 3 were found to exhibit dynamic behavior. An NMR investigation of the dynamics of two fluorinated α-diimine ligands, as well as some palladium complexes of these ligands, is discussed in Chapter 4.

The polymerization of 1-hexene and propylene by nickel complexes bearing electrophilic α-diimine ligands is presented in Chapter 5. The effects of the diimine ligands on the resulting polymer products are discussed. A brief account of the reactivity of these nickel complexes towards norbornene and mixtures of norbornene and ethylene is also presented.

Chapter 6 focuses on two major areas: the synthesis of well-defined, cationic nickel complexes, and mechanistic studies of olefin polymerization as catalyzed by these well-defined Ni complexes. The preparation of a series of (α-diimine)nickel dimethyl complexes is described, and conversion of these dialkyl complexes into their corresponding cationic solvent adducts is discussed. Kinetic studies of ethylene and propylene chain growth initiated by the cationic solvent adducts are also presented. This chapter is adapted from a communication which has been submitted to the *Journal of the American Chemical Society* for publication.

Chapter 7 is an extension of the work begun in Chapter 6, and further development of the synthesis and reactivity of well-defined cationic nickel diimine complexes is described. This chapter contains a summary of preliminary investigations of Ni(II)-β-agostic complexes, and studies which help to shed some light on the mechanism of chain isomerization that takes place during the course of Ni(II)-catalyzed olefin polymerizations are presented.

References

(1) Reisch, M. S. *Chem. Eng. News* **1997**, *75* (May 26), 14.

(2) Ziegler, K.; Holzkamp, E.; Briel, H.; Martin, H. *Angew. Chem.* **1955**, *67*, 541-547.

(3) Natta, G.; Pino, P.; Corradini, P.; Dannusso, F.; Mantica, E.; Mazzanti, G.; Moraglio, G. *J. Am. Chem. Soc.* **1955**, *77*, 1708-1710.

(4) Theopold, K. H. *Eur. J. Inorg. Chem.* **1998**, 15-24.

(5) McKnight, A. L.; Waymouth, R. M. *Chem. Rev.* **1998**, *98*, 2857-2868.

(6) Bochmann, M. *J. Chem. Soc., Dalton Trans.* **1996**, 255-270.

(7) Brintzinger, H. H.; Fischer, D.; Mülhaupt, R.; Rieger, B.; Waymouth, R. M. *Angew. Chem., Int. Ed. Engl.* **1995**, *34*, 1143-1170.

(8) Coates, G. W.; Waymouth, R. M. *Science* **1995**, *267*, 217-219.

(9) Yang, X.; Stern, C. L.; Marks, T. J. *J. Am. Chem. Soc.* **1994**, *116*, 10015-10031.

(10) Coughlin, E. B.; Bercaw, J. E. *J. Am. Chem. Soc.* **1992**, *114*, 7606-7607.

(11) Crowther, D. J.; Baenziger, N. C.; Jordan, R. F. *J. Am. Chem. Soc.* **1991**, *113*, 1455-1457.

(12) Ewen, J. A.; Jones, R. L.; Razavi, A.; Ferrara, J. D. *J. Am. Chem. Soc.* **1988**, *110*, 6255-6256.

(13) Kaminsky, W.; Külper, K.; Brintzinger, H. H.; Wild, F. R. W. P. *Angew. Chem., Int. Ed. Engl.* **1985**, *24*, 507-508.

(14) Ewen, J. A. *J. Am. Chem. Soc.* **1984**, *106*, 6355-6364.

(15) Kaminsky, W.; Miri, M.; Sinn, H.; Woldt, R. *Makromol. Chem., Rapid Commun.* **1983**, *4*, 417-421.

(16) Sinn, H.; Kaminsky, W. *Adv. Organomet. Chem.* **1980**, *18*, 99-149.

(17) Muthukumaru Pillai, S.; Ravindranathan, M.; Sivaram, S. *Chem. Rev.* **1986**, *86*, 353-399.

(18) Skupinska, J. *Chem. Rev.* **1991**, *91*, 613-648.

(19) Chauvin, Y.; Olivier, H. Dimerization and Codimerization. In *Applied Homogeneous Catalysis with Organometallic Compounds*; Cornils, B., Herrmann, W. A., Eds.; VCH Publishers: New York, 1996; Vol. 1, pp 258-268.

(20) Andrews, J. W. *Hydrocarbon Process.* **1982**, *61*, 110.

(21) Chauvin, Y.; Gaillard, J. F.; Quang, D. V.; Andrews, J. W. *Chem. Ind. (London)* **1974**, 375-378.

(22) Vogt, D. Oligomerization of Ethylene to Higher Linear α-Olefins. In *Applied Homogeneous Catalysis with Organometallic Compounds*; Cornils, B., Herrmann, W. A., Eds.; VCH Publishers: New York, 1996; Vol. 1, pp 245-258.

(23) Bonnet, M. C.; Dahan, F.; Ecke, A.; Keim, W.; Schulz, R.; Tkatchenko, I. *J. Chem. Soc., Chem. Commun.* **1994**, 615-616.

(24) Hirose, K.; Keim, W. *J. Mol. Catal.* **1992**, *73*, 271-276.

(25) Keim, W. *Angew. Chem., Int. Ed. Engl.* **1990**, *29*, 235-244.

(26) Müller, U.; Keim, W.; Krüger, C.; Betz, P. *Angew. Chem., Int. Ed. Engl.* **1989**, *28*, 1011-1013.

(27) Keim, W. *J. Mol. Catal.* **1989**, *52*, 19-25.

(28) Keim, W. *New J. Chem.* **1987**, *11*, 531-534.

(29) Keim, W.; Behr, A.; Gruber, B.; Hoffmann, B.; Kowaldt, F. H.; Kürschner, U.; Limbäcker, B.; Sistig, F. P. *Organometallics* **1986**, *5*, 2356-2359.

(30) Peuckert, M.; Keim, W. *Organometallics* **1983**, *2*, 594-597.

(31) Keim, W.; Hoffmann, B.; Lodewick, R.; Peuckert, M.; Schmitt, G. *J. Mol. Catal.* **1979**, *6*, 79-97.

(32) Keim, W.; Kowaldt, F. H.; Goddard, R.; Krüger, C. *Angew. Chem., Int. Ed. Engl.* **1978**, *17*, 466.

(33) Ostoja Starzewski, K. A.; Witte, J. *Angew. Chem., Int. Ed. Engl.* **1987**, *26*, 63-64.

(34) Ostoja Starzewski, K. A.; Witte, J. *Angew. Chem., Int. Ed. Engl.* **1985**, *24*, 599-601.

(35) Klabunde, U.; Ittel, S. D. *J. Mol. Catal.* **1987**, *41*, 123-134.

(36) Klabunde, U.; Mulhaupt, R.; Herskovitz, T.; Janowicz, A. H.; Calabrese, J.; Ittel, S. D. *J. Poly. Sci., Part A: Polym. Chem.* **1987**, *25*, 1989-2003.

(37) Möhring, V. M.; Fink, G. *Angew. Chem., Int. Ed. Engl.* **1985**, *24*, 1001-1003.

(38) Keim, W.; Appel, R.; Storeck, A.; Krüger, C.; Goddard, R. *Angew. Chem., Int. Ed. Engl.* **1981**, *20*, 116-117.

(39) Johnson, L. K.; Killian, C. M.; Brookhart, M. *J. Am. Chem. Soc.* **1995**, *117*, 6414-6415.

(40) Tempel, D. J. Mechanistic Studies of Pd(II)- and Ni(II)-Catalyzed Olefin Polymerization. Ph.D. Dissertation, University of North Carolina at Chapel Hill, 1998.

(41) Killian, C. M.; Tempel, D. J.; Johnson, L. K.; Brookhart, M. *J. Am. Chem. Soc.* **1996**, *118*, 11664-11665.

(42) Killian, C. M. Ni(II)-Based Catalysts for the Polymerization and Copolymerization of Olefins: A New Generation of Polyolefins. Ph.D. Dissertation, University of North Carolina-Chapel Hill, 1996.

(43) Gates, D. P.; Brookhart, M. Manuscript in preparation.

(44) Johnson, L. K.; Mecking, S.; Brookhart, M. *J. Am. Chem. Soc.* **1996**, *118*, 267-268.

(45) Mecking, S.; Johnson, L. K.; Wang, L.; Brookhart, M. *J. Am. Chem. Soc.* **1998**, *120*, 888-899.

(46) McLain, S. J.; Feldman, J.; McCord, E. F.; Gardner, K. H.; Teasley, M. F.; Coughlin, E. B.; Sweetman, K. J.; Johnson, L. K.; Brookhart, M. *Macromolecules* **1998**, *31*, 6705-6707.

(47) Killian, C. M.; Johnson, L. K.; Brookhart, M. *Organometallics* **1997**, *16*, 2005-2007.

(48) Tempel, D. J.; Brookhart, M. *Organometallics* **1998**, *17*, 2290-2296.

(49) Tempel, D. J.; Johnson, L. K.; Huff, R. L.; Brookhart, M. Manuscript in preparation.

(50) Svejda, S. A.; Brookhart, M. *Organometallics* **1999**, *18*, 65-74.

CHAPTER 2

Ethylene Oligomerization and Propylene Dimerization Using Cationic (α-Diimine)Ni(II) Catalysts

Introduction

Transition-metal-catalyzed oligomerization of ethylene and dimerization of α-olefins are important processes that are used to convert these basic feedstocks into useful value-added products. Ethylene oligomerization by nickel catalysts is the first step of the Shell Higher Olefin Process (SHOP).[1-4] The SHOP process is highly selective for producing linear α-olefins in the C_4-C_{20+} range, which are used as comonomers to synthesize linear low-density polyethylene, and in the production of lubricants, plasticizers, surfactants, and detergents.[5] The IFP Dimersol® process utilizes a cationic nickel catalyst to nonselectively dimerize and codimerize propylene and 1-butene; the dimer products are used as gasoline additives.[6-8]

Olefin dimerization[9] and oligomerization[10] reactions are typically carried out using homogeneous late transition metal catalysts, particularly nickel-based catalysts. A wide variety of ligands have been employed successfully with these systems,[11-20] and careful tuning of ligands can be used to vary product composition from lower oligomers to polymer.[21-24] Neutral nickel catalysts based on phosphorus-oxygen chelates are particularly well-developed and are employed in industrial SHOP reactors.[3,4,25] A series of extremely active Ni(II) ethylene oligomerization catalysts containing

dithioacetylacetonate chelating ligands have been reported,[26-28] and the mechanism by which they dimerize propylene has been investigated.[29] Recently, we reported highly active iron-based catalysts for ethylene oligomerization.[30]

The strong propensity of late transition metal-based catalysts to undergo β-hydrogen elimination reactions has largely relegated this class of catalysts for applications in dimerization or oligomerization processes. We recently reported the development of cationic Ni(II) and Pd(II) α-diimine complexes that *polymerize* ethylene and α-olefins (eq 2.1).[31,32] The key to the ability of

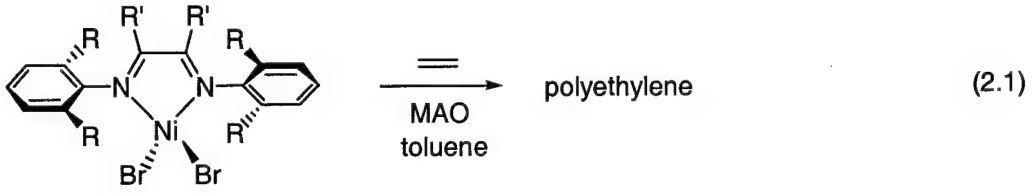

(2.1)

R = *i*-Pr
R' = H, Me, or R', R' = 1,8-naphth-diyl

these late transition-metal catalysts to form polymer lies in the steric bulk of the α-diimine ligands. The aryl rings of the α-diimine ligands are approximately orthogonal to the plane formed by the metal and coordinated nitrogen atoms. This ring orientation places the bulky substituents in axial sites, which effectively retards the rate of chain transfer relative to chain propagation. In a recent communication we reported that when diimine ligands lacking bulky aryl ortho substituents are used, the resulting Ni(II)-based systems produce a Schulz-Flory distribution of ethylene oligomers (eq 2.2).[33] We have subsequently undertaken a series of detailed studies investigating the electronic

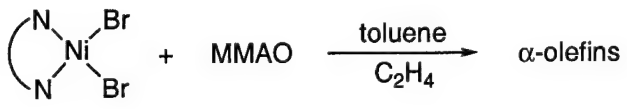

(2.2)

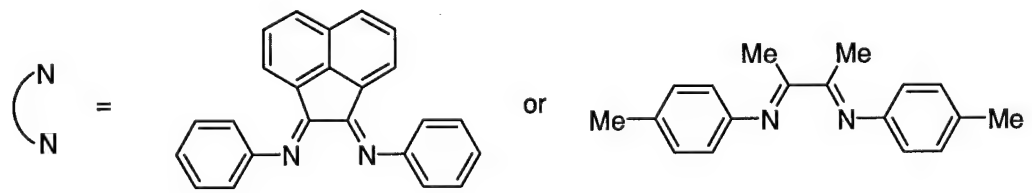

effects of the α-diimine ligand on the oligomerization of ethylene. In addition, the effects of the aluminum alkyl cocatalyst on catalyst activity, catalyst lifetime, and product composition have been examined. We have discovered that these sterically unhindered Ni(II) catalysts dimerize propylene, and have investigated the effects of α-diimine ligand electronics coupled with variations in reaction conditions on the dimer product distribution. Proposed mechanisms for both ethylene oligomerization and propylene dimerization are discussed.

Results and Discussion

A. Catalyst Preparation. Extensive studies on the synthesis and reactivity of a wide variety of d^8 α-diimine complexes have been reported by Elsevier et. al.[34-38] Using similar synthetic methods, a series of *para*-aryl substituted α-diimine ligands and their corresponding nickel(II) dibromide complexes were prepared as shown in Scheme 2.1. Synthesis and characterization of ligands **1b-e** and nickel(II) dibromide complexes **2b-e** have been previously reported.[37,39,40] Acenaphthoquinone and slightly more than 2 equivalents of the appropriate aniline were combined in toluene containing camphorsulfonic acid (ca. 2-3 mol %) and the mixture was heated to reflux. Water evolution was observed by collecting the toluene/water azeotrope using a Dean-Stark trap. Electron-rich anilines react smoothly under these conditions to form the corresponding diimines, but even at these temperatures the reaction using electron-poor 4-trifluoromethylaniline is sluggish. Efforts to prepare the diimine derived from 4-nitroaniline and acenaphthoquinone using these reaction conditions proved unsuccessful. Crude ligands were purified via precipitation from chloroform with pentane, followed by several pentane washes.

The nickel(II) dibromide complexes **2a-e** were prepared from the ligands **1a-e** by reaction of a slight excess of the free diimine ligand with (1,2-dimethoxyethane)nickel(II) bromide in methylene chloride (Scheme 2.1). The nickel complexes precipitated from solution, and were purified by washing away the 1,2-dimethoxyethane and excess ligand with diethyl ether. Complexes **2a-e** are air-

stable solids and are insoluble in common organic solvents, including CH_2Cl_2, $CHCl_3$, Et_2O, toluene, and hydrocarbon solvents. They are sparingly soluble in 1,2-difluorobenzene.

Scheme 2.1. α-Diimine ligands **1a-e** and synthesis of corresponding Ni(II) dibromide complexes **2a-e**.

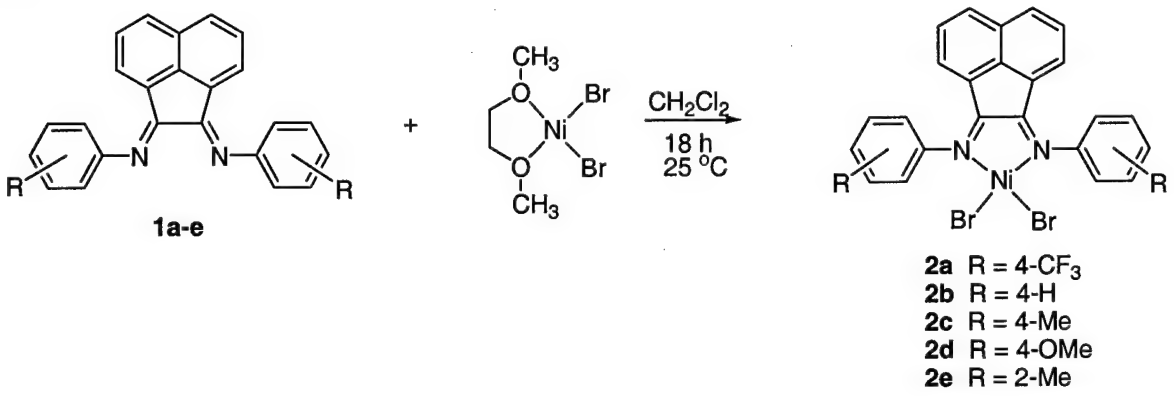

B. Oligomerization of Ethylene. Treatment of catalyst precursors **2a-d** with MAO, modified MAO (MMAO), MAO-IP[41] or Et_2AlCl in toluene generates active ethylene oligomerization catalysts. The results of a series of these oligomerization reactions are summarized in Table 2.1. A Schulz-Flory distribution[42-45] of oligomers is produced, which is characterized by a constant, α, where α represents the probability of chain propagation (eq 2.3). An oligomer distribution with a small

$$\alpha = \frac{\text{rate of propagation}}{\text{rate of propagation + rate of chain transfer}} = \frac{\text{moles of } C_{n+2}}{\text{moles } C_n} \qquad (2.3)$$

Schulz-Flory α (e.g. $\alpha < 0.5$) will therefore consist mainly of dimers and lower oligomers, while the bulk of an oligomer distribution with a high Schulz-Flory α (e.g. $\alpha > 0.8$) will consist of higher oligomers. The olefins produced are primarily linear α-olefins, with the remainder consisting of linear 2-alkenes. Branched olefins are not observed when reaction times are 1 hour or less. Very long reactions (e.g. 3 hours or more) with the most active catalysts occasionally have very small amounts of branched products present (<2% of total products), which we believe are formed from reincorporation of oligomerization products which build to high concentrations after long reaction periods.

The oligomerization mechanism is proposed to be that shown in Scheme 2.2 and is similar to that proposed for polymerization using analogous Ni(II) complexes.[31] Evidence suggests the intermediate cationic nickel alkyl complexes exist as β-agostic species.[46-48] Metal migration along the chain occurs as shown through olefin hydride species such as **III**.[49] When chain transfer occurs from species **II/III**, only α-olefins can be produced. Internal olefins (2-alkenes) can be produced only when chain transfer occurs from secondary alkyl agostic species **IV/IV'** (α-olefins could arise from these species as well). We have suggested that chain transfer may occur through associative displacement of olefin from an olefin hydride species such as **III**. Theoretical calculations suggest that chain transfer may occur via a direct β-H migration from the alkyl group to bound ethylene in a species such as **I**.[50,51] No experimental evidence is currently available which distinguishes these possible chain transfer mechanisms.

Table 2.1. Oligomerization of Ethylene in 200 mL Toluene with **2**/Al Cocatalyst.[a]

Entry	Catalyst	Pressure (atm)	Temp (°C)	Time (min)	TON[b] X 10^{-3}	% α-olefin[c]	Schulz-Flory α
1	**2a**/MMAO	1	35	60	22	57	0.50
2	**2a**/MMAO	15	35	60	116	81	0.59
3	**2a**/MMAO	28	35	60	136	87	0.61
4	**2a**/MMAO	56	35	60	113	91	0.68
5	**2a**/MMAO	56	15	60	26	94	0.71
6	**2a**/MMAO	56	55	60	103	88	0.66
7	**2a**/MMAO	56	75	60	74	88	0.63
8	**2b**/MMAO	56	35	60	49	92	0.70
9	**2c**/MMAO	56	35	60	45	91	0.71
10	**2d**/MMAO	15	35	60	102	84	0.64
11	**2d**/MMAO	28	35	60	114	88	0.67
12	**2d**/MMAO	56	35	60	50	95	0.74
13	**2a**/MMAO	28	35	30	65	94	0.68
14	**2a**/MAO	28	35	30	80	94	0.68
15	**2a**/MAO-IP	28	35	30	23	96	0.67
16	**2a**/Et_2AlCl	28	35	30	51	90	0.81

[a]Reaction conditions: entries 1-12, [Ni] = 1.00 X 10^{-4} M, 240 equivalents Al:Ni; entries 13-16, [Ni] = 2.50 X 10^{-5} M, 200 equivalents Al:Ni. [b]Turnover number = moles ethylene consumed/moles Ni catalyst. [c]Remainder of product is 2-alkenes.

Some general trends are observed in the data in Table 2.1, particularly the effects of ethylene pressure and temperature, which can be rationalized with the mechanism shown in Scheme 2.2.

Increasing the ethylene pressure results in an increase in the selectivity for α-olefins, as well as an increase in the Schulz-Flory α constant (entries 1-4, 10-12, Table 2.1). According to Scheme 2.2, an increase in ethylene concentration (pressure) should favor increased selectivity for α-olefins over internal olefins because the rate of chain transfer from species **II/III** relative to the rate of chain isomerization to species **IV/IV'** increases with increasing ethylene concentration. The fact that the

Scheme 2.2. Proposed mechanism of olefin oligomerization.

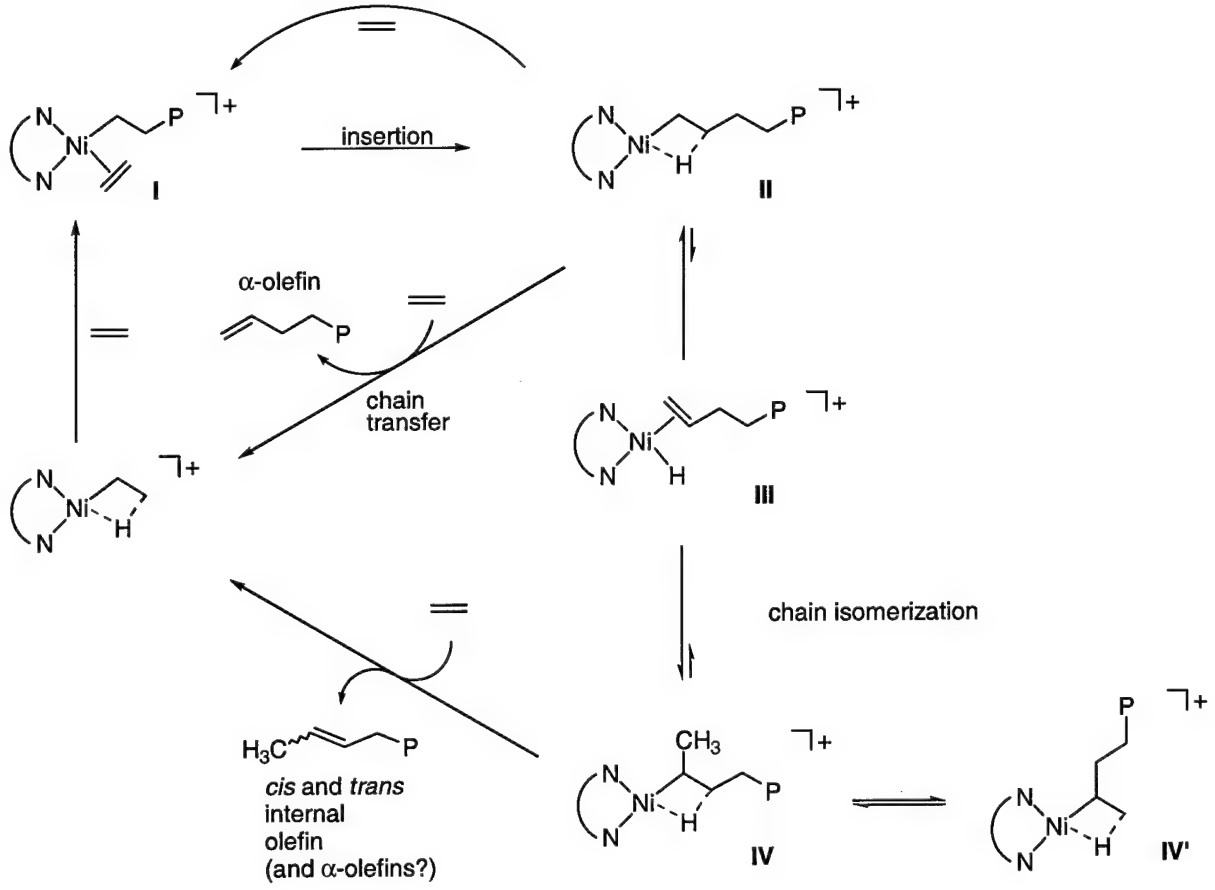

Schulz-Flory α values decrease with decreasing $[C_2H_4]$ suggests that the ratio of chain transfer:propagation (k_{ct}/k_p) is much greater for secondary alkyl complexes **IV/IV'** than for primary alkyl species **II**. This is supported by the observation that no branched α-olefins are produced and all internal olefins produced are 2-alkenes (*cis* and *trans* $CH_3CH{=}CHR$). These observations suggest that once metal migration occurs to give **IV/IV'** no ethylene insertion occurs and no further metal

migration occurs. Thus, the secondary alkyl species **IV/IV'** either undergo chain transfer or isomerize back to **II** as shown in Scheme 2.3. Schulz-Flory α values should track the percent α-olefin produced. Inspection of Table 2.1 shows this trend is followed, with the exception of the oligomerization carried out with Et_2AlCl as activator (run 16; this activator behaves differently from MAO activators, see below).

Scheme 2.3. Proposed mechanism of chain isomerization/transfer for secondary alkyl species.

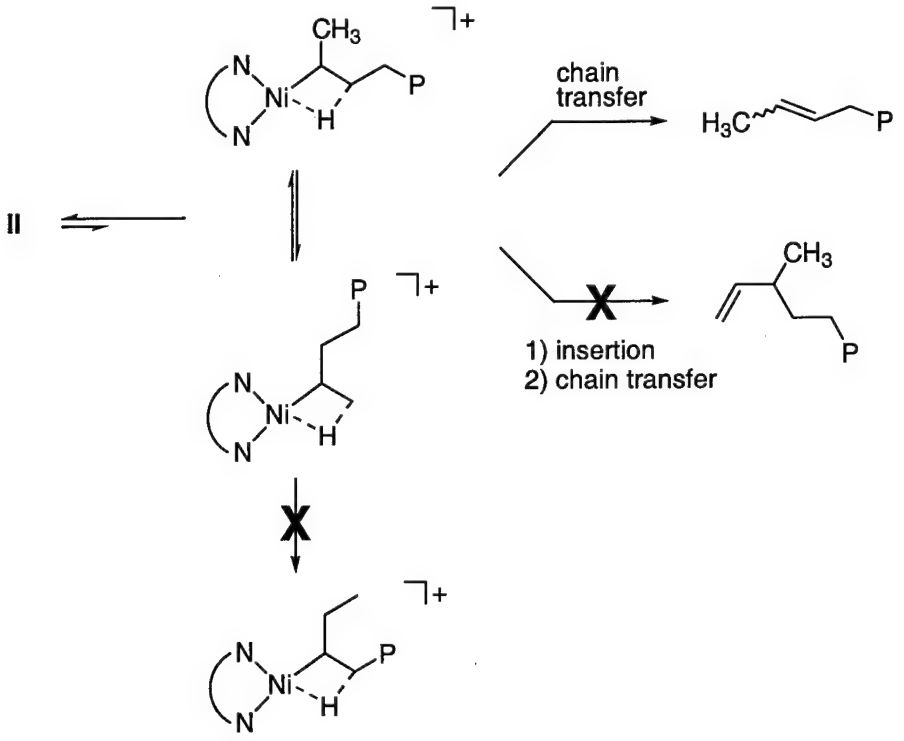

Turnover frequencies are also ethylene-dependent, reaching a maximum value when the ethylene pressure is near 30 atm. Further increases in ethylene pressure result in a decrease in the apparent turnover frequency. The reason for this decrease in turnover frequency is not understood. Possibilities include a decrease in the solvent polarity at higher ethylene concentrations[52,53] or inhibition due to formation of an inactive (or less active) five-coordinate intermediate.

In addition to ethylene pressure effects, the oligomerization reaction is strongly affected by the temperature. As the temperature is increased, both selectivity for α-olefins and the Schulz-Flory constant α decrease (entries 4-7, Table 2.1). These results indicate that the rate of chain transfer

relative to the rate of chain propagation increases with temperature. Since ethylene solubility in toluene decreases with increasing temperature,[54] the loss of selectivity for α-olefins and concomitant decrease in the Schulz-Flory α constant as the temperature increases could be due in part to lower concentrations of ethylene in solution. Thus, the same arguments given for ethylene pressure effects on these parameters apply to the observed temperature effects. Furthermore, the first-order chain isomerization reaction of **II** should show a stronger temperature dependence than the second-order reaction with ethylene required to effect chain transfer. This same trend is seen with increased branching of polyethylene as temperature is increased at constant pressure.[31] Turnover frequencies also increase with temperature (compare entries 4 and 5), but significant catalyst decomposition occurs over 60 min when the reaction temperature is raised above 55 °C (compare entries 6 and 7 with entry 4).

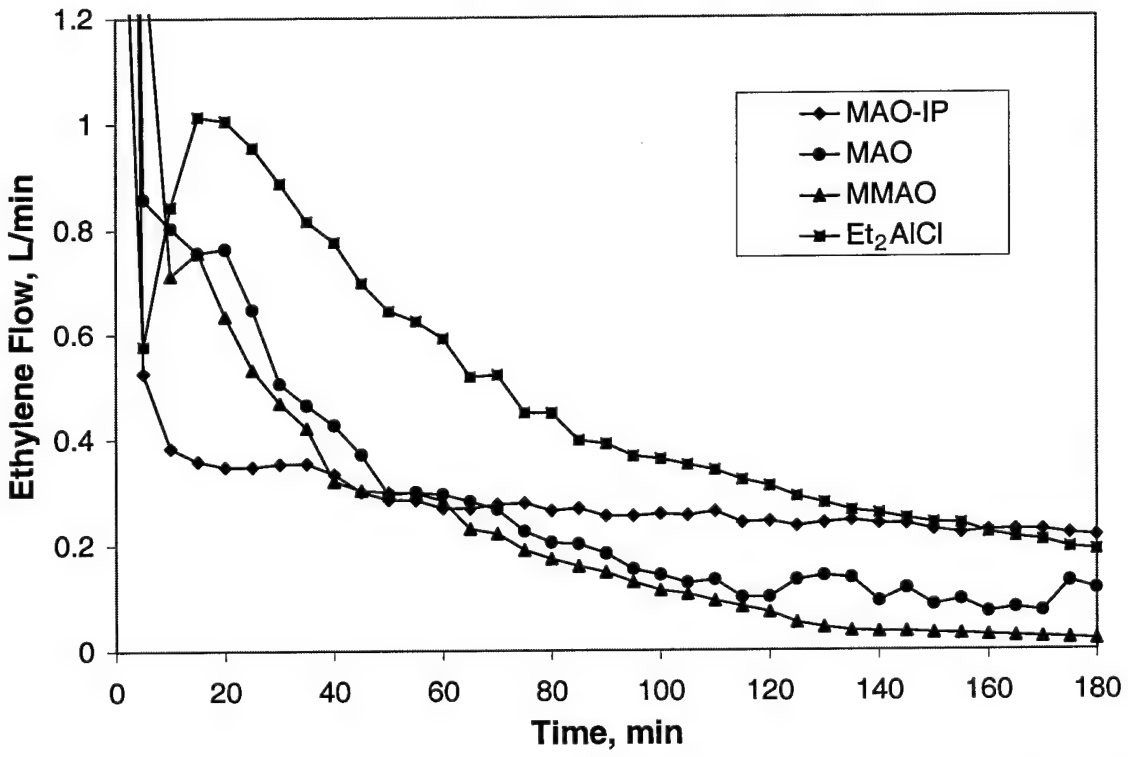

Figure 2.1. Ethylene flow profiles in oligomerization reactions with **2a** and various cocatalysts (400 eq Al:Ni, 200 psig ethylene, 35 °C).

No substantial ligand electronic effects on selectivity for α-olefins or the Schulz-Flory α constant are observed. There does appear to be a trend of increasing turnover frequencies as the metal center becomes more electrophilic. For example, as the *para* substituents on the ligand aryl groups are varied from methyl to trifluoromethyl, turnover frequencies double (entries 4, 8, 9, Table 2.1). The electron-poor trifluoromethyl substituent is expected to lead to a more electrophilic metal center relative to that when more electron-rich substituents are present, which leads to an increased rate of ethylene insertion, the turnover-limiting step. However, the methoxy substituent leads to turnover frequencies that are higher than expected (entries 10-12, Table 2.1). The reason for this behavior is not clear, but formation of Lewis acid-base complexes of the methoxy group with excess aluminum cocatalyst would be expected to reduce electron density on the ligand, and therefore lead to a more electrophilic metal center than would normally be expected.

The choice of aluminum cocatalyst has a significant effect on the ethylene oligomerization reactions. MAO, MMAO, MAO-IP, and Et_2AlCl are all effective cocatalysts. Reactions activated by MAO, MMAO, and MAO-IP all show similar Schulz-Flory values, but those activated by Et_2AlCl produce oligomer mixtures with a higher Schulz-Flory α constant (entries 13-16, Table 2.1).

Catalyst lifetimes were investigated by measuring the ethylene flow into the reactor with a mass flowmeter. The lifetimes of catalysts generated by activation of **2a** with various cocatalysts in ethylene oligomerization reactions are shown in Figure 2.1. The high ethylene flow rates indicated during the initial 5-10 minutes of each reaction reflect the process of ethylene saturation of the toluene solvent. Overall, Et_2AlCl generates the most active catalyst over 3 hour reaction periods. However, comparison of entries 13-16 (Table 2.1) show that over the first 30 min, the MAO-activated catalyst, for example, produces more turnovers than the Et_2AlCl-activated catalyst. Judging from the flow profiles (Figure 2.1) this is likely due to a more rapid catalyst activation by MAO, thus more turnovers at early times. MAO and MMAO cocatalysts produce catalysts that are most active during the first 20 minutes of the reaction, after which time catalyst activity steadily declines. After 3 hours,

the catalyst produced from MMAO is almost completely inactive. MAO-IP generates the least active catalyst during early reaction times, but this catalyst shows more constant activity throughout 3 hour reactions than reactions using MAO or MMAO. Longer runs with **2a**/MAO-IP show the catalyst is still active after 12 hours, although the catalyst activity at this point is less than 10% of the activity observed 30 minutes into the reaction.

The effects of various Al:Ni ratios in ethylene oligomerizations were investigated using **2a** and Et_2AlCl and the results are shown in Figure 2.2. Generally, a threshold amount of cocatalyst is needed to effectively activate the precatalyst, presumably to scavenge impurities that may poison the active catalyst. Figure 2.2 suggests that a period of 15-25 min is required for full activation of the precatalyst using Et_2AlCl, depending on the Al:Ni ratio used. No similar induction period is seen when using MAO-type activators.[55] The activation periods when using Et_2AlCl as the cocatalyst were found to be variable and not well defined. Since turnover numbers shown in Table 2.1 were determined by measuring the amount of reaction products formed over set reaction periods, the combination of variable activation periods and catalyst deactivation makes turnover number comparisons between various cocatalysts difficult and very qualitative at best. Higher amounts of cocatalyst (e.g. > 1000 eq Al:Ni) in the ethylene oligomerization reactions lead to faster degradation of the active catalyst. The reason for this trend is not understood, but it was observed with all cocatalysts tested. Cavell and Masters noted that contamination of Et_2AlCl with Et_3Al reduced the activity of cationic Ni catalysts in olefin oligomerizations.[26] Similarly, Kissin and Beach have reported that sulfonated nickel ylide ethylene oligomerization catalysts are reduced to inactive Ni(0) species by Et_3Al.[17] Attempts to use Me_3Al to activate dibromide precatalyst **2d** in the presence of ethylene failed to form an active catalyst. These observations may suggest that trialkylaluminum impurities in the cocatalyst could in part be responsible for catalyst degradation.

Adding certain ortho substituents to the aryl rings of the α-diimine ligands leads to much longer-lived catalysts.[56] In addition, the ethylene flow experiments described above show that lower Al:Ni

ratios result in more active and longer-lived catalyst systems. These results seem to indicate that catalytic intermediates formed from precursors containing diimine ligands lacking steric bulk near the metal center could possibly deactivate through reaction with excess cocatalyst.

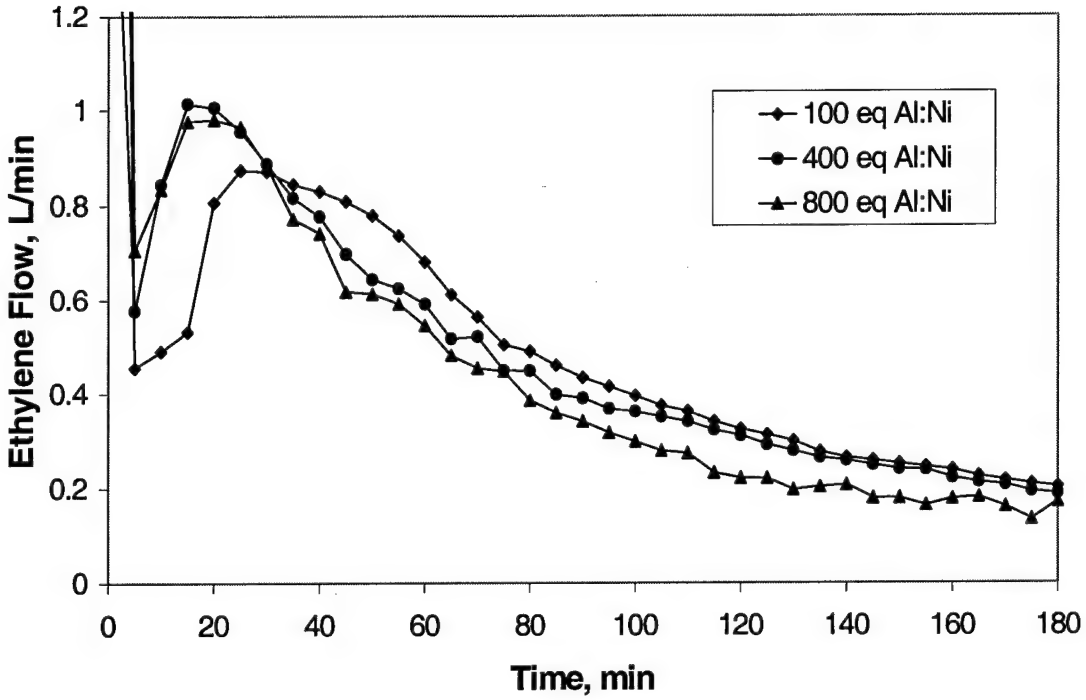

Figure 2.2. Ethylene flow profiles in oligomerization reactions with various ratios of **2a** to Et_2AlCl (200 psig ethylene, 35 °C).

The oligomer composition and distribution at various points during the reaction was investigated by running a series of ethylene oligomerization reactions catalyzed by **2a**/MMAO using identical reaction conditions, but different reaction times. The results are summarized in Table 2.2. Total turnover numbers are not proportional to reaction time; i.e., turnover frequencies appear to drop as the reaction progresses, which supports the data obtained in the monomer flow measurement experiments, indicating significant catalyst decay occurs in ½-2 hours. Although catalyst performance degrades with time, selectivity for α-olefins and the Schulz-Flory α value remain essentially unchanged throughout the duration of catalysis. Relatively constant α-olefin to internal olefin ratios indicate no significant isomerization of the reaction products is taking place at longer

reaction times, and this data supports a previous control experiment where no observable isomerization of added 1-nonene was seen.[33]

Table 2.2. Oligomerization of Ethylene with **2a**/MMAO.[a]

Entry	Time (min)	TON X 10^{-3}	% α-olefin	Schulz-Flory α[b]
1	15	41	94	0.67
2	30	75	93	0.67
3	60	113	91	0.68
4	120	185	90	0.68

[a]Reaction conditions: [Ni] = 1.00 X 10^{-4} M, 240 equivalents Al:Ni, 200 mL toluene, 800 psig ethylene, 35 °C. [b]Determined from ratios of 1-tetradecene/1-dodecene GLC areas.

C. Dimerization of Propylene. Treatment of precatalysts **2a-e** with MMAO or Et_2AlCl in toluene generates active catalysts which dimerize propylene. The results of a series of propylene dimerization reactions with these catalysts are summarized in Table 2.3. Under the reaction conditions described in Table 2.3, these catalysts are greater than 99% selective for production of propylene dimers as determined by GLC. No trimers or higher oligomers are observed in 30 min runs. The products referred to in Table 2.3 are shown in Scheme 2.5.

Table 2.3. Dimerization of Propylene in 50 mL Toluene with **2**/Al Cocatalyst.[a]

					Product Distribution, mol %[b]				
Entry	Catalyst	Pressure (atm)	Temp (°C)	TOF[c]	Path A	Path B	Path C	Path D	Isomerization products[d]
1	**2a**/MMAO	1.1	0	4410	19	38	8	21	14
2	**2a**/MMAO	2	0	14,600	19	41	9	20	11
3	**2a**/MMAO	3	0	19,600	19	42	8	20	11
4	**2a**/MMAO	4	0	19,500	18	40	8	23	11
5	**2a**/MMAO	5	0	19,400	19	43	8	21	9
6	**2a**/MMAO	2	-15	2760	18	37	8	29	8
7	**2a**/MMAO	2	28	10,000	21	38	8	18	15
8	**2b**/MMAO	1.1	0	3730	20	39	9	20	12
9	**2c**/MMAO	1.1	0	3310[e]	24	41	9	16	10
10	**2d**/MMAO	1.1	0	1800	20	38	10	22	10
11	**2a**/Et_2AlCl	2	0	1520	19	40	8	25	8
12	**2a**/MMAO[f]	1.1	0	3140[g]	17	34	8	25	16
13	**2a**/MMAO[h]	1.1	0	2640[g]	14	28	8	29	21
14	**2e**/MMAO	1.1	0	230	13	13	6	43	25

[a]1300 equivalents Al:Ni; 30 min reaction times. [b]Product distribution according to pathways shown in Scheme 2.5. [c]TOF = turnover frequency (moles C_3H_6/mol Ni • h). [d]Percentage of product mixture containing double-bond shift isomers of the dimerization products. [e]35 Min reaction time. [f]870 Equivalents Al:Ni. [g]60 Min reaction time. [h]1700 Equivalents Al:Ni.

At low propylene concentrations, the turnover frequencies are dependent on the propylene concentration. As the propylene concentration is increased, the turnover frequency becomes

independent of propylene concentration (entries 1-5, Table 2.3). This behavior may be due to an equilibrium between an alkyl agostic resting state species and an alkyl olefin resting state species at lower propylene concentrations. This equilibrium would shift in favor of the alkyl olefin species at higher propylene concentrations. The turnover-limiting step is believed to be migratory insertion of the alkyl olefin complex, so the observed rate of dimerization should be independent of propylene concentration when the sole resting state species is the alkyl olefin species. The dimer product distribution is essentially unaffected by changes in the propylene concentration, although the degree of isomerization of the reaction products decreases with increasing propylene concentration.

Turnover frequencies at 2 atm propylene pressure increase as the temperature is raised from -15 °C to 0 °C, but decline as the temperature is raised further (entries 2, 6-7, Table 2.3). We believe this observed decrease in turnover frequency is due to a lower concentration of propylene in solution at 28 °C than at 0 °C, since the solubility of propylene in toluene decreases dramatically with increasing temperature.[54] The observation that maximum turnover frequency at 2 atm occurs near 0 °C therefore indicates the point of balance between monomer concentration in solution and the expected increasing rate of insertion with increasing temperature. The product distribution is only slightly affected by temperature changes, but the degree of isomerization of the reaction products was nearly double for reactions run 28 °C as opposed to those run at -15 °C (compare entries 6 and 7).

Turnover frequencies increase as the electrophilic nature of the catalyst increases (entries 1, 8-10, Table 2.3). Dimerizations catalyzed by **2a**/MMAO proceed at more than twice the rate as those catalyzed by **2d**/MMAO over the first 30 minutes following catalyst activation. The dimer product distribution is relatively independent of electronic effects, but the degree of product isomerization increases as the catalyst becomes more electrophilic.

The nature and quantity of aluminum cocatalyst affects the outcome of the propylene dimerization reactions. For example, use of Et_2AlCl as the cocatalyst results in turnover frequencies that are an order of magnitude lower than when MMAO is used (compare entries 2 and 11, Table 2.3). Since

long induction periods were observed when Et_2AlCl was used as a cocatalyst in ethylene oligomerizations at 35 °C, it is likely that the apparent low activity of **2a**/Et_2AlCl in dimerizing propylene is due to an even longer induction period since this reaction was run at 0 °C. While the overall product distribution is essentially unchanged, the degree of isomerization observed when Et_2AlCl is used is substantially lower. Varying the amount of MMAO used led to different turnover frequencies; 1300 equivalents Al:Ni was found to be the optimal ratio of cocatalyst to precatalyst for maximizing turnover frequency (entries 1, 12-13, Table 2.3). In contrast, lower cocatalyst:precatalyst ratios led to optimal turnover frequencies in the ethylene oligomerization reactions (see above).

The isomerization of dimer products was probed in a control experiment in which 1-pentene was added to a propylene dimerization reaction catalyzed by **2a**/MMAO (Table 2.4). Over the course of 2 hours, 1-pentene was slowly isomerized to the internal isomers, which suggests that isomerization of the reaction products takes place to some extent after chain transfer. Although isomerization is taking place, it is slow as compared to the rate of dimer production.

Table 2.4. Isomerization of 1-Pentene by **2a**/MMAO under Propylene Dimerization Conditions.[a]

Isomer	Relative Mol %[b]		
	5 min	1 h	2 h
1-pentene	100	79	71
trans-2-pentene	0	12	16
cis-2-pentene	0	9	13

[a][Ni] = 4.00 X 10^{-5} M, 1300 eq Al:Ni, 50.0 mL toluene, 0 °C, 1 atm propylene.
[b]Areas relative to an octane internal standard as determined by GLC.

Even though some isomerization of the dimerization products takes place during the reaction, some conclusions about the regiochemistry of propylene insertion can be drawn based on product distributions. A commonly advanced mechanism for nickel-catalyzed dimerization assumes a propylene-free nickel hydride intermediate[57,58] which in this case would be (N^N)Ni-H^+. As discussed above it is unlikely such a discrete hydride intermediate is generated; the proposed general catalytic dimerization cycle is shown in Scheme 2.4. Scheme 2.5 outlines the specific steps which lead to formation of various hexene isomers. As shown in Scheme 2.5, the isomers formed depend on

(1) whether *n*-propyl or *i*-propyl group migration occurs, (2) whether migration occurs in a 1,2 or 2,1 fashion and (3) the direction of β-H elimination when two possibilities exist (routes B and D). Based on the analysis of ethylene oligomerization above and the observation of branching in ethylene polymerization by similar Ni catalysts as well as recent observations concerning cationic palladium alkyl complexes,[46] it is likely that the cationic nickel propyl complexes **V** and **VI** as well as the nickel propyl propylene complexes **VII** and **VIII** partially or fully equilibrate prior to migratory insertion.

Scheme 2.4. General catalytic cycle for propylene dimerization.

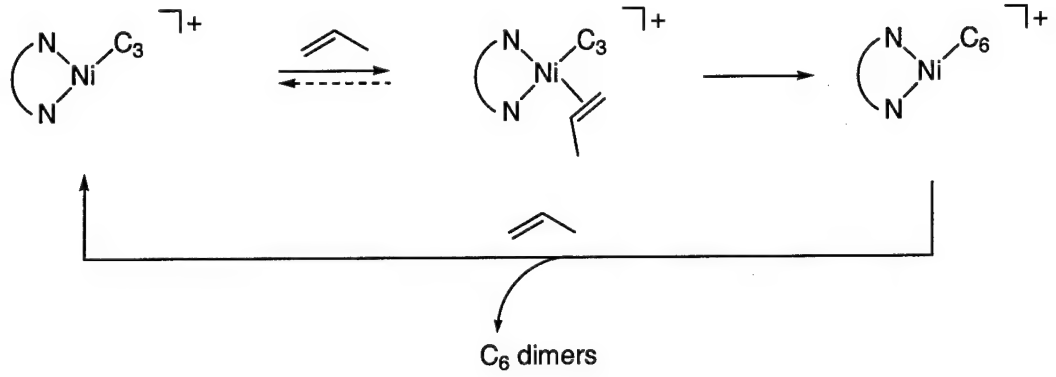

Some isomerization of primary dimerization products takes place (see Table 3). Since 2-methyl-2-pentene is the major isomerization product and it can arise from either pathway A or D, the fraction of reaction through one or both of these pathways may be underestimated using ratios of primary products. However, since isomerization products account for only 10% of total product, qualitative conclusions can be drawn from primary product ratios. Clearly pathway B involving 2,1 insertions of the *n*-propyl complex is the major pathway for dimerization, accounting for 40% of primary products observed. Products from migration of an *n*-propyl group (both 2,1 and 1,2) are favored over products from migration of an *i*-propyl group by ca. 2:1 (paths A+B : paths C+D). However, since the ratios of propyl propylene complexes **VII**:**VIII** undergoing insertion is not known (and they may be in equilibrium) it is not valid to conclude that the barrier to migration of the *n*-propyl group is less than

Scheme 2.5. Propylene dimerization pathways.

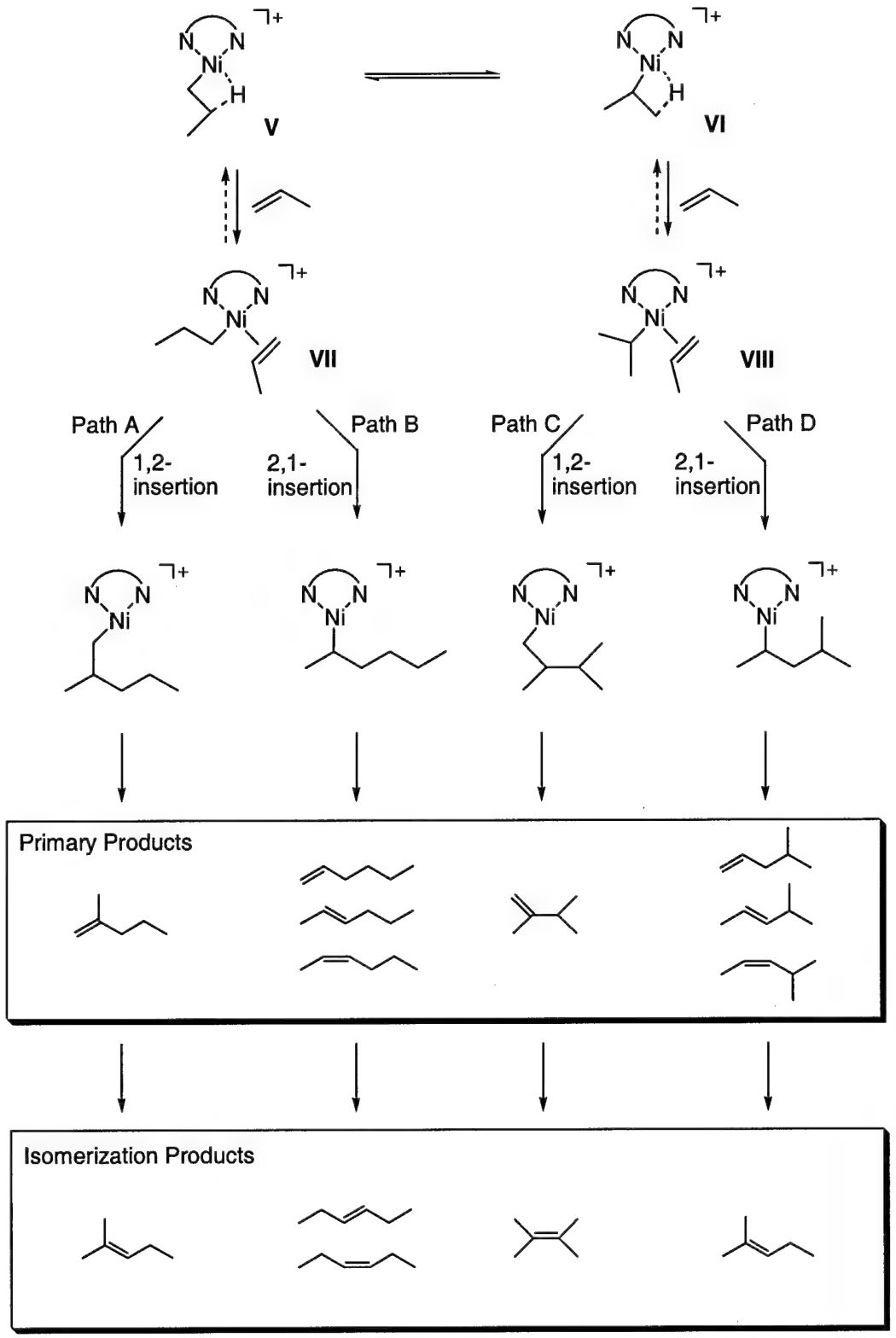

that of the *i*-propyl group. Overall, 2,1 insertion is favored over 1,2 insertion by ca. 2:1 (paths B+D : paths A+C).

It is also instructive to examine the 2,1:1,2 insertion ratio as a function of which group, *n*-propyl or *i*-propyl, is migrating. Again, based on ratios of primary products, the *n*-propyl group exhibits a ca. 2:1 ratio of 2,1:1,2 insertion (path B:A) while the corresponding *i*-propyl group ratio (path D:C) is ca. 2.5:1. Thus, 2,1 insertion is somewhat preferred for the secondary alkyl group. This preference may be somewhat greater when considering that the 2-methyl-2-pentene isomerization product, no matter which pathway it forms from, either decreases the B:A ratio or increases the D:C ratio.

The catalyst lifetimes under typical propylene dimerization conditions used to construct Table 2.3 were examined by analyzing aliquots of dimerization reactions catalyzed by **2a**/MMAO and **2c**/MMAO and plotting the total propylene turnover number vs. time (Figure 2.3). Both catalysts demonstrate relatively steady activity for the first 40 min following activation, but subsequently their performance degrades. Following 2 h of reaction time, the catalysts are still functioning, but slowly. The dimer product distribution remains constant throughout the duration of the experiment, as well as the extent to which these products are isomerized (Table 2.5). During the early periods of the

Table 2.5. Dimerization of Propylene with **2a**/MMAO.[a]

Reaction Time (min)	Dimer Product Distribution, mol %			
	n-Hexenes	2-Methyl-pentenes	2,3-Dimethyl-butenes	Isomerization products
20	44	47	9	12
40	45	46	9	12
60	45	46	9	12
90	46	45	9	12
120	45	46	9	12
180	45	46	9	13

[a]Reaction conditions: 2.0×10^{-6} mol **2a**, 1300 eq Al:Ni, 50 mL toluene, 1.1 atm propylene, 0 °C.

reaction the sole reaction products are dimers. At longer reaction times (e.g. after 2 h), small amounts of trimers appear, but even after 3 hours they compose less than 2% of the total product mixture. No tetramers or higher oligomers were detected by gas chromatography. Similar results were obtained from the dimerization reaction catalyzed by **2c**/MMAO.

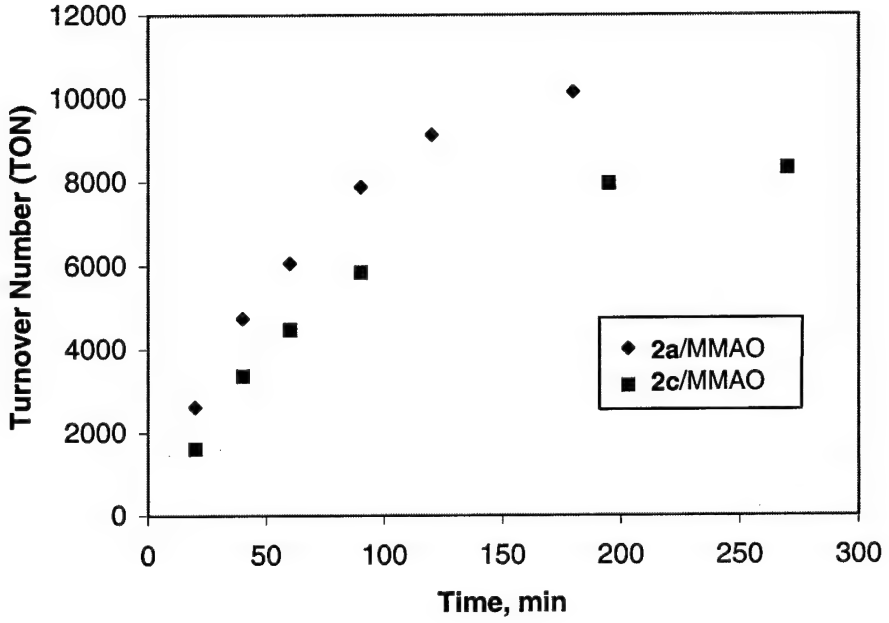

Figure 2.3. Propylene turnover number (TON) vs. time using **2a**/MMAO and **2c**/MMAO in toluene at 0 °C.

D. Dimerization of Higher Olefins. Dimerization reactions of 1-butene and 4-methyl-1-pentene run under conditions similar to the propylene dimerization reactions were analyzed by GLC and found to proceed only very slowly as compared to propylene dimerizations. 1-Butene is dimerized by **2a**/MMAO at a rate less than 10% of that observed for propylene dimerizations run under similar reaction conditions.

The results of dimerization of 4-methyl-1-pentene by **2a**/MMAO are listed in Table 2.6. While small amounts of dimers are produced, this catalyst system actually isomerizes 4-methyl-1-pentene at a faster rate than it dimerizes it. Turnover frequencies are less than 5% of those measured for propylene dimerizations carried out under similar conditions. Overall, these results suggest that uptake of olefin products in ethylene oligomerizations should occur much more slowly than ethylene, and this is experimentally borne out by both the observed Schulz-Flory oligomer distributions and the lack of branched olefin products.

Table 2.6. Dimerization of 4-Methyl-1-pentene by **2a**/MMAO in Toluene.

	Product Distribution, Mol %	
Species	1 h Aliquot	2 h Aliquot
4-Methyl-1-pentene	89.6	86.9
cis-4-Methyl-2-pentene	1.3	1.6
trans-4-Methyl-2-pentene	1.4	1.8
2-Methyl-1-pentene	1.4	1.7
2-Methyl-2-pentene	1.5	1.9
Dimers[a]	4.8	6.1
Dimer TON (mol dimers/mol Ni)	205	270

[a]Includes all C_{12} alkenes.

Conclusions

The findings that sterically-unhindered (α-diimine)Ni(II) catalysts actively oligomerize ethylene and dimerize propylene further demonstrate the versatility of this class of catalysts, and illustrate their sensitivity to steric tuning. The temperature and pressure sensitivity of these catalysts in ethylene oligomerization reactions allows control of the reaction products through simple variation of these reaction conditions. Ethylene oligomer mixtures with longer average chain lengths can be produced by increasing ethylene pressure, lowering the reaction temperature, and using Et_2AlCl as the cocatalyst, while oligomer mixtures with shorter average chain lengths can be produced by lowering ethylene pressure, raising the reaction temperature, and using MAO or MMAO as the cocatalyst. Lowering the electron density on the metal center through addition of electron-withdrawing groups on the ligand produces more active catalysts, but leads to slightly lower selectivity for α-olefins. Catalyst longevity in ethylene oligomerization reactions is dependent upon the nature and concentration of aluminum cocatalyst, and MAO-IP was found to be the best cocatalyst for generating long-lived catalysts.

These catalysts are very active propylene dimerization catalysts, and demonstrate some selectivity for linear products. Maximum turnover frequencies are realized using electrophilic precatalysts activated with MMAO at temperatures near 0 °C and propylene pressures above 2 atm. Slow dimer product isomerization takes place under typical reaction conditions, and can be minimized by lower

temperatures and higher propylene pressures. The dimer product distribution indicates a 2:1 preference for an initial 1,2 propylene insertion (versus a 2,1 insertion). Furthermore, a 2:1 preference for the second propylene inserting in a 2,1 fashion is observed. Higher olefins such as 1-butene and 4-methyl-1-pentene are dimerized very slowly relative to propylene, which is further evidence that reincorporation of higher olefin reaction products in both ethylene oligomerization and propylene dimerization reactions is not favorable.

Experimental Section

General Methods. All manipulations of air- and/or water-sensitive compounds were performed using standard high-vacuum or Schlenk techniques. Argon was purified by passage through columns of BASF R3-11 catalyst (Chemalog) and 4-Å molecular sieves. Solid organometallic compounds were transferred in an argon-filled Vacuum Atmospheres drybox. ^{1}H, ^{13}C, and ^{19}F NMR spectra were recorded on Varian XL-400 MHz or Gemini 300 MHz spectrometers. Chemical shifts are reported relative to residual $CHCl_3$ (δ 7.24 for ^{1}H), $CDCl_3$ (δ 77.00 for ^{13}C), and CCl_3F (δ 0.00 for ^{19}F). The dimer and oligomer products were analyzed on a Hewlett-Packard 5890A gas chromatograph using a Supelco Petrocol DH 50.2 capillary column (50 m, 0.20 mm i.d., 0.50 μm film thickness) and a flame ionization detector. Ethylene flow measurements were made with an Omega FMA-869 mass flowmeter and recorded with an Omega RD-853-T paperless recorder. Elemental analyses were performed by Atlantic Microlab of Norcross, GA.

Materials. Toluene, diethyl ether, pentane, and methylene chloride were purified using procedures recently reported by Pangborn et. al.[59] Polymer-grade ethylene and propylene were purchased from National Specialty Gases. Propylene was passed through a Drierite gas drying jar (6.7 cm X 29 cm column) before use, while ethylene was used without further purification. 7% Al (wt %) and 6.4% Al solutions of modified methylalumoxane (MMAO) in heptane containing 23-27% isobutyl groups were purchased from Akzo Nobel. MAO-IP (13.5 wt% Al in toluene) was purchased from Akzo Nobel. Diimine ligands **1b-e** and corresponding nickel(II) bromide complexes **2b-e** were

prepared according to modified literature procedures.[31,37,39,40] Acenaphthoquinone, 4-trifluoromethylaniline, (DME)$NiBr_2$, MAO, Et_2AlCl, and 1-pentene were purchased from Aldrich Chemical Co. and used as received. The hexene isomer standards were purchased from Aldrich, Lancaster, and Fluka.

Synthesis of (ArN=C(An)-C(An)=NAr) (Ar = *p*-$CF_3C_6H_4$) (1a). Acenaphthoquinone (0.514 g, 2.82 mmol) and *p*-trifluoromethylaniline (1.00 g, 6.20 mmol) were added to 40 mL of dry toluene in a round bottom flask equipped with a magnetic stir bar. Camphorsulfonic acid catalyst (15 mg) was added to the reaction mixture, and a Dean-Stark trap was attached to the flask. The solution was refluxed for 5 days. Toluene was then removed on a vacuum line, leaving an orange solid. The solid was dissolved in 5 mL $CHCl_3$, and 40 mL pentane was then added to precipitate the diimine. The precipitate was washed with 2 X 20 mL of pentane and dried in vacuo. The product was isolated as a yellow solid (1.06 g, 80% yield). ^{1}H NMR ($CDCl_3$, 400 MHz, 30 °C) δ 7.94 (d, J = 8.1 Hz, 2 H), 7.73 (d, J = 8.1 Hz, 4 H), 7.42 (pseudo t, 2 H), 7.21 (d, J = 8.1 Hz, 4 H), 6.84 (d, J = 7.2 Hz, 2 H); ^{13}C NMR ($CDCl_3$, 100 MHz, 30 °C) δ 161.3, 154.5, 142.0, 131.4, 129.6, 128.0, 127.9, 126.8 (q, $^3J_{C\text{-}F}$ = 3.3 Hz), 126.7 (q, $^2J_{C\text{-}F}$ = 33.4 Hz), 124.4 (q, $^1J_{C\text{-}F}$ = 271 Hz, CF_3), 124.1, 118.3; ^{19}F NMR ($CDCl_3$, 282 MHz, 20 °C) δ -62.3 (s, CF_3). Anal. Calcd. for $C_{26}H_{14}F_6N_2$: C, 66.67; H, 3.01; N, 5.98. Found C, 66.69; H, 3.08; N, 5.90.

Synthesis of (ArN=C(An)-C(An)=NAr)$NiBr_2$ (Ar = *p*-$CF_3C_6H_4$) (2a). (DME)$NiBr_2$ (77 mg, 0.25 mmol) and **1a** (150 mg, 0.32 mmol) were combined in a Schlenk flask under an argon atmosphere. CH_2Cl_2 (20 mL) was added, and the reaction stirred at room temperature for 20 hours. The supernatant liquid was removed, and the product washed with 3 X 10 mL Et_2O and dried in vacuo. The product was isolated as an olive-green powder (141 mg, 82% yield). MS (FAB): m/z[%] 610, 609, 608, 607, 606, 605 [12, 35, 32, 100, 23, 72, M^+-Br], 529, 528, 527, 526 [6, 15, 13, 35, M^+-Br_2], 470, 469, 468 [10, 26, 8, M^+-$NiBr_2$], 450, 449 [17, 52, M^+-$NiBr_2F$]. Anal. Calcd. for $C_{26}H_{14}Br_2F_6N_2Ni$: C, 45.46; H, 2.05; N, 4.08. Found C, 45.31; H, 2.70; N, 3.75.

General Procedure for Ethylene Oligomerization. A mechanically-stirred 1000 mL Parr autoclave was heated overnight to 100 °C under vacuum, then cooled to 30 °C under an ethylene atmosphere. The autoclave was charged with 198 mL toluene and MMAO. The autoclave was sealed, and ethylene was added (100 psig). The solution was stirred for 10 min, during which time the desired reaction temperature was established. The ethylene pressure was then released, and a suspension of the appropriate catalyst precursor (**2a-d**, 2.0×10^{-5} mol in 2 mL toluene) was added to the reaction mixture via cannula. The reactor was then sealed and pressurized with ethylene to the desired reaction pressure. The reaction was stirred under constant ethylene pressure for 1 h, after which time the pressure was released and the catalyst quenched with acetone and water. An aliquot of the reaction mixture was analyzed by GLC to determine the Schulz-Flory α constant. The integrated areas of the C_{12} and C_{14} oligomers were used to calculate the Schulz-Flory α constants. The GLC conditions used are as follows: injector and detector temperatures, 250 °C; oven temperature program, 100 °C/4 min, 8 °C/min ramp, 250 °C/70 min. Oligomer peaks in the C_4-C_{26} range were resolved under these analytical conditions. The solvents were removed on a rotary evaporator, and the residual toluene was removed in vacuo overnight. The mass of the remaining olefin products was obtained, and lower olefins lost during workup were calculated using the Schulz-Flory α constant and a gas chromatograph taken of the olefin products following workup. α-Olefin selectivity was determined by comparing the ratios of terminal olefin proton areas to internal olefin proton areas as measured by ^{1}H NMR spectroscopy.

Ethylene Flow Rate Measurements. A mechanically-stirred 1000 mL Parr autoclave under an ethylene atmosphere was charged with 198 mL toluene and the appropriate aluminum cocatalyst. The reactor was sealed, pressurized with ethylene to 200 psig, and the temperature allowed to equilibrate at 35 °C. Once the system reached equilibrium, the ethylene flow baseline was established with a mass flowmeter positioned between the ethylene supply cylinder and the autoclave. A small flame-dried Schlenk tube under an argon atmosphere was charged with **2a** (1.0×10^{-5} mol, 6.9 mg) and 2

mL toluene to form a precatalyst slurry. The reactor was vented, and the precatalyst slurry was transferred into the reactor via cannula. The reactor was repressurized to 200 psig with ethylene, and the temperature maintained at 35 °C. Ethylene flow rates were recorded at 5 to 15 second intervals throughout the duration of the reaction.

General Procedure for Propylene Dimerization. A dry Fisher-Porter bottle was charged with a magnetic stir bar, evacuated, then filled with propylene. Toluene (47.0 mL) and MMAO (1.4 mL of 7% heptane solution) were added to the bottle via syringe. The reaction mixture was then cooled to the reaction temperature while stirring under constant propylene pressure. A suspension of the appropriate catalyst precursor (**2a-d**, 2.00 X 10^{-6} mol in 2.0 mL toluene) and 50 μL octane (internal standard) were transferred via cannula to the reaction vessel. The bottle was then sealed and pressurized with propylene. After a 30 min reaction period, the reactor was depressurized, and an aliquot of the reaction mixture was removed for GLC analysis. The GLC conditions used: injector temperature 220 °C; detector temperature 250 °C; oven temperature program, 30 °C/18 min, 20 °C/min ramp, 150 °C/25 min.

Analysis of Propylene Dimers. Standard solutions of the propylene dimers and octane were prepared by adding 2.5, 5.0, 10.0, and 15.0 μL of authentic samples of each compound to toluene in 10.0 mL volumetric flasks. The solutions were diluted to 10.0 mL with toluene, and GLC calibration curves were obtained. Aliquots of the dimerization reaction mixtures (ca. 5 mL) were removed via cannula and added to 10.0 mL volumetric flasks containing about 4 mL acetone. The aliquots were warmed to 20 °C, diluted to volume with acetone, and injected into the gas chromatograph. Each dimer was qualitatively identified by retention time. Retention times for the dimers under the analytical conditions used are as follows: 4-methyl-1-pentene, 10.92 min; 2,3-dimethyl-1-butene, 11.55 min; *cis*-4-methyl-2-pentene, 11.65 min; *trans*-4-methyl-2-pentene, 11.85 min; 2-methyl-1-pentene, 13.19 min; 1-hexene, 13.28 min; *trans*-3-hexene, 14.48 min; *cis*-3 hexene, 14.57 min; *trans*-2-hexene, 14.73 min; 2-methyl-2-pentene, 14.96 min; *cis*-2-pentene, 15.66 min; 2,3-dimethyl-2-

butene, 17.59 min. The dimers were quantified by first determining the volume of the aliquot withdrawn via comparison of the octane internal standard area with an octane calibration curve, then using the GLC areas of each propylene dimer versus their respective standard calibration curves to determine the mass of each dimer present in the reaction mixture.

1-Pentene Isomerization Control Experiment. The general procedure described for propylene dimerization was followed (vide supra). A slurry of precatalyst **2a** (1.37 mg, 2.00 X 10^{-6} mol) in 2.0 mL toluene was added to MMAO (1.5 mL of 6.4% heptane solution, 1300 eq Al:Ni) in 46.5 mL toluene containing 50 μL 1-pentene and 50 μL octane at 0 °C. The propylene pressure was maintained at 1 atm throughout the duration of the experiment. Aliquots (ca. 5 mL) of the reaction mixture were removed at 5 min, 1 h, and 2 h after catalyst activation and analyzed by GLC. The areas of 1-pentene, *cis*-2-pentene, and *trans*-2-pentene relative to an octane internal standard were determined for each aliquot.

Propylene Dimerization Longevity Experiments. The general procedure described for propylene dimerization was followed (vide supra). A slurry of precatalyst **2a** (1.37 mg, 2.00 X 10^{-6} mol) or **2c** (1.16 mg, 2.00 X 10^{-6} mol) in 2.0 mL toluene was added to MMAO (1.4 mL of 7% solution, 1300 eq Al:Ni) in 46.6 mL toluene containing 50 μL octane at 0 °C. The propylene pressure was maintained at 1.1 atm throughout the duration of the experiment. Aliquots (ca. 4 mL) of the reaction mixture were removed via cannula and quantified by GLC (vide supra). The amount of catalyst, solvent, and dimer products removed with each aliquot was determined using the octane internal standard, and utilized in subsequent turnover number calculations.

Dimerization of 1-Butene. Precatalyst **2a** (5.0 X 10^{-6} mol, 3.4 mg) and 50 mL toluene were combined in a 100 mL Schlenk flask equipped with a magnetic stir bar. 1-Butene was purged through the solution for 10 min, then 1.2 mL MMAO (7% in heptane) was added via syringe. The reaction was allowed to proceed at 25 °C for 75 min under 1 atm 1-butene pressure. Aliquots were removed at 10 min and 75 min, quenched with acetone, and injected into the GLC (60 °C isothermal).

A mixture of butene dimers was observed. Comparison of total dimer GLC areas with propylene dimer standards shows the turnover frequencies for 1-butene dimerization are less than 10% of those observed for analogous propylene dimerization reactions.

Dimerization of 4-Methyl-1-Pentene. Dry, degassed toluene (48 mL) was added to a dry, Ar-filled 100 mL Schlenk flask equipped with a magnetic stir bar. 4-Methyl-1-pentene (ca. 1 mL) was added to the reaction mixture via syringe, followed by MMAO (1.5 mL of a 6.42% solution). Precatalyst **2a** (2.00×10^{-6} mol, 1.37 mg), octane (52.5 μL, GLC internal standard) and 2 mL toluene were added to a flame-dried Schlenk tube. The precatalyst slurry was transferred into the reaction flask via cannula. The reaction was allowed to proceed at 25 °C under a static Ar atmosphere for 2 h. Aliquots of the reaction mixture were removed after 1 h and 2 h, quenched in acetone, and analyzed by GLC using the procedure described above for quantitative analysis of propylene dimers. The product distributions are listed in Table 7. Turnover numbers based on dimer masses calculated using the 4-methyl-1-pentene GLC calibration curve are 205 mol dimers/mol Ni (1 h aliquot) and 270 mol dimers/mol Ni (2 h aliquot).

References and Notes

(1) Keim, W.; Kowaldt, F. H.; Goddard, R.; Krüger, C. *Angew. Chem., Int. Ed. Engl.* **1978**, *17*, 466.

(2) Keim, W.; Hoffmann, B.; Lodewick, R.; Peuckert, M.; Schmitt, G. *J. Mol. Catal.* **1979**, *6*, 79-97.

(3) Peuckert, M.; Keim, W. *Organometallics* **1983**, *2*, 594-597.

(4) Keim, W. *Angew. Chem., Int. Ed. Engl.* **1990**, *29*, 235-244.

(5) Vogt, D. Oligomerization of Ethylene to Higher Linear α-Olefins. In *Applied Homogeneous Catalysis with Organometallic Compounds*; Cornils, B.; Herrmann, W. A., Eds.; VCH Publishers: New York, 1996; Vol. 1, pp 245-258.

(6) Chauvin, Y.; Olivier, H. Dimerization and Codimerization. In *Applied Homogeneous Catalysis with Organometallic Compounds*; Cornils, B.; Herrmann, W. A., Eds.; VCH Publishers: New York, 1996; Vol. 1, pp 258-268.

(7) Andrews, J. W. *Hydrocarbon Process.* **1982**, *61*, 110.

(8) Chauvin, Y.; Gaillard, J. F.; Quang, D. V.; Andrews, J. W. *Chem. Ind. (London)* **1974**, 375-378.

(9) Muthukumaru Pillai, S.; Ravindranathan, M.; Sivaram, S. *Chem. Rev.* **1986**, *86*, 353-399.

(10) Skupinska, J. *Chem. Rev.* **1991**, *91*, 613-648.

(11) Keim, W. *J. Mol. Catal.* **1989**, *52*, 19-25.

(12) Keim, W. *New J. Chem.* **1987**, *11*, 531-534.

(13) Keim, W.; Behr, A.; Gruber, B.; Hoffmann, B.; Kowaldt, F. H.; Kürschner, U.; Limbäcker, B.; Sistig, F. P. *Organometallics* **1986**, *5*, 2356-2359.

(14) Keim, W.; Behr, A.; Limbäcker, B.; Krüger, C. *Angew. Chem., Int. Ed. Engl.* **1983**, *22*, 503.

(15) Bonnet, M. C.; Dahan, F.; Ecke, A.; Keim, W.; Schulz, R.; Tkatchenko, I. *J. Chem. Soc., Chem. Commun.* **1994**, 615-616.

(16) Matt, D.; Huhn, M.; Fischer, J.; DeCian, A.; Kläui, W.; Tkatchenko, I.; Bonnet, M. C. *J. Chem. Soc., Dalton Trans.* **1993**, 1173-1178.

(17) Kissin, Y. V.; Beach, D. L. *J. Poly. Sci., Part A: Polym. Chem.* **1989**, *27*, 147-155.

(18) Strömberg, S.; Oksman, M.; Zhang, L.; Zetterberg, K. *Acta Chemica Scandinavica* **1995**, *49*, 689-695.

(19) Braunstein, P.; Pietsch, J.; Chauvin, Y.; Mercier, S.; Saussine, L.; DeCian, A.; Fischer, J. *J. Chem. Soc., Dalton Trans.* **1996**, 3571-3574.

(20) Desjardins, S. Y.; Cavell, K. J.; Jin, H.; Skelton, B. W.; White, A. H. *J. Organomet. Chem.* **1996**, *515*, 233-243.

(21) Ostoja Starzewski, K. A.; Witte, J. *Angew. Chem., Int. Ed. Engl.* **1985**, *24*, 599-601.

(22) Ostoja Starzewski, K. A.; Witte, J. *Angew. Chem., Int. Ed. Engl.* **1987**, *26*, 63-64.

(23) Klabunde, U.; Mulhaupt, R.; Herskovitz, T.; Janowicz, A. H.; Calabrese, J.; Ittel, S. D. *J. Poly. Sci., Part A: Polym. Chem.* **1987**, *25*, 1989-2003.

(24) Hirose, K.; Keim, W. *J. Mol. Catal.* **1992**, *73*, 271-276.

(25) Keim, W.; Schulz, R. P. *J. Mol. Catal.* **1994**, *92*, 21-33.

(26) Abeywickrema, R.; Bennett, M. A.; Cavell, K. J.; Kony, M.; Masters, A. F.; Webb, A. G. *J. Chem. Soc., Dalton Trans.* **1993**, 59-68.

(27) Brown, S. J.; Masters, A. F. *J. Organomet. Chem.* **1989**, *367*, 371-374.

(28) Cavell, K. J.; Masters, A. F. *Aust. J. Chem.* **1986**, *39*, 1129-1134.

(29) Brown, S. J.; Clutterbuck, L. M.; Masters, A. F.; Sachinidis, J. I.; Tregloan, P. A. *Applied Catalysis* **1989**, *48*, 1-11.

(30) Small, B. L.; Brookhart, M. *J. Am. Chem. Soc.* **1998**, *120*, 7143-7144.

(31) Johnson, L. K.; Killian, C. M.; Brookhart, M. *J. Am. Chem. Soc.* **1995**, *117*, 6414-6415.

(32) Brookhart, M. S.; Johnson, L. K.; Killian, C. M.; Arthur, S. D.; Feldman, J.; McCord, E. F.; McLain, S. J.; Kreutzer, K. A.; Bennett, A. M.; Coughlin, B. E.; Ittel, S. D.; Parthasarathy, A.; Tempel, D. J. *Pat. Appl.* WO 96/23010, **1996**.

(33) Killian, C. M.; Johnson, L. K.; Brookhart, M. *Organometallics* **1997**, *16*, 2005-2007.

(34) van Asselt, R.; Rijnberg, E.; Elsevier, C. J. *Organometallics* **1994**, *13*, 706-720.

(35) van Asselt, R.; Gielens, E. E. C. G.; Rülke, R. E.; Vrieze, K.; Elsevier, C. J. *J. Am. Chem. Soc.* **1994**, *116*, 977-985.

(36) van Asselt, R.; Elsevier, C. J.; Smeets, W. J. J.; Spek, A. L. *Inorg. Chem.* **1994**, *33*, 1521-1531.

(37) van Asselt, R.; Elsevier, C. J.; Smeets, W. J. J.; Spek, A. L.; Benedix, R. *Recl. Trav. Chim. Pays-Bas* **1994**, *113*, 88-98.

(38) van Asselt, R. Ph.D. Thesis, Universiteit van Amsterdam, Amsterdam, The Netherlands, 1993.

(39) tom Dieck, H.; Svoboda, M.; Grieser, T. *Naturforsch* **1981**, *36b*, 823-832.

(40) Svoboda, M.; tom Dieck, H. *J. Organomet. Chem.* **1980**, *191*, 321-328.

(41) MAO-IP is a new proprietary product sold by Akzo Nobel.

(42) Flory, P. J. *J. Am. Chem. Soc.* **1940**, *62*, 1561-1565.

(43) Schulz, G. V. *Z. Phys. Chem., Abt. B* **1935**, *30*, 379-398.

(44) Schulz, G. V. *Z. Phys. Chem., Abt. B* **1939**, *43*, 25-46.

(45) Henrici-Olivé, G.; Olivé, S. *Adv. Polym. Sci.* **1974**, *15*, 1-29.

(46) Tempel, D. J.; Brookhart, M. *Organometallics* **1998**, *17*, 2290-2296.

(47) McLain, S. J.; Feldman, J.; McCord, E. F.; Gardner, K. H.; Teasley, M. F.; Coughlin, E. B.; Sweetman, K. J.; Johnson, L. K.; Brookhart, M. *Polym. Mater. Sci. Eng.* **1997**, *76*, 20.

(48) McLain, S. J.; Feldman, J.; McCord, E. F.; Gardner, K. H.; Teasley, M. F.; Coughlin, E. B.; Sweetman, K. J.; Johnson, L. K.; Brookhart, M. *Macromolecules* **1998**, *31*, 6705-6707.

(49) Theoretical studies suggest such species do not lie in potential energy minima and are thus transition states for interconversion of agostic species.

(50) Musaev, D. G.; Froese, R. D. J.; Morokuma, K. *Organometallics* **1998**, *17*, 1850-1860.

(51) Deng, L.; Woo, T. K.; Cavallo, L.; Margl, P. M.; Ziegler, T. *J. Am. Chem. Soc.* **1997**, *119*, 6177-6186.

(52) Longo, P.; Oliva, L.; Grassi, A.; Pellecchia, C. *Makromol. Chem.* **1989**, *190*, 2357-2361.

(53) Further evidence of turnover frequency dependence on solvent polarity is that turnover frequencies decrease as the solvent is changed from chlorobenzene to toluene to a 1/1 mixture of toluene/pentane.

(54) Fogg, P. G. T.; Gerrard, W. *Solubility of Gases in Liquids*; John Wiley & Sons Ltd.: West Sussex, England, 1991.

(55) In addition to the mass flow data, reactions initiated with MAO-type cocatalysts are exothermic at the start of the reaction, while reactions initiated with Et_2AlCl exhibit maximum exotherms 10-20 min after the reaction start.

(56) Svejda, S. A.; Onate, E.; Gates, D. P.; Brookhart, M. Manuscript in preparation.

(57) Müller, U.; Keim, W.; Krüger, C.; Betz, P. *Angew. Chem., Int. Ed. Engl.* **1989**, *28*, 1011-1013.

(58) Collman, J. P.; Hegedus, L. S.; Norton, J. R.; Finke, R. G. *Principles and Applications of Organotransition Metal Complexes*; University Science Books: Mill Valley, CA, 1987, pp 578-596.

(59) Pangborn, A. B.; Giardello, M. A.; Grubbs, R. H.; Rosen, R. K.; Timmers, F. J. *Organometallics* **1996**, *15*, 1518-1520.

CHAPTER 3

The Synthesis of Branched Polyethylene Using (α-Diimine)Nickel(II) Catalysts: The Influence of Temperature, Ethylene Pressure, and Ligand Structure on Polymer Properties

This chapter is taken from a manuscript that will soon been submitted for publication, and consists of experimental work performed mainly by three people: Dr. Derek Gates, Dr. Enrique Oñate, and Steve Svejda. The work has been left in the form of the prepared manuscript in order to present a complete account of this work to the reader. The contributions of the other Brookhart group members to this work are as follows: Dr. Oñate synthesized ligands **1c** and **1d**, and Ni complexes **4c** and **4d**. In addition, he performed most of the polymerization experiments conducted with **4c** and **4d**, and grew the crystals used to obtain X-ray structures of **4c** and **4d**. Dr. Peter White performed the crystallographic structural determinations of **4c** and **4d**. Dr. Gates synthesized ligand **3**, Ni complexes **5** and **6**, thoroughly characterized ligand **2** (previously prepared by Dr. Dan Tempel), and conducted the polymerization experiments with **4-6**. Mr. Scott Shultz performed some of the DSC analyses. Mr. Steve Gross (Professor DeSimone's laboratory) assisted with the DMA experiment. The high-temperature GPC analyses were performed by DuPont. Dr. Gates and Professor Brookhart contributed extensively to the writing and revision of the final manuscript.

Introduction

The development of well-defined early transition metal- and lanthanide-based catalysts for the polymerization of ethylene and α-olefins has been the subject of intense recent study.[1] These homogeneous catalysts represent a significant technological advance over traditional heterogeneous

Ziegler-Natta systems in that insight into mechanism of polymerization can be gained, and rational changes to the catalyst structure can be used to control polymer microstructure and properties. Although early metal catalysts currently dominate industrial polymerization processes, there has been a trend towards the development of catalysts containing late transition metal elements. Relative to early metal catalysts, these systems have the potential to yield polymers with different microstructures and should be less oxophilic and therefore more tolerant of functionalized monomers. Currently, well-defined catalysts based on complexes of cobalt,[2-4] rhodium,[5,6] nickel,[7-24] palladium,[8,25,26] platinum,[6] and iron[27-29] have been reported to polymerize olefins.

Scheme 3.1. (α-Diimine)Ni(II) and Pd(II) olefin polymerization catalysts/catalyst precursors.

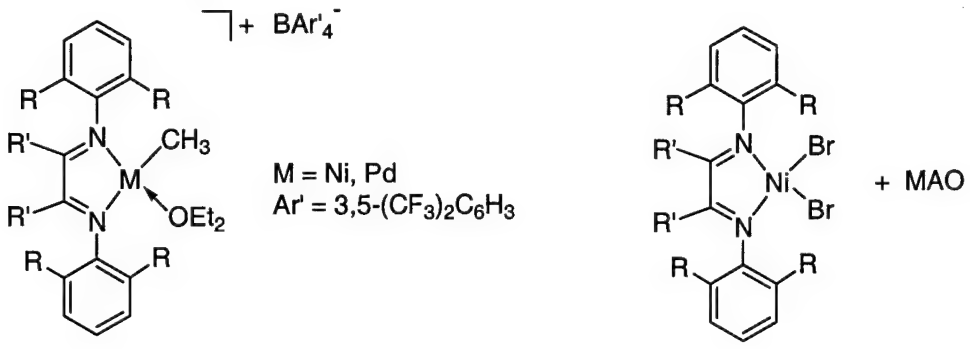

I **II**

A major focus of our work has involved the development of olefin polymerization catalysts based upon cationic α-diimine complexes of nickel and palladium of general structure **I**, the first report of which appeared in 1995.[8,9] Alternatively, active catalysts may be readily generated and used in situ by reaction of dibromide **II** and methylaluminoxane (MAO). Subsequently, other groups have reported olefin polymerizations using identical or closely related catalyst systems.[17,19-23] These catalysts polymerize ethylene and α-olefins to high molecular weight polymer with activities of the nickel(II) system comparable to early metal systems. Dramatic differences in the microstructure and properties of polymers made using these nickel- and palladium-based catalysts are observed as

compared to polymers made using early metal Ziegler-Natta and metallocene technology. For example, branching in polyethylene prepared with nickel(II)- or palladium(II)-based catalysts can vary from highly branched to linear and the properties thus vary from rigid plastics to soft elastomers. The polymer properties observed are greatly dependent on reaction conditions, ligand structure and the metal. For example, catalysts lacking bulky substituents in the ortho aryl positions have been found to oligomerize ethylene selectively to α-olefins.[11,12] Furthermore, bulky nickel(II) catalysts have been shown to catalyze the living polymerization of α-olefins (i.e. propylene, 1-hexene, etc.) at -10 °C, and thus provide access to diblock and multiblock copolymers. Palladium-based catalysts have proven to be tolerant of certain functional groups and will copolymerize alkyl acrylates with ethylene and α-olefins.[25,26] Recently, internal olefins such as cyclopentene have been polymerized with both nickel- and palladium-based catalysts forming unique high molecular weight poly(cyclopentene) with 1,3-enchainment via an addition mechanism rather than expected 1,2-enchainment.[13]

A general mechanism for the polymerization has been proposed and is shown in Scheme 3.2. The catalyst resting state for the Pd(II) systems is the alkyl olefin complex **A** as established by ^{1}H NMR spectroscopy.[8,30] The same resting state appears to apply in the Ni(II) systems at low temperature.[31] The turnover limiting step is the migratory insertion reaction to yield an intermediate cationic alkyl complex **B**. This species has been shown to be a β-agostic species in the Pd(II) systems,[13,30] but for simplicity is shown in Scheme 3.2 without the M-β-H-C interaction. Metal migration (chain running) along the alkyl chain can occur in these species via β-H elimination/readdition reactions (to **C** and **D**) as shown in Scheme 3.2.[8,9,26,30] (A similar proposal was made by Fink to account for structures of 1-hexene oligomers from certain Ni(II) catalysts).[14,15] These migration reactions occur without chain transfer. Successive migratory insertion and ethylene trapping cycles from **A** leads to linear polymer. Insertion following chain running leads to the introduction of branches in the polymer chain. The greater the extent of chain running prior to insertion the more highly branched the polymer.[8,9,32] In

the case of nickel, trapping and insertion are competitive with chain running and thus the extent of branching is sensitive to ethylene pressure, decreasing with increasing ethylene pressure.

Scheme 3.2. Proposed mechanism of propagation for the preparation of branched polyethylene using Ni(II) catalysts.

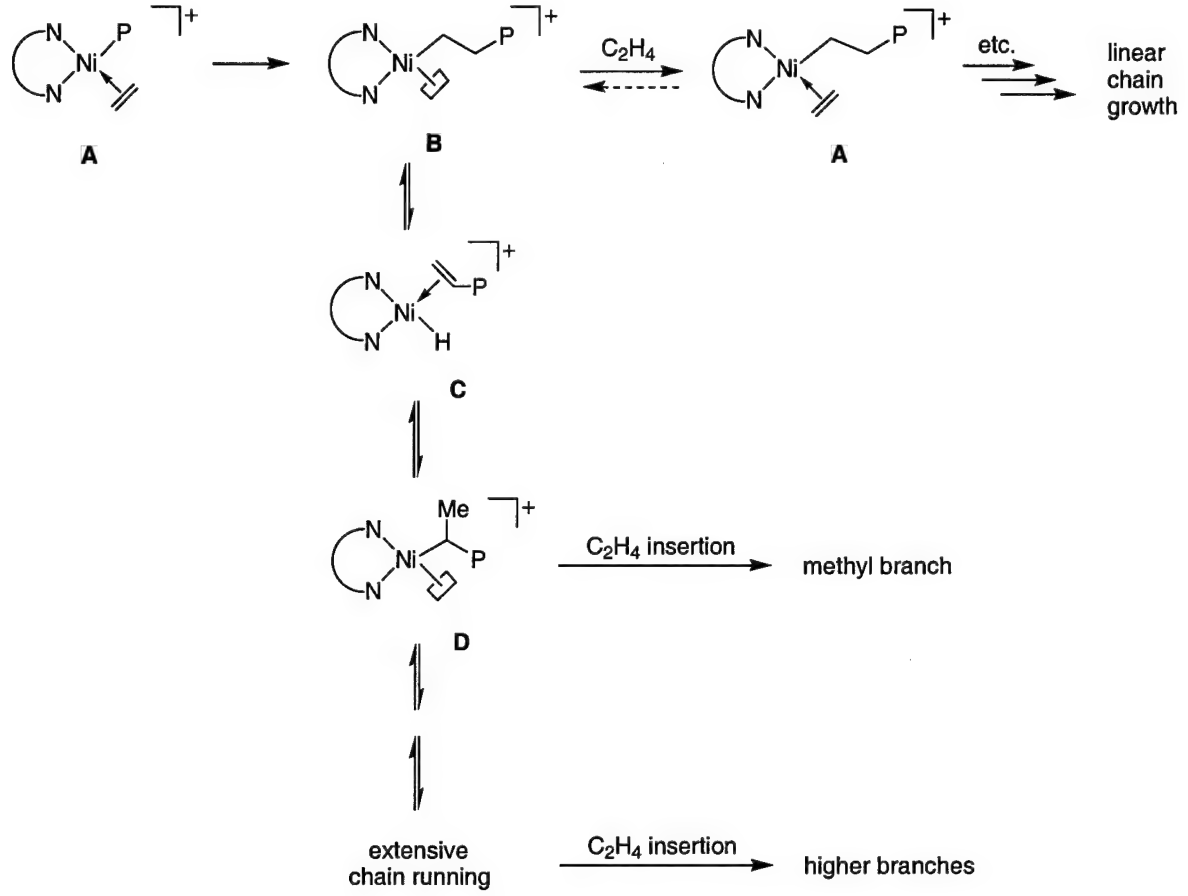

A critical feature of these catalysts is that, unlike most late metal systems, the rate of chain transfer (k_{ct}) is much slower than the rate of propagation (k_p) and thus high polymer results from polymerization of ethylene and α-olefins. The key feature leading to slow chain transfer is the presence of bulky ortho aryl substituents which are situated above and below the axial positions of the square planar complex. Generally, the more sterically encumbering the substituents, the higher the polymer molecular weights (i.e. the greater k_p/k_{ct}). Initially, the slow rate of chain transfer was ascribed to a slow associative displacement of the unsaturated polymer chain as a result of the bulky ortho substituents blocking axial approach of the monomer (see Scheme 3.3). Recent calculations by

Ziegler et al. have suggested that chain transfer occurs by direct β-H transfer to monomer in the alkyl olefin resting state **A** and that this barrier increases with increasing steric bulk of the ortho substituents.[33,34] Currently, no firm experimental evidence is available which distinguishes these mechanisms. Several other theoretical analyses of these systems have appeared which agree in large measure with the mechanistic details derived from our experimental studies.[35,36]

Scheme 3.3. Proposed mechanisms of chain transfer.

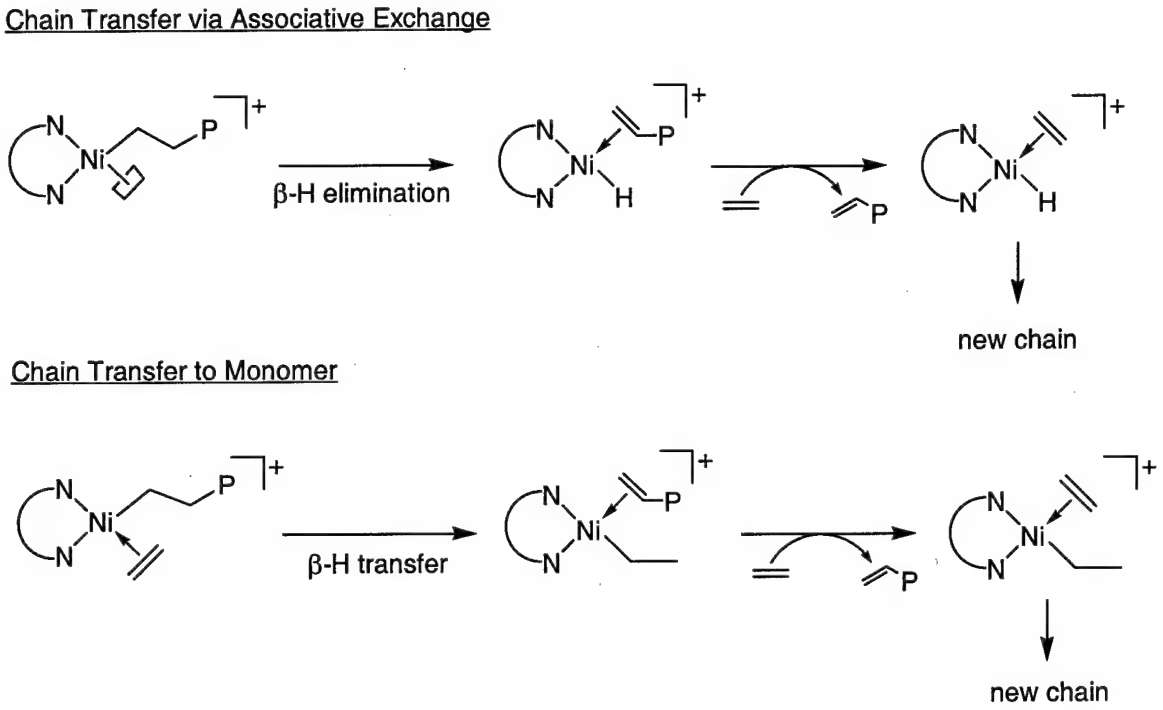

In this chapter, as follow-up work to the initial communication,[8] we report on our detailed investigations of the polymerization of ethylene using (α-diimine)nickel(II) catalysts. In order to gain more insight into the factors controlling the activity of the catalysts and the effect of catalyst structure on polymer structure and properties, we have examined several aryl-substituted α-diimine systems with variable ortho substituents including *i*-propyl, methyl, trifluoromethyl, and pentafluorophenyl groups as well as variations in substitution at the backbone carbon atoms of the α-diimine ligand. The effect of temperature and ethylene pressure on activity and polymer microstructure, and the effect of catalyst structure on chain transfer and catalyst lifetime will also be presented.

Results and Discussion

A. Synthesis of α–Diimine Ligands and Corresponding Ni(II) Bromide Complexes.

The α-diimine ligands and the corresponding Ni(II) dibromide complexes prepared for study are summarized in Schemes 3.4 and 3.5, respectively. Compounds **1e-g** are known[37] and certain aspects of the polymerization behavior of activated complexes **4f** and **4g** have been previously reported by us.[8] Compounds **1e-g**, **2**, and **3** were prepared using the formic acid catalyzed condensation of the appropriate aniline with the corresponding diketone in methanol. These conditions were not optimal for the preparation of α-diimines containing electron-withdrawing groups. Thus, **1a-d** were prepared by the reaction of diketone with amine in the presence of catalytic amounts of H_2SO_4 in toluene with removal of water by azeotropic distillation. We have fully characterized the previously unknown ligands by ^1H, ^{13}C, and where appropriate, ^{19}F NMR spectroscopy as well as elemental analysis. Compounds **1a-d** exhibit a complex fluxional behavior in solution which involves interconversion between (*E*, *E*) and (*E*, *Z*) forms as well as net rotation about the carbon-nitrogen aryl bond to interconvert syn and anti forms (see Chapter 4). A complete analysis of this fluxional behavior is beyond the scope of this work but similar behavior has been reported.[37] Interestingly, **2** was isolated and characterized spectroscopically not as the α-diimine, but rather as the imine/enamine tautomer. This tautomerization has also been observed for a similar compound which was reported by van Asselt and co-workers,[37] as well as a β-diimine ligand reported by Feldman et. al.[16]

Scheme 3.4. Structures of α-diimine ligands **1-3**.

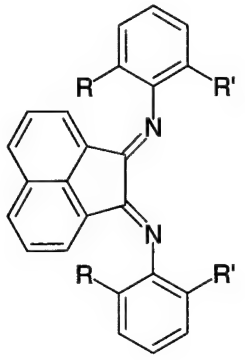

	R	R'
1a	CF_3	H
1b	CF_3	Me
1c	C_6F_5	H
1d	C_6F_5	Me
1e	Me	H
1f	Me	Me
1g	^{i}Pr	^{i}Pr

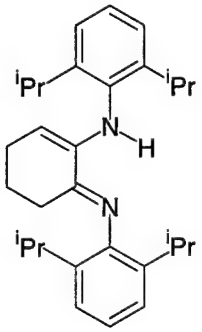

2

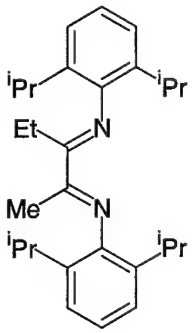

3

As previously reported, the nickel(II) dibromide complexes were readily obtained from reaction of the α-diimine with (DME)$NiBr_2$.[38] Characterization of these complexes was difficult because of their poor solubility in organic solvents, and the fact that they are paramagnetic, and thus high resolution NMR spectroscopic analysis is not possible. Fortunately, crystals of **4c** and **4d** which were suitable for X-ray diffraction analysis were obtained by slow diffusion of pentane into a dichloromethane solution of the Ni(II) complexes.

Scheme 3.5. Structures of (α-diimine)$NiBr_2$ complexes **4-6**.

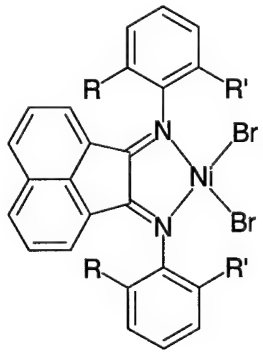

	R	R'
4a	CF_3	H
4b	CF_3	Me
4c	C_6F_5	H
4d	C_6F_5	Me
4e	Me	H
4f	Me	Me
4g	^{i}Pr	^{i}Pr

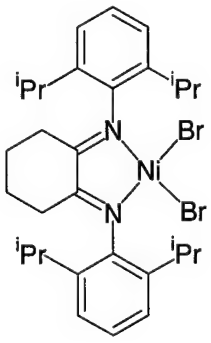

5

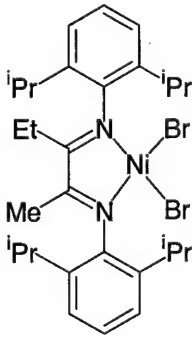

6

The crystal structure of **4c** (Figure 3.1) with a 2-pentafluorophenyl substituent crystallized with two molecules of water coordinated to nickel, making this a six-coordinate octahedral complex. As in

related structures,[17,37] the aryl rings of the α-diimine lie nearly perpendicular to the plane formed by the metal and coordinated nitrogen atoms. Of particular note is the C_2 symmetry of the complex about the nickel atom, with the pentafluorophenyl rings in an anti conformation above and below the coordination plane. Similarly, complex **4d** (Figure 3.2) crystallizes with the pentafluorophenyl rings in the anti conformation, but in this case no water was coordinated to the tetrahedral nickel center. However, in both cases, this does not preclude the alternative conformation in which the pentafluorophenyl groups are in a syn conformation. In both structures, the pentafluorophenyl rings are oriented with the face of each ring directed approximately over the axial sites of the nickel atom.

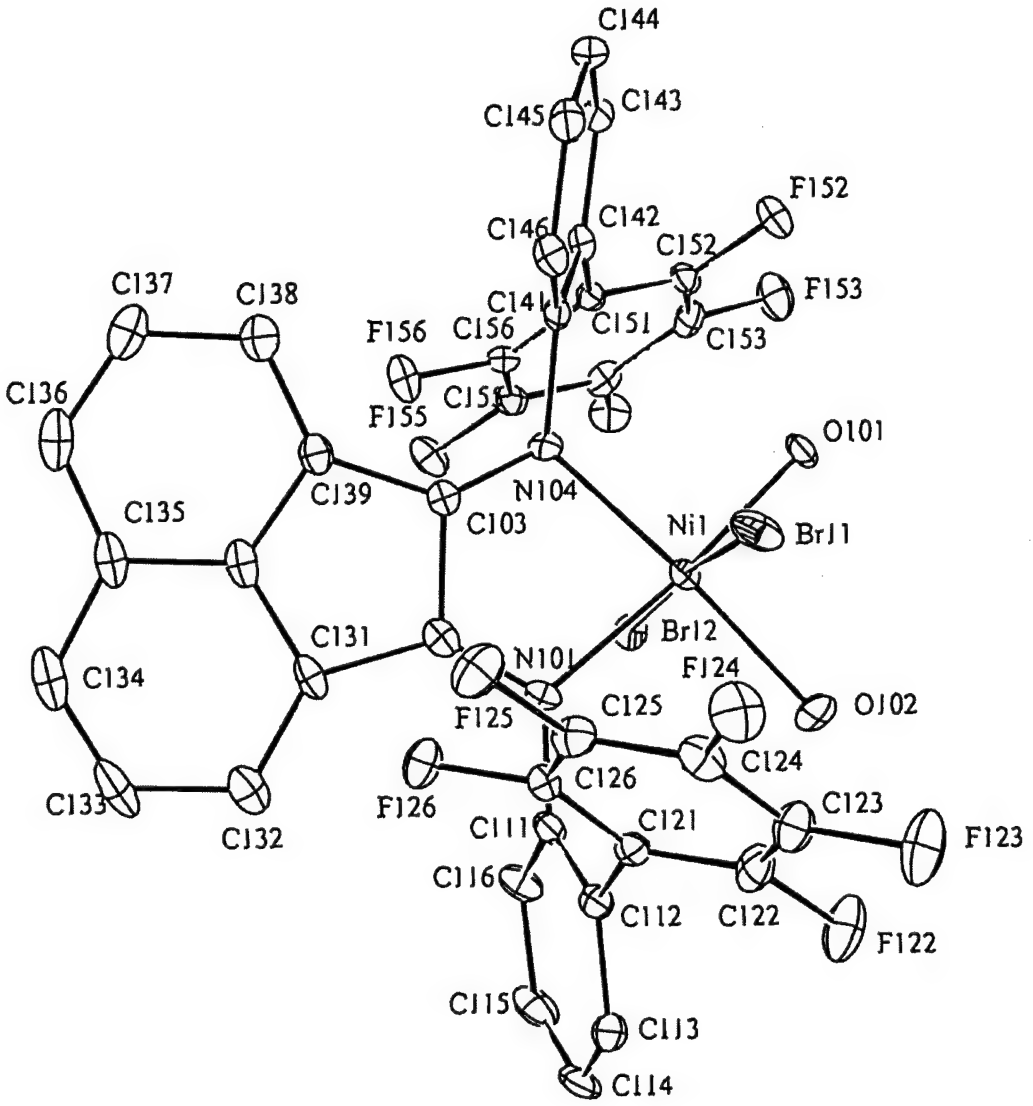

Figure 3.1. Molecular structure of **4c**. Selected bond lengths (Å) and angles (°): Ni(1)-Br(11) 2.493(1), Ni(1)-Br(12) 2.612(8), Ni(1)-O(101) 2.063(3), Ni(1)-O(102) 2.100(3), Ni(1)-N(101) 2.109(4), N(101)-C(102) 1.283(6), C(102)-C(103) 1.515(7), C(103)-N(104) 1.280(6), Ni(1)-N(104) 2.093(4), Br(11)-Ni(1)-Br(12) 174.41(3), N(101)-Ni(1)-N(104) 80.3(1), Ni(1)-N(101)-C(102) 111.0(3), N(101)-C(102)-C(103) 134.9(5), C(102)-C(103)-N(104) 117.6(4), C(103)-N(104)-Ni(1) 112.1(3).

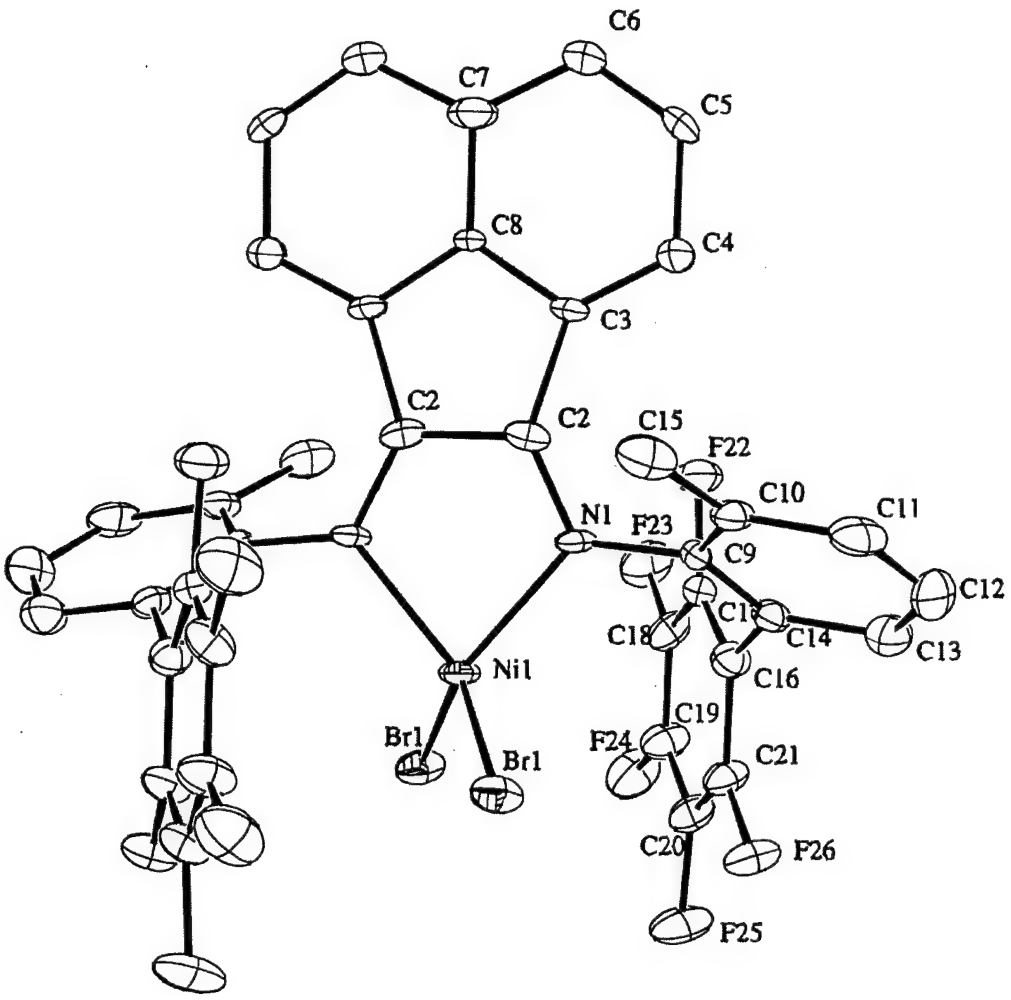

Figure 3.2. Molecular structure of **4d** (Molecule 1). Selected bond lengths (Å) and angles (°): Molecule 1: Ni(1)-Br(1) 2.323(1), Ni(1)-N(1) 2.025(7), N(1)-C(2) 1.296(11), C(2)-C(2)a 1.48(2), Br(1)-Ni(1)-Br(1)a 117.43(7), N(1)-Ni(1)-N(1)a 82.4(3), Ni(1)-N(1)-C(2) 111.6(6), N(1)-C(2)-C(2)a 117.2(7); Molecule 2: Ni(2)-Br(2) 2.288(1), Ni(2)-N(31) 2.013(6), N(31)-C(32) 1.279(11), C(32)-C(32)b 1.47(2), Br(2)-Ni(2)-Br(2)b 123.44(8), N(31)-Ni(2)-N(31)b 83.0(3), Ni(2)-N(31)-C(32) 110.6(5), N(31)-C(32)-C(32)b 117.7(7).

B. Polymerization Experiments at 35 °C.

While well-defined catalysts of the type $[(\alpha\text{-diimine})Ni(CH_3)(solvent)]^+ BAr'_4^-$ (Ar' = 3,5-$(CF_3)_2C_6H_3$) can be prepared, these salts are exceedingly sensitive to moisture, air and heat.[8] A much more convenient method for generation of catalysts involves in situ activation of the Ni(II) dibromide complexes with methylalumoxane (MAO) or its derivatives.[8,9] In this study, we have consistently employed modified methylalumoxane (MMAO, see Experimental Section for details) as the activator.

In order to make meaningful comparisons of the effect of catalyst structure on catalyst activity and polymer structure and properties, all data were collected under similar conditions. A temperature of 35 °C was chosen for the initial polymerization experiments because of the ease in maintaining constant temperature in both the ambient pressure runs and, more importantly, the high pressure runs. The reactions at high ethylene pressures are observed to exotherm rapidly as the reactor is pressurized and throughout the polymerization run. Thus, a reaction starting at room temperature (25 °C) can rapidly warm to >60 °C throughout a 10-20 min experiment without efficient cooling. The most reproducible temperatures for runs conducted at 35 °C were obtained when the reactor was initially stabilized at 27 °C; upon addition of the activator (MMAO), and the catalyst, and subsequent pressurization with ethylene, the temperature in the reactor then rapidly rose to 35 °C within ca. 30 seconds, where it could be maintained by cooling with an ice-cooled water circulator for the rest of the run (10 or 20 min).

1. Effects of Varying Ligand Structure on Catalyst Activity and Polymer Properties.

The results for ethylene polymerization experiments conducted at 1 atm ethylene pressure and 35 °C are shown in Table 3.1, and polymerizations run at 35 °C and 200 psig ethylene pressure (ca. 15 atm) are summarized in Table 3.2. Reactions run at 1 atm ethylene pressure suffer from monomer mass transport limitations at this low ethylene concentration,[39] and therefore accurate comparisons of catalyst turnover frequencies are difficult under these conditions. Monomer mass transport is not a factor when the ethylene pressure is raised to 200 psig, and thus a more accurate determination of the high turnover frequencies attainable by these catalysts is possible. In addition, a comparison of trends in turnover frequencies for these catalysts can be made at this pressure.

A striking feature observed in the data is that the catalysts with only one aryl ortho substituent R [R = CF_3 (**4a**), C_6F_5 (**4c**), CH_3 (**4e**); Table 3.1, entries 1, 3 and 5] do not yield high molecular weight polymer, but instead produce oligomers for which olefinic endgroups could be detected by ^1H NMR spectroscopy (% α-olefin: **4a**, 55%; **4c**, 35% **4e**, 37%). Integration of the olefinic ^1H resonances with respect to the methylene resonances gave degrees of polymerization (DP) less than 150.

Table 3.1. Polymerization Data for 1 Atmosphere Runs at 35 °C.

entry	catalyst	mol cat (X 10^6)	temp (°C)	reaction time (min)	TOF (x10^{-3}/h)	M_n[a]	PDI	branches per 1000 carbons	thermal transitions (°C)	
									T_g	T_m
1	**4a**	2.0	30	30	150	4100[b]	-	31[c]	-	92,107
2	**4b**	2.0	35	30	45	240000	2.5	75	-40	56
3	**4c**	2.8	35	20	4	1020[b]	-	29[c]	-	-
4	**4d**	3.7	35	20	5	41400	4.4	34	-	107
5	**4e**	10	35	30	8	920[b]	-	3[c]	-	-
6	**4f**	2.0	35	30	24	14300	1.8	67	-44	29,60
7	**4g**	1.6	35	30	56	125000	1.8	106	-	- 17
8	**5**	1.8	35	30	30	268000	1.5	108	-	- 8
9	**6**	1.8	35	30	15	171000	1.6	101	-52	-2

a) Molecular weights of the polymers were determined by GPC (using a universal calibration) in trichlorobenzene at 135 °C. b) Molecular weights of low molecular weight samples were determined by end-group analysis using ^{1}H NMR spectroscopy. c) Branching numbers for low molecular weight samples (M_n<5000) were corrected for endgroups.

When a methyl substituent is introduced into the remaining ortho position of these catalysts the molecular weight increases dramatically (see Table 3.1). For example, comparing **4a** (2-CF_3) with **4b** (2-CF_3-6-CH_3) the M_n increases from 4,100 to 240,000. Similar trends are noted for **4c** (2-C_6F_5) versus **4d** (2-C_6F_5-6-CH_3) (M_n = 1,020 and 41,400, respectively) and **4e** (2-CH_3) versus **4f** (2,6-$(CH_3)_2$) (M_n = 920 versus 14,300). Polymerizations carried out at 200 psig ethylene pressure and 35 °C (Table 3.2) exhibit similar trends. For example, **4a** yields polyethylene with M_n = 3,800 while **4b** yields polyethylene with M_n = 400,000. Similarly, molecular weights of polyethylenes formed by catalysts **4d** and **4f** under these conditions were significantly higher than polyethylenes prepared with **4c** and **4e**, respectively. These observations are all in accord with our previous observation that increased steric bulk in the axial sites will lead to a decrease in the rate of chain transfer relative to the rate of propagation.

Table 3.2. Summary of Polymerization Data for 200 Psig Runs at 35 °C.

entry	catalyst	mol cat (X 10^6)	temp (°C)	pressure (psig)	reaction time (min)	TOF (X 10^{-3}/h)	M_n[a]	PDI	branches per 1000 carbons	thermal transitions (°C)
1	**4a**	1.1	35	200	20	1100	3800[b]		5[c]	125 (T_m)
2	**4b**	2.0	35	200	20	500	400000	3.3	27	127 (T_m)
3	**4c**	1.7	35	200	20	650	970[b]		5[c]	-
4	**4d**	0.5	35	200	20	1100	73700	2.6	4	134 (T_m)
5	**4e**	5.0	35	200	20	230	1300[b]		2[c]	-
6	**4f**	1.5	35	200	10	1600	59200	2.5	13	128 (T_m)
7	**4g**	0.83	35	200	10	2400	337000	1.8	24	110 (T_m)
8	**5**	0.89	35	200	10	1600	844000	1.7	39	100 (T_m)
9	**6**	0.95	35	200	10	900	766000	1.7	28	96 (T_m)

a) Molecular weights of the polymers were determined by GPC (using a universal calibration) in trichlorobenzene at 135 °C. b) Molecular weights of low molecular weight samples were determined by end-group analysis using ^{1}H NMR spectroscopy. c) Branching numbers for low molecular weight samples (M_n<5000) were corrected for endgroups.

It is significant to note that the molecular weight distributions of polyethylene formed by **4b** and **4d** at 1 atm ethylene pressure are 2.5 and 4.4, respectively, which are substantially broader than the polydispersities produced by the other catalysts. A possible explanation for this broadening is that two isomers of complexes **4b** and **4d** are present: a C_2 symmetric form, and a C_S symmetric form. Species of both symmetries may be formed when the nickel complexes are synthesized,[40] thus the broadening of the molecular weight distribution may be attributable to the presence of more than one type of catalyst in solution (see Chapter 4 for further discussion). However, it was not possible to resolve a bimodal feature by GPC and we have no additional evidence for a two-site catalyst system.

The measured turnover frequencies (TOFs) of these catalysts are affected by several variables and are often difficult to interpret.[41] For example, for highly active catalysts, mass transfer limitations may apply and at 1 atm ethylene pressure it is clear that these effects do limit observed turnover frequencies of the active catalysts in Table 3.1. Catalyst instability can reduce calculated TOFs in

runs over extended time periods or at high temperatures (see below) relative to conditions where no catalyst decay occurs. In cases where insoluble polymer is formed, TOFs often fall when catalysts become heterogeneous due to precipitation. In addition, of course, TOFs are affected by electronic[12] and steric effects of substituents. Under conditions reported in Table 3.2 (low catalyst loading, 200 psig, 35 °C, short reaction time) previous experiments,[42] together with those discussed below suggest that mass transfer limitations do not apply, the catalyst resting state is the nickel alkyl ethylene complex, and catalysts are stable over these time periods at 35 °C. Thus, the observed differences in TOFs in Table 3.2 can be largely attributed to substituent effects.

The basic trend observed, consistent with previous observations, is that increases in the bulk of the ortho substituents result in increased TOFs. For example, the TOF of **4g** (2,6-$^{i}Pr_2$) is 2.4 X 10^6 hr^{-1} compared to the less bulky **4f** (2,6-Me_2) of 1.6 X 10^6 hr^{-1}. Consistent with this trend the TOF of the mono-methyl substituted catalyst, **4e** drops to 2.3 X 10^5 hr^{-1}. Similarly, the TOF of **4d** (2-C_6F_5-6-CH_3) of 1.1 X 10^6 hr^{-1} is about twice that of the TOF of the less bulky **4c** (2-C_6F_5) of 6.5 X 10^5 hr^{-1}. The one catalyst pair which exhibits the opposite trend is **4a** (2-CF_3) with a measured TOF of 1.1 X 10^6 hr^{-1} versus **4b** (2-CF_3-6-CH_3) with a TOF of 5.0 x 10^5 hr^{-1}. A possible explanation here may involve the rapid precipitation of the high molecular weight polymer formed by **4b** and thus, even under these conditions, reduction of the measured TOF due to precipitation.

The mono-CF_3 substituted catalyst **4a** is considerably more active than the mono-CH_3 system **4e** (1.8 X 10^6 hr^{-1} vs. 2.3 X 10^5 hr^{-1} TOF). While part of the explanation may be steric, the fairly similar sizes of -CF_3 versus -CH_3 groups suggests also that the electron-withdrawing nature of the -CF_3 group may increase the TOF. This result is consistent with substituent effects noted in ethylene oligomerization reactions.[12]

Since the catalyst resting state under these conditions is the alkyl olefin complex, the TOFs (assuming no complications as enumerated above) will simply be the rate of migratory insertion. The

fact that bulkier substituents accelerate this rate can be ascribed to more relief of strain in going from the more crowded ground state alkyl olefin complex to the less crowded transition state.[34]

A strong correlation exists between the magnitude of steric bulk exerted by the ortho substituents and the degree of branching observed in the resulting polymers. The branching numbers for polyethylene can be determined by ^{1}H NMR spectroscopy using the ratio of the number of methyl groups to the overall number of carbons (e.g. methyl + methylene + methine),[43] and are reported as branches per thousand carbons.

In general, the branching numbers were observed to increase with more steric bulk (Table 3.1). For example, in experiments run under 1 atm ethylene pressure, the branching number determined for polyethylene prepared using catalyst **4f** is 67, whereas 106 branches were observed when bulkier **4g** was employed. In addition, a comparison of the branching numbers for the series of catalysts with single substituents in the 2- position of the aryl rings (i.e. **4a**, **4c**, and **4e**) and catalysts containing substituents in the 2- and 6-positions (i.e. **4b**, **4d**, and **4e**), shows that the branching is consistently higher for the latter catalysts. For example, catalyst **4a** (2-CF_3) yields polyethylene with 31 branches per thousand carbons whereas the bulkier catalyst **4b** (2-CF_3-6-CH_3) affords polyethylene with 75 branches per thousand carbons.

These observations suggest that trapping of the intermediate alkyl cation (e.g. **B**, Scheme 3.2) by ethylene is slowed by bulky substituents more than the rate of chain running. Thus, more chain running and branching can occur in the catalysts that bear bulky substituents relative to those which possess less bulky substituents. The same trend is also noted in the 200 psig polymerizations (Table 3.2); however, at this increased pressure branching is reduced for all catalysts since the rate of trapping and insertion is now faster for all catalysts. This feature will be further illustrated and discussed below.

In a previous communication, we reported that changes to the α-diimine backbone can have a remarkable effect on polymer microstructure and catalyst activity.[8] We have investigated this

backbone effect further using complexes **4g**, **5**, and **6**, all of which contain the same bulky 2,6-diisopropylphenyl groups as imine substituents. Complex **4g** contains a planar acenapthyl backbone, whereas the other two catalysts **5** and **6** contain saturated alkyl groups as substituents on the backbone carbons. All three catalysts are very active polymerization catalysts (entries 7-9, Tables 3.1 and 3.2) with turnover frequencies on the order of 10^5/hr at 1 atm and 10^6/hr at 200 psig. Catalyst **4g** exhibits a slightly higher turnover frequency (2.4 X 10^6/h at 200 psig) than **5** and **6** (1.6 X 10^6 and 9.0 X 10^5/h respectively).

Although the turnover frequencies are higher for **4g**, the molecular weights of polyethylene produced with catalyst **4g** are less than the molecular weights for polyethylene produced with catalysts **5** and **6**. For example, for polymerization experiments conducted at 200 psig, the molecular weight (M_n) of polymer generated from catalyst **4g** was 337,000 whereas from catalysts **5** and **6** the molecular weights were 844,000 and 766,000 respectively. A significant effect of the alkyl substituted backbone is that the molecular weight distributions of the polyethylene are significantly less than those of the planar acenapthyl systems. This effect on molecular weight distributions can be seen clearly in Figure 3.3, which shows the GPC chromatograms for polyethylene produced with catalysts **4g**, **5** and **6** at one atmosphere and 35 °C. The polydispersity of polyethylene formed with catalysts **5** (Figure 3.3b) and **6** (Figure 3.3c) are 1.5 and 1.6 respectively (1 atm ethylene, 35 °C) compared with 1.8 for polymer produced by **4g** (Figure 3.3a) under identical conditions. When the ethylene pressure is raised to 200 psig, polydispersities increase slightly, but still remain below 2.0. The fact that molecular weight distributions remain below 2 under these conditions implies that the M_n values are not yet limited by chain transfer and longer reaction times would produce higher molecular weight materials.

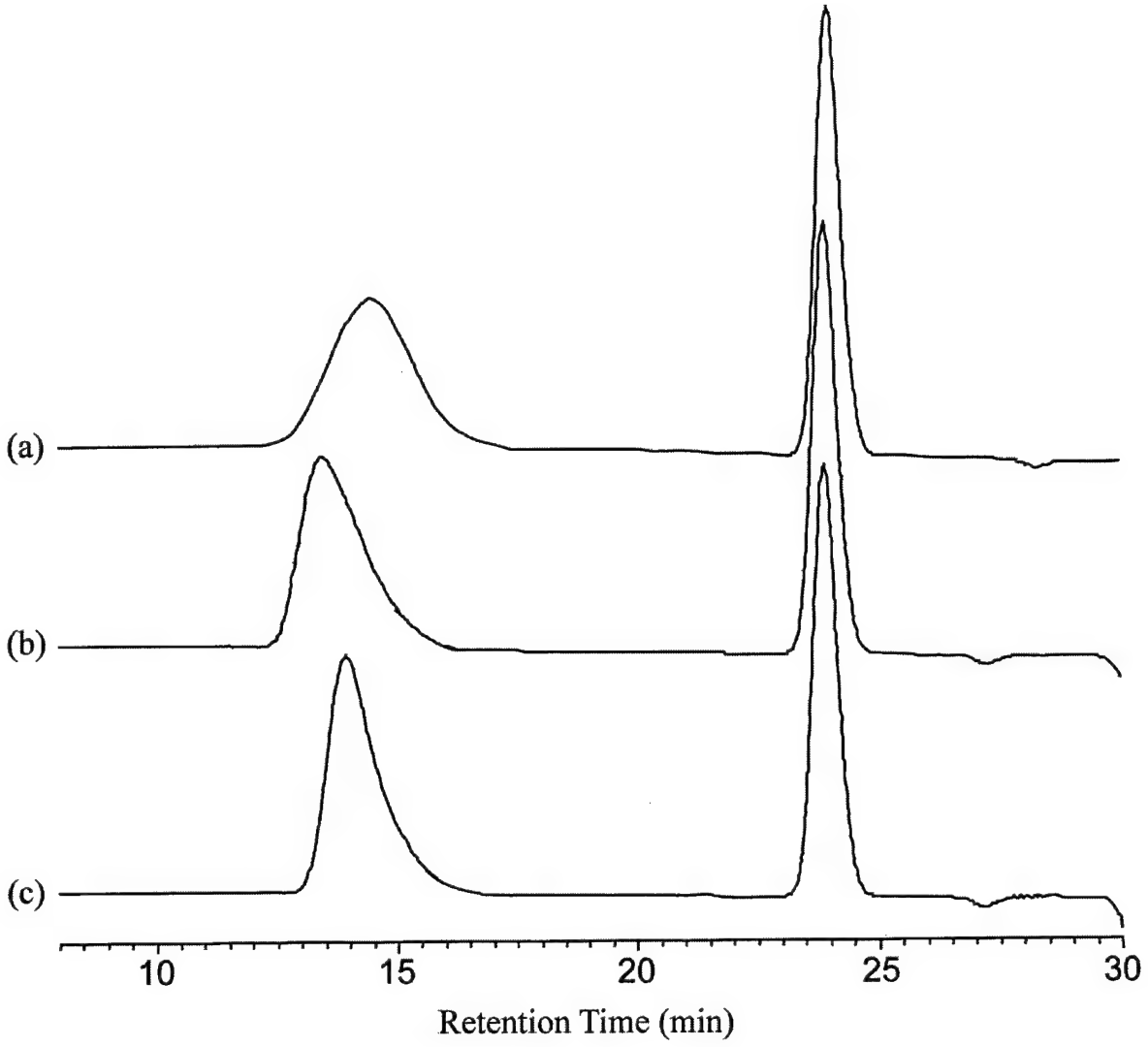

Figure 3.3. GPC chromatograms of polyethylene produced at 35 °C and 1 atm (ethylene) using catalyst: (a) **4g**, (b) **5**, (c) **6**.

2. Effects of Changes in Ethylene Pressure on Polymer Properties

A series of polymerization experiments in which the ethylene pressure was varied, but the temperature held at 35 °C, is summarized in Table 3.3. This data can be compared to that in Table 3.1 for polymerizations carried out at 1 atm ethylene pressure. The most significant effect noted in these studies is a trend towards more linear, less branched polymers as the ethylene pressure is increased. For example, catalyst **4f** (2,6-$(CH_3)_2$) exhibits 67 branches per thousand carbons at 1 atm which drops to 13 branches per throusand carbons at 200 psig and to ca. 5 branches per thousand

carbons at 600 psig ethylene. Melting points (T_m's) determined using DSC range from 60 °C (a broad transition) to 132 °C (sharp transition) for these branching numbers. Similarly, catalyst **5** yields polyethylene containing 108 branches per thousand carbons at 1 atm ethylene, 39 branches per thousand carbons at 200 psig and 11 branches per thousand carbons at pressures of 400 and 600 psig. T_m values for these likewise increase with decreasing branching. Catalyst **4b** (2-CF_3-6-CH_3) yields polyethylene with 75 branches per thousand carbons at 1 atm ethylene, 27 branches per thousand carbons at 200 psig and 5-7 branches per thousand carbons at 400 psig and 600 psig. An unusual feature of the polyethylene made at 200 psig is that despite having 27 branches per thousand carbons, the T_m is remarkably high (127 °C) in comparison to the other polyethylene samples with similar branching numbers (compare entry 4 with entry 22).

The trend of decreased branching with increasing ethylene pressure in these cases reinforces our earlier observations. In essence, chain running originates from the cationic alkyl complex (**B**; Scheme 3.2; see Chapter 7 for further discussion) and the lifetime of this complex (and thus the extent of chain running) is decreased as ethylene concentration increases. The rate of insertion (chain growth) will either be *independent* of ethylene pressure if the resting state is predominantly the alkyl olefin complex (**A**; Scheme 3.2) or *increase* with ethylene pressure if a significant fraction of the catalyst rests as the cationic alkyl complex (e.g., if the polymerization is mass transfer limited).

There is little variation of molecular weight with ethylene pressure for individual catalysts. The small variations observed are likely due to variations in experimental conditions (e.g., polymer precipitation and variable extent of catalyst decay) since no clear trend is observed as pressure is varied. The trends apparent in comparing different catalysts are consistent with the discussions above for the 1 atm results; that is, increasing steric bulk of ortho substituents results in increasing polymer molecular weight. For catalyst **6**, M_n values reach 1 X 10^6 and are not yet limited by chain transfer processes since M_w/M_n values are still below 2.

Table 3.3. The Effect of Pressure on Polymer Activity and Properties.

entry	catalyst	mol cat (X 10^6)	temp (°C)	pressure (psig)	reaction time (min)	TOF (X 10^{-3}/h)	M_n[a]	PDI	branches per 1000 carbons	thermal transitions (°C)
1	**4a**	1.1	35	200	20	1100	3800[b]		5[c]	125 (T_m)
2	**4a**	0.8	35	400	20	1300	4100[b]		4[c]	131 (T_m)
3	**4a**	0.8	35	600	20	2800	4000[b]		2[c]	129 (T_m)
4	**4b**	2.0	35	200	20	500	400000	3.3	27	127 (T_m)
5	**4b**	2.0	35	400	20	560	533000	2.8	5	130 (T_m)
6	**4b**	2.0	35	600	20	1000	314000	3.7	7	131 (T_m)
7	**4c**	1.7	35	200	20	650	970[b]		5[c]	-
8	**4c**	1.8	35	400	20	970	715[b]		3[c]	-
9	**4c**	1.9	35	600	20	1600	776[b]		2[c]	-
10	**4d**	0.5	35	200	20	1100	73700	2.6	4	134 (T_m)
11	**4d**	0.5	35	400	20	1300	94000	2.2	1	137 (T_m)
12	**4d**	0.5	35	600	20	1200	90300	2.3	1	138 (T_m)
13	**4f**	1.5	35	200	10	1600	59200	2.5	13	128 (T_m)
14	**4f**	1.5	35	400	10	1900	64400	2.2	12	126 (T_m)
15	**4f**	1.5	35	600	10	2500	59300	2.6	5	132 (T_m)
16	**4g**	0.83	35	200	10	2400	337000	1.8	24	110 (T_m)
17	**4g**	0.83	35	400	10	3700	226000	2.4	19	106 (T_m)
18	**4g**	0.81	35	600	10	3000	318000	2.4	17	119 (T_m)
19	**5**	0.89	35	200	10	1600	844000	1.7	39	100 (T_m)
20	**5**	0.85	35	400	10	2800	1010000	1.7	11	108 (T_m)
21	**5**	0.91	35	600	10	2600	799000	1.9	11	114 (Tm)
22	**6**	0.95	35	200	10	900	766000	1.7	28	96 (T_m)
23	**6**	0.86	35	400	10	2000	1030000	1.6	12	105 (T_m)
24	**6**	0.86	35	600	10	2300	1000000	1.6	15	105 (T_m)

a) Molecular weights of the polymers were determined by GPC (using a universal calibration) in trichlorobenzene at 135 °C. b) Molecular weights of low molecular weight samples were determined by end-group analysis using ^{1}H NMR spectroscopy. c) Branching numbers for low molecular weight samples (M_n<5000) were corrected for endgroups.

C. Polymerization Experiments at Higher Temperatures

The experiments described above have all been carried out at 35 °C. In this section we report polymerizations at higher temperature and the impact of increasing temperature on catalyst activities and lifetimes as well as on polymer branching and molecular weights.

In general, at 60 °C and above catalyst lifetimes are sufficiently short that they have a significant impact on the total turnovers (TON, turnover number) which can be achieved over 10-30 min time periods. While a decrease in ethylene solubility at increased temperatures may play a role, it is clear that the major effect on the total turnover number is catalyst decay. Table 3.4 reports polymerizations carried out at 1 atm ethylene pressure and temperatures of 35 °C, 60 °C and 85 °C. For catalyst **4b** (2-CF_3-6-CH_3) the TON calculated for a 30 min run decreases from 23,000 at 35 °C to 3,800 at 60 °C. At 85 °C, catalyst decay is sufficiently rapid that no polymer is isolated. Similar behavior is observed for **4g**, **5**, and **6** except that at 85 °C some activity is observed for these catalysts.

Table 3.5 reports polymerizations run under 200 psig ethylene pressure and at 35 °C, 60 °C and 85 °C. At 200 psig ethylene pressure, considerably higher TONs are achieved relative to 1 atm runs. In general, TONs at 60 °C decrease by a factor of 2 or less relative to those observed at 35 °C, but at 85 °C TONs drop off quite significantly. For example, for **4b** the TON decreases from 170,000 (20 min run) at 35 °C to 140,000 at 60 °C, but then drops to 30,000 at 85 °C. For **4d** (2-C_6F_5-6-CH_3) the TON increases to 950,000 at 60 °C from 430,000 at 35 °C then drops to 520,000 at 85 °C.

Table 3.4. Summary of 1 Atmosphere Runs at High Temperature.

entry	catalyst	mol cat (X 10^6)	temp (°C)	reaction time (min)	TON (X 10^{-3})	M_n[a]	PDI	branches per 1000 carbons	thermal transitions (°C)	
									T_g	T_m
1	**4b**	2.0	35	30	23	240000	2.5	75	-40	56
2	**4b**	2.0	60	30	3.8	56000	2.8	90	-44	-
3	**4b**	2.0	85	30	Decomp	N/A				
4	**4g**	1.6	35	30	28	125000	1.8	106	-	- 17
5	**4g**	1.6	60	30	17	48600	2.7	122	- 65	- 43
6	**4g**	1.6	85	30	5	27000	2.7	124	- 67	-
7	**5**	1.8	35	30	15	268000	1.5	108	-	- 8
8	**5**	2.1	60	30	10	139000	2.0	115	-60	-30
9	**5**	1.6	85	30	1.8	56000	1.9	136	-60	-
10	**6**	1.8	35	30	7.5	171000	1.6	101	-52	-2
11	**6**	2.1	60	30	5.5	129000	1.6	100	-40	-17
12	**6**	1.7	85	30	0.6	42000	2.2	112	- 53	- 17

a) Molecular weights of the polymers were determined by GPC (using a universal calibration) in trichlorobenzene at 135 °C.

Table 3.5. Summary of High Temperature Runs at 200 Psig.

entry	catalyst	mol cat (X 10^6)	temp (°C)	pressure (psig)	reaction time (min)	TON (X 10^{-3})	M_n[a]	PDI	branches per 1000 carbons	thermal transitions (°C)	
										T_g	T_m
1	**4b**	2.0	35	200	20	170	400000	3.3	27	-	127
2	**4b**	2.0	60	200	20	140	237000	3.3	46	-	102
3	**4b**	2.0	85	200	20	30	68000	4.4	52	-37	81
4	**4d**	0.5	35	400	20	430	94000	2.2	1	-	137
5	**4d**	0.5	60	400	20	950	53900	1.9	12	-	130
6	**4d**	0.5	85	400	20	520	29400	2.1	19	-	121
7	**4f**	1.5	35	200	10	270	59200	2.5	13	-	128
8	**4f**	1.5	60	200	10	150	22800	2.3	25	-	114
9	**4f**	2.0	85	200	10	25	12900	2.9	44	-	90, 114
10	**4g**	0.83	35	200	10	400	337000	1.8	24	-	110
11	**4g**	0.82	60	200	10	230	155000	1.8	58	-42	68
12	**4g**	0.82	85	200	10	70	62700	1.9	83	-45	24
13	**5**	0.89	35	200	10	270	844000	1.7	39	-	100
14	**5**	0.89	60	200	10	130	395000	1.7	60	-42	57
15	**5**	0.92	85	200	10	50	211000	1.8	93	-50	20
16	**6**	0.95	35	200	10	150	766000	1.7	46	-	96
17	**6**	0.83	60	200	10	100	331000	1.9	73	-44	54
18	**6**	0.92	85	200	10	10	196000	1.8	85	-49	23

a) Molecular weights of the polymers were determined by GPC (using a universal calibration) in trichlorobenzene at 135 °C.

The productivity of catalyst **5** was examined over 10 to 20 min reaction times at 60 °C and 85 °C at 200 psig (see Table 3.6). At 60 °C there is a significant increase in TON from the 10 min run (130,000) to the 20 min run (200,000) indicating that a significant fraction of the catalyst is still active after 10 min. However, at 85 °C the minor increase in TON at 20 min (64,000) relative to 10 min (53,000) reaction time indicates that most of the catalyst has deactivated after 10 min at 85 °C.

Table 3.6. Catalyst Lifetime of **5**/MMAO at High Temperature/Pressure.

Entry	mol cat (X 10^6)	temp (°C)	pressure (psig)	reaction time (min)	TON (X 10^{-3})	M_n	PDI	branches per 1000 carbons
1	0.89	60	200	10	129	395000	1.7	60
2	0.84	60	200	20	201	407000	1.8	71
3	0.92	85	200	10	53	211000	1.8	93
4	0.93	85	200	20	64	205000	1.8	93

The mode of catalyst decay is unknown. One possibility for decay is a C-H activation of an *ortho*-alkyl substituent.[44] Thus, our motivation for preparing catalysts containing *ortho*-C_6F_5 and -CF_3 substituents was the possibility that these catalysts would exhibit much higher stabilities than those possessing *ortho*-alkyl substituents. We have noted that TONs for polymerizations using catalyst **4d** (2-C_6F_5-6-CH_3) remain high for 20 min runs at 60 °C and 85 °C and 200 psig ethylene. However, we chose catalyst **4c** (2-C_6F_5) for stability studies since the low molecular weight polyethylene formed (M_n ca. 900) does not form insoluble polymer in the reactor and result in inactivity due to precipitation and inaccessibility of catalyst sites. The results of a set of experiments monitoring productivity over time periods from 20 min to 4 h are summarized in Table 3.7. At 35 °C and 200 psig ethylene pressure, the productivity increases essentially linearly with time (entries 1-5). Thus, under these conditions, very little catalyst decomposition is occurring over this time period. A similar set of experiments at 0 °C and 1 atm ethylene pressure (entries 6-10) shows that activity does begin to decrease after 3-4 h, suggesting that catalyst stability is greater at higher ethylene pressures for this catalyst system.

Table 3.7. Summary of Ethylene Polymerization Activity for **4c**/MMAO.[a]

entry	mol catalyst (X 10^6)	reaction time (min)	temp (°C)	ethylene pressure (atm)	TON (X 10^{-4})[b]	M_n[c]	% α-olefin[c]	branches per 1000 carbons[c]
1	1.7	20	35	15	22	970	90	5
2	1.1	60	35	15	64	770	87	7
3	1.1	120	35	15	130	960	91	8
4	1.1	180	35	15	198	970	90	5
5	0.8	240	35	15	244	960	86	6
6	2.4	30	0	1	3.2	1020	77	5
7	2.5	60	0	1	6.1	1000	78	7
8	1.4	120	0	1	12.2	890	79	4
9	1.6	180	0	1	16.8	750	79	4
10	1.1	240	0	1	17.6	790	78	5

a) Reaction conditions: 200 mL toluene (entries 1-5) or 100 mL toluene (entries 6-10), 1700 equiv Al/equiv Ni. b) Turnover number. C) Determined by ^{1}H NMR spectroscopy (corrected for endgroups).

Monomer flow measurements using **4c**/MMAO were conducted to gain additional data concerning catalyst activity. These data are summarized in Figure 3.4. At 35 °C and 200 psig ethylene pressure, very slow catalyst deactivation was observed over a 5 h time period. The decay rate was independent of catalyst concentration. At 60 °C, the catalyst decay rate was considerably accelerated. Qualitatively, the stability of this catalyst is not significantly different from those bearing *ortho*-alkyl substituents studied above. This latter experiment suggests that C-H bond activation is not a major route for deactivation of catalysts bearing *ortho*-alkyl substituents.

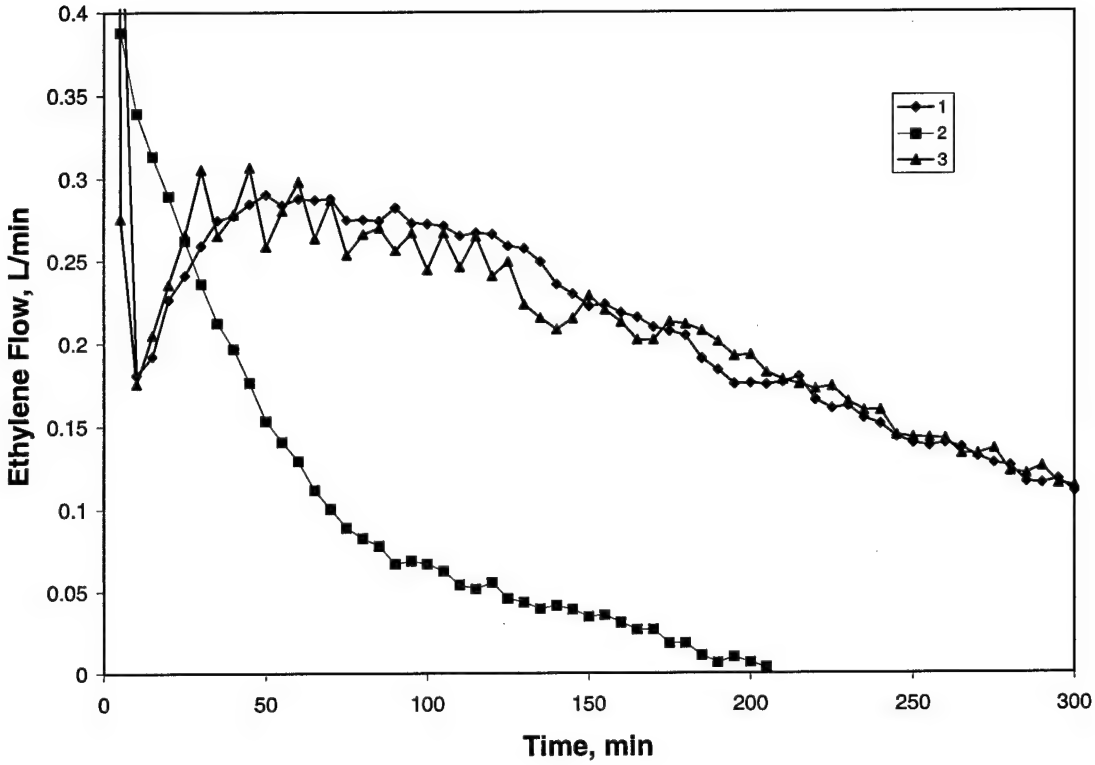

Figure 3.4. Ethylene flow profiles in polymerization reactions of **4c**/MMAO in toluene under 200 psig ethylene pressure. Line 1: 400 mL toluene, 35 °C. Line 2: 400 mL toluene, 60 °C. Line 3: 200 mL toluene, 35 °C.

The molecular weight of the polyethylene produced by each catalyst was found to decrease as the temperature was increased. For example, when catalyst **4b** (2-CF_3-6-CH_3) is employed at 200 psig ethylene pressure, the molecular weight drops from M_n = 400,000 when carried out at 35 °C to M_n = 237,000 at 60 °C to M_n = 68,000 at 85 °C. Similar effects are also observed with all the other catalysts, with a decrease in M_n of approximately 50% when the temperature is increased 25 °C. These results suggest that at higher temperatures there is an increase in the rate of chain transfer, although further complications with catalyst degradation may also affect molecular weights. The distribution of molecular weights is also observed to increase as the reaction temperature is increased.

The branching numbers are observed to increase dramatically with increasing temperature with a corresponding decrease in T_m values. For example, the branching numbers obtained for catalyst **5** increase from 39 per thousand carbons at 35 °C to 60 per thousand carbons at 60 °C, to 93 per

thousand carbons at 85 °C. This trend can be clearly observed by a comparison of the ^{1}H NMR spectra shown in Figure 3.5. The small doublet observed at 0.83 ppm which is assigned to the methyl groups at the end of branches increases in intensity relative to the methylene resonances at 1.24 ppm as the temperature is increased. Also, the methine resonances, which are observed as broad resonances at 1.1 ppm, increase with increasing temperature. Furthermore, the fact that the methyl resonances are split into doublets indicates that the branches in these polyethylenes are mainly CH_3 branches; however, the small shoulder visible at 0.80 ppm suggests the presence of other longer branches.

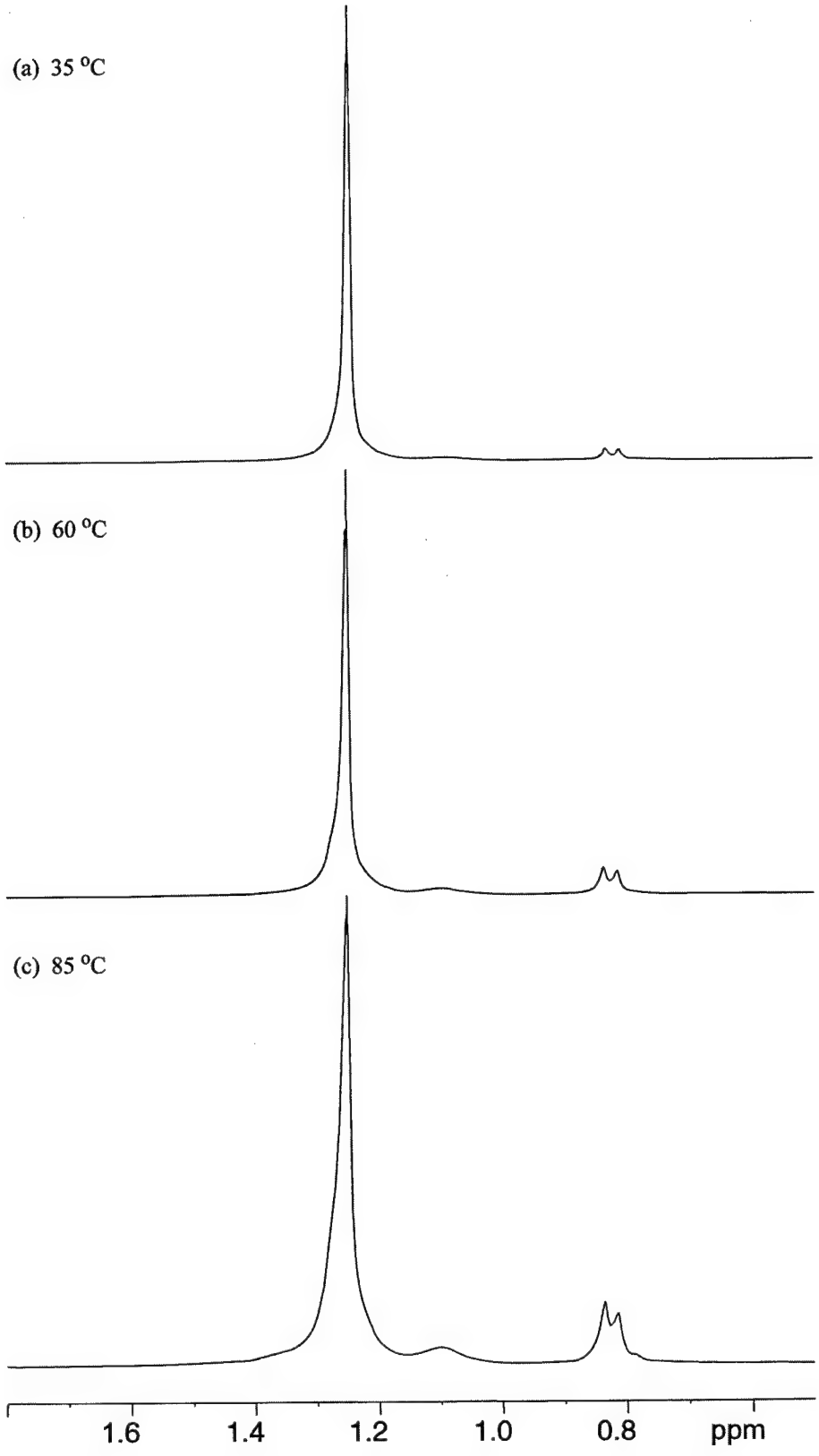

Figure 3.5. ^{1}H NMR spectra (300 MHz, C_6D_5Br, 120 °C) of polyethylene prepared with **5**/MMAO and 200 psig ethylene showing the effect of reaction temperature on branching.

D. Thermal Properties of Highly Branched Polyethylenes.

The physical appearance of the unprocessed polyethylene samples isolated from the reactor varies dramatically as the nature of the catalyst structure changes. For example, polymers formed with bulky 2,6-diisopropylphenyl substituted catalysts (**4g**, **5**, and **6**) at 1 atm ethylene pressure and 35 °C are clear, colorless rubbery materials, whereas with catalyst **4b** a white rubbery material is formed. At 200 psig ethylene pressure, the polymer formed with **4b** is a tough flexible white solid, and with **4g**, **5**, and **6**, the materials are rigid solids.

In order to gain more insight into the thermal properties of these highly branched polyethylenes, we have characterized the polymers by differential scanning calorimetry (DSC). The linear polymers (<5 branches per thousand carbons) were found to exhibit melt transitions (T_m's) between 125 and 135 °C, which is typical of high density polyethylene (HDPE) which has a T_m of 135 °C.[45] For example, the linear polyethylene produced at high pressures with catalyst **4d** (see Table 3.3) has a branching number of 1 per thousand carbons and a T_m of 137-138 °C. With other bulky catalysts (**4g**, **5** and **6**), the branched materials produced at similar pressures exhibit melting points of ca. 100 °C.

A complex thermal behavior is observed for the highly branched polyethylenes prepared at 1 atm or 200 psig ethylene pressure, which we attribute to the irregularity of the polymer structure. For example, the polyethylene produced at 35 °C with catalysts **5** and **6** (108 and 101 branches per thousand carbons, respectively) show melting transitions below room temperature (-8 and -2 °C, respectively), and also exhibit a second-order transition. As the branching numbers increase (at higher temperatures), the second-order transition becomes more pronounced, and the melting points shift to lower temperature and occur over a much broader temperature range. For example, Figure 3.6 shows the DSC thermograms for polyethylene prepared using catalyst **5** at 200 psig ethylene pressure and at temperatures of 35, 60 and 85 °C. The polyethylene produced at 35 °C (Figure 3.6a) and 60 °C (Figure 3.6b) exhibit broad melting transitions on the heating curves, but these are much sharper upon crystallization on the cooling curve. In addition, the second-order transition at ca. -42 °C, which is barely visible on the heating curve, is clearly observed on the cooling curve. The second-order

transition is observed upon repeated scanning of the sample between -100 °C and 140 °C. This transition is even more pronounced for the polymer obtained from catalyst **5** at 85 °C (Figure 3.6c).

It is worth noting that the thermal properties of low-density polyethylene have been studied extensively, and three second-order transitions have been observed. The α transition usually occurs between 30 and 120 °C, the β transition is typically detected between -30 and 10 °C, and the γ transition is seen in the range of -150 to -120 °C.[46,47] The second-order transitions observed in this study are likely β transitions, which are usually observed using dynamic mechanical techniques,[48] and have been attributed to the onset of motion at branch points.[45,47] The unique highly branched structures of the present polymers makes the second-order transitions detectable by DSC. We have also carried out a dynamic mechanical analysis (DMA) experiment on a polyethylene fiber produced using catalyst **4g** (200 psig ethylene pressure, 60 °C) (Table 3.5, entry 11) which is shown in Figure 3.7. The β transition is clearly observed at -30 °C (1 Hz) as the peak maximum in the tan(Δ) curve. This transition was observed at -42 °C by DSC. In addition, the γ transition was also detected at -126 °C. These results are consistent with those previously reported for low density polyethylene.

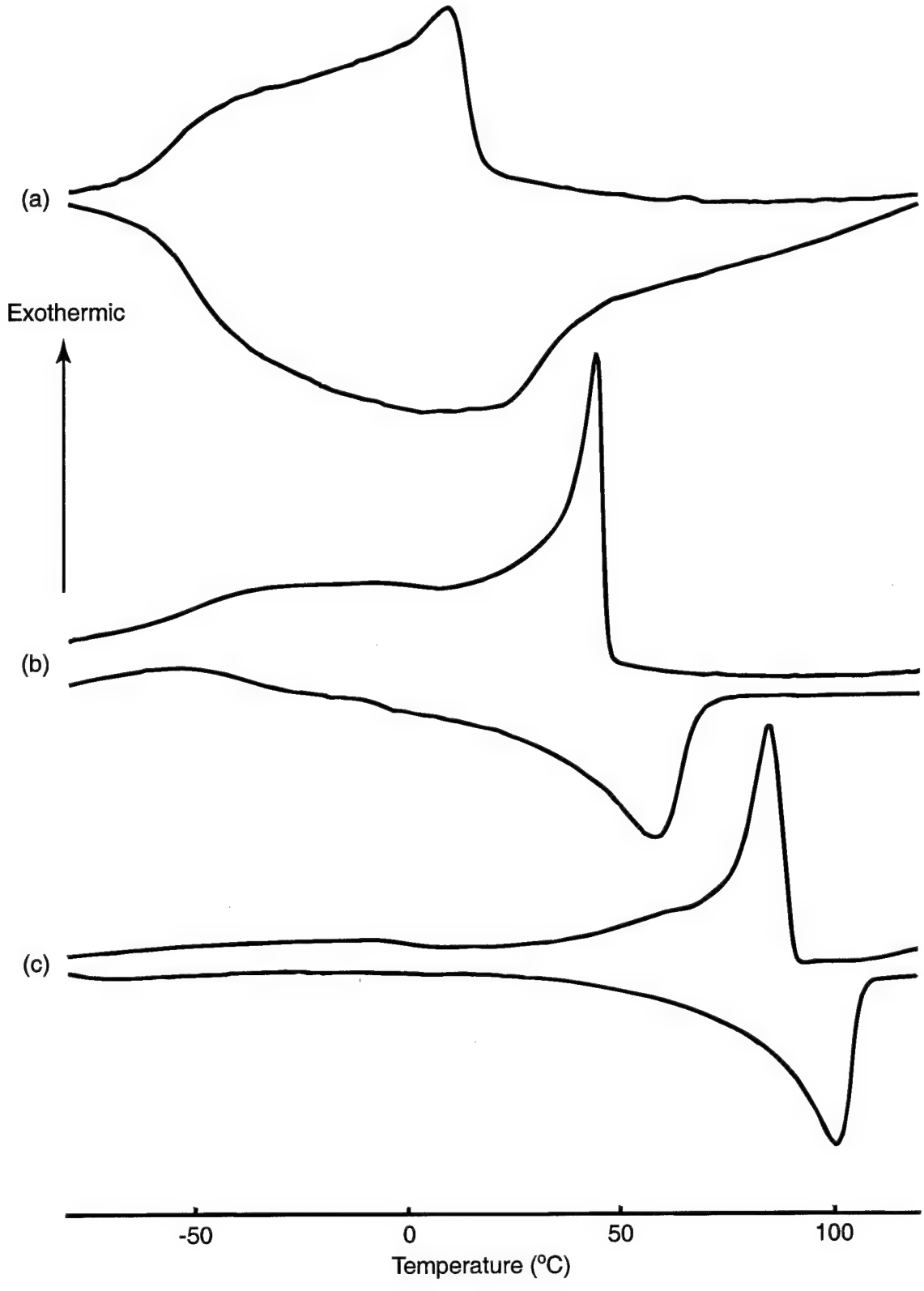

Figure 3.6. DSC thermograms of polyethylene prepared at 200 psig with **5**/MMAO: (a) 35 °C; (b) 60 °C; (c) 85 °C. Y axis is heat flow and is not drawn to scale.

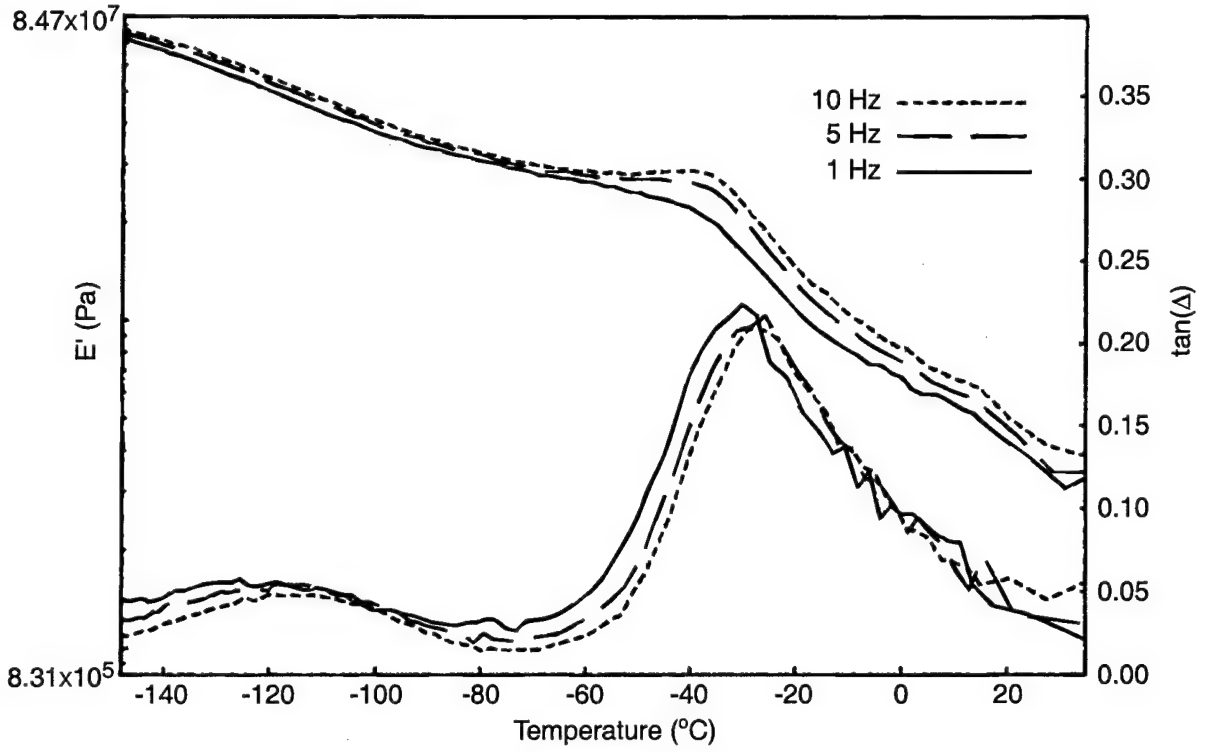

Figure 3.7. DMA of polyethylene produced using **4g**/MMAO (200 psig, 60 °C) with sampling frequencies of 10, 5, 2, 1, and 0.5 Hz (for clarity, only the 10, 5, and 1 Hz slices are shown). The top curve corresponds to E' while the bottom curve corresponds to tan(Δ).

Conclusions

Several conclusions can be drawn from these studies which reinforce our earlier observations concerning effects of ethylene pressure, temperature, and ligand variation on these ethylene polymerizations. All of the effects are completely consistent with our proposed mechanistic scheme for chain growth.

(1) As the bulk of the ortho aryl substituents on the α-diimine ligand increases, the molecular weights of the polyethylenes increase. With mono ortho substituted aryl α-diimine catalysts, M_n values as low as ca. 1000 are seen, while with the bulkiest ortho diisopropyl-substituted systems, M_n values reach 10^6.

(2) Increased steric bulk of the ortho substituents also increases the extent of branching in the polyethylenes as well as the turnover frequencies. The electron-withdrawing substituent, *o*-CF_3, appears to increase the TOF more then expected based simply on steric effects, and is consistent with earlier observed electronic effects.

(3) Catalysts bearing alkyl substituents on the backbone carbon atoms tend to give higher molecular weight polymers with more narrow molecular weight distributions than the catalysts bearing the planar aromatic acenaphthyl backbone. Catalyst activities are comparable.

(4) Increases in ethylene pressure lead to dramatic reductions in the extent of branching in the polymer presumably due to an increased rate of trapping and insertion relative to the rate of chain isomerization which is independent of $[C_2H_4]$.

(5) Increases in polymerization temperatures result in increased branching and decreased molecular weights. Catalysts are stable over hours at 35 °C, but lifetimes are reduced to minutes at temperatures above 60 °C. The catalyst decay mechanism is unknown, but results with fluorinated ortho substituents show decay is likely not due to C-H bond activation of ortho alkyl substituents.

The physical properties of the homopolyethylenes produced by these catalyst systems vary widely depending on the extent of branching and polymer molecular weight. It is clear from these studies that structural variations of the α-diimine ligand coupled with the conditions of polymerization (temperature and ethylene pressure) can be used to control branching and molecular weight in a predictable way. Thus, variably branched polyethylenes can be produced without the use of an α-olefin comonomer (as is required for early metal catalysts) with properties which not only span the range of HDPE to LLDPE to LDPE but also include amorphous, elastomeric homopolymers.

Experimental Section

General Methods. All manipulations of air- and/or water-sensitive compounds were performed using standard high-vacuum or Schlenk techniques. Argon was purified by passage through columns

of BASF R3-11 catalyst (Chemalog) and 4-Å molecular sieves. Solid organometallic compounds were transferred in an argon-filled Vacuum Atmospheres drybox. ^{1}H, ^{13}C, and ^{19}F NMR spectra were recorded on Bruker Avance-500, -400, -300, or Varian Gemini 300 MHz spectrometers. Chemical shifts are reported relative to residual $CHCl_3$ (δ 7.24 for ^{1}H), $CDCl_3$ (δ 77.00 for ^{13}C), and CCl_3F (δ 0.00 for ^{19}F). ^{1}H NMR spectra of polyethylene were taken in C_6D_5Br at 120 °C. Ethylene flow measurements were made with an Omega FMA-869 mass flowmeter and recorded with an Omega RD-853-T paperless recorder. High temperature gel permeation chromatography (GPC) was performed by DuPont (Wilmington, DE) in 1,2,4-trichlorobenzene at 135 °C using a Waters HPLC 150C equipped with Shodex columns. A calibration curve was established with polystyrene standards and universal calibration was applied using Mark-Houwink constants for polyethylene ($k = 4.34 \times 10^{-4}$, $\alpha = 0.724$). Differential scanning calorimetry was recorded on a Seiko Instruments DSC 220 calibrated with the melting transition of indium. Samples were heated to ca. 50 °C above their T_m and cooled rapidly to -120 °C and held for 20-30 min prior to scanning (scan rate: 10 °C/min). Dynamic mechanical analysis was carried out using a Seiko Instruments DMS210 with a scan rate of 2 °C/min between -150 °C and 50 °C, and frequencies of 10, 5, 2, 1, and 0.5 Hz. Elemental analyses were performed by Atlantic Microlab of Norcross, GA.

Materials. Toluene, diethyl ether, pentane, and methylene chloride were purified using procedures recently reported by Pangborn et al.[49] High pressure polymerizations were performed in a mechanically stirred 1000 mL Parr autoclave. Polymer-grade ethylene (99.5%) was purchased from National Specialty Gases and used without further purification. 7% Al (wt %) and 6.4% Al solutions of modified methylalumoxane (MMAO) in heptane (d = 0.73 g/mL) containing 23-27% isobutyl groups were purchased from Akzo Nobel. Diimine ligands **1e-g**, **2**, and **3** as well as nickel(II) bromide complexes **4-6** were prepared according to modified literature procedures.[8,37,38,50] Acenaphthenequinone, aniline, 1,2-cyclohexanedione, iodopentafluorobenzene, 2,6-diisopropylaniline, 2,3-pentanedione, *o*-toluidine, 2-trifluoromethylaniline, and $(DME)NiBr_2$, were purchased from Aldrich Chemical Co. C_6D_5Br was purchased from Cambridge Isotope Laboratories

and stored over activated 4-Å molecular sieves. 2-(Pentafluorophenyl)aniline[51] and 2-methyl-6-trifluoromethylaniline[52] were prepared according to literature procedures.

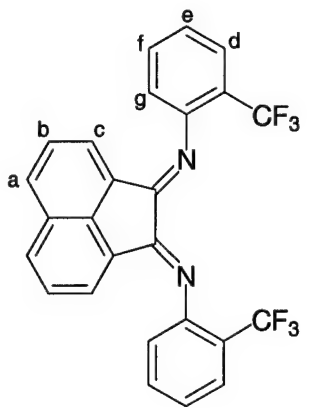

1a

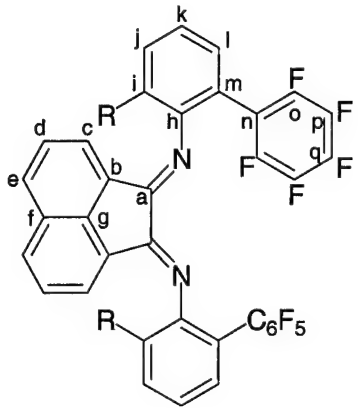

1c (R = H)
1d (R = CH_3)

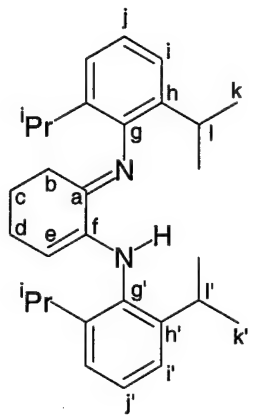

2

Synthesis of (ArN=C(An)-C(An)=NAr) (Ar = 2-$CF_3C_6H_4$) (1a). Acenaphthenequinone (2.73 g, 15.0 mmol) and *o*-trifluoromethylaniline (6.43 g, 40.0 mmol) were stirred in toluene (100 mL) and sulfuric acid (1 drop) was added. The solution was refluxed for 3 days using a Dean-Stark trap to collect H_2O eliminated. K_2CO_3 (5 g) was added at room temperature to neutralize, followed by filtration, and toluene was removal in vacuo. The orange solid obtained was dissolved in CH_2Cl_2 (40 mL) and pentane (40 mL) was added. After 1 d at -30 °C, yellow-orange crystals formed which were isolated by filtration and washing with pentane (2 X 10 mL), and dried in vacuo. Yield of **1a** = 5.70 g (81%). Two isomers are observed by ^{1}H NMR in a 3.8:1 ratio ($C_2D_2Cl_4$, 295 K); the major isomer has a C_2 or C_S symmetry, while all resonances are unique for the minor isomer (C_1 symmetry). Many of the NMR resonances corresponding to the minor isomer are obscured by those from the major isomer, and are therefore not reported. ^{1}H NMR (500 MHz, $C_2D_2Cl_4$, 295 K, major isomer) δ 7.86 (d, J = 8.0 Hz, 2H, a), 7.73 (d, J = 8.0 Hz, 2H, d), 7.57 (dd, J = 8.0, 7.5 Hz, 2H, f), 7.34 (dd, J = 8.5, 7.5 Hz, 2H, b), 7.31 (dd, J = 8.0, 7.5 Hz, 2H, e), 7.04 (d, J = 8.0 Hz, 2H, g), 6.57 (d, J = 7.0 Hz, 2H, c); ^{13}C{^{1}H} NMR (75 MHz, $CDCl_3$, 293 K, major isomer) δ 161.4, 149.9, 141.9, 132.9, 131.7 (q, $^1J_{CF}$ =

284 Hz, CF_3), 131.1, 129.3, 128.3, 127.8, 126.9 (q, $^3J_{CF}$ = 4.5 Hz), 124.0, 123.8, 118.8, 117.2 (q, $^2J_{CF}$ = 32 Hz); ^{19}F NMR (376 MHz, $C_2D_2Cl_4$, 293 K, major isomer) δ -61.6 (br s, CF_3). Anal. Calcd. for $C_{26}H_{14}F_6N_2$: C, 66.67; H, 3.01; N, 5.98. Found C, 66.55; H, 3.04; N, 5.92.

Synthesis of (ArN=C(An)-C(An)=NAr) (Ar = 2-CH_3-6-$CF_3C_6H_3$) (1b). Acenaphthenequinone (0.91 g, 5.0 mmol) and 2-methyl-6-trifluoromethylaniline (1.9 g, 11 mmol) were stirred in toluene (40 mL) and sulfuric acid (2 drops) was added. The solution was refluxed for 1 day using a Dean-Stark trap to collect H_2O eliminated. The ruby-red solution was filtered while still hot into a clean flask containing 5 g K_2CO_3, and allowed to stand for 15 min. A second filtration to remove K_2CO_3, and solvent removal in vacuo, yielded an orange solid. The crude product was purified by column chromatography on 200-400 mesh, 60-Å silica gel using a gradient of 5% ethyl acetate/1% triethylamine/hexanes (initial) to 50% ethyl acetate/1% triethylamine/hexanes (final). The product eluted as the first major orange band. The product was isolated after solvent removal as a yellow solid. Yield of **1b** = 1.0 g (40%). The product ^{1}H NMR resonances are broad at room temperature; however, at 248 K the product exists as four distinct isomers in (49:30:14:7 ratio). The two major isomers have C_2/C_S symmetry, while the two minor isomers have C_1 symmetry. ^{1}H NMR (500 MHz, $C_2D_2Cl_4$, 248 K, most abundant isomer) δ 7.88 (d, J = 8.4 Hz, 2H), 7.56 (d, J = 7.2 Hz, 2H), 7.45 (d, J = 7.6 Hz, 2H), 7.35 (virtual t, 2H), 7.20 (virtual t, 2H), 6.47 (d, J = 7.2 Hz, 2H), 2.04 (s, 6H, CH_3); ^{13}C{^{1}H} NMR (125 MHz, $C_2D_2Cl_4$, 243 K, most abundant isomer) δ 162.4, 148.3, 141.4, 135.1, 131.1, 130.1, 128.9, 128.8, 127.1, 126.4 (q, $^1J_{CF}$ = 293 Hz, CF_3), 124.9, 124.2, 123.4, 117.7 (q, $^2J_{CF}$ = 31 Hz, CCF_3), 18.0 (CH_3); ^{19}F NMR (376 MHz, $C_2D_2Cl_4$, 243 K, most abundant isomer) δ -61.3 (s, CF_3). Anal. Calcd. for $C_{28}H_{18}F_6N_2$: C, 67.74; H, 3.65; N, 5.64. Found C, 67.83; H, 3.68; N, 5.57.

Synthesis of (ArN=C(An)-C(An)=NAr) (Ar = 2-(C_6F_5)C_6H_4) (1c). To a stirred solution of 2-(pentafluorophenyl)aniline (1.0 g, 3.8 mmol) in 100 mL toluene were added acenaphthenequinone (0.32 g, 1.7 mmol) and H_2SO_4 (0.01 mL, 0.1 mmol). After refluxing 48 h the solvent was removed on a vacuum line, leaving the crude product as an orange residue. The crude orange residue was purified by column chromatography (15% ethyl acetate/hexanes, 60 mm silica gel) to yield the product as an

orange solid. Yield: 0.4 g (30%). Two isomers are observed by ^{1}H NMR in a 3.5:1 ratio ($CDCl_3$, room temperature); the major isomer has a C_2 axis or C_S plane of symmetry, while all resonances are unique for the minor isomer (C_1 symmetry). Many of the NMR resonances corresponding to the minor isomer are obscured by those from the major isomer, and are therefore not reported. ^{1}H NMR (300 MHz, $CDCl_3$, 293 K, major isomer): δ 7.92 (d, $^3J_{HH}$ = 8.1 Hz, 2H, e), 7.49 (dt, $^3J_{HH}$ = 7.6 Hz, $^4J_{HH}$ = 1.8 Hz, 2H, j), 7.41 (t, $^3J_{HH}$ = 8.1 Hz, 2H, d), 7.39 (t, $^3J_{HH}$ = 7.6 Hz, 2H, k), 7.35 (broad d, $^3J_{HH}$ = 7.6 Hz, 2H, l), 7.12 (d, $^3J_{HH}$ = 8.1 Hz, 2H, c), 7.04 (d, $^3J_{HH}$ = 7.6 Hz, 2H, i); ^{13}C{^{1}H} NMR (75 MHz, $CDCl_3$, 293 K, major isomer): δ 162.2 (a), 150.5 (h), 144.0 (broad d, $^1J_{CF}$ = 264 Hz, o), 141.9 (g), 140.7 (broad d, $^1J_{CF}$ = 226 Hz, q), 138.4 (broad d, $^1J_{CF}$ = 257 Hz, p), 132.1 (f), 131.3 (b), 130.6 (e), 129.5 (d), 128.0 (j), 127.6 (l), 124.9 (k), 124.0 (c), 119.0 (C-9), 116.9 (m), 113.5 (t, $^2J_{CF}$ = 23 Hz, n); ^{19}F NMR (282 MHz, $CDCl_3$, 293 K, major isomer): δ -139.0 (broad, 4F, F_{ortho}), -155.1 (t, $^3J_{FF}$ = 17.0 Hz, 2F, F_{para}), -162.9 (broad, 4F, F_{meta}). Anal. Calcd for $C_{36}H_{14}F_{10}N_2$: C, 65.07; H, 2.12; N, 4.22. Found: C, 65.12; H, 2.17; N, 4.22.

Synthesis of 2-methyl-6-(pentafluorophenyl)aniline. Under a nitrogen atmosphere, a stirred solution of C_6F_5I (13.2 g, 44.9 mmol), *o*-toluidine (16.1 g, 149 mmol) and acetonitrile (150 mL) in a Pyrex flask was irradiated with a medium-pressure mercury lamp (450 W) for 3 days at 80 °C. The mixture was concentrated and the residue was extracted with diethyl ether (100 mL). The ether solution was then washed with 5% aqueous $NaHCO_3$, dried over $MgSO_4$, and the solvent removed. Excess *o*-toluidine was removed via vacuum distillation. The oily residue was purified using column chromatography (6% diethyl ether/hexanes, 60 mm silica gel) to give 2-methyl-6-(pentafluorophenyl)aniline as a white powder (0.3 g, 3%). 2-Methyl-3-(pentafluorophenyl)aniline and 2-methyl-4-(pentafluorophenyl)aniline were also produced; the identity of the desired isomer was confirmed by X-ray crystallography. ^{1}H NMR (300 MHz, $CDCl_3$, 293 K): δ 7.17 (d, $^3J_{HH}$ = 7.4 Hz, 1H, Ar*H*), 6.93 (d, $^3J_{HH}$ = 7.4 Hz, 1H, Ar*H*), 6.78 (t, $^3J_{HH}$ = 7.4 Hz, 1H, Ar*H*), 3.55 (br s, 2H, NH_2), 2.23 (s, 3 H, CH_3); ^{13}C{^{1}H} NMR (75 MHz, $CDCl_3$, 293 K): δ 144.4 (m, Ar *C*F), 142.8 (s, *C*=N), 140.8 (m, *C*F), 137.9 (m, Ar *C*F), 131.8 (t, J_{CF} = 7.5 Hz, *C*CH3), 129.0 (s, Ar *C*H), 123.2 (s, Ar *C*H),

118.1 (s, Ar *C*H), 113.3 (dt, $^2J_{CF}$ = 23 Hz, $^4J_{CF}$ = 7.6 Hz, C_{ipso} of C_6F_5 ring), 110.8 (s, *C*-(C_6F_5)), 17.6 (m, *C*H_3); ^{19}F NMR (282 MHz, $CDCl_3$, 293 K): δ -139.0 (dd, $^3J_{FF}$ = 22.1 Hz, $^4J_{FF}$ = 7.9 Hz, 2F, F_{ortho}), -154.5 (t, $^3J_{FF}$ = 22.1 Hz, 1F, F_{para}), -161.2 (dt, $^3J_{FF}$ = 22.1 Hz, $^4J_{FF}$ = 7.9 Hz, 2F, F_{meta}). Anal. Calcd for $C_{13}H_8F_5N$: C, 57.15; H, 2.95; N, 5.13. Found: C, 57.13; H, 2.91; N, 5.11.

Synthesis of (ArN=C(An)-C(An)=NAr) (Ar = 2-CH_3-6-(C_6F_5)C_6H_3) (1d). To a stirred solution of 2-methyl-6-(pentafluorophenyl)aniline (1.2 g, 4.4 mmol) in 50 mL of methanol were added acenaphthenequinone (0.33 g, 1.8 mmol) and formic acid (0.10 mL, 2.6 mmol). The solution was stirred at room temperature for 48 h, then the solvent was removed to yield an orange residue. The residue was purified via column chromatography (5% ethyl acetate/hexanes, 60 mm silica gel) to give **1d** as a yellow powder (0.4 g, 32%). An equilibrium between two isomers exists; following chromatography, a 90:10 ratio of isomers is seen, which shifts to a 50:50 ratio after 24 h in $CDCl_3$ at room temperature. Isomer 1: ^{1}H NMR (300 MHz, $CDCl_3$, 293 K, isomer 1): δ 8.1-6.7 (br m, 12H, Ar*H*), 2.03 (s, 6H, C*H*$_3$); ^{13}C{^{1}H} NMR (75 MHz, $CDCl_3$, 293 K): δ 161.7 (a), 149.1 (h), 146-135 (multiplets for o, p, q), 140.6 (g), 132.1 (f), 130.9 (b), 129.6-129.5 (e and i), 128.5 (d), 127.8 (j), 126.5 (l), 124.1 (k), 122.9 (c), 115.0 (m), 113.9 (t, $^2J_{CF}$ = 15 Hz, n), 17.4 (*C*H_3); ^{19}F NMR (282 MHz, $CDCl_3$, 293 K): δ -136.2 (dd, $^3J_{FF}$ = 22.3 Hz, $^4J_{FF}$ = 7.7 Hz, 2F, F_{ortho}), -139.0 (dd, $^3J_{FF}$ = 22.3 Hz, $^4J_{FF}$ = 7.7 Hz, 2F, F_{ortho}), -155.6 (t, $^3J_{FF}$ = 22.3 Hz, 2F, F_{para}), -162.3 (dt, $^3J_{FF}$ = 22.3 Hz, $^4J_{FF}$ = 7.7 Hz, 2F, F_{meta}), -163.5 (dt, $^3J_{FF}$ = 22.3 Hz, $^4J_{FF}$ = 7.7 Hz, 2F, F_{meta}). Isomer 2: ^{1}H NMR (300 MHz, $CDCl_3$, 293 K): δ 8.1-6.7 (br m, 12H, Ar*H*), 2.05 (s, 6H, C*H*$_3$); ^{13}C{^{1}H} NMR (75 MHz, $CDCl_3$, 293 K): δ 162.5 (a), 149.3 (h), 146-135 (multiplets for o, p, q), 140.9 (g), 132.3 (f), 131.0 (b), 129.6-129.5 (e and i), 128.6 (d), 127.9 (j), 125.9 (l), 124.1 (k), 123.1 (c), 115.6 (m), 113.7 (t, $^2J_{CF}$ = 15 Hz, n), 17.9 (*C*H_3); ^{19}F NMR (282 MHz, $CDCl_3$, 293 K): δ -137.2 (dd, $^3J_{FF}$ = 21.7 Hz, $^4J_{FF}$ = 5.9 Hz, 2F, F_{ortho}), -139.6 (dd, $^3J_{FF}$ = 22.0 Hz, $^4J_{FF}$ = 6.2 Hz, 2F, F_{ortho}), -155.0 (broad t, $^3J_{FF}$ = 14.1 Hz, 2F, F_{para}), -162.9 (broad, 2F, F_{meta}), -163.3 (broad, 2F, F_{meta}). Anal. Calcd for $C_{38}H_{18}F_{10}N_2$: C, 65.90; H, 2.62; N, 4.04. Found: C, 65.61; H, 2.58; N, 3.90.

Synthesis of 2. A solution of 2,6-diisopropylaniline (2.66 g, 15.0 mmol) in methanol (20 mL) was added to 1,2-cyclohexanedione (0.73 g, 6.5 mmol). Formic acid (ca. 1 mL) was added to the light yellow solution. After stirring for two days at room temperature a white solid precipitated from the red solution and was separated by filtration. The white solid was washed with methanol (3 X 5 mL). NMR analysis indicates the product exists as the imine/enamine tautomer (**2**). Yield of **2** = 1.27 g (45%). ^{1}H NMR (500 MHz, $CDCl_3$, 293 K): δ 7.25-7.05 (m, 6H, Ar*H*), 6.43 (s, 1H, N*H*), 4.82 (t, *J* = 5 Hz, 1H, e-*H*), 3.27 (septet, *J* = 7 Hz, 2H, l or l'), 2.84 (septet, *J* = 6.9 Hz, 2H, l' or l), 2.20 (m, 4H, d and b), 1.74 (quintet, *J* = 5 Hz, 2H, c), 1.22, 1.20 (2 x d, *J* = 7 Hz, k and k'); ^{13}C {^{1}H} NMR (126 MHz, $CDCl_3$, 293 K): δ 162.1 (a), 147.3 (h'), 145.8 (g), 139.6 (f), 137.0 (g'), 136.4 (h), 126.5 (j or j'), 123.4 (i'), 122.9 (i), 106.1 (e), 29.4 (b), 28.4 (l'), 28.3 (l), 24.2 (d), 23.30 (c), 23.25 (k'), 22.9 (k). Assignments were made using HMQC and HMBC experiments. Anal. Calcd for $C_{30}H_{42}N_2$: C, 83.67; H, 9.83; N, 6.50. Found: C, 83.32; H, 9.79; N, 6.67.

Synthesis of (ArN=C(Et)-C(Me)=NAr) (Ar = 2,6-C_6H_3(*i*-Pr)$_2$) (3). A solution of 2,6-diisopropylaniline (4.23 g, 23.9 mmol) in methanol (5.0 mL) was added to 2,3-pentanedione (1.15 g, 11.5 mmol). Formic acid (ca. 0.5 mL) was added to the light yellow solution. The product was isolated using a chromatographic separation on silica gel (0-10% gradient of ethyl acetate in hexanes). The product was a viscous yellow oil which solidified on standing. Yield of **3** = 1.25 g (26%). ^{1}H NMR (500 MHz, $CDCl_3$, 293 K): δ 7.1 (m, 6H, Ar*H*), 2.73 (septet, *J* = 6.9 Hz, 4H, C*H*Me$_2$), 2.56 (q, *J* = 7.6 Hz, 2H, C*H*$_2$CH$_3$), 2.05 (s, 3H, C*H*$_3$), 1.23, 1.19, 1.17, 1.14 (all d, *J* = 6.9 Hz, 24H, CH*Me*$_2$), 1.06 (t, *J* = 7.6 Hz, 3H, CH$_2$C*H*$_3$); ^{13}C{^{1}H} NMR (126 MHz, $CDCl_3$, 293 K): δ 172.0, 167.8 (2 x *C*=N), 146.2, 145.7 (2 x *ipso*-Ar), 135.2, 135.0 (2 x *ortho*-Ar), 123.7, 123.5 (2 x *para*-Ar), 123.0, 122.8 (2 x *meta*-Ar), 28.4 (*C*H(CH$_3$)$_2$), 23.2 (CH(*C*H$_3$)$_2$), 22.7 (*C*H$_2$CH$_3$) 22.2 (CH(*C*H$_3$)$_2$), 17.2 (CH$_3$), 10.6 (CH$_2$). Assignments were made using an HMQC experiment. Anal. Calcd for $C_{29}H_{42}N_2$: C, 83.20; H, 10.11; N, 6.69. Found: C, 83.24; H, 10.11; N, 6.67.

Synthesis of (ArN=C(An)-C(An)=NAr)NiBr$_2$ (Ar = 2-$CF_3C_6H_4$) (4a). (DME)NiBr$_2$ (111 mg, 0.36 mmol) and **1a** (187 mg, 0.40 mmol) were combined in a Schlenk flask under an argon

atmosphere. CH_2Cl_2 (20 mL) was added, and the reaction stirred at room temperature for 18 hours. The supernatant liquid was removed, and the product washed with 2 X 10 mL Et_2O and dried in vacuo. The product was isolated as a red-brown powder (220 mg, 89% yield).

Synthesis of (ArN=C(An)-C(An)=NAr)NiBr$_2$ (Ar = 2-CH$_3$-6-CF$_3$C$_6$H$_3$) (4b). Following the above procedure, **4b** was isolated as a red powder in 94% yield.

Synthesis of (ArN=C(An)-C(An)=NAr)NiBr$_2$ (Ar = 2-(C$_6$F$_5$)C$_6$H$_4$) (4c). Following the above procedure, **4c** was isolated as a yellow powder (0.3 g, 42% yield). Crystals suitable for an X-ray diffraction experiment were obtained by slow diffusion of pentane into a saturated dichloromethane solution of **4c**. Anal. Calcd for $C_{36}H_{14}Br_2F_{10}N_2Ni$: C, 48.97; H, 1.60; N, 3.17. Found: C, 48.77; H, 1.64; N, 3.08.

Synthesis of (ArN=C(An)-C(An)=NAr)NiBr$_2$ (Ar = 2-CH$_3$-6-(C$_6$F$_5$)C$_6$H$_3$) (4d). Following the above procedure, **4d** was isolated as an orange powder (0.25 g, 42% yield). Crystals suitable for an X-ray diffraction experiment were obtained by slow diffusion of pentane into a saturated dichloromethane solution of **4d**. Anal. Calcd for $C_{38}H_{18}Br_2F_{10}N_2Ni$: C, 50.10; H, 1.99; N, 3.07. Found: C, 49.88; H, 1.94; N, 3.03.

Synthesis of (ArN=C(CH$_2$CH$_2$CH$_2$CH$_2$)C=NAr)NiBr$_2$ (Ar = 2,6-C$_6$H$_3$(*i*-Pr)$_2$) (5). Following the above procedure, **5** was isolated as a red powder in 48% yield.

Synthesis of (ArN=C(CH$_2$CH$_3$)-C(CH$_3$)=NAr)NiBr2 (Ar = 2,6-C$_6$H$_3$(*i*-Pr)$_2$) (6). Following the above procedure, **6** was isolated as a red powder in 84% yield.

General Procedure for 1 atm Polymerizations. Toluene (100 or 200 mL) was added to a flask under 1 atm of ethylene pressure at the desired temperature (regulated by a water bath). MMAO (1.6 mL; Al:Ni = 1000-3000) was added to the stirred solution and the temperature was allowed to equilibrate for 10-15 min. The appropriate Ni(II) complex was dissolved/suspended in 5 mL of toluene and was rapidly added to the reaction mixture. The polymerization mixture was stirred for 30

min open to ethylene, then was quenched by addition of methanol, acetone, and ca. 5 mL 6 M HCl. Polyethylene precipitated from solution, and was isolated by removal of the solvents and dried in vacuo. For the 85 °C runs, the polymer did not precipitate from the quenched reaction mixture, and had to be isolated by solvent evaporation on a rotary evaporator, followed by washing with HCl (6M), methanol and acetone, and drying in vacuo.

General Procedure for High Pressure Polymerizations. A 1000 mL Parr autoclave was heated under vacuum at 60 °C for several hours, then was cooled and backfilled with ethylene. Toluene (200 mL) and MMAO (1.6 mL; Al:Ni = 1000-3000) were added, the autoclave sealed, and the ethylene pressure raised to ca. 50 psig. The reaction temperature was established and the mixture allowed to stir for 15 min. The autoclave was then vented, the precatalyst solution/suspension added, and the autoclave sealed and pressurized to the desired ethylene pressure while stirring. For 35 °C runs the temperature was maintained by cooling with an ice/water cooled circulator. The reaction was quenched by venting ethylene from the autoclave, followed by addition of methanol or acetone. The precipitated polymers were filtered from solution and dried in vacuo.

Ethylene Flow Rate Measurements. A mechanically-stirred 1000 mL Parr autoclave under an ethylene atmosphere was charged with 198 mL toluene and MMAO. The reactor was sealed, pressurized with ethylene to 200 psig, and the temperature allowed to equilibrate at the reaction temperature. Once the system reached equilibrium, the ethylene flow baseline was established with a mass flowmeter positioned between the ethylene supply cylinder and the autoclave. The reactor was vented, and a suspension of **4c** (0.6 mg, 7 X 10^{-7} mol) in toluene (2 mL) was transferred into the reactor via cannula. The reactor was repressurized to 200 psig with ethylene, and the temperature maintained within 1 °C of the desired reaction temperature. Ethylene flow rates were recorded at 5 to 15 second intervals throughout the duration of the reaction.

Crystallographic structural determinations: Crystals of **4c** and **4d** suitable for X-ray crystallography were grown at room temperature from a saturated CH_2Cl_2 solution with slow

diffusion of diethyl ether. Single crystals were mounted in oil on the end of a fiber. Intensity data were collected on a Bruker SMART 1K diffractometer with CCD detector using MoKα radiation of wavelength 0.71073 Å using 0.3° ω corrected intensity data. The structures were solved by direct methods and refined by least squares techniques using the NRCVAX[53] suite of programs. All non-hydrogen atoms were refined to ride on the atoms to which they were bonded. Crystal data, data collection, and refinement parameters are listed in Table 3.8.

Table 3.8. Structural Parameters for **4c** and **4d**.

	4c	**4d**
formula	$NiBr_2C_{36}H_{18}F_{10}N_2O_2 \cdot (1/3)H_2O$	$NiBr_2C_{38}H_{18}F_{10}N_2$
FW	925.05	911.07
crystal class	triclinic	monoclinic
space group	$P\bar{1}$	P2/c
color	yellow	orange
a [Å]	14.3043(6)	17.3143(8)
b [Å]	15.0408(6)	11.3596(5)
c [Å]	25.9407(11)	19.8097(9)
α [°]	96.9580(10)	
β [°]	105.2400(10)	113.3180(10)
γ [°]	107.5340(10)	
V [Å^3]	5011.4(4)	3578.0(3)
Z	6	4
D(calc) [g cm^{-3}]	1.839	1.691
RF [I > 3σ(I)]	0.047	0.060
R_W [all data]	0.050	0.074
GoF	2.01	1.96

[a] Definition of R indices: $RF = \Sigma(F_O-F_C)/\Sigma(F_O)$, $R_W = [\Sigma[w(F_O-F_C)^2]/\Sigma[w(F_O)^2]]^{1/2}$.

References and Notes

(1) See for example: (a) Brintzinger, H. H.; Fischer, D.; Mülhaupt, R.; Rieger, B.; Waymouth, R. M. *Angew. Chem., Int. Ed. Engl.* **1995**, *34*, 1143; (b) McKnight, A. L.; Waymouth, R. M. *Chem. Rev.* **1998**, *98*, 2587; (c) Yang, X.; Stern, C. L.; Marks, T. J. *J. Am. Chem. Soc.* **1994**, *116*, 10015; (d) Britovsek, G. J. P.; Gibson, V. C.; Wass, D. F. *Angew. Chem., Int. Ed. Engl.* **1999**, *38*, 429; (e) Bochmann, M. *J. Chem. Soc., Dalton Trans.* **1996**, 255; (f) Fink, G.; Mülhaupt, R.; Brintzinger, H. H., Eds. *Ziegler Catalysts: Recent Scientific Innovations and Technological Improvement*; Springer-Verlag: Berlin, 1995.

(2) Schmidt, G. F.; Brookhart, M. *J. Am. Chem. Soc.* **1985**, *107*, 1443.

(3) Brookhart, M.; Volpe, A. F.; Lincoln, D. M.; Horvath, I. T.; Millar, J. M. *J. Am. Chem. Soc.* **1990**, *112*, 5634.

(4) Brookhart, M.; DeSimone, J. M.; Grant, B. E.; Tanner, M. J. *Macromolecules* **1995**, *28*, 5378.

(5) Wang, L.; Flood, T. C. *J. Am. Chem. Soc.* **1992**, *114*, 3169.

(6) Timonen, S.; Pakkanen, T. T.; Pakkanen, T. A. *J. Mol. Catal.* **1996**, *111*, 267.

(7) For early examples of Ni-catalyzed ethylene polymerization see: (a) Keim, W.; Appel, R.; Storeck, A.; Krüger, C.; Goddard, R. *Angew. Chem., Int. Ed. Engl.* **1981**, *20*, 116; (b) Klabunde, U.; Ittel, S. D. *J. Mol. Catal.* **1987**, *41*, 123; (c) Klabunde, U.; Mülhaupt, R.; Herskovitz, T.; Janowicz, A. H.; Calabrese, J.; Ittel, S. D. *J. Polym. Sci., Part A: Polym. Chem.* **1987**, *25*, 1989; (c) Ostoja Starzewski, K. A.; Witte, J. *Angew. Chem., Int. Ed. Engl.* **1987**, *26*, 63.

(8) Johnson, L. K.; Killian, C. M.; Brookhart, M. *J. Am. Chem. Soc.* **1995**, *117*, 6414. Following initial discoveries at UNC, collaborative efforts were initiated with the group at DuPont.

(9) (a) Johnson, L. K.; Killian, C. M.; Arthur, S. D.; Feldman, J.; McCord, E. F.; McLain, S. J.; Kreutzer, K. A.; Bennett, A. M. A.; Coughlin, E. B.; Ittel, S. D.; Parthasarathy, A.; Tempel, D. J.; Brookhart, M. S. WO 96/23010; (b) Brookhart, M. S.; Johnson, L. K.; Arthur, S. D.; Feldman, J.; Kreutzer, K. A.; Bennett, A. M. A.; Coughlin, E. B.; Ittel, S. D.; Parthasarathy, A.; Tempel, D. J. U.S. Patent 5 866 224, 1999; (c) Brookhart, M. S.; Johnson, L. K.; Killian, C. M.; Arthur, S. D.;

Feldman, J.; McCord, E. F.; McLain, S. J.; Kreutzer, K. A.; Bennett, A. M. A.; Coughlin, E. B.; Ittel, S. D.; Parthasarathy, A.; Wang, L.; Yang, Z. U.S. Patent 5 866 663, 1999; (d) Brookhart, M. S.; Johnson, L. K.; Killian, C. M.; Arthur, S. D.; McCord, E. F.; McLain, S. J. U.S. Patent 5 891 963, 1999; (e) Brookhart, M. S.; Johnson, L. K.; Killian, C. M.; McCord, E. F.; McLain, S. J.; Kreutzer, K. A.; Ittel, S. D.; Tempel, D. J. U.S. Patent 5 880 241, 1999.

(10) Killian, C. M.; Tempel, D. J.; Johnson, L. K.; Brookhart, M. *J. Am. Chem. Soc.* **1996**, *118*, 11664.

(11) Killian, C. M.; Johnson, L. K.; Brookhart, M. *Organometallics* **1997**, *16*, 2005.

(12) Svejda, S. A.; Brookhart, M. *Organometallics* **1999**, *18*, 65.

(13) McLain, S. J.; Feldman, J.; McCord, E. F.; Gardner, K. H.; Teasley, M. F.; Coughlin, E. B.; Sweetman, K. J.; Johnson, L. K.; Brookhart, M. *Macromolecules* **1998**, *31*, 6705.

(14) Möhring, V. M.; Fink, G. *Angew. Chem., Int. Ed. Engl.* **1985**, *24*, 1001.

(15) Schubbe, R.; Angermund, K.; Fink, G.; Goddard, R. *Macromol. Chem. Phys.* **1995**, *196*, 467.

(16) Feldman, J.; McLain, S. J.; Parthasarathy, A.; Marshall, J.; Calabrese, J. C.; Arthur, S. D. *Organometallics* **1997**, *16*, 1514.

(17) Schleis, T.; Spaniol, T. P.; Okuda, J.; Heinemann, J.; Mülhaupt, R. *J. Organomet. Chem.* **1998**, *569*, 159.

(18) Wang, C.; Friedrich, S.; Younkin, T. R.; Li, R. T.; Grubbs, R. H.; Bansleben, D. A.; Day, M. W. *Organometallics* **1998**, *17*, 3149.

(19) Pellecchia, C.; Zambelli, A. *Macromol. Rapid Commun.* **1996**, *17*, 333.

(20) Pappalardo, D.; Mazzeo, M.; Pellecchia, C. *Macromol. Rapid Commun.* **1997**, *18*, 1017.

(21) Pellecchia, C.; Zambelli, A.; Mazzeo, M.; Pappalardo, D. *J. Mol Catal.* **1998**, *128*, 229.

(22) Galland, G. B.; de Souza, R. F.; Mauler, R. S.; Nunes, F. F. *Macromolecules* **1999**, *32*, 1620.

(23) Zeng, X.; Zetterberg, K. *Macromol. Chem. Phys.* **1998**, *199*, 2677.

(24) Kim, J. S.; Pawlow, J. H.; Wojcinski, L. M.; Murtuza, S.; Kacker, S.; Sen, A. *J. Am. Chem. Soc.* **1998**, *120*, 1932.

(25) Johnson, L. K.; Mecking, S.; Brookhart, M. *J. Am. Chem. Soc.* **1996**, *118*, 267.

(26) Mecking, S.; Johnson, L. K.; Wang, L.; Brookhart, M. *J. Am. Chem. Soc.* **1998**, *120*, 888.

(27) Small, B. L.; Brookhart, M.; Bennett, A. M. A. *J. Am. Chem. Soc.* **1998**, *120*, 4049.

(28) Britovsek, G. J. P.; Gibson, V. C.; Kimberly, B. S.; Maddox, P. J.; McTavish, S. J.; Solan, G. A.; White, A. J. P.; Williams, D. J. *Chem. Commun.* **1998**, 849.

(29) (a) Small, B. L.; Brookhart, M. *Macromolecules* **1999**, *32*, 2120; (b) Pellecchia, C.; Mazzeo, M.; Pappalardo, D. *Macromol. Rapid Commun.* **1998**, *19*, 651.

(30) Tempel, D. J.; Brookhart, M. *Organometallics* **1998**, *17*, 2290.

(31) Svejda, S. A.; Johnson, L. K.; Brookhart, M. *J. Am. Chem. Soc.*, manuscript submitted for publication.

(32) ^{13}C NMR spectroscopic and light scattering studies have shown that the polyethylene produced with (α-diimine)palladium(II) catalysts is hyperbranched. See reference 9, and Guan, Z.; Cotts, P. M.; McCord, E. F.; McLain, S. J. *Science*, **1999**, *283*, 2059.

(33) Deng, L.; Margl, P. M.; Ziegler, T. *J. Am. Chem. Soc.* **1997**, *119*, 1094.

(34) Deng, L.; Woo, T. K.; Cavallo, L.; Margl, P. M.; Ziegler, T. *J. Am. Chem. Soc.* **1997**, *119*, 6177.

(35) Musaev, D. G.; Froese, R. D. J.; Morokuma, K. *Organometallics* **1998**, *17*, 1850.

(36) Froese, R. D. J.; Musaev, D. G.; Morokuma, K. *J. Am. Chem. Soc.* **1998**, *120*, 1581.

(37) van Asselt, R.; Elsevier, C. J.; Smeets, W. J. J.; Spek, A. L.; Benedix, R. *Recl. Trav. Chim. Pays-Bas* **1994**, *113*, 88.

(38) tom Dieck, H.; Svoboda, M.; Grieser, T. *Z. Naturforsch* **1981**, *36b*, 823.

(39) Due to the high activity of these catalysts, even under conditions of high dilution and low catalyst loadings, the consumption of monomer is very rapid and the catalyst rapidly becomes starved for monomer.

(40) It is also possible that the 2,6-disubstituted aryl groups undergo slow rotation in solution, however, on the timescale of the polymerization reactions, it is likely that these groups are fixed either in the C_2 or C_S conformations.

(41) Turnover frequencies given assume complete catalyst activation. Recent results suggest the initial reaction with methylaluminoxane may produce some inactive nickel materials: Gates, D. P.; Brookhart, M. Unpublished results.

(42) Killian, C. M. Ni(II)-Based Catalysts for the Polymerization and Copolymerization of Olefins: A New Generation of Polyolefins. Ph.D. Dissertation, University of North Carolina-Chapel Hill, 1996.

(43) The branching numbers determined by ^{1}H NMR give no information about the types of branches (i.e. methyl, ethyl, propyl). A series of multidimensional NMR experiments conducted by E. F. McCord on polyethylene produced from nickel diimine catalysts indicate the frequency of branching to be Me>Et>Pr>Bu, etc. See reference 9.

(44) Activation of an ortho C-H bond in a (DAD)$NiBr_2$ compound [DAD = glyoxalbis(diisopropylmethylimine)] has been observed in reactions with bulky *o*-tolylmagnesium bromide. See tom Dieck, H.; Svoboda, M. *Chem. Ber.* **1976**, *109*, 1657. We have also observed an intramolecular C-H activation in (2,6-diisopropyl)phenyl substituted [(α-diimine)Pd(Me)(OEt_2)]$^+$ complexes in solution (Johnson, L. K.; Tempel, D. J.; Brookhart, M. Unpublished results.

(45) Doak, K. W. In *Encyclopedia of Polymer Science and Engineering*, Revd. Ed.; Mark, H. F.; Kroschwitz, J. I., Eds.; Wiley-Interscience: New York, 1986; Vol. 6, see p. 410.

(46) Hoffman, J. D.; Williams, G.; Passaglia, E. *J. Polymer Sci.: Part C* **1966**, *14*, 173.

(47) Popli, R.; Glotin, M.; Mandelkern, L.; Benson, R. S. *J. Polymer Sci.: Polymer Phys.* **1984**, *22*, 407.

(48) Alberola, N.; Cavaille, J. Y.; Perez, J. *Eur. Polym. J.* **1992**, *28*, 935.

(49) Pangborn, A. B.; Giardello, M. A.; Grubbs, R. H.; Rosen, R. K.; Timmers, F. J. *Organometallics* **1996**, *15*, 1518.

(50) Svoboda, M.; tom Dieck, H. *J. Organomet. Chem.* **1980**, *191*, 321.

(51) Chen, Q. Y.; Li, Z. T. *J. Org. Chem.* **1993**, *58*, 2599.

(52) Chupp, J. P.; Balthazor, T. M.; Miller, M. J.; Pozzo, M. J. *J. Org. Chem.* **1984**, *49*, 4711.

(53) Gabe, E. J.; LePage, Y.; Charland, J. P.; Lee, F. L.; White, P. S. *J. Appl. Cryst.* **1989**, *22*, 284.

CHAPTER 4

Dynamic NMR Analysis of Electron-Deficient α-Diimine Ligands and Corresponding Pd(II) Complexes

Introduction

Metal complexes bearing α-diimine ligands have been known for nearly fifty years.[1] In this time, a tremendous amount of information about the synthesis and reactivity of these complexes has been developed.[1-14] The recent discovery that late transition-metal complexes bearing sterically bulky α-diimine ligands polymerize ethylene and α-olefins to high polymer[15] has stimulated extensive experimental[16-31] and theoretical[32-38] studies of the olefin polymerization behavior of these complexes.

α-Diimines have the general formula RN=C(R')-C(R")=NR, and they usually exist in solution in the *E* (trans) configuration at each imine functionality with an *s-trans* conformation about the C-C bond in the N=C-C=N backbone. Diimines containing a rigid napthalene backbone (Scheme 4.1) are not free to rotate about the C-C bond in the backbone, and the imine nitrogen atoms are fixed in a cis orientation. The aryl rings lie perpendicular to the plane formed by the conjugated napthylene/imine backbone system. As a consequence, addition of a single ortho substituent to each *N*-aryl ring leads to the formation of seven possible isomers: three pairs of enantiomers, and a meso compound (Scheme 4.1). Elsevier et. al. reported that in solution, only one isomer of each of the two diimines shown in Scheme 4.1 is observed by ^{1}H NMR spectroscopy, and that the isomer of each compound observed was one of the (*E*,*E*) forms.[39] Furthermore, these authors conclude that (1) one isomer is present in solution, or (2) fast exchange of all isomers is occurring on the NMR time scale. They

speculate that rotation of the phenyl rings about the N-C(Ar) bond will be hindered by an unfavorable steric interaction of the ortho aryl substituent with the naphthylene ring, and so interconversion of the syn and anti (*E*,*E*) isomers will therefore only proceed through the (*E*,*Z*) isomers. Elsevier and coworkers support this speculation with experimental evidence of similar behavior in camphorquinone dioximes,[40-44] as well as their own observation of a solvent-dependent equilibrium between the (*E*,*E*) and (*E*,*Z*) isomers of bis(phenylimino)camphane (Figure 4.1).[39]

Scheme 4.1. Mechanism of syn and anti isomer interconversion as proposed by Elsevier et. al. (R,R = Me, Me or *i*-Pr, *i*-Pr).[39] Enantiomers have been omitted for clarity.

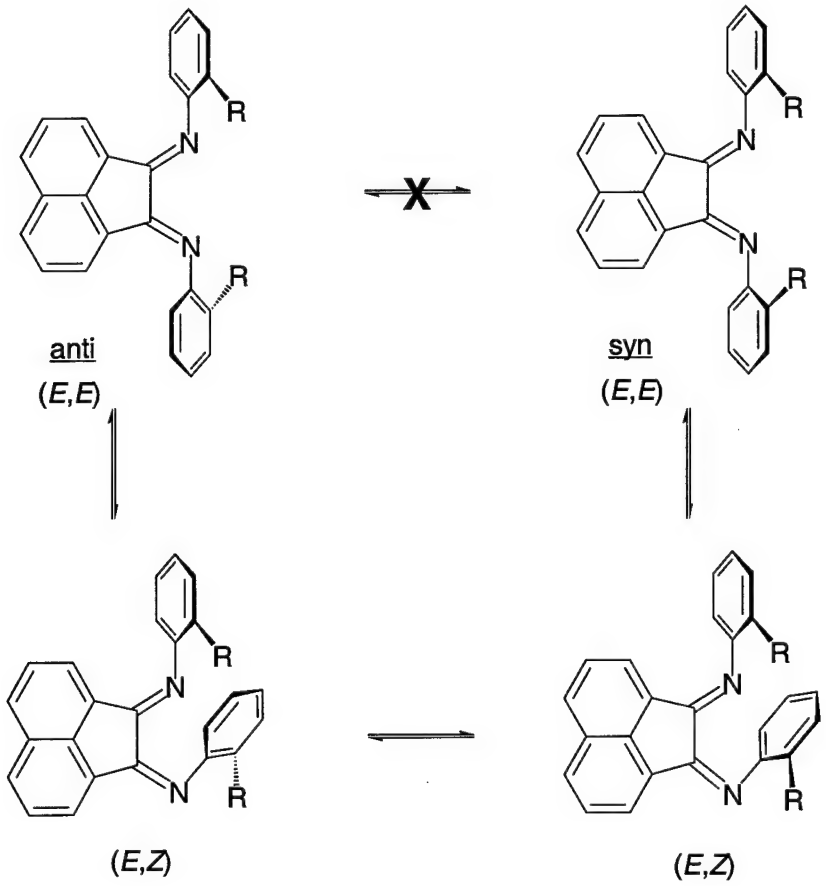

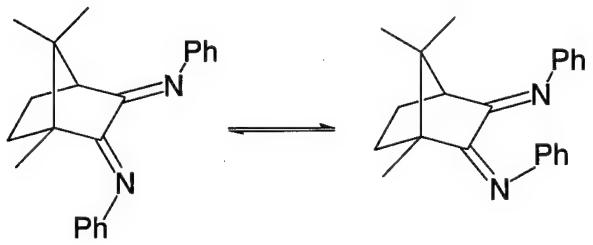

(*E*,*E*) (*E*,*Z*)

Figure 4.1. (*E*,*E*) and (*E*,*Z*) isomers of bis(phenylimino)camphane.[39]

Dr. Dan Tempel successfully separated the cis and trans isomers of a bulky 2-*tert*-butyl-6-methylphenyl substituted diimine by chromatography (Figure 4.2). No observable line broadening was observed when a $CDCl_3$ solution of the trans isomer was heated to 55 °C over several hours, and no appearance of the cis isomer was seen.[45] These results clearly indicate that isomerization of sterically bulky α-diimines containing a rigid backbone is highly unfavorable.

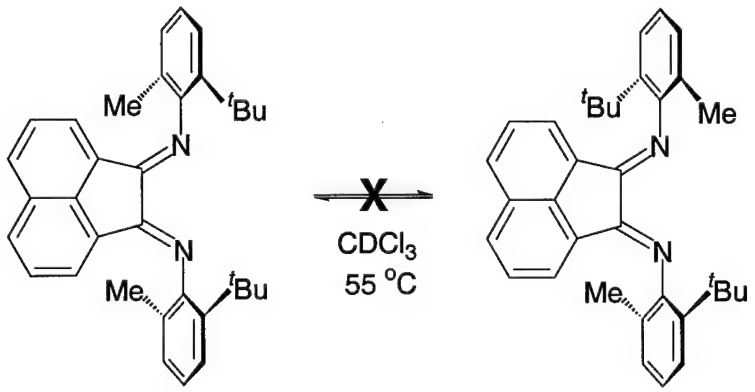

Figure 4.2. Cis and trans isomers of a sterically bulky diimine.[45]

The coordination of an unsymmetrically-substituted α-diimine ligand such as one of those shown in Figure 4.2 to a metal center leads to the possible formation of two isomers of the resulting metal complex. One isomer will have C_2 symmetry (the anti isomer), while the other will have C_S symmetry (the syn isomer). The presence of complexes of two different symmetries will have stereochemical consequences when the mixture is used as a catalyst. In olefin polymerization

reactions, such a mixture would be expected to lead to broadened polydispersities in the polymer products due to different rates of chain transfer and/or propagation for the two different complexes.

The synthesis of the unsymmetrically-substituted diimines **1** and **2** were described in Chapter 3. These diimines display complex dynamic behavior, which has been investigated and is described in this chapter. In addition, palladium dichloride and palladium methyl chloride complexes of **1** have been prepared in order to investigate the likelihood of rotation of the phenyl ring about the N-C(Ar) bond when the diimine is bound to a metal center. The dynamics of the palladium methyl chloride have been explored, and the results are presented below. The consequences of two different aryl ortho substituents upon coordination of the diimine to a metal center, and possible behavior of these complexes in olefin polymerization reactions, are discussed herein.

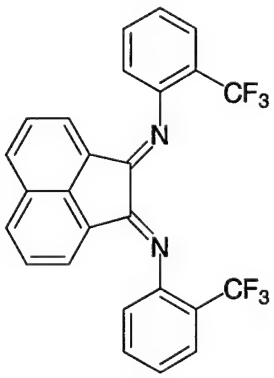

1

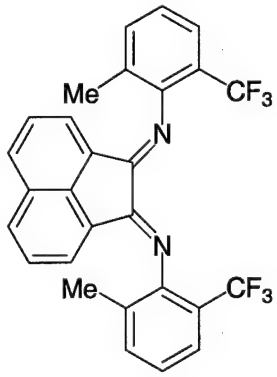

2

Results and Discussion

A. Dynamic Behavior of 1. Seven different structures (three pairs of enantiomers and a meso compound) for α-diimine **1** are possible. For the sake of simplicity, only one enantiomer from each enantiomeric pair will be used to represent these different structures, and these are shown in Figure 4.3. Since the *N*-aryl rings are perpendicular to the plane formed by the N=C(Nap)-C(Nap)=N backbone (Nap = 1,8-naphth-diyl), the *o*-CF_3 substituents on these aryl rings can be oriented in either a syn or an anti fashion to each other with respect to this plane. In addition, three (*E*,*E*) and four (*E*,*Z*) isomers are possible. Of the three (*E*,*E*) isomers, two are a pair of C_2-symmetric enantiomers ($\mathbf{1}_{anti}$), and the third is the C_S-symmetric meso compound ($\mathbf{1}_{syn}$); $\mathbf{1}_{anti}$ and $\mathbf{1}_{syn}$ are interconverted via an overall 180° rotation of an aryl ring about the N-C(Ar) bond. The four (*E*,*Z*) structures are C_1-symmetric ($\mathbf{1'}_{anti}$ and $\mathbf{1'}_{syn}$). Net inversion at a nitrogen atom interconverts **1** and **1'**.[46]

Diimine **1** exhibits a series of dynamic processes that may be studied by NMR spectroscopy. The simplest technique for monitoring these is ^{19}F NMR spectroscopy, since the CF_3 groups appear as singlets in these spectra. A series of ^{19}F NMR spectra were obtained over the temperature range of -100 to 30 °C in CD_2Cl_2 (Figure 4.4), and another series was collected from -30 to 140 °C in $C_2D_2Cl_4$ (Figure 4.5). Both series of spectra exhibit some dependence of the chemical shifts with changing temperature. At -100 °C, peaks corresponding to $\mathbf{1}_{syn}$, $\mathbf{1}_{anti}$, $\mathbf{1'}_{syn}$, and $\mathbf{1'}_{anti}$ are present. The symmetry of these isomers, and examination of the ^1H NMR spectra at this temperature, allows the assignment of the two major species to $\mathbf{1}_{anti}$ and $\mathbf{1}_{syn}$. At -100 °C, there is substantial viscosity broadening of the signals. As the temperature is increased from -100 °C to -30 °C, the peaks corresponding to $\mathbf{1'}_{anti}$ and $\mathbf{1'}_{syn}$ broaden and coalesce, indicating exchange is occurring between these isomers. At higher temperatures (e.g. -50 to 10 °C), the peaks corresponding to the (*E*,*E*) isomers $\mathbf{1}_{anti}$ and $\mathbf{1}_{syn}$ also broaden and coalesce, indicating exchange is occurring between these two isomers. At temperatures above 20 °C, all peaks broaden, and eventually coalesce into a single peak at 110 °C. Fast exchange of all isomers therefore occurs at high temperature.

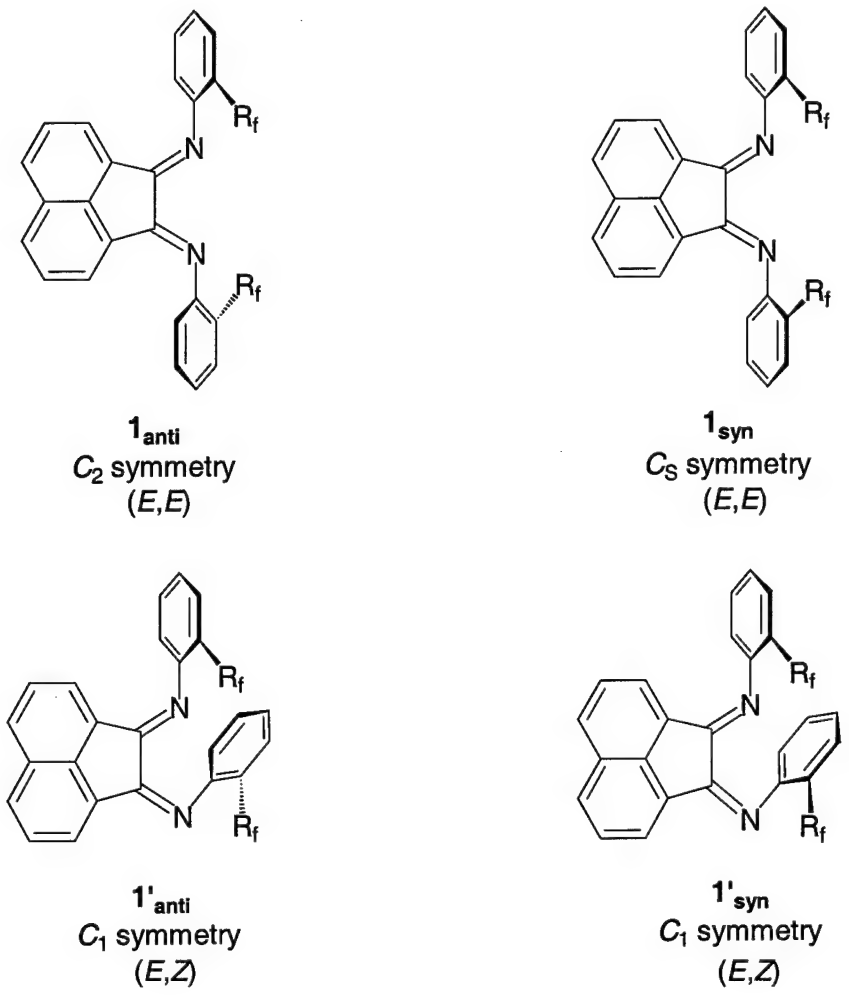

Figure 4.3. Possible structures of α-diimine **1** ($R_f = CF_3$, the enantiomers of each isomer are omitted for clarity).

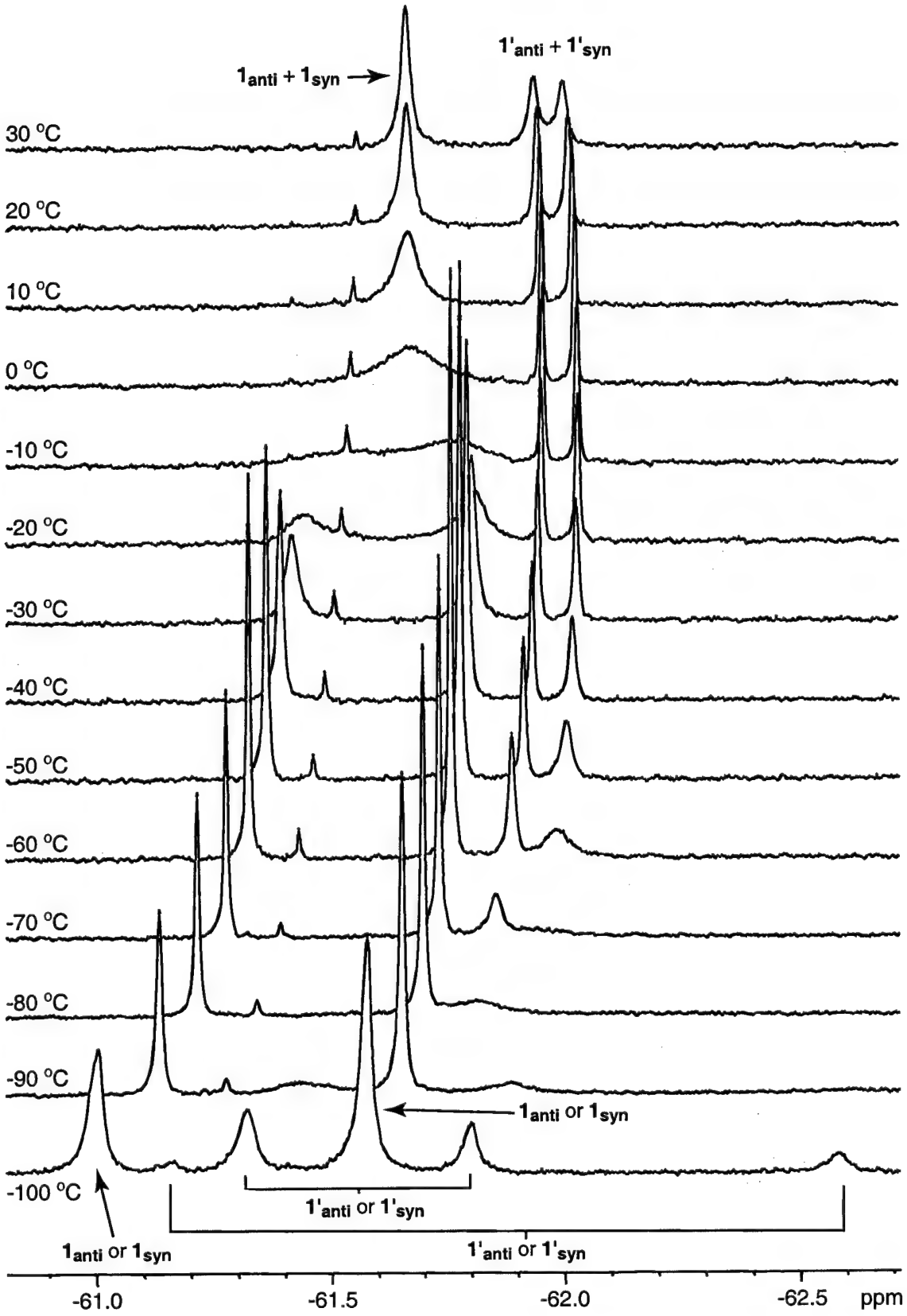

Figure 4.4. Variable-temperature ^{19}F NMR spectra of **1**, CD_2Cl_2, 471 MHz.

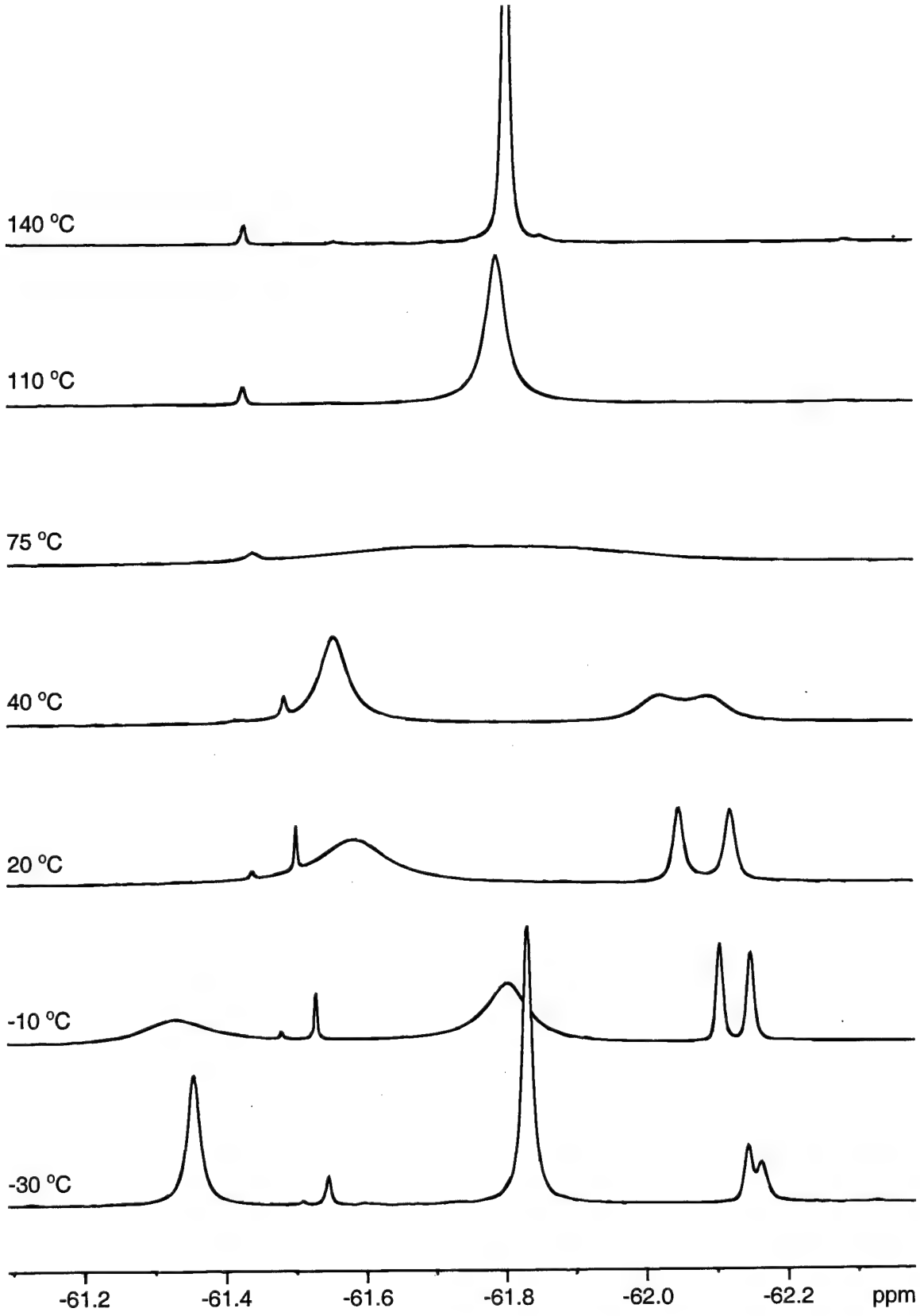

Figure 4.5. Variable-temperature ^{19}F NMR spectra of **1**, $C_2D_2Cl_4$, 376 MHz.

The dynamic processes in **1** observed by ^{19}F NMR spectroscopy are summarized in Scheme 4.2. Three distinct processes are observed: (1) exchange of the C_1-symmetric species ($\mathbf{1'}_{anti}$ and $\mathbf{1'}_{syn}$, process A), (2) exchange of the C_2/C_S-symmetric species ($\mathbf{1}_{anti}$ and $\mathbf{1}_{syn}$, process B), and (3) exchange of the C_2/C_S-symmetric species with the C_1-symmetric species (**1** and **1'**, process C). Approximate rate constants for these processes can be obtained from line-shape analysis of the spectra, and these are shown in Table 4.1. Because there are unequal populations of the various isomers exchanging with one another, there are two rates (and two energy barriers) associated with each exchange process. Since the assignment of the peaks observed in the NMR spectra to unique structures is not possible, assignment of a given rate and corresponding barrier may only be made to a particular exchange process, but not to a specific direction within that exchange process.

The variable-temperature ^{19}F NMR experiments establish that exchange of $\mathbf{1}_{anti}$ and $\mathbf{1}_{syn}$ does not take place through $\mathbf{1'}_{anti}$ and $\mathbf{1'}_{syn}$ as intermediates, which is the pathway proposed by Elsevier et. al. (Scheme 4.1)[39] Instead, $\mathbf{1}_{anti}$ and $\mathbf{1}_{syn}$ exchange directly with each other via rotation of a phenyl ring about a N-C(Ar) bond, with a barrier to rotation of about 12.5 kcal/mol. Furthermore, $\mathbf{1'}_{anti}$ and $\mathbf{1'}_{syn}$ exchange directly with one another, presumably through the same aryl ring rotation process, and the barrier to this exchange is low (ca. 9 kcal/mol). Exchange of **1** with **1'** has the highest energy barrier of the three processes, about 16 kcal/mol.

Scheme 4.2. Dynamic processes in **1**.

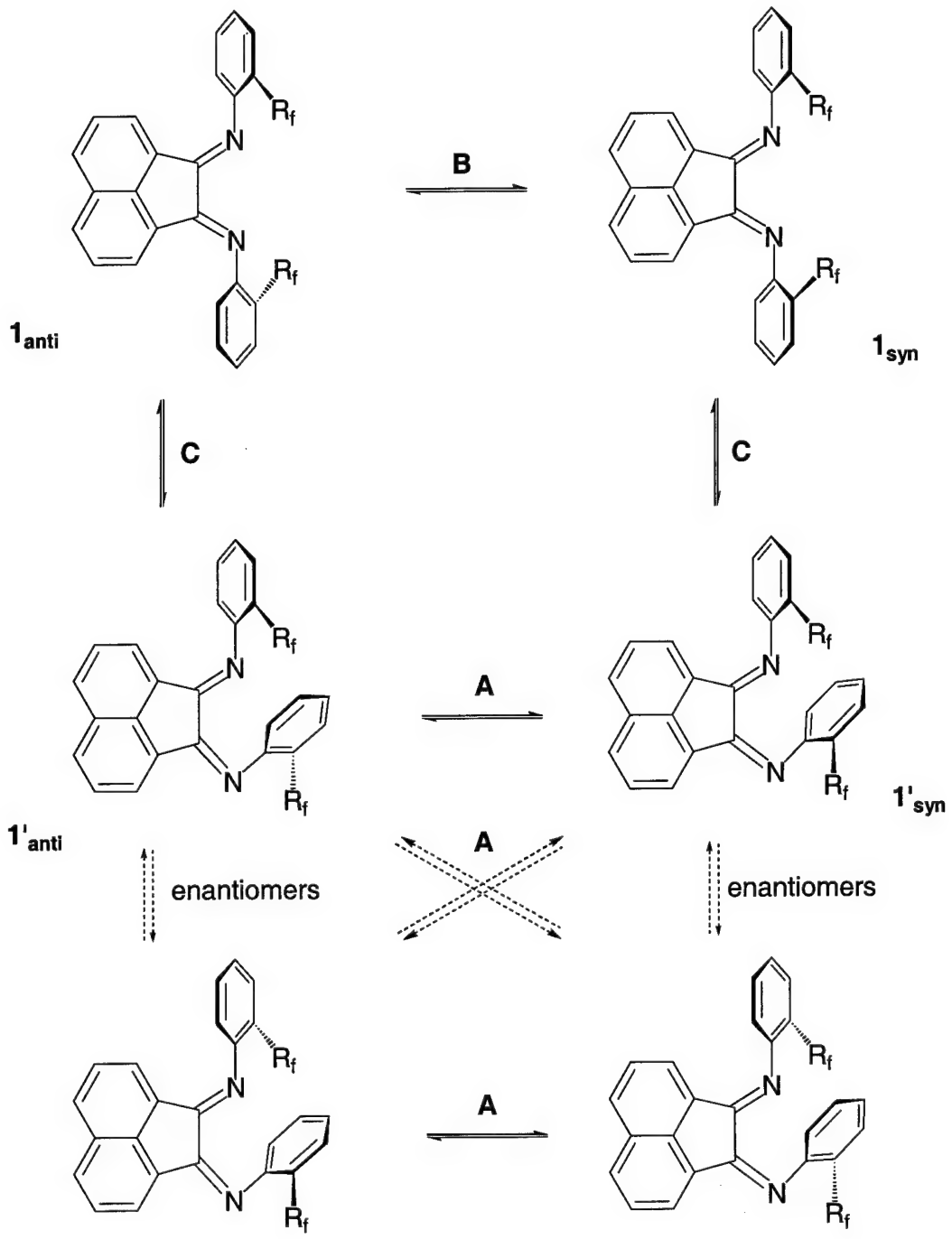

Table 4.1. Exchange Rate Constants and Energy Barriers for **1**.

Exchange Process[a]	ΔW[b]	k (temp)[c]	$\Delta G^{\ddagger}$, kcal/mol
A	10 Hz[d]	31 s^{-1} (-95 °C)	9.0
	5 Hz[d]	16 s^{-1} (-95 °C)	9.3
B	10.7 Hz	34 s^{-1} (-30 °C)	12.4
	7.5 Hz	24 s^{-1} (-30 °C)	12.6
C	8.0 Hz	25 s^{-1} (30 °C)	15.8
	7.3 Hz	23 s^{-1} (30 °C)	15.9

[a]Exchange processes shown in Scheme 4.2. [b]Difference in linewidth (half-height) at this temperature as compared to the non-broadened (natural) linewidth. [c]From the slow exchange approximation: $k = \pi(\Delta W)$. [d]Natural linewidth estimated as 2 Hz.

B. Dynamic Behavior of 2. Diimine **1** only has one *o*-aryl substituent on each phenyl ring, which allows the rotation about the N-C(Ar) bond in the (*E*,*E*) isomers to take place. Incorporation of a non-hydrogen substituent in the second ortho position would be anticipated to make this rotation much more unfavorable, especially when the diimine is coordinated to a metal. The effect of a second *o*-aryl substituent (a methyl group) on the dynamic processes just described for **1** was investigated using **2**. Diimine **2** has the same spectroscopic "handle" as **1** (the *o*-CF_3 group), making it an ideal candidate for dynamic studies. Diimine **2** has the same number of possible isomers (3 pairs of enantiomers plus a meso compound) with the same symmetry elements that are possible for **1**, and these are shown in Figure 4.6.

Due to the symmetry of the possible isomers of diimine **2**, a maximum of four isomers are expected to be observed by ^1H or ^{19}F NMR spectroscopy. All four are indeed visible, and as was observed for **1**, the two major isomers in a $C_2D_2Cl_4$ solution are the (*E*,*E*) isomers ($\mathbf{2}_{syn}$ and $\mathbf{2}_{anti}$). The four isomers are found in the ratio of 49:30:14:7 as determined by ^1H NMR spectroscopy (-25 °C, $C_2D_2Cl_4$). Once again, it was not possible to assign NMR resonances to a particular isomer. A ^1H-^1H NOESY spectrum (two-dimensional nuclear Overhauser spectroscopy) was acquired in the hope that cross peaks would be seen for the isomers with methyl substituents in near proximity ($\mathbf{2}_{syn}$ and $\mathbf{2'}_{syn}$), but no cross peaks were observed.[47]

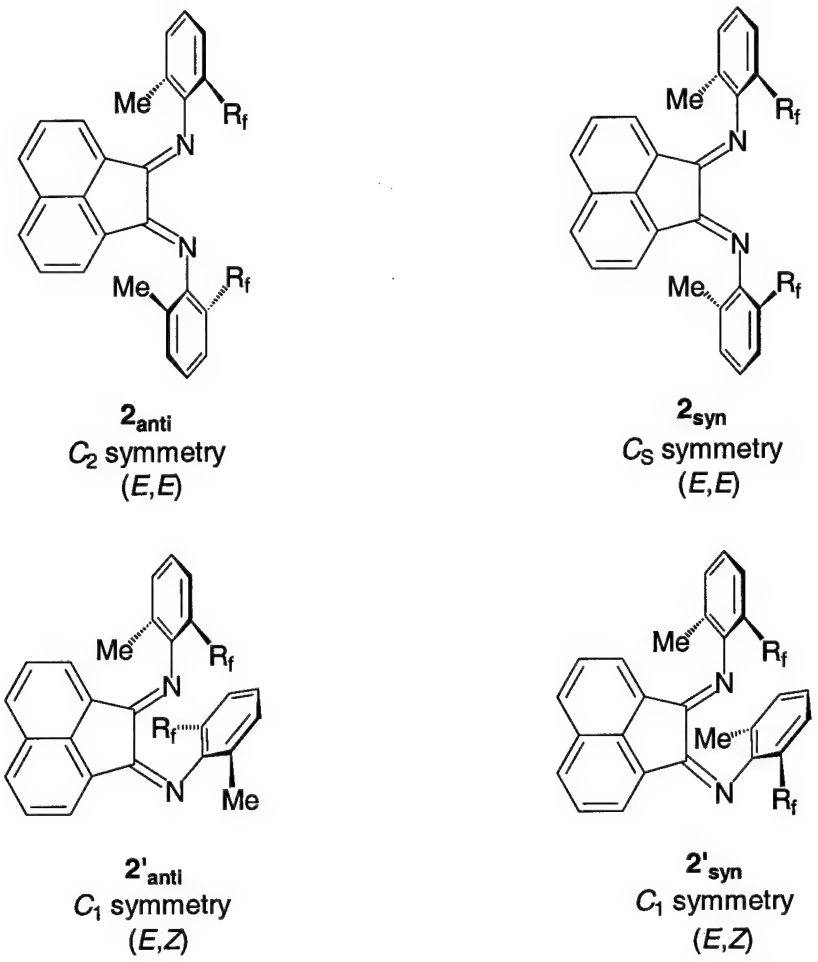

Figure 4.6. Possible structures of α-diimine **1** ($R_f = CF_3$, the enantiomers of each isomer are omitted for clarity).

Diimine **2** demonstrated dynamic behavior that could be followed by variable-temperature ^{19}F NMR spectroscopy. A series of ^{19}F NMR spectra of **2** in $C_2D_2Cl_4$ were acquired over the temperature range of -30 to 120 °C (Figure 4.7). At -30 °C, all four isomers are visible. As the temperature was warmed through room temperature, all peaks began to broaden, then coalesced into two peaks of unequal areas above 80 °C. These two peaks continue to sharpen as the temperature is increased to 120 °C. Seven signals for each species are observed in the ^1H NMR spectrum at 120 °C, which indicates that the two species have C_2 or C_S symmetry on the NMR time scale.

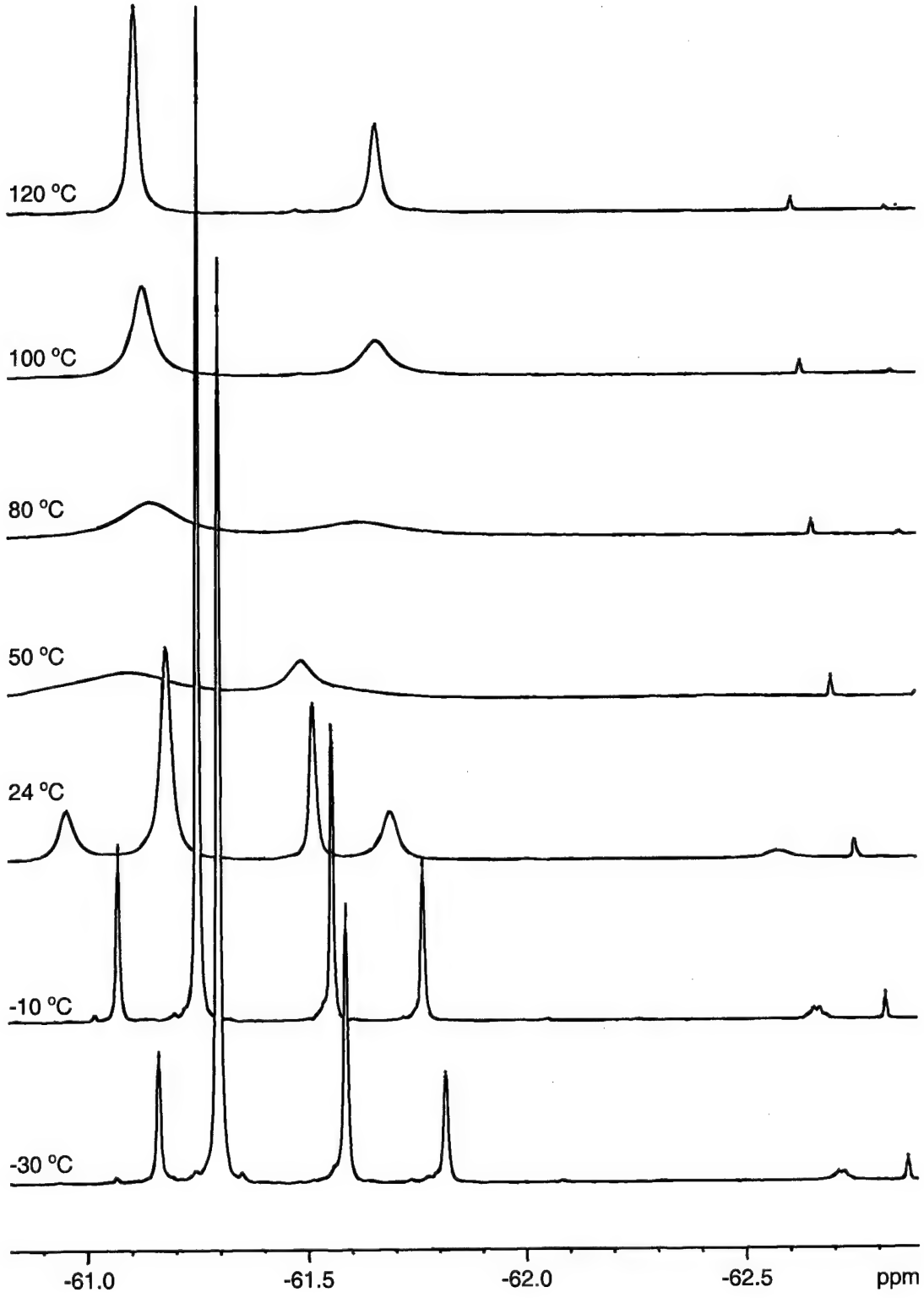

Figure 4.7. Variable-temperature ^{19}F NMR spectra of **2**, $C_2D_2Cl_4$, 376 MHz.

The dynamic processes that are observed in **2** are summarized in Scheme 4.3. Direct exchange between $\mathbf{2}_{anti}$ and $\mathbf{2}_{syn}$ (Path B) is not observed on the NMR time scale, even at 120 °C. In addition, exchange between the $\mathbf{2'}_{syn}$ and $\mathbf{2'}_{anti}$ isomers is not observed. An important implication of these observations is that the aryl rings will be locked in place upon coordination to a metal. An unsymmetrically-substituted diimine such as **2** will therefore form two different isomers upon formation of the nickel or palladium complexes used in olefin polymerizations. Furthermore, the ratio of these two isomers will remain fixed throughout the duration of the polymerization.

Scheme 4.3. Dynamic processes in **2**.

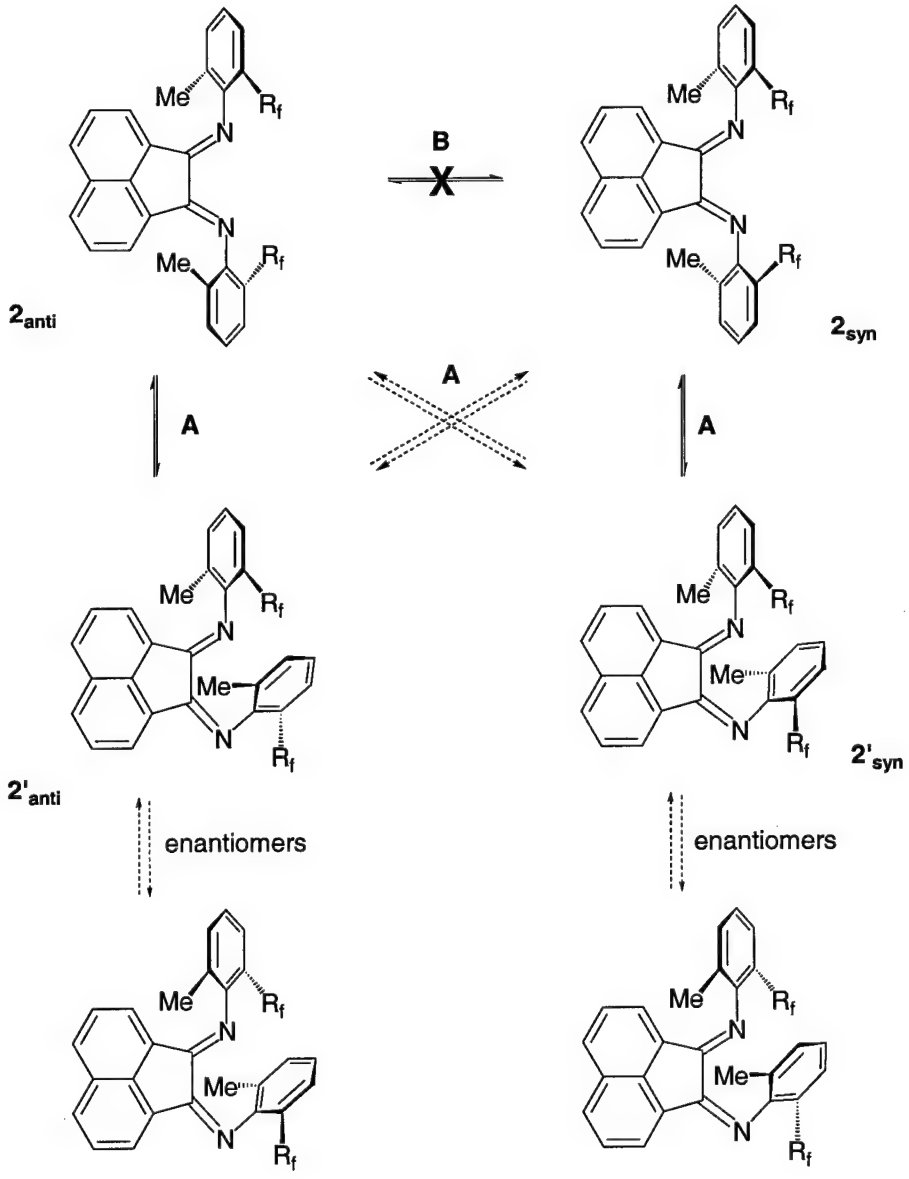

C. Dynamic Behavior of Palladium Complexes of 1. The spectroscopic "handle" present in diimine **1** in the form of the trifluoromethyl substituents makes it possible to observe whether or not net rotation of the aryl rings occurs while the ligand is coordinated to a metal. To further investigate this possibility, the palladium dichloride and palladium methyl chloride complexes of diimine ligand **1** were synthesized.

The synthesis of the palladium dichloride complex **3** is shown in Scheme 4.4. Palladium dichloride complex **3** was isolated as an air-stable yellow-orange solid. This complex is insoluble in diethyl ether, and is only sparingly soluble in chloroform. Only one isomer is observed in the ^{1}H NMR spectrum. Two isomers are observed by ^{19}F NMR ($CDCl_3$ solvent), and are presumably the syn and anti isomers. At -50 °C, these isomers exist in a 25:1 ratio. At 40 °C, the smaller peak broadens considerably, but it is still clearly visible. The integral of the smaller peak was not reliable at 40 °C, so the ratio of the two species was not determined at this temperature. The broadening of the smaller peak at 40 °C hints that slow exchange between the syn and anti isomers may be taking place at this temperature. The observed isomer ratios are somewhat surprising given the more equal relative ratios of the free ligand $\mathbf{1}_{syn}$ and $\mathbf{1}_{anti}$.

Scheme 4.4. Synthesis of palladium dichloride complex **3**.

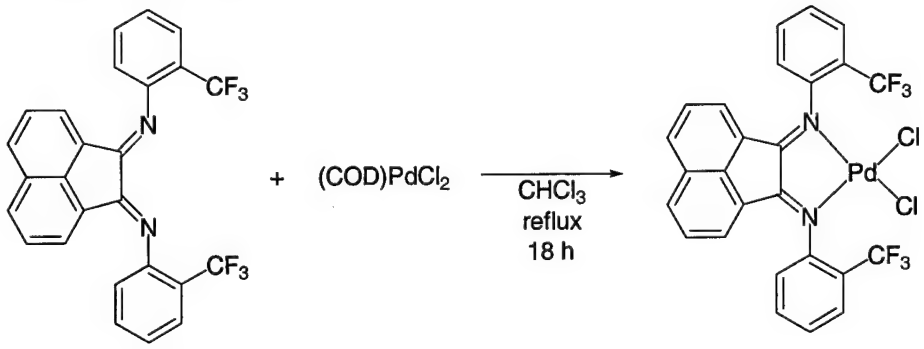

1 **3**

The poor solubility of **3** coupled with the observed isomer ratios made this complex a poor candidate for dynamic studies. However, the palladium methyl chloride complex **4** proved to be a better choice for dynamic studies. Complex **4** was synthesized by reaction of diimine ligand **1** with

(COD)Pd(Me)Cl in Et_2O (Scheme 4.5). Complex **4** is an air-stable brick-red solid, and is soluble in diethyl ether and halogenated hydrocarbon solvents. Only one set of resonances is clearly visible in the ^1H NMR spectrum, but resonances for both $\mathbf{4}_{anti}$ and $\mathbf{4}_{syn}$ are easily observed by ^{19}F NMR. The ratio of these isomers is 18:1 at 20 °C ($C_2D_2Cl_4$ solvent), and this ratio remains essentially constant over a time period of 30 min at this temperature. As was the case with the diimine compounds **1** and **2**, assignment of NMR resonances to specific isomers of **4** was not possible. At higher temperatures, **4** exhibits dynamic behavior.

Scheme 4.5. Synthesis of palladium methyl chloride complexes $\mathbf{4}_{anti}$ and $\mathbf{4}_{syn}$ from **1**.

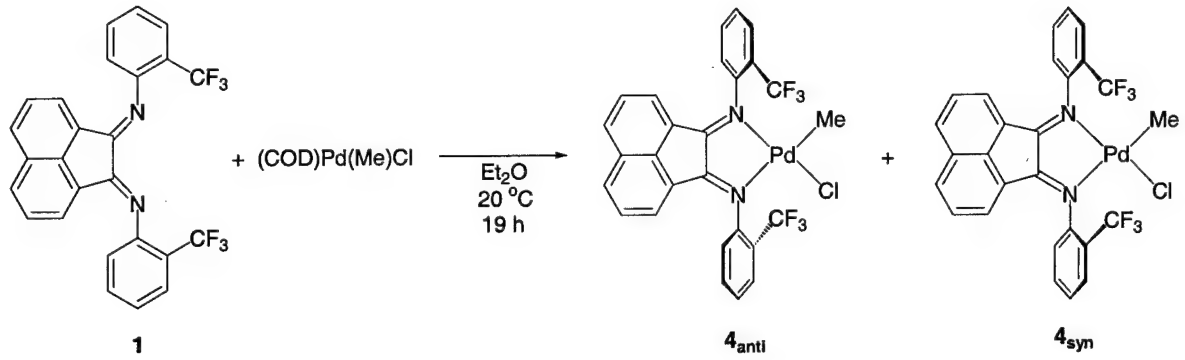

1 $\mathbf{4}_{anti}$ $\mathbf{4}_{syn}$

A series of variable-temperature ^{19}F NMR spectra of complex **4** were acquired (Figure 4.8). Spectra were obtained at temperatures ranging from -30 to 120 °C. From -30 to 20 °C, no significant changes are observed, so these spectra were not included in Figure 4.8. At 40 °C, the signals of the *major* isomer begin to broaden. At 60 °C, the minor isomer signals begin to broaden as well. However, coalescence of the major and minor resonances is not observed, even at temperatures as high as 120 °C. Upon cooling to 25 °C, the two isomers are present in a 2:1 ratio, which is not changed further after additional heating. Slow decomposition of the palladium complex is observed at temperatures above 100 °C. Free diimine ligand **1** is slowly formed, as well as some unidentified fluorinated species. Methane and methyl chloride are also slowly formed at these elevated temperatures. A palladium mirror was seen in the NMR tube upon removal from the probe.

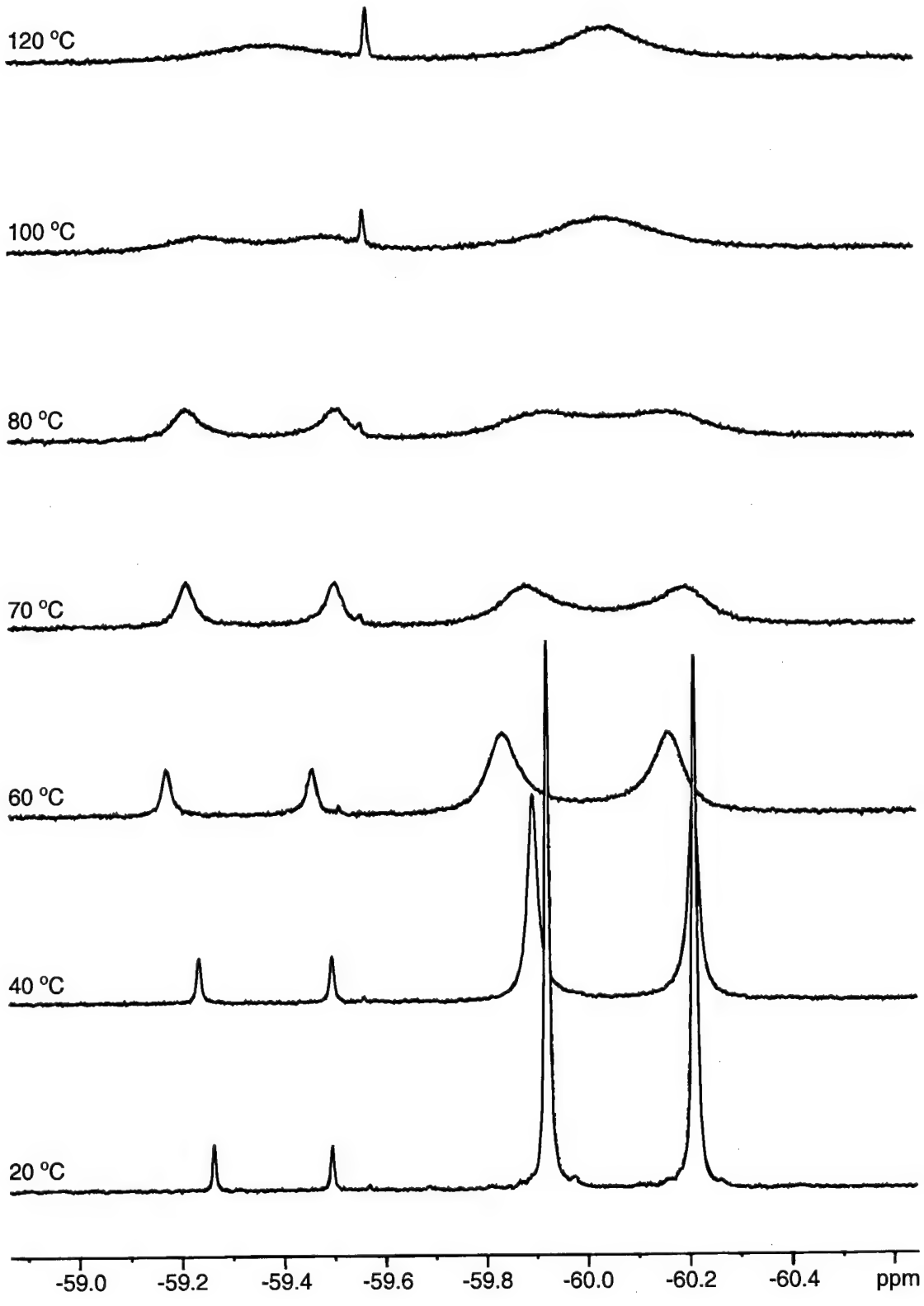

Figure 4.8. Variable-temperature ^{19}F NMR spectra of **4**, $C_2D_2Cl_4$, 376 MHz.

Several conclusions may be drawn from these variable-temperature NMR experiments. The initial broadening of the major isomer indicates that exchange of the two trifluoromethyl groups is occurring within this isomer. Since the major isomer signals begin to broaden before the minor isomer signals, the observed trifluoromethyl exchange is not an exchange of the syn and anti isomers. Instead, this data indicates site exchange is taking place through inversion at the palladium atom (Scheme 4.6). The precise mechanism by which this inversion proceeds was not determined, but inversion through a tetrahedral intermediate is one likely possibility. A rate constant of 19 s^{-1} (40 °C) for the inversion process occurring in the major isomer was determined by lineshape analysis. This corresponds to an "inversion barrier" at Pd of 16.5 kcal/mol at this temperature.

Scheme 4.6. Interconversion of $\mathbf{4}_{syn}$ and $\mathbf{4}_{anti}$, and site exchange of CF_3 and CF_3* nuclei through inversion at Pd.

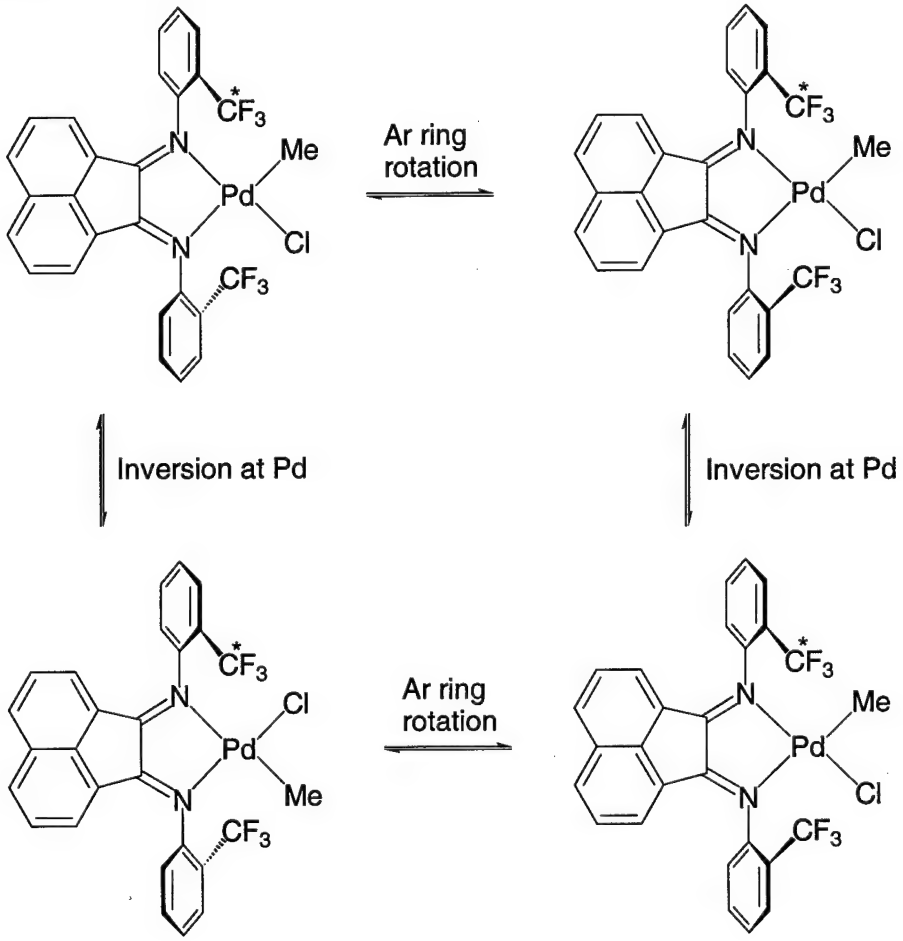

The observed ratios of $\mathbf{4}_{syn}$:$\mathbf{4}_{anti}$ at various temperatures indicates that an equilibrium exists between these two isomers. After the temperature was raised to 120 °C for 20 min, and then rapidly lowered to 25 °C, a 2:1 ratio of the two isomers was seen. Further heating and cooling resulted in no further changes in this ratio. Assuming the syn and anti isomers have reached equilibrium at 120 °C, the rapid cooling to 25 °C is essentially a thermal quenching of the equilibrium ratios of the two isomers that exists at 120 °C. The 18:1 ratio observed immediately following the synthesis of **4** reflects a kinetic ratio that results from "trapping" of the various isomers of **1** upon coordination of the metal. Since the kinetic ratio is essentially constant at 25 °C, the barrier to exchange of $\mathbf{4}_{syn}$ and $\mathbf{4}_{anti}$ is high. Assuming that exchange of these isomers is a simple first-order process, and furthermore, that $t_{1/2}$ for this process is approximately 1 h, a lower boundary estimate of the barrier for interconversion of $\mathbf{4}_{syn}$ and $\mathbf{4}_{anti}$ is 22 kcal/mol at 25 °C. This high barrier indicates that rotation of a ligand aryl ring while the ligand is bound to a metal is unfavorable. Furthermore, since this experiment was conducted with a ligand bearing only a single, relatively small ortho aryl substituent, ligands with aryl rings incorporating two bulkier ortho aryl substituents will be essentially locked in place throughout the duration of a typical polymerization experiment. In addition, diimine ligands with two different ortho aryl substituents can form two possible isomers (syn and anti) upon coordination to a metal. Consequently, metal complexes of two different symmetries will be present in olefin polymerization mixtures in which these complexes are employed as catalysts, which could result in broadening of the polydispersities of the polymers formed by these complex mixtures.

Conclusions

Diimine compounds containing an *o*-CF_3 substituent demonstrate dynamic behavior corresponding to exchange of syn and anti, as well as (*E*,*E*) and (*E*,*Z*) isomers. The ratio of the (*E*,*E*):(*E*,*Z*) isomers of the mono *o*-CF_3 substituted diimine **1** is 3.8:1 at 23 °C in $C_2D_2Cl_4$. Dynamic NMR studies of **1** found that the barriers to exchange increases in the order $(E,Z)_{syn}/(E,Z)_{anti} < (E,E)_{syn}/(E,E)_{anti} <$

(*E*,*E*)/(*E*,*Z*). Direct exchange of the $(E,E)_{syn}$ and $(E,E)_{anti}$ isomers is observed, which presumably occurs via rotation of the aryl ring about the N-C(Ar) bond.

Addition of a methyl group to the other ortho aryl position in **1** forms diimine **2**. Dynamic NMR studies of **2** show that at higher temperatures, exchange of the $(E,E)_{syn}$ isomer with either the $(E,Z)_{syn}$ or $(E,Z)_{anti}$ isomer takes place, while a similar exchange of the $(E,E)_{anti}$ isomer with either the $(E,Z)_{anti}$ or $(E,Z)_{syn}$ isomer takes place. Direct exchange of the $(E,E)_{syn}$ and $(E,E)_{anti}$ isomers is not observed, even at 120 °C. The rotation of the aryl ring about the N-C(Ar) bond is therefore greatly hindered by the presence of two ortho aryl substituents on each phenyl ring.

Upon complexation of **1** to palladium, a mixture of syn and anti kinetic products is obtained. Dynamic studies of the palladium methyl chloride complex of **1** showed that upon heating to 120 °C, the initial ratio of kinetic isomers (18:1 at 20 °C) is reduced to a 2:1 ratio. The studies also found that an inversion process occurs at palladium by which the Me and Cl substituents are exchanged. The "inversion barrier" at palladium of 16.5 kcal/mol (40 °C) was calculated for one of the two isomers. The mechanism of this inversion was not determined, but it is likely taking place through a square-planar-tetrahedral-square planar isomerization process at palladium.

These experiments confirm that the aryl rings of diimine ligands containing two non-hydrogen ortho aryl substituents are locked in place once coordinated to palladium. It is anticipated that this conclusion also holds true for nickel diimine complexes. If the substituents are different, two kinetic isomers are possible upon formation of the metal complexes. Due to the high barriers to rotation about the diimine N-C(Ar) bond in the metal complexes, this kinetic isomer ratio will persist on the time scale of most typical olefin polymerization reactions catalyzed by these complexes.

Experimental Section

General Methods. All manipulations of air- and/or water-sensitive compounds were performed using standard high-vacuum or Schlenk techniques. Argon was purified by passage through columns of BASF R3-11 catalyst (Chemalog) and 4-Å molecular sieves. Solid organometallic compounds were transferred in an argon-filled Vacuum Atmospheres drybox. ^{1}H, ^{13}C, and ^{19}F NMR spectra were recorded on Bruker Avance-500, -400, or -300 MHz spectrometers. Chemical shifts are reported relative to residual $CHCl_3$ (δ 7.24 for ^{1}H), C_2HDCl_4 (δ 5.93 for ^{1}H), $CDCl_3$ (δ 77.00 for ^{13}C), and CCl_3F (δ 0.00 for ^{19}F). NMR probe temperatures were calibrated with an external methanol sample. Temperatures beyond the liquid range of methanol were extrapolated.

Materials. Diethyl ether was purified using procedures reported by Pangborn et. al.[48] The α-diimine ligands were prepared using the procedures described in Chapter 3. (COD)PdMeCl was prepared according to the literature.[49]

(ArN=C(An)-C(An)=NAr) (Ar = 2-$CF_3C_6H_4$) (1). The synthesis of this compound as well as the ^{1}H, ^{13}C, and ^{19}F NMR spectra for the averaged structures of $\mathbf{1}_{syn}$ and $\mathbf{1}_{anti}$ were reported in Chapter 3. At 23 °, the ^{1}H, ^{13}C, and ^{19}F spectra of $\mathbf{1}_{syn}$ and $\mathbf{1}_{anti}$ are averaged on the NMR time scale, as are the ^{1}H and ^{19}F spectra of $\mathbf{1'}_{syn}$ and $\mathbf{1'}_{anti}$. The ratio of **1**:**1'** is 3.8:1 at 23 °C in $C_2D_2Cl_4$. The spectroscopic assignments for the averaged isomers $\mathbf{1'}_{syn}$ and $\mathbf{1'}_{anti}$ were determined by ^{1}H (Figure 4.9) and ^{1}H-^{1}H COSY (Figure 4.10) NMR spectroscopy and are reported here. Several of these peaks were obscured by the averaged resonances of $\mathbf{1}_{syn}/\mathbf{1}_{anti}$, but the chemical shifts and multiplicities of these peaks could be determined by the cross peaks in the COSY spectrum: ^{1}H NMR ($C_2D_2Cl_4$, 23 °C, 500 MHz, **1'**) δ 8.13 (d, J = 7.5 Hz, 1H, H_c'), 7.99 (d, J = 7.5 Hz, 1H, H_a'), 7.90 (d, J = 8.0 Hz, 1H, H_a), 7.77 (apparent t, 1H, H_b'), 7.57 (d, 1H, H_d or H_d'), 7.52 (d, J = 7.0 Hz, 1H, H_d' or H_d), 7.40 (apparent t, 1H, H_f or H_f'), 7.38 (apparent t, 1H, H_f' or H_f), 7.29 (apparent t, 1H, H_b), 7.17 (apparent t, 1H, H_e or H_e'), 7.03 (apparent t, 1H, H_e' or H_e), 6.90 (d, J = 7.0 Hz, 1H, H_g' or H_g), 6.65 (d, J = 7.5 Hz, H_g or

H_g'), 6.45 (d, J = 6.5 Hz, 1H, H_c); ^{19}F NMR ($C_2D_2Cl_4$, 20 °C, 471 MHz) δ -61.9 (s, 3F, CF_3), -62.0 (s, 3F, CF_3').

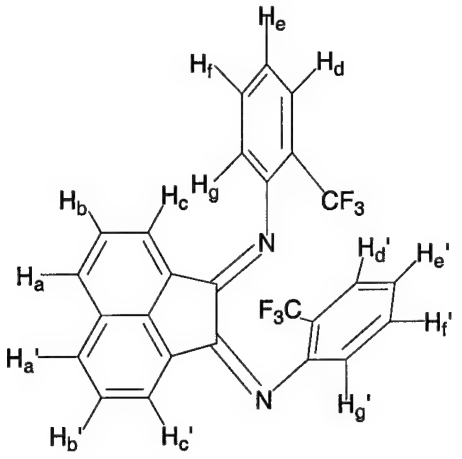

1'

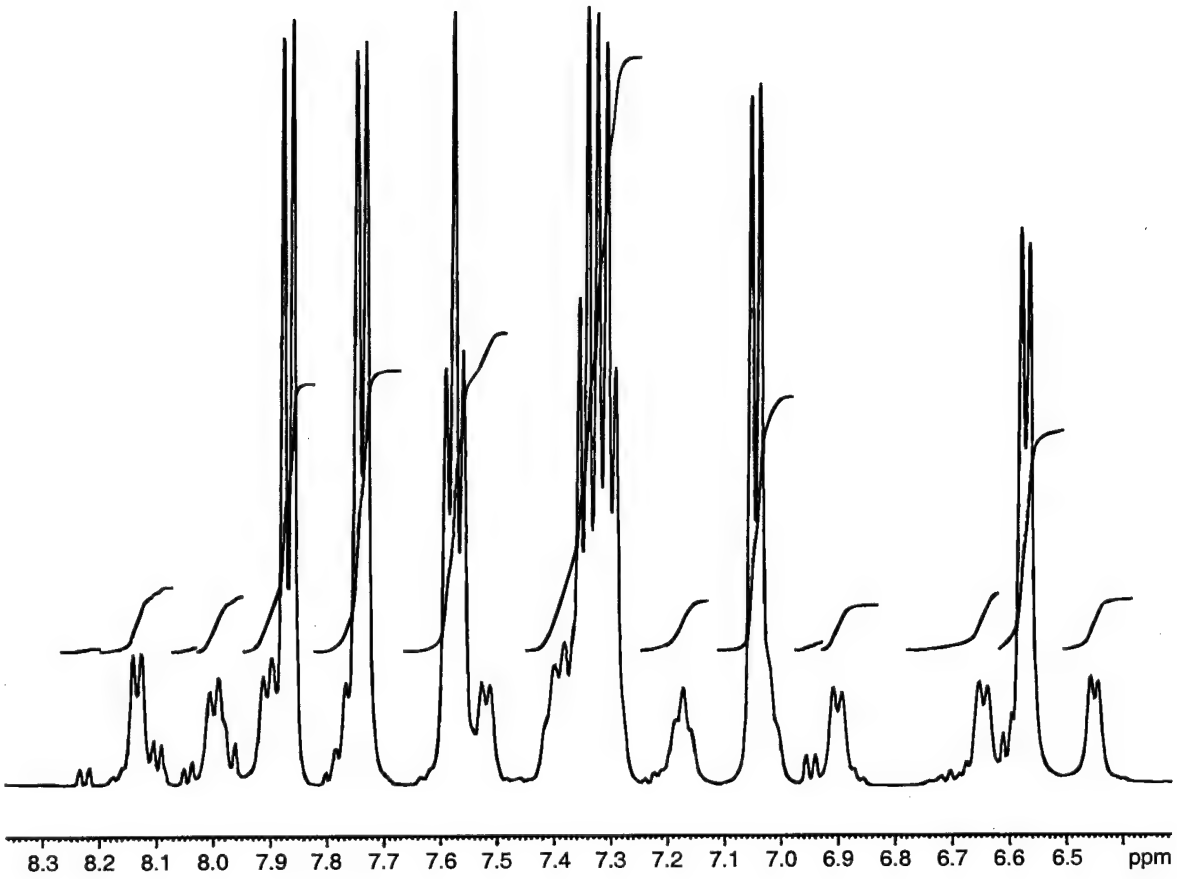

Figure 4.9. ^{1}H NMR spectrum of **1**, $C_2D_2Cl_4$, 22 °C, 500 MHz.

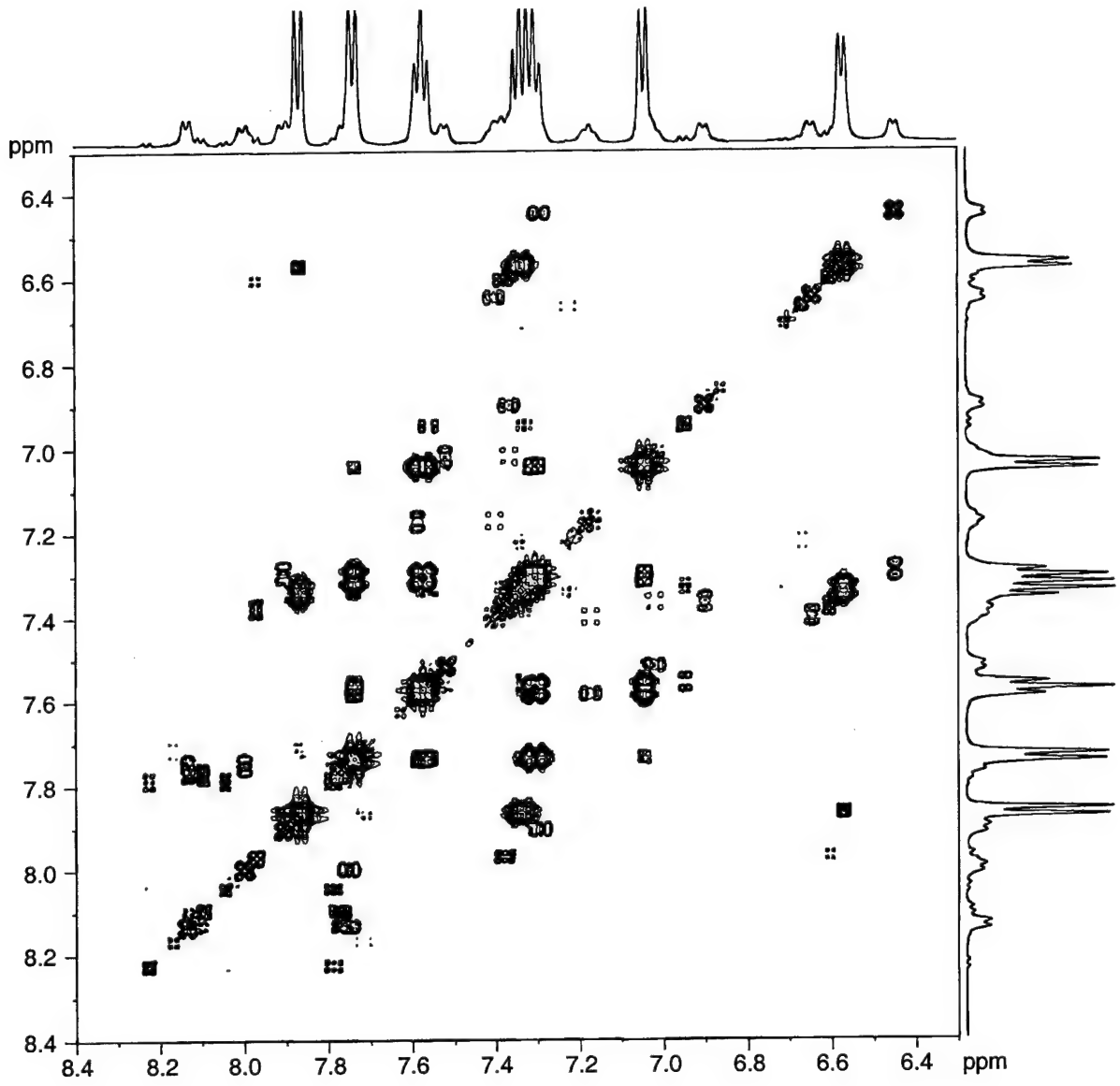

Figure 4.10. ^{1}H-^{1}H COSY NMR spectrum of **1**, $C_2D_2Cl_4$, 22 °C, 500 MHz.

(ArN=C(An)-C(An)=NAr) (Ar = (2-CF_3-6-CH_3)C_6H_3) (2). The synthesis of this compound as well as the ^{1}H and ^{13}C NMR spectra for the most abundant isomer were reported in Chapter 3. The product exists as four distinct isomers at -25 °C in $C_2D_2Cl_4$. Two major isomers and two minor isomers are present in a 49:30:14:7 ratio. The two major isomers have C_2/C_S symmetry, while the two minor isomers have C_1 symmetry. The ^{1}H NMR spectrum of **2** (Figures 4.11 and 4.12) is sufficiently complex to preclude a complete spectroscopic assignment of all isomers. However, the ^{1}H-^{1}H COSY NMR spectrum (Figure 4.13) confirms that four product isomers with the

aforementioned symmetry are present in solution. An effort was made to assign resonances to specific isomers through a NOESY experiment, but no useful information was obtained from this experiment.

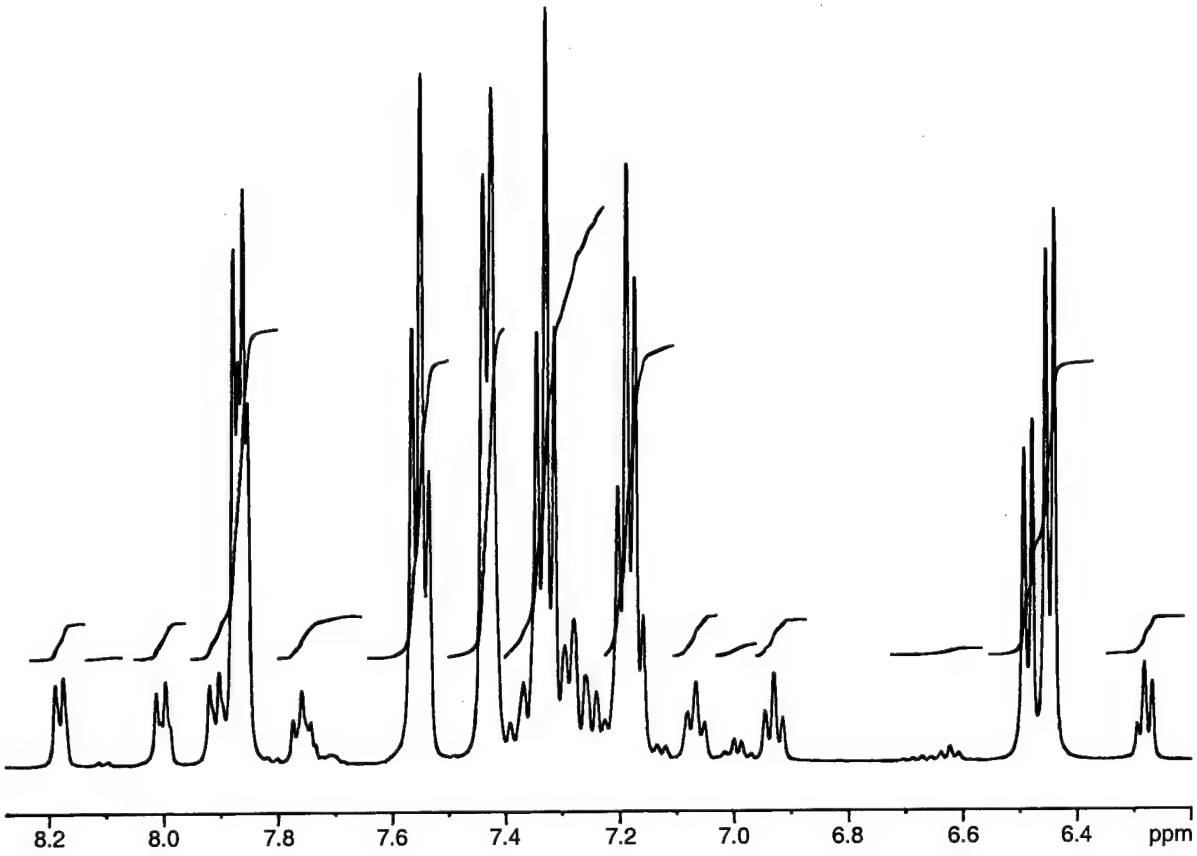

Figure 4.11. ^{1}H NMR spectrum (aromatic region) of **2**, $C_2D_2Cl_4$, -30 °C, 500 MHz.

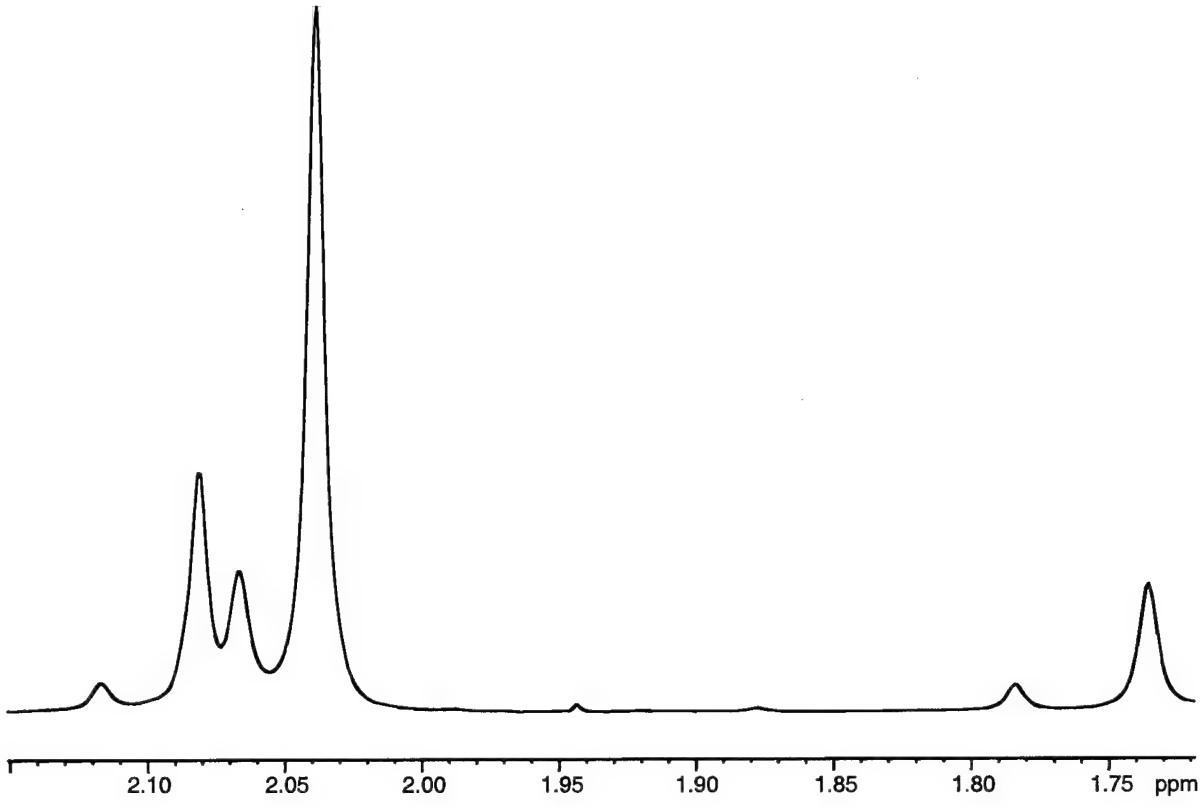

Figure 4.12. ^{1}H NMR spectrum (methyl region) of **2**, $C_2D_2Cl_4$, -10 °C, 500 MHz.

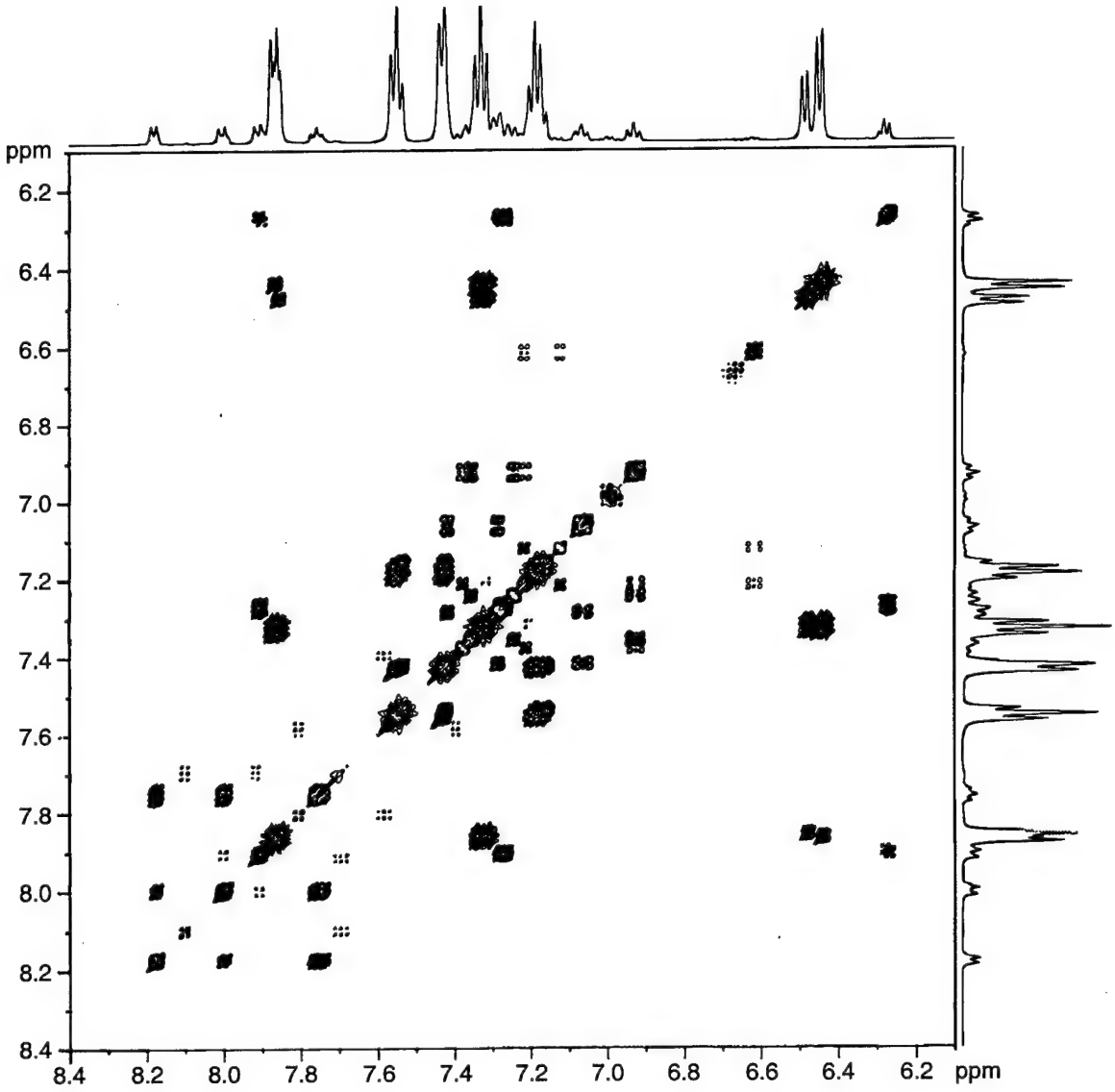

Figure 4.13. ^{1}H-^{1}H COSY NMR spectrum (aromatic region) of **2**, $C_2D_2Cl_4$, -30 °C, 500 MHz.

(ArN=C(An)-C(An)=NAr)$PdCl_2$ (Ar = 2-$CF_3C_6H_4$) (3). Diimine ligand **1** (580 mg, 1.25 mmol) and (COD)$PdCl_2$ (314 mg, 1.10 mmol) were combined in a Schlenk flask under an argon atmosphere. $CHCl_3$ (30 mL) was added via syringe, and the solution was purged with argon for 5 min. The reaction was heated to reflux, and stirred for 18 hours. Initially, the solution was a heterogeneous, yellow-orange solution. After 2 h, an orange precipitate formed, and the solution gradually changed to a red-brown color. After 18 h, the solution was cooled to room temperature, and the supernatant liquid was removed via a filter cannula. The product was washed with 2 X 10 mL Et_2O and dried in

vacuo. The palladium complex **3** was isolated as a yellow-orange powder. Complex **3** is insoluble in Et_2O, and is only sparingly soluble in $CHCl_3$. Only one isomer is clearly visible by ^1H NMR spectroscopy. Two isomers are observed by ^{19}F NMR spectroscopy ($CDCl_3$): the ratio of isomers is ca. 85:1 at 20 °C, and 25:1 at -50 °C. ^1H NMR ($CDCl_3$, -50 °C, 400 MHz) δ 8.20 (d, J = 8.3 Hz, 2H), 7.89 (d, J = 7.7 Hz, 2H), 7.82 (apparent t, 2H), 7.68 (apparent t, 2H), 7.55 (apparent t, 2H), 7.49 (d, J = 8.3 Hz, 2H), 6.53 (d, J = 7.3 Hz, 2H); ^{19}F NMR ($CDCl_3$, -50 °C, 376 MHz) δ -60.1 (major isomer), -59.2 (minor isomer).

(ArN=C(An)-C(An)=NAr)PdMeCl (Ar = 2-$CF_3C_6H_4$) (4). Diimine ligand **1** (580 mg, 1.25 mmol) and (COD)PdMeCl (300 mg, 1.10 mmol) were combined in a Schlenk flask under an argon atmosphere. Et_2O (30 mL) was added via syringe. The solution turned dark red. A red precipitate formed within the first 10 min of the reaction period. The reaction was allowed to stir at room temperature for 19 h. The filtrate was then removed via a filter cannula, then the precipitate was washed with 3 X 10 mL Et_2O and dried in vacuo. The palladium complex **4** was isolated as a brick-red powder (550 mg, 80% yield). An 18:1 ratio of two isomers is present in the ^{19}F NMR spectrum at 20 °C. Upon heating to 120 °C for ca. 20 min, followed by cooling back to room temperature, a 2:1 ratio of isomers is present. Only the resonances for the major isomer may be assigned in the ^1H and ^{13}C NMR spectra. ^1H NMR ($C_2D_2Cl_4$, 22 °C, 500 MHz) δ 8.07 (d, J = 8.3 Hz, 1H, An H_p), 8.03 (d, J = 8.3 Hz, 1H, An H_p'), 7.88 (d, J = 8.0 Hz, 1H), 7.80 (m, 2H), 7.73 (apparent t, 1H), 7.60 (apparent t, 1H), 7.43 (m, 2H, An H_m, H_m'), 7.31 (overlapping doublets, 2H), 6.57 (d, J = 2.5 Hz, 1H, An H_o'), 6.35 (d, J = 7.3 Hz, 1H, An H_o), 0.72 (s, 3H, Pd-CH_3); ^{13}C NMR ($C_2D_2Cl_4$, 0 °C, 125.8 MHz) δ 173.3, 168.6, 145.2, 144.5, 144.1, 134.2, 133.5, 132.3, 131.9, 131.5, 129.41, 129.37, 128.5, 128.2 (q, $^3J_{CF}$ = 4.6 Hz), 127.5, 127.4, 126.5, 125.6, 125.5, 125.4, 123.5 (q, $^1J_{CF}$ = 273 Hz, CF_3), 123.2 (q, $^1J_{CF}$ = 273 Hz, $C'F_3$), 122.7, 122.1, 122.0, 121.3 (q, $^2J_{CF}$ = 32 Hz), 2.5 (Pd-CH_3); ^{19}F NMR ($C_2D_2Cl_4$, 20 °C, 376 MHz) δ -59.9 (s, CF_3), -60.2 (s, CF_3'). Only one signal is visible in the ^1H NMR spectrum for the minor isomer: ^1H NMR ($C_2D_2Cl_4$, 22 °C, 500 MHz, minor isomer) δ 0.73 (s, Pd-CH_3); ^{19}F NMR ($C_2D_2Cl_4$, 20 °C, 376 MHz, minor isomer) δ -59.3 (s, CF_3), -59.5 (s, CF_3').

General Procedure for Variable-Temperature NMR Experiments. A high-grade 5 mm NMR tube (Wilmad 528-PP or 535-PP) was charged with ca. 15 mg of 1, 2, or 4, then was sealed with a rubber septum. The septum was wrapped with teflon tape to secure it in place, then ~700 μL of the appropriate solvent (CD_2Cl_2, $C_2D_2Cl_4$, or $CDCl_3$) was added via syringe. A small amount of CCl_3F (e.g. 2-3 drops) was added via a 22 gauge cannula as an internal standard for ^{19}F NMR spectra. The septum was wrapped with Parafilm and shaken until the sample was homogeneous. Variable-temperature NMR spectra were then recorded on high-field instruments (400 or 500 MHz). Following temperature adjustments, the NMR probe temperatures were allowed to stabilize for 15 min prior to acquisition of the next spectrum.

References and Notes

(1) van Koten, G.; Vrieze, K. *Adv. Organomet. Chem.* **1982**, *21*, 151-239.

(2) Klein, R. A.; Hartl, F.; Elsevier, C. J. *Organometallics* **1997**, *16*, 1284-1291.

(3) van Asselt, R.; Elsevier, C. J.; Amatore, C.; Jutand, A. *Organometallics* **1997**, *16*, 317-328.

(4) Groen, J. H.; Delis, J. G. P.; van Leeuwen, W. N. M.; Vrieze, K. *Organometallics* **1997**, *16*, 68-77.

(5) Groen, J. H.; Elsevier, C. J.; Vrieze, K.; Smeets, W. J. J.; Spek, A. L. *Organometallics* **1996**, *15*, 3445-3455.

(6) van Asselt, R.; Gielens, E. E. C. G.; Rülke, R. E.; Vrieze, K.; Elsevier, C. J. *J. Am. Chem. Soc.* **1994**, *116*, 977-985.

(7) van Asselt, R.; Rijnberg, E.; Elsevier, C. J. *Organometallics* **1994**, *13*, 706-720.

(8) van Asselt, R.; Elsevier, C. J.; Smeets, W. J. J.; Spek, A. L. *Inorg. Chem.* **1994**, *33*, 1521-1531.

(9) van Asselt, R.; Gielens, E. E. C. G.; Rülke, R. E.; Elsevier, C. J. *J. Chem. Soc., Chem. Commun.* **1993**, 1203-1205.

(10) Yang, K.; Lachicotte, R. J.; Eisenberg, R. *Organometallics* **1998**, *17*, 5102-5113.

(11) Yang, K.; Lachicotte, R. J.; Eisenberg, R. *Organometallics* **1997**, *16*, 5234-5243.

(12) Ganis, P.; Orabona, I.; Ruffo, F.; Vitagliano, A. *Organometallics* **1998**, *17*, 2646-2650.

(13) Fusto, M.; Giordano, F.; Orabona, I.; Ruffo, F.; Panunzi, A. *Organometallics* **1997**, *16*, 5981-5987.

(14) Carfagna, C.; Formica, M.; Gatti, G.; Musco, A.; Pierleoni, A. *Chem. Commun.* **1998**, 1113-1114.

(15) Johnson, L. K.; Killian, C. M.; Brookhart, M. *J. Am. Chem. Soc.* **1995**, *117*, 6414-6415.

(16) Svejda, S. A.; Brookhart, M. *Organometallics* **1999**, *18*, 65-74.

(17) Tempel, D. J.; Brookhart, M. *Organometallics* **1998**, *17*, 2290-2296.

(18) Mecking, S.; Johnson, L. K.; Wang, L.; Brookhart, M. *J. Am. Chem. Soc.* **1998**, *120*, 888-899.

(19) LaPointe, A. M.; Brookhart, M. *Organometallics* **1998**, *17*, 1530-1537.

(20) Killian, C. M.; Johnson, L. K.; Brookhart, M. *Organometallics* **1997**, *16*, 2005-2007.

(21) Killian, C. M.; Tempel, D. J.; Johnson, L. K.; Brookhart, M. *J. Am. Chem. Soc.* **1996**, *118*, 11664-11665.

(22) Johnson, L. K.; Mecking, S.; Brookhart, M. *J. Am. Chem. Soc.* **1996**, *118*, 267-268.

(23) Galland, G. B.; de Souza, R. F.; Mauler, R. S.; Nunes, F. F. *Macromolecules* **1999**, *32*, 1620-1625.

(24) McLain, S. J.; Feldman, J.; McCord, E. F.; Gardner, K. H.; Teasley, M. F.; Coughlin, E. B.; Sweetman, K. J.; Johnson, L. K.; Brookhart, M. *Macromolecules* **1998**, *31*, 6705-6707.

(25) Pellecchia, C.; Zambelli, A.; Mazzeo, M.; Pappalardo, D. *J. Mol Catal.* **1998**, *128*, 229-237.

(26) Schleis, T.; Spaniol, T. P.; Okuda, J.; Heinemann, J.; Mülhaupt, R. *J. Organomet. Chem.* **1998**, *569*, 159-167.

(27) Zeng, X.; Zetterberg, K. *Macromol. Chem. Phys.* **1998**, *199*, 2677-2681.

(28) Feldman, J.; McLain, S. J.; Parthasarathy, A.; Marshall, J.; Calabrese, J. C.; Arthur, S. D. *Organometallics* **1997**, *16*, 1514-1516.

(29) Pappalardo, D.; Mazzeo, M.; Pellecchia, C. *Macromol. Rapid Commun.* **1997**, *18*, 1017-1023.

(30) Pellecchia, C.; Zambelli, A.; Oliva, L.; Pappalardo, D. *Macromolecules* **1996**, *29*, 6990-6993.

(31) Pellecchia, C.; Zambelli, A. *Macromol. Rapid Commun.* **1996**, *17*, 333-338.

(32) Deng, L.; Woo, T. K.; Cavallo, L.; Margl, P. M.; Ziegler, T. *J. Am. Chem. Soc.* **1997**, *119*, 6177-6186.

(33) Deng, L.; Margl, P. M.; Ziegler, T. *J. Am. Chem. Soc.* **1997**, *119*, 1094-1100.

(34) Froese, R. D. J.; Musaev, D. G.; Morokuma, K. *J. Am. Chem. Soc.* **1998**, *120*, 1581-1587.

(35) Musaev, D. G.; Froese, R. D. J.; Morokuma, K. *Organometallics* **1998**, *17*, 1850-1860.

(36) Musaev, D. G.; Froese, R. D. J.; Svensson, M.; Morokuma, K. *J. Am. Chem. Soc.* **1997**, *119*, 367-374.

(37) Musaev, D. G.; Svensson, M.; Morokuma, K.; Stromberg, S.; Zetterberg, K.; Siegbahn, P. E. M. *Organometallics* **1997**, *16*, 1933-1945.

(38) Musaev, D. G.; Froese, R. D. J.; Morokuma, K. *New J. Chem.* **1997**, *21*, 1269-1282.

(39) van Asselt, R.; Elsevier, C. J.; Smeets, W. J. J.; Spek, A. L.; Benedix, R. *Recl. Trav. Chim. Pays-Bas* **1994**, *113*, 88-98.

(40) Ma, M. S.; Angelici, R. J.; Powell, D.; Jacobson, R. A. *Inorg. Chem.* **1980**, *19*, 3121-3128.

(41) Ma, M. S.; Angelici, R. J. *Inorg. Chem.* **1980**, *19*, 924-927.

(42) Ma, M. S.; Angelici, R. J. *Inorg. Chem.* **1980**, *19*, 363-370.

(43) Nakamura, A.; Konishi, A.; Otsuka, S. *J. Chem. Soc., Dalton Trans.* **1979**, 488-495.

(44) Ma, M. S.; Angelici, R. J.; Powell, D.; Jacobson, R. A. *J. Am. Chem. Soc.* **1978**, *100*, 7068-7069.

(45) Tempel, D. J. Mechanistic Studies of Pd(II)- and Ni(II)-Catalyzed Olefin Polymerization. Ph.D. Dissertation, University of North Carolina at Chapel Hill, 1998.

(46) The mechanism through which the (*E*,*E*)/(*E*,*Z*) interconversion takes place in these diimines is not known, but two possible pathways are via pyramidal inversion at the nitrogen atom, or by a 180° rotation about the C=N bond. This latter process would of course necessitate breaking the π-bond, so this bond would have to be weak in order for this rotation to take place.

(47) This spectrum was only acquired once with one mixing time. Experimentation with the mixing time may yield useful results.

(48) Pangborn, A. B.; Giardello, M. A.; Grubbs, R. H.; Rosen, R. K.; Timmers, F. J. *Organometallics* **1996**, *15*, 1518-1520.

(49) Rülke, R. E.; Ernsting, J. M.; Spek, A. L.; Elsevier, C. J.; van Leeuwen, P. W. N. M.; Vrieze, K. *Inorg. Chem.* **1993**, *32*, 5769-5778.

CHAPTER 5

Polymerization of α-Olefins and Norbornene by Electron-Deficient(α-Diimine)Ni(II) Complexes

Introduction

Transition metal-catalyzed polymerization of α-olefins, particularly propylene, has exploded into an area of tremendous commercial significance and intense academic research since its beginnings[1,2] in the 1950s. The development of homogeneous, well-defined metallocene complexes and subsequent mechanistic studies have led to many important advances in catalyst design, especially in the regime of stereocontrol of monomer enchainment.[3-8] These early transition-metal complexes typically enchain α-olefins of C_n carbons with strict 1,2-regiochemistry, forming linear polymers with a branch of length C_{n-2} on every other main-chain carbon. Recently, Fe complexes have been reported that polymerize propylene to moderate molecular-weight polymer via a 2,1 insertion mechanism with chain-end stereocontrol.[9]

While transition-metal catalyzed ethylene and propylene polymerization reactions are the most commercially significant and well-studied olefin polymerization processes, other monomers are also gaining research interest. Recent reports describe the copolymerization of norbornene and ethylene catalyzed by early transition-metal metallocene complexes.[10-14] Transition metal-catalyzed norbornene polymerizations have been found to proceed via a ring-opening metathesis mechanism or by an addition mechanism (Figure 5.1). The ethylene/norbornene copolymerization reactions proceed via an addition mechanism, and the resulting materials possess very high glass transitions and superior optical properties. Although early transition-metal complexes have been used more

extensively than late transition metals to polymerize norbornene, there are some examples of late-transition metal catalyzed norbornene polymerizations. For example, the homopolymerization of norbornene to high polymers with cationic palladium complexes such as $[Pd(CH_3CN)_4][BF_4]_2$[15,16] and cobalt neodecanoate/methylaluminoxane[17] has been described. While early transition-metal catalysts copolymerize norbornene and ethylene,[18] ethylene and α-olefins have been found to function as chain-transfer agents in norbornene polymerization reactions catalyzed by cationic palladium or nickel π-allyl complexes.[19]

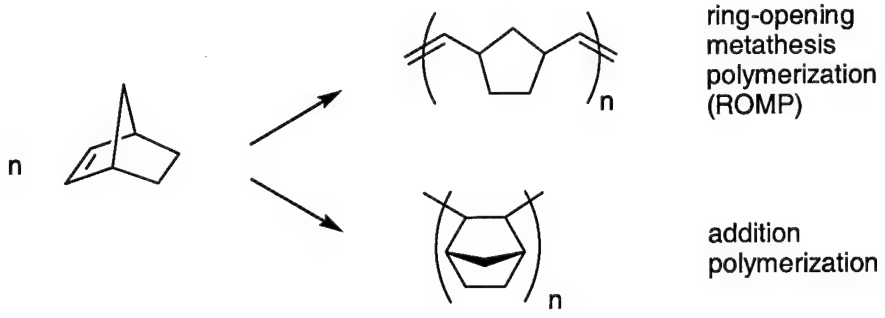

Figure 5.1. Norbornene polymerization mechanisms.

While early transition-metal olefin polymerization catalysts are highly effective in the polymerization of unfunctionalized alkenes, they are oxophilic and therefore ineffective in polymerizing olefins containing functional groups such as esters, ethers, and ketones. In addition, many such functional groups are incompatible with the aluminum alkyl cocatalysts that are needed to activate metallocene complexes. Since late transition-metal complexes are more electron-rich because of their high d-electron count, they should in theory be less oxophilic and therefore more functional group tolerant than their early transition-metal counterparts. Unfortunately, the high electron density of late transition metal complexes makes β-hydride elimination and subsequent chain transfer much more facile than is found in early metal systems. Indeed, nickel and palladium complexes are typically ethylene dimerization[20] or oligomerization[21] catalysts due to rapid chain transfer relative to chain propagation.

In 1985, Möhring and Fink reported the oligomerization of α-olefins[22] using an aminobis(imino)phosphorane nickel complex that was first synthesized by Keim et al.[23] This neutral complex was reported to oligomerize C_3-C_{20} olefins, yielding materials with 2,ω-enchainment of the α-olefin (C_1 forms a methyl branch). This unusual enchainment was proposed to be a result of migration of the metal to the end of the growing oligomer chain, followed by regioselective 1,2-monomer insertion, metal migration, etc. The metal migration (so-called chain running) takes place through a series of facile β-hydrogen elimination/reinsertion steps.

The first reported late transition-metal catalysts that were capable of polymerizing α-olefins are sterically bulky (α-diimine)Ni(II) and Pd(II) systems.[24] Many interesting features of these complexes have been discovered. These include the ability to form poly(α-olefin)s with fewer branches than expected (chain straightening, or 1,ω-enchainment), precise control of the polymer microstructure through variation of the diimine ligand or reaction conditions, the ability to polymerize α-olefins at -10 °C in a living fashion,[25] and the capability to copolymerize ethylene and α-olefins with polar monomers such as acrylates and vinyl ketones.[26,27] In addition, mechanistic studies using well-defined palladium diimine complexes have revealed details of chain propagation and chain isomerization.[24,28,29] The chain propagation mechanism of nickel-catalyzed 1-hexene polymerization has also been investigated,[29] and the current understanding of this mechanism is summarized in Scheme 5.1.

Scheme 5.1. Chain propagation mechanism of nickel-catalyzed 1-hexene polymerizations.[29]

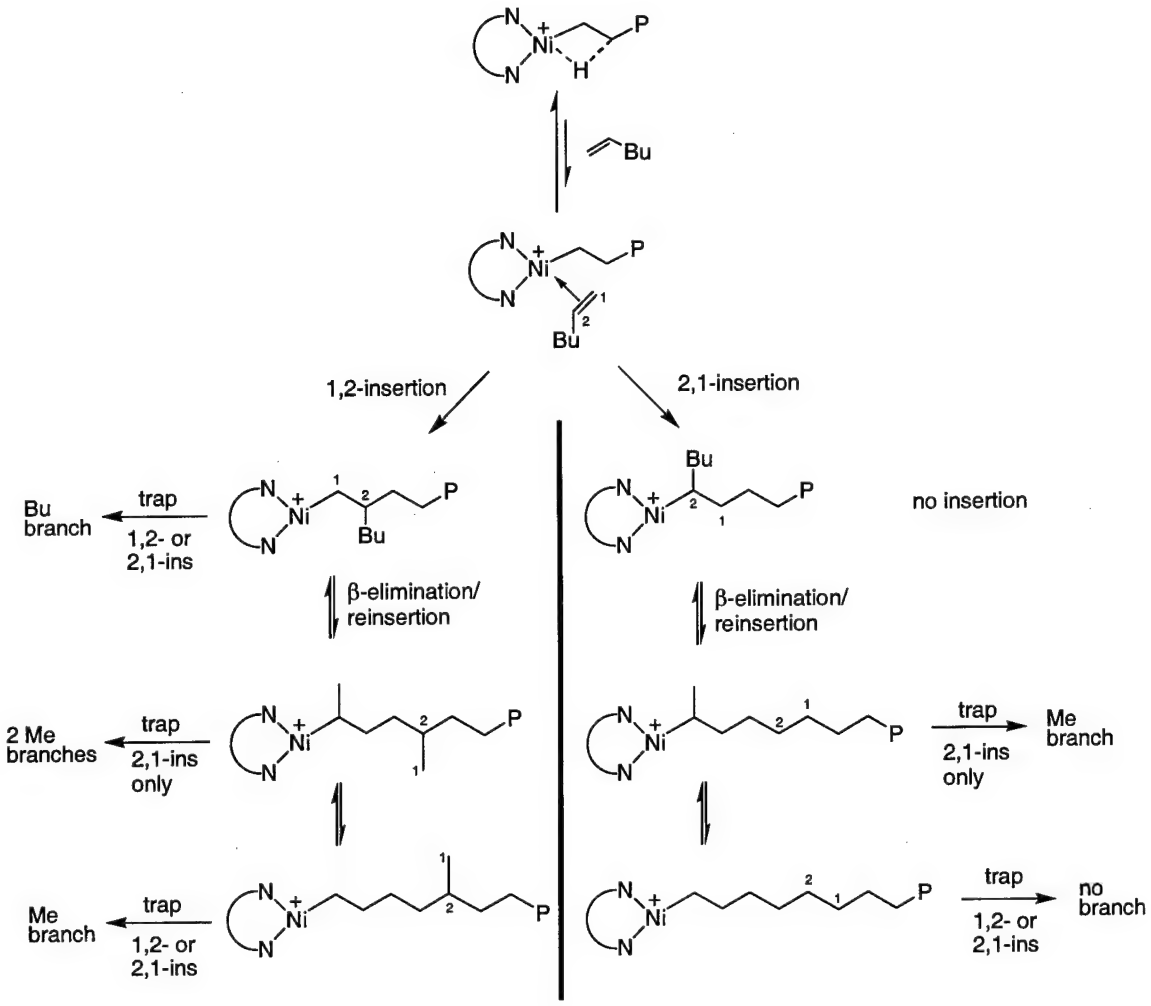

In Chapter 3, a detailed investigation of ethylene polymerizations catalyzed by nickel diimine complexes was described. Diimine ligands containing relatively non-bulky, fluorinated *ortho*-aryl substituents were among those studied, and complexes incorporating these ligands were found to be highly active ethylene polymerization catalysts. The low to moderate steric bulk of these complexes makes them attractive targets for studies involving bulkier olefin monomers. In this chapter, the utility of these complexes for the polymerization of 1-hexene and propylene is explored. In addition, a description of the behavior of these complexes in norbornene polymerizations is presented.

Results and Discussion

The (α-diimine)nickel dibromide catalyst precursors **1-6** (Scheme 5.2) were prepared according to the procedures described in Chapter 3. Catalyst precursor **7** was prepared by Dr. Chris Killian, and polymerization results obtained from the use of **7** are included in some of the data tables for comparison purposes and are referenced from his Ph.D. dissertation.[30] The polymerization reactions were conducted by activating the nickel dibromide complexes with modified methylaluminoxane (MMAO)[31] in toluene in the presence of the olefin monomer (Scheme 5.2). In contrast to many of the ethylene polymerization reactions described in Chapter 3, polymerization reactions of α-olefins are much easier to control. For example, the poly(α-olefin) products are highly soluble in toluene, and so polymerization reactions remain homogeneous throughout the duration of the reaction. In addition, no observable exotherms are observed, so temperature control is much more precise. Polymerizations of α-olefins occur more slowly than polymerizations of ethylene, so higher catalyst loadings are possible, resulting in more accurate calculations of monomer turnover numbers. Since 1-hexene is a liquid, very accurate monomer concentrations are known when it is used as the monomer. All of these factors lead to much more precise reaction control when polymerizing α-olefin monomers, particularly 1-hexene.

Scheme 5.2. General polymerization reactions and catalyst labeling scheme.

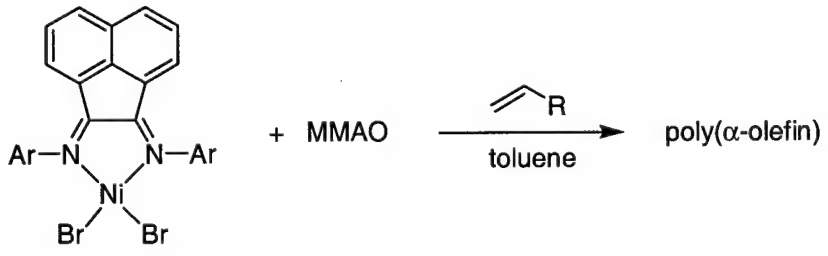

(1) Ar = (2-CF_3)C_6H_4
(2) Ar = (2-CH_3-6-CF_3)C_6H_3
(3) Ar = (2-C_6F_5)C_6H_4
(4) Ar = (2-CH_3-6-C_6F_5)C_6H_3
(5) Ar = (2-CH_3)C_6H_4
(6) Ar = (2,6-(CH_3)$_2$)C_6H_3
(7) Ar = (2,6-(*i*-Pr)$_2$)C_6H_3

A. Polymerization of 1-Hexene. The results for the polymerization of 1-hexene using 10 vol % monomer and catalyst precursors **1-6** are shown in Table 5.1. As a comparison, an entry performed by Dr. Chris Killian using **7** is included (entry 8).[30] The data in Table 5.1 contrasts the effects of the diimine ligand ortho substituents on catalyst productivity, extent of branching in the polymer products, and polymer molecular weights.

Table 5.1. Ligand Effects on 1-Hexene Polymerization in Toluene.[a]

							GPC (UNC)[b]		GPC (DuPont)[c]	
Entry	Complex	Temp (°C)	1-Hexene Conc. (vol %)	Time (min)	TO	Branches/ 1000 C	M_n (X 10^{-3})	PDI	M_n (X 10^{-3})	PDI
1	**1**	22	10%	60	660	93[d]	6.7	1.8	1.5	3.4
2	**2**	22	10%	60	440	89	119	3.4	76	2.5
3	**3**	22	10%	60	920	93[d]	1.7	1.5	0.5	1.7
4	**4**	22	10%	60	480	100	62	1.4	22	1.9
5	**5**	22	10%	60	42	87[d]	Oligomer	-	-	-
6	**6**	22	10%	60	1750	107	105	1.7	32	2.5
7	**2**	22	10%	20	160	99	121	1.6	95	1.6
8	**7**[e]	23	10%	60	1400	120	-	-	91	1.6

[a]Reaction conditions: 1.0 X 10^{-5} mol precatalyst **1-6**, 1.5 mL MMAO (6.68% wt % Al in heptane), 50 mL total solution volume. [b]Molecular weights determined by GPC (vs. polystyrene standards) in THF. [c]Molecular weights determined by GPC (using a universal calibration) in 1,2,4-trichlorobenzene. [d]Branching numbers were corrected for methyl endgroups (determined from ^{1}H NMR spectra). [e]This entry was run by Dr. Chris Killian: Killian, C. M. Ni(II)-Based Catalysts for the Polymerization and Copolymerization of Olefins: A New Generation of Polyolefins. Ph.D. Dissertation, University of North Carolina at Chapel Hill, 1996, p. 73.

The catalyst turnover numbers shown in Table 5.1 were calculated from the moles of 1-hexene in the poly(1-hexene) products divided by the moles of nickel dibromide catalyst precursor placed in the reaction mixture. This calculation assumes complete activation of the catalyst precursor (each nickel atom is catalytically active), and also assumes each active catalyst site remains active throughout the duration of the reaction. Recent evidence indicates that the assumption of complete catalyst activation is probably not valid,[32] which results in underestimation of the actual turnover numbers. In addition, evidence suggests that these catalysts slowly deactivate over time (see Chapters 2 and 3). Catalyst deactivation would further reduce the apparent turnover numbers of these reactions. Therefore, the turnover numbers shown in Table 5.1 represent lower limits to the actual turnover

numbers, which may be considerably higher than the values reported here. Caution must be exercised when comparing turnover numbers for various catalysts, since the extent of catalyst activation and the rate of catalyst deactivation may be variable for complexes bearing different ligands.

Some comparisons of the turnover numbers in Table 5.1 may be made. When compared to ethylene polymerization reactions (Chapter 3),[33] the apparent turnover numbers for 1-hexene are roughly three orders of magnitude lower (see discussion below). Complexes containing two alkyl substituents on the diimine aryl rings demonstrate the highest apparent turnover numbers (entries 6 and 8). In addition, polymerizations run with complex **2** over 20 min (entry 7) and 60 min reaction periods (entry 2) show that the catalyst appears to retain its activity throughout the 60 min reaction period; the apparent turnovers roughly triple as the reaction period is tripled.

As was observed in ethylene polymerizations (Chapter 3), the number of ortho aryl substituents on the diimine ligand (e.g. overall steric bulk), as well as the nature of the substituents affect the degree of branching of the poly(1-hexene)s. When the aryl substituents are varied from one methyl group (**5**), to two methyl groups (**6**), to two isopropyl groups (**7**), the degree of branching increases (entries 5, 6, and 8, Table 5.1). To put this another way, overall chain-straightening increases as ligand steric bulk decreases. An additional observation is that chain-straightening is more pronounced for the asymmetrically-substituted complex **2** (2-Me-6-CF_3, 89 branches/1000 C) as compared to the symmetrical complex **6** (2,6-Me_2, 107 branches/1000 C). These trends can be explained in terms of the monomer enchainment mechanism. In the case of α-olefin enchainment, a 1,2-monomer insertion *always* leads to at least one branch, but 2,1-enchainment may lead to no branches, depending on the extent of chain-running following a 2,1-insertion (Scheme 5.1). In order to form the observed chain-straightened polymers, a significant portion of the overall migratory insertions must proceed in a 2,1-fashion, followed by migration of nickel to the end of the chain. As the steric bulk of the diimine ortho aryl substituents is decreased, the ability of an α-olefin monomer to coordinate in a manner that will lead to a 2,1-insertion is increased (Figure 5.2). Asymmetric substitution of the diimine ortho

aryl substituents (e.g. R' ≠ R'') has been demonstrated to promote 2,1-insertions of α-olefins in similar nickel diimine complexes.[29] Such asymmetric substitution may be the reason why more chain running is seen in the poly(1-hexene)s formed with **2** as compared to those made with **6**.

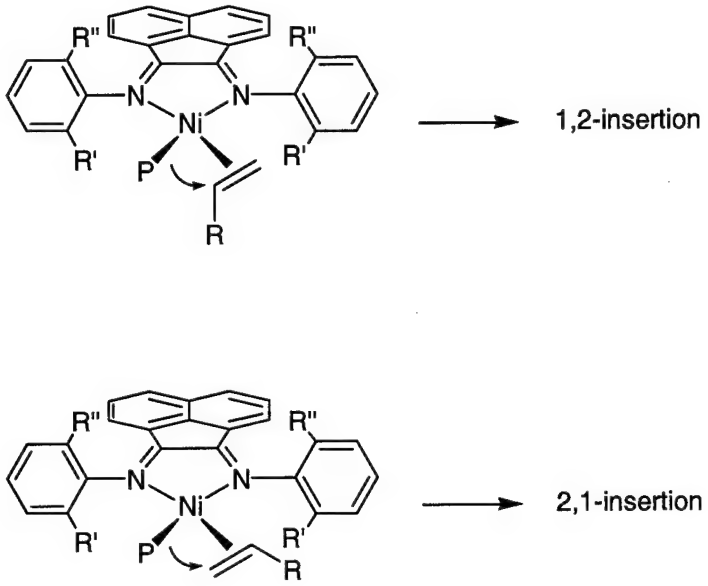

Figure 5.2. Influence of ligand aryl substituents on olefin coordination.

The ^{1}H NMR spectra of the poly(hexene)s produced in Table 5.1 are characterized by a doublet at 0.83 ppm (Figure 5.3). This resonance corresponds to methyl branches on the main chain of the polymer. This conclusion is supported by detailed NMR studies that show methyl branches are the most numerous branches found in these types of polymers.[34,35] Resonances appearing slightly downfield of the methyl doublet correspond to the endgroups of longer branches. The prominent triplet at 0.87 ppm in some of the spectra are likely due to the methyl groups of butyl branches. The qualitative appearance of the methyl region (0.90-0.65 ppm) of the ^{1}H NMR spectra shown in Figure 5.3 varies with the diimine ligands. These variations indicate different branch length distributions, and/or the different types of branches promoted by the various diimine ligand substituents. A detailed analysis of the polymer branching is well beyond the scope of this work, but such an analysis may expose further subtle effects of the diimine substituents on the number and type of branches formed in the poly(1-hexene)s.

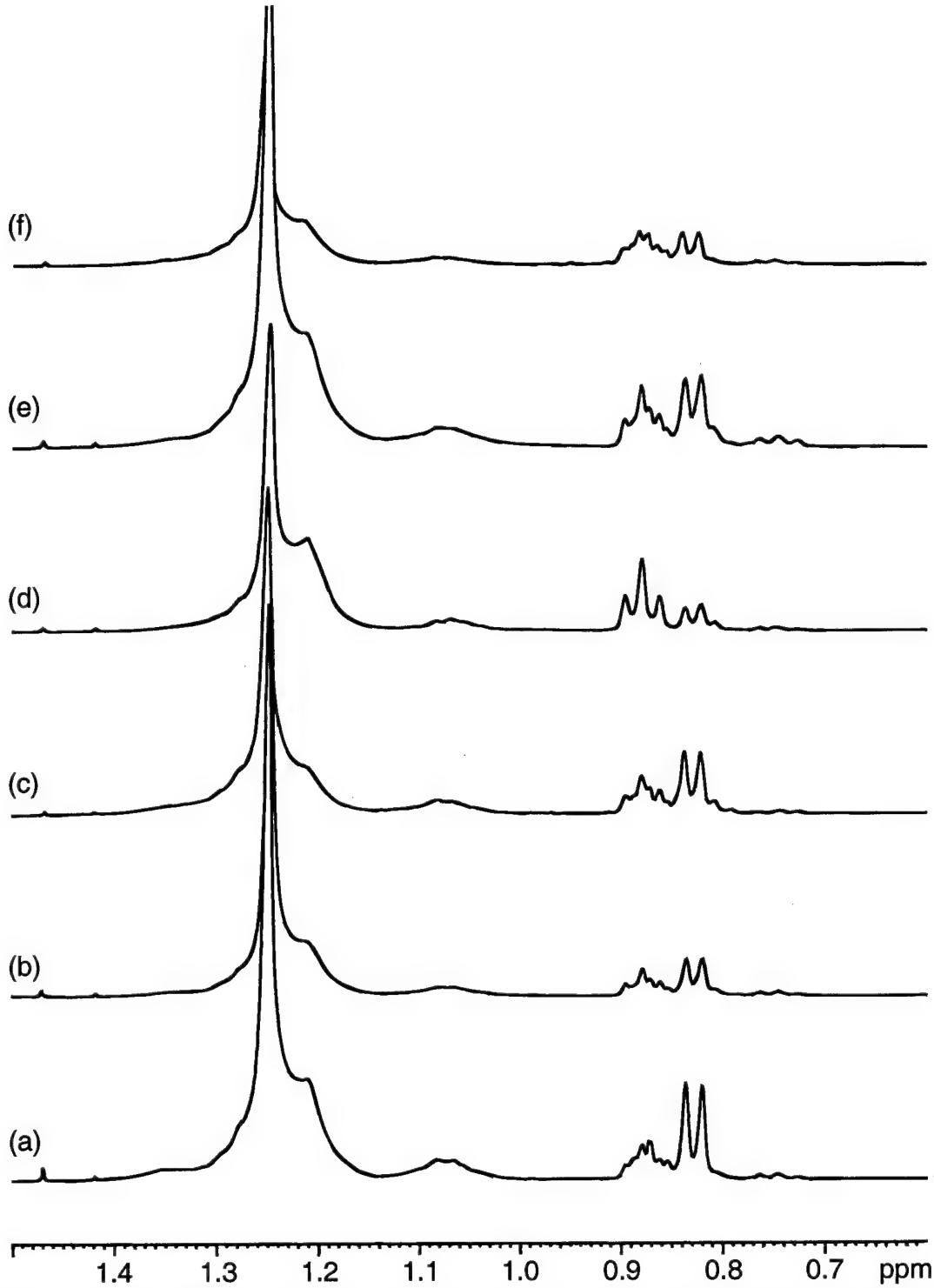

Figure 5.3. ^{1}H NMR spectra (400 MHz, $CDCl_3$, 40 °C) of poly(1-hexene) prepared at 22 °C, 10 vol % monomer, and precatalyst: (a) **1**; (b) **2**; (c) **3**; (d) **4**; (e) **5**; (f) **6**.

The molecular weights and polydispersities of the poly(1-hexene)s shown in Table 5.1 were determined by gel permeation chromatography (GPC). GPC analyses were performed on two different instruments under different conditions. One set of analyses was performed in tetrahydrofuran at 35 °C, and the polymer molecular weights were determined by comparison of the polymer elution times with those of polystyrene standards. These conditions have become the standard conditions by which we determine polymer molecular weights of poly(α-olefin)s in our laboratory since these polymers are usually soluble in THF. An additional set of GPC analyses was performed at DuPont. These GPC analyses were carried out in 1,2,4-trichlorobenzene at 135 °C. The molecular weights were determined by comparing elution curves with a calibration curve established with polystyrene standards, followed by application of a universal calibration using Mark-Houwink constants for polyethylene ($k = 4.34 \times 10^{-4}$; $\alpha = 0.724$). The high-temperature GPC method is typically used for polyethylene samples, which are not often soluble in THF. A more valid comparison of molecular weight data obtained for both polyethylene samples and poly(α-olefin) samples may then be made when all such data is measured by high-temperature GPC.

A couple of clear trends with regard to the effect of the diimine substituents on polymer molecular weight are seen in the data shown in Table 5.1. Consistent with the polyethylene results (Chapter 3), the combination of MMAO and catalyst precursors **1**, **3**, or **5** produces only oligomers or low molecular-weight polymer (entries 1, 3, and 5). Nonhydrogen substituents are required in each ortho position on the diimine aryl rings in order to obtain high polymer. The molecular weights of the polymers formed by **2** (2-Me-6-CF_3) and **7** (2,6-*i*-Pr_2) are roughly equivalent, even though the substituents on **2** are smaller. Enhancement of turnover numbers by the presence of a CF_3 group on the diimine aryl rings has been previously observed (Chapters 2 and 3),[33,36] and may be due to a lowering of the olefin migratory insertion barrier by the electron-withdrawing CF_3 group. Polymers formed by **2** (2-Me-6-CF_3) have substantially higher molecular weights than those formed by **4** (2-Me-6-C_6F_5) or **6** (2,6-Me_2) (Table 5.1, entries 2, 4, and 6).

It is interesting to compare the molecular weight distributions of the polymers formed by **2** after 20 min (entry 7) and 60 min (Table 5.1, entry 2). After the short reaction period, the polydispersity index (PDI) is relatively low (1.6), but increases to 2.5 after 60 min. The polymer number-average molecular weights are similar over both reaction periods. Since active catalysts of two possible symmetries are possible (Chapter 4), this broadening of the molecular weight distribution at extended reaction periods may be due to selective activation of one catalyst type over the early periods of the reaction, and/or selective deactivation of one of the catalyst types as the reaction progresses. Broadened molecular weight distributions were also noted when this catalyst was used to make polyethylene (Chapter 3).

The effect of monomer concentration on catalyst productivity, branching frequency, and molecular weight is shown in Table 5.2. One of the most striking results is the dependence of the turnover numbers on the monomer concentration. When the monomer concentration is doubled, the apparent turnover number is roughly doubled as well. Two explanations for this turnover dependence on the monomer concentration are likely: (1) the turnover limiting step is not migratory olefin insertion in the alkyl olefin complex, but rather trapping of the agostic intermediate formed following migratory insertion or chain isomerization, or (2) an equilibrium exists between an agostic intermediate and the alkyl olefin resting state complex. Based on experimental evidence, this monomer concentration effect on the turnover frequency is probably due to the existence of an equilibrium between a β-agostic species and the corresponding alkyl olefin complex (eq 5.1).[37,38] If the turnover-limiting step in the overall catalytic cycle is migratory olefin insertion from the alkyl olefin complex, then the

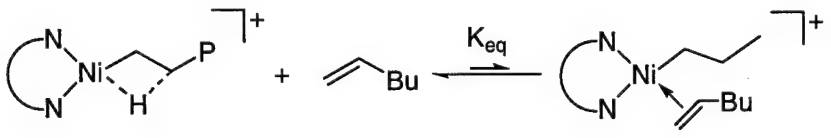

(5.1)

equilibrium shown in eq 5.1 would have to lie far to the left in order to obtain the observed linear increase in turnovers with increasing monomer concentration. As the monomer concentration is

increased, the equilibrium shifts in favor of the alkyl olefin complex. Since the presumed turnover-limiting step is migratory insertion of the olefin (Chapter 6), the apparent turnover numbers will increase as the equilibrium is shifted more in favor of the alkyl olefin complex.

Table 5.2. Monomer Concentration Effects on 1-Hexene Polymerization in Toluene.[a]

							GPC (UNC)[b]		GPC (DuPont)[c]	
Entry	Complex	Temp (°C)	1-Hexene Conc. (vol %)	Time (min)	TO	Branches/ 1000 C	M_n (X 10^{-3})	PDI	M_n (X 10^{-3})	PDI
1	**2**	22	10%	60	440	89	119	3.4	76	2.5
2	**2**	22	20%	60	920	108	240	2.4	101	2.9
3	**2**	22	40%	60	1650	124	306	2.4	120	3.2

[a]Reaction conditions: 1.0 X 10^{-5} mol precatalyst **2**, 1.5 mL MMAO (6.68% wt % Al in heptane), 50 mL total solution volume. [b]Molecular weights determined by GPC (vs. polystyrene standards) in THF. [c]Molecular weights determined by GPC (using a universal calibration) in 1,2,4-trichlorobenzene.

The branching numbers also increase with increasing monomer concentration. Since chain running is therefore decreasing with increasing monomer concentration, the mechanistic interpretation of this effect is that branched intermediates from 2,1-insertions are trapped at increasing rates. Increased trapping rates of branched intermediates retards chain running, and subsequent migratory insertions lead to increased branching frequencies in the polymer.

The effect of temperature on the polymerization of 1-hexene catalyzed by **2**/MMAO is shown in Table 5.3. Turnover numbers tend to decrease with increasing reaction temperature. This trend is probably due to increased rates of catalyst deactivation at higher temperatures. The mechanism through which these complexes deactivate is not known, but experiments with nickel dialkyl complexes (Chapter 6 and 7) may hint at one possibility. Complexes of the form (α-diimine)NiR_2 (R = Me, Et, Pr) have been found to be very unstable thermally, and readily undergo reductive elimination of the alkyl groups, even at temperatures below -20 °C. Overalkylation of the nickel dibromide catalyst precursors by MMAO, or more likely, by small amounts of residual Me_3Al present in the MMAO,[39,40] could conceivably form nickel dimethyl complexes. Reductive elimination of ethane from these complexes prior to methide abstraction could result in the formation of inactive species. This process may be occurring prior to initiation of polymer chain growth, so that only a

fraction of the nickel present is in the form of a catalytically-active complex. Lower reaction temperatures would be anticipated to slow down such a process, which could be the explanation for the trend of decreasing turnovers at elevated temperatures. Alkylation of the active cationic catalyst to form a nickel dialkyl complex might also occur, and subsequent reductive elimination of an alkane from this dialkyl complex to form an inactive species could take place. Therefore, over extended reaction periods, the number of active catalyst sites would be expected to decrease through one or both of these processes.

Table 5.3. Temperature Effects on 1-Hexene Polymerization in Toluene.[a]

							GPC (UNC)[b]		GPC (DuPont)[c]	
Entry	Complex	Temp (°C)	1-Hexene Conc. (vol %)	Time (min)	TO	Branches/ 1000 C	M_n (X 10^{-3})	PDI	M_n (X 10^{-3})	PDI
1	**2**	0	10%	60	470	110	187	1.2	72	1.3
2	**2**	22	10%	60	440	89	119	3.4	76	2.5
3	**2**	40	10%	60	290	94	123	2.9	54	3.2
4	**2**	60	10%	60	100	83	24.8	6.0	d	d

[a]Reaction conditions: 1.0 X 10^{-5} mol precatalyst **2**, 1.5 mL MMAO (6.68% wt % Al in heptane), 50 mL total solution volume. [b]Molecular weights determined by GPC (vs. polystyrene standards) in THF. [c]Molecular weights determined by GPC (using a universal calibration) in 1,2,4-trichlorobenzene. [d]Insufficient sample quantity for analysis.

Polymer molecular weights tend to decrease dramatically with increasing reaction temperature.[41] A higher rate of chain transfer relative to chain propagation is reflected in the broadened polydispersities measured for the polymers formed at higher temperatures. At 60 °C, the catalyst lifetime is apparently short, as the pink color of the active catalyst solution quickly fades during the course of the reaction, and a black precipitate (presumably decomposition product) is formed. This short catalyst lifetime probably accounts for the low molecular weight of the polymer formed at this temperature, above and beyond the increased rate of chain transfer.

An interesting result is the low polydispersity (1.16) of the polymer formed by **2** at 0 °C (Table 5.3, entry 1). Living polymerizations have been carried out with nickel complexes bearing bulkier diimine ligands (e.g. isopropyl substituents, complex **7**) at -10 °C.[25] The ortho-aryl substituents on

complex **2** are not nearly as large, but yet this system appears to be approaching a living system at 0 °C. This is even more interesting considering the possibility that two possible catalyst types can exist in solution due to the asymmetric ortho substituents on the diimine ligand. The low PDI may indicate that at 0 °C, only one of the two possible catalysts is actively polymerizing the monomer.

B. Polymerization of Propylene. Polymerization experiments with catalyst precursors **1-6** activated by MMAO were also carried out as an additional comparison of the effects of the diimine ligand substituent(s) on α-olefin polymerizations. Polymerizations of propylene are somewhat complicated by the fact that propylene is a gas at the temperatures these reactions were performed, and that its solubility in toluene varies substantially with reaction temperature. This makes monomer concentration studies more difficult to interpret. However, the same general trends observed in the 1-hexene polymerizations were again observed in the following propylene polymerizations. Discussion of the effects of the diimine ligand and reaction conditions on the polymerization reactions mentioned in the case of 1-hexene is valid for the following propylene polymerizations. There are a few additional points to be made, and these will be described briefly in the following sections.

The results of a series of propylene polymerization reactions using nickel complexes bearing different diimine ligands are summarized in Table 5.4. The turnover numbers observed in these propylene polymerizations are similar to those measured for the 1-hexene polymerizations. As was seen previously, two ortho substituents on each diimine aryl ring are necessary to obtain high polymer. Olefinic groups are again seen in the ^{1}H NMR spectra of the low molecular weight material produced by **1** and **3**. Complex **5** did not produce any recoverable polymer. One interesting difference in the data as compared to the 1-hexene polymerization results (Table 5.1) is the degree of branching observed in the polymers produced by **1** and **2** versus **3** and **4**. These four complexes generated very similar branching numbers in their 1-hexene polymers, but there is a large difference in the branching numbers in their propylene polymers. Polypropylene produced by complexes **1** and

2 exhibits a high degree of chain straightening, but polypropylene produced by **3** and **4** is much more branched. The reason for this result is not readily apparent.

Table 5.4. Ligand Effects on Propylene Polymerization in Toluene.[a]

						GPC (UNC)[b]		GPC (DuPont)[c]	
Entry	Complex	Temp (°C)	Propylene Pressure (atm)	TO	Branches/ 1000 C	M_n (X 10^{-3})	PDI	M_n (X 10^{-3})	PDI
1	**1**	22	1	650	184[d]	4.0	1.6	2.7	1.8
2	**2**	22	1	410	183	107	2.4	93	2.0
3	**3**	22	1	1130	260[d]	1.7	1.4	1.1	1.4
4	**4**	22	1	690	277	59	1.3	50	1.3
5	**5**	22	1	e	-	-	-	-	-
6	**6**	22	1	1540	259	69	1.7	49	1.9
7	**7**[f]	23	1	4200	265	-	-	144	1.2

[a]Reaction conditions: 1.0 X 10^{-5} mol precatalyst **1-6**, 1.5 mL MMAO (6.68% wt % Al in heptane), 50 mL total solution volume, 60 min reaction time. [b]Molecular weights determined by GPC (vs. polystyrene standards) in THF. [c]Molecular weights determined by GPC (using a universal calibration) in 1,2,4-trichlorobenzene. [d]Branching numbers were corrected for methyl endgroups (determined from ^{1}H NMR spectra). [e]No polymer recovered. [f]This entry was run by Dr. Chris Killian: Killian, C. M. Ni(II)-Based Catalysts for the Polymerization and Copolymerization of Olefins: A New Generation of Polyolefins. Ph.D. Dissertation, University of North Carolina at Chapel Hill, 1996, p. 73.

The nature of the branches appears to vary with the ligand used in the polymerization. The ^{1}H NMR spectra of several of the polymer samples listed in Table 5.4 are shown in Figure 5.4. A comparison of the methyl region (0.90-0.65 ppm) of each polymer indicates that there are significant differences in the types of branches produced by each of the diimine ligands. As mentioned previously, a detailed investigation of the polymer branching is beyond the scope of this work.

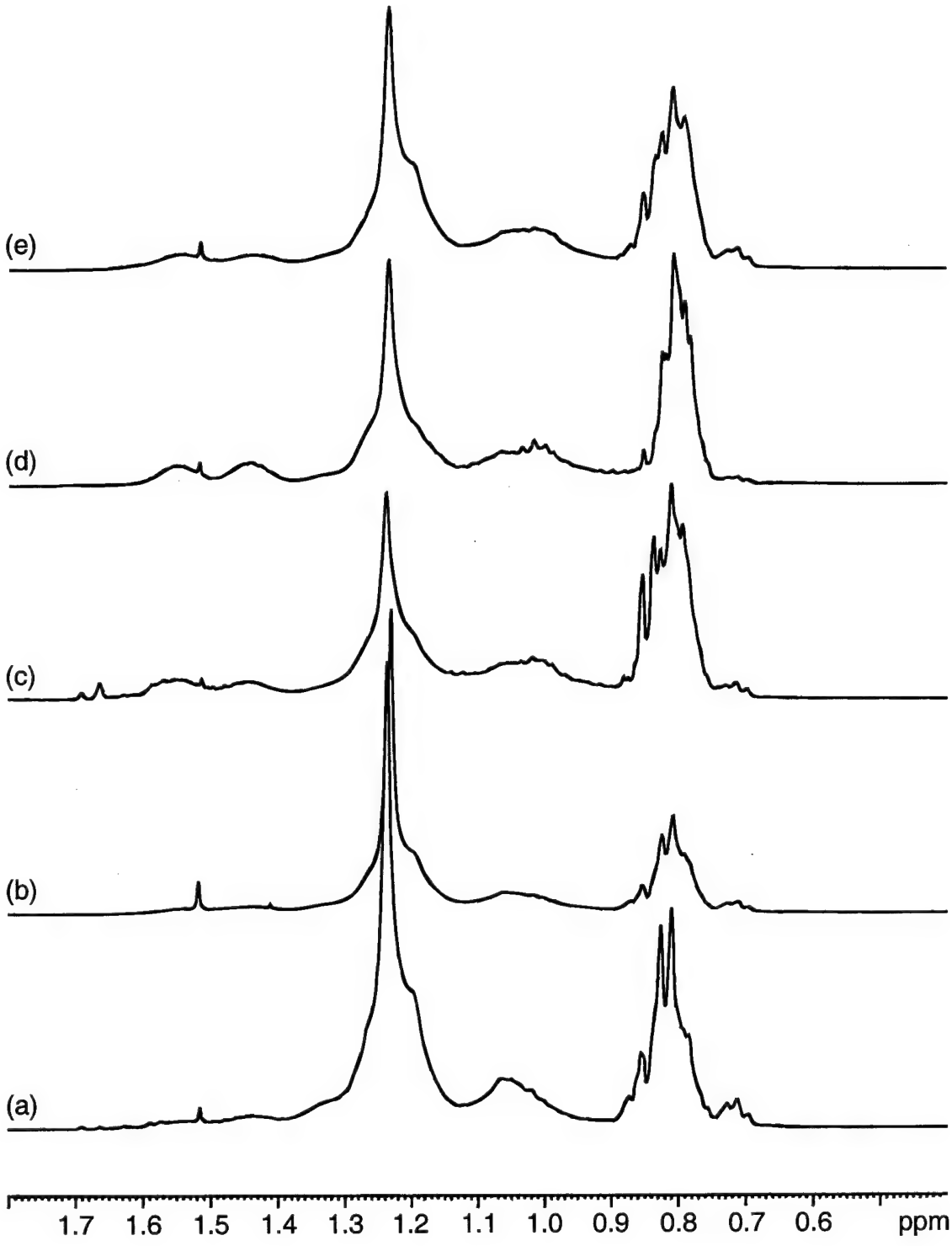

Figure 5.4. ^{1}H NMR spectra (400 MHz, $CDCl_3$, 40 °C) of polypropylene prepared at 22 °C, 1 atm propylene pressure, and precatalyst: (a) **1**; (b) **2**; (c) **3**; (d) **4**; (e) **6**.

The effect of propylene concentration (pressure) on the productivity of **2** and **6**, and some of the corresponding polymer properties, are listed in Table 5.5. The presence of a mixed resting state equilibrium between a β-agostic complex and an alkyl olefin complex is again observed, as indicated by the trend of increasing turnover numbers with increasing propylene pressure. The molecular weights of the polypropylene produced by **2** are significantly higher than the polypropylene formed by **6**. Polymer branching numbers increase with increasing propylene pressure when **2** is used, but are largely unaffected by monomer concentration when complex **6** is employed.

Table 5.5. Propylene Concentration (Pressure) Effects on Propylene Polymerization in Toluene.[a]

						GPC (UNC)[b]		GPC (DuPont)[c]	
Entry	Complex	Temp (°C)	Propylene Pressure (atm)	TO	Branches/ 1000 C	M_n (X 10^{-3})	PDI	M_n (X 10^{-3})	PDI
1	**2**	22	1	410	183	107	2.4	93	2.0
2	**2**	22	2	500	221	201	2.5	180	2.2
3	**2**	22	3	840	227	224	2.7	192	2.6
4	**2**	22	4	1280	241	261	2.6	202	2.8
5	**6**	22	1	1540	259	69	1.7	49	1.9
6	**6**	22	2	2070	245	78	2.0	62	1.9
7	**6**	22	3	2340	247	84	1.7	64	1.7

[a]Reaction conditions: 1.0 X 10^{-5} mol precatalyst **1-6**, 1.5 mL MMAO (6.68% wt % Al in heptane), 50 mL total solution volume, 60 min reaction time. [b]Molecular weights determined by GPC (vs. polystyrene standards) in THF. [c]Molecular weights determined by GPC (using a universal calibration) in 1,2,4-trichlorobenzene.

The effect of temperature on the polymerization of propylene by **2**/MMAO (Table 5.6) is very similar to its effect on the polymerization of 1-hexene. As the temperature is increased, the observed turnover numbers decrease, the degree of branching decreases, the molecular weights drop, and the polydispersities broaden. It is interesting to again note that the molecular weight distribution of the polymer produced at 0 °C is again very narrow (PDI = 1.16). The changes in the branching numbers are quite dramatic, and a glance at the ^{1}H NMR spectra of these polymers (Figure 5.5) shows

substantial changes in the appearance of the methyl region (0.90-0.65 ppm) over this reaction temperature range.

Table 5.6. Temperature Effects on Propylene Polymerization in Toluene.[a]

						GPC (UNC)[b]		GPC (DuPont)[c]	
Entry	Complex	Temp (°C)	Propylene Pressure (atm)	TO	Branches/ 1000 C	M_n (X 10^{-3})	PDI	M_n (X 10^{-3})	PDI
1	**2**	0	1	810	266	149	1.2	113	1.2
2	**2**	22	1	410	183	107	2.4	93	2.0
3	**2**	40	1	130	188	63	2.0	42	2.2
4	**2**	60	1	29	168	26	Bimodal	d	d

[a]Reaction conditions: 1.0 X 10^{-5} mol precatalyst **1-6**, 1.5 mL MMAO (6.68% wt % Al in heptane), 50 mL total solution volume, 60 min reaction time. [b]Molecular weights determined by GPC (vs. polystyrene standards) in THF. [c]Molecular weights determined by GPC (using a universal calibration) in 1,2,4-trichlorobenzene. [d]Insufficient sample for analysis.

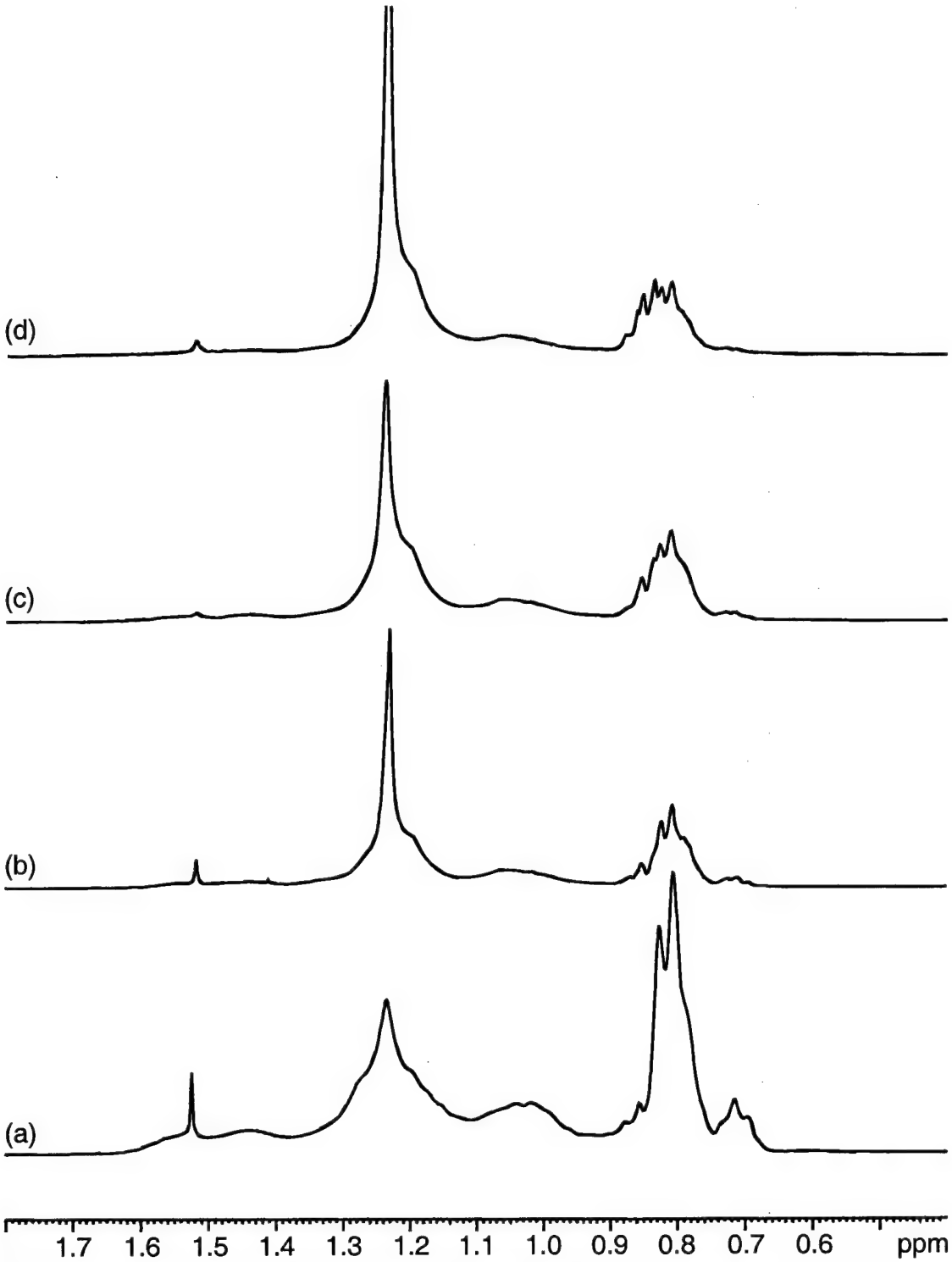

Figure 5.5. ^{1}H NMR spectra (400 MHz, $CDCl_3$, 40 °C) of polypropylene prepared using precatalyst **2**, 1 atm propylene pressure, at the following temperatures: (a) 0 °C; (b) 22 °C; (c) 40 °C; (d) 60 °C.

As mentioned previously, olefinic groups can be observed by ^{1}H NMR for the low molecular-weight poly(1-hexene)s and polypropylenes formed by **1**, **3** and **5** (Table 5.1, entries 1, 3, and 5; Table 5.4, entries 1 and 3). The distribution of the olefin groups in these materials is summarized in Table 5.7. As an illustrative example, the olefinic region of the ^{1}H NMR spectrum of poly(1-hexene) made with **3** is shown in Figure 5.6. Four distinct groups of olefins are observed: α-olefins, internal olefins, vinylidenes ($RR'C=CH_2$) and trisubstituted olefins. The major olefin type observed in all cases is internal olefin. Trisubstituted olefins made up only a very minor fraction of the total distribution.

Table 5.7. Olefin Distribution in Polymers Made by **1**, **3**, and **5**.[a]

			Olefin Distribution, %			
Entry	Complex	Monomer	α-Olefins	Internal Olefins	Vinylidenes	Trisubstituted Olefins
1	**1**[b]	1-hexene	10.7	82.8	4.1	2.4
2	**3**[b]	1-hexene	12.5	80.4	4.3	2.8
3	**5**[b]	1-hexene	7.3	83.2	6.7	2.8
4	**1**[c]	propylene	20.2	60.9	13.1	5.8
5	**3**[c]	propylene	12.7	52.0	30.3	5.0

[a]Determined by ^{1}H NMR. [b]From Table 5.1. [c]From Table 5.4.

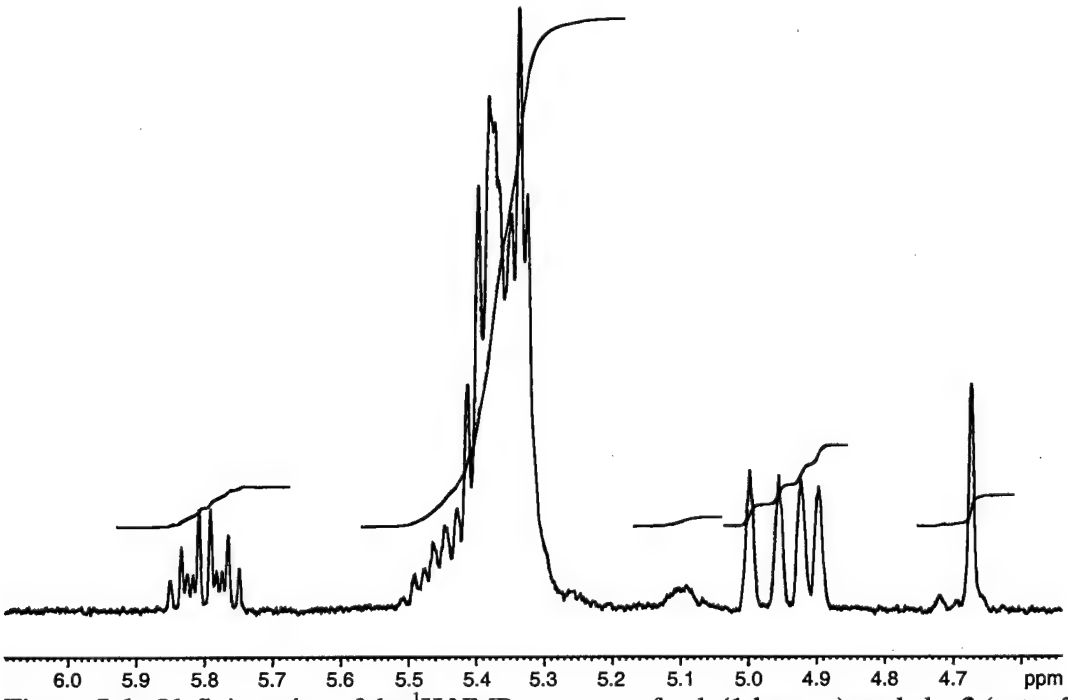

Figure 5.6. Olefinic region of the ^{1}H NMR spectrum of poly(1-hexene) made by **3** (entry 3, Table 5.1).

An investigation of the chain growth mechanism indicates that vinylidene and trisubstituted olefin groups may arise directly following a 1,2-insertion (Schemes 5.1, 5.3), or following a chain isomerization process in which the nickel migrates along the polymer chain until it runs to a methyl branch. Either pathway is possible, but the first is more probable since the nickel begins in the required position for formation of these olefin groups. The α-olefin and internal olefin groups can be formed following either 1,2- or 2,1-insertions. Inspection of the data in Table 5.7 shows that vinylidene groups are more common when propylene is used as the monomer. These results do not confirm whether 1,2-insertions become more prevalent when propylene is used as the monomer, or whether the rate of chain transfer from species directly leading to vinylidene groups is faster relative to chain transfer from other species. The second reason makes more sense based on steric arguments. According to Scheme 5.3, an internal olefin is formed when chain transfer occurs from olefin hydride **I**. Internal olefins may also form from several other possible intermediates. An α-olefin may be formed once the metal runs to the end of the chain following a 2,1-insertion. Chain transfer from olefin hydrides **II** and **III** forms vinylidene and trisubstituted olefins, respectively. Olefin hydrides **II** and **III** are more sterically crowded about the metal center than **I**, and so associative olefin displacement in **II** and **III** should be more favorable when the incoming olefin is propylene instead of 1-hexene.

Scheme 5.3. Chain transfer to form vinylidenes and trisubstituted olefins.

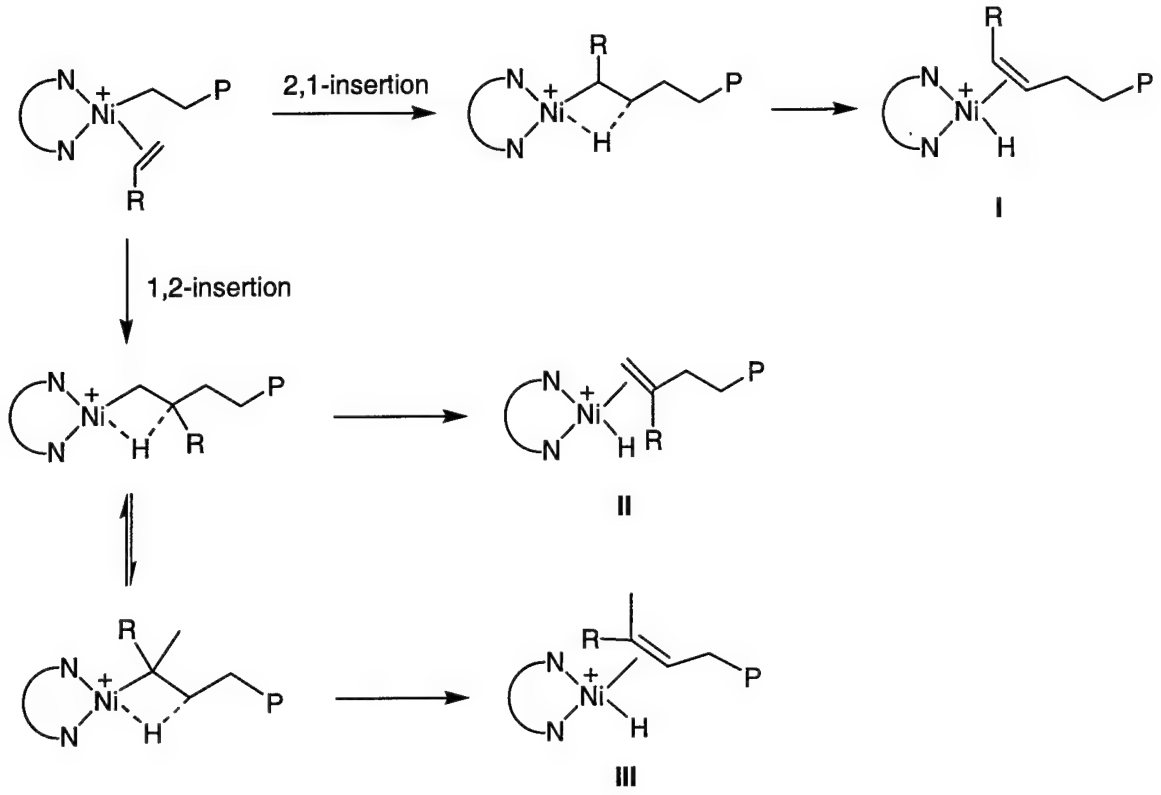

C. Polymerization of Norbornene. The relatively small size of the aryl substituents of complexes **1** and **2**, combined with their high activity in the polymerization of ethylene and α-olefins, makes these complexes attractive systems for the polymerization of bulky olefins such as norbornene. A brief series of polymerization experiments were carried out using norbornene as the monomer and **1** or **2** as catalyst precursors. The results of these polymerizations are shown in Table 5.8.

Table 5.8. Norbornene Homopolymerization Data.

Entry	Complex	Mol Ni ($X 10^{-6}$)	Temp (°C)	Norbornene concentration (mol/L)	Solvent	Time (min)	TO	g polymer
1	**1**	10	23	1.10 (3.10 g)	chlorobenzene	120	3300	3.10
2	**1**	1.0	23	1.06 (3.00 g)	chlorobenzene	210	30,900	2.90
3	**1**	10	23	1.07 (3.01 g)	toluene	120	760	0.71
4	**2**	10	23	1.07 (3.01 g)	chlorobenzene	120	3030	2.85

Reaction conditions: 2.5 mL MMAO (6.42% wt % Al in heptane), 30.0 mL total solution volume.

The norbornene homopolymerization experiments were usually carried out using chlorobenzene as the solvent. The polymerization solutions were a deep maroon color upon catalyst activation, and

they remained homogeneous throughout the duration of the reaction. Reaction solutions warmed noticeably over the first 20 min of the reaction in chlorobenzene solvent, and became quite viscous over this period as well. Reactions run in chlorobenzene proceeded to completion, and no odor of norbornene was evident as the reactions were quenched. Reactions run in toluene proceeded at a much slower rate, and only partial conversion of the monomer to polymer took place under the same conditions in which quantitative conversion was observed in chlorobenzene. The polymer reaction mixtures were quenched by dropwise addition into acidified methanol. Polynorbornene immediately precipitated as an intractible white solid. The precipitated polymers are insoluble in THF, CH_2Cl_2, and $CHCl_3$. Very small amounts (NMR samples) could be dissolved in boiling bromobenzene (156 °C) over several hours. The ^{1}H NMR spectra showed no alkene resonances, indicating the absence of olefinic endgroups, and thus high molecular weight material was formed. In addition, the ^{1}H NMR spectra were consistent with polynorbornene formed through an addition mechanism (Figure 5.1). The molecular weights and distributions of these polynorbornenes could not be measured due to their poor solubility, even in 1,2,4-trichlorobenzene at 135 °C.

Copolymers of norbornene and ethylene are much more processible than norbornene homopolymers, and in addition, the copolymers retain the desirable optical properties, thermal behavior, and chemical inertness of polynorbornene.[10,13,14] Since the combination of MMAO with precatalysts **1** or **2** forms very active ethylene and norbornene homopolymerization systems, copolymerization of these two monomers was naturally the next logical course of action. The results of attempted copolymerization reactions of norbornene and ethylene are shown in Table 5.9.

Table 5.9. Copolymerization of Ethylene and Norbornene with **1** or **2**.[a]

				Monomer				
Entry	Complex	Mol Ni (X 10^6)	Solvent Vol. (mL)	Norbornene	Ethylene	Temp (°C)	Rxn Time (min)	Polymer Yield
1	**1**	10	30	3.00 g	1 atm	0	60	1.13 g
2	**1**	10	30	0.50 g	1 atm	0	60	0.14 g
3	**1**	10	200	1.00 g	15 atm	23	30	-
4	**2**	2	200	1.00 g	15 atm	35	60	-

[a]Reaction conditions: chlorobenzene solvent, MMAO cocatalyst: 430 equiv Al:Ni (entries 1-3); 1400 equiv Al:Ni (entry 4).

Polymer was only obtained when the ratio of norbornene to ethylene was relatively high (compare entries 1-3, Table 5.9). An α-olefin endgroup was seen in the ^{1}H NMR spectrum of the product formed in entry 1. In addition, this spectrum showed a 60:1 ratio of norbornene units to the α-olefin group. The ^{1}H NMR spectrum of the product formed in entry 2 showed a 25:1 ratio of norbornene units to an α-olefin endgroup. Neither spectrum contained the prominent methylene singlet at 1.25 ppm that is associated with polyethylene repeat units. Therefore, the polymers formed are likely low molecular weight norbornene homopolymers with α-olefin endgroups. These results show that lowering the ratio of norbornene to ethylene results in a decrease in the incorporation of norbornene in the polymer chain, and that ethylene appears to inhibit norbornene polymerization. In addition, at relatively high ratios of ethylene to norbornene, no polymer is formed at all (entries 3 and 4), possibly indicating that norbornene acts as a catalyst poison in ethylene polymerizations. No ethylene oligomers were found in these reaction mixtures as determined by gas chromatography.

Late transition-metal catalysts are able to homopolymerize norbornene to high polymer because β-hydride elimination is unfavorable due to the orientation of β-hydrogen atoms on the metal-bound norbornyl fragment. Since β-hydrogen elimination is unfavorable, the formation of olefin hydrides does not occur, and therefore chain transfer from olefin hydride intermediates is not significant.[16] Since mixtures of norbornene and ethylene do not polymerize well, an experiment was run (Scheme 5.4) in which norbornene was first homopolymerized under conditions that left virtually no unreacted norbornene in solution. Ethylene was then added to the reaction mixture in an effort to form a block

copolymer. After 15.5 h under ethylene the reaction was quenched in the standard fashion. Upon workup, no copolymer was formed, only polynorbornene.

Scheme 5.4. Attempted preparation of poly(norbornene-*b*-ethylene).

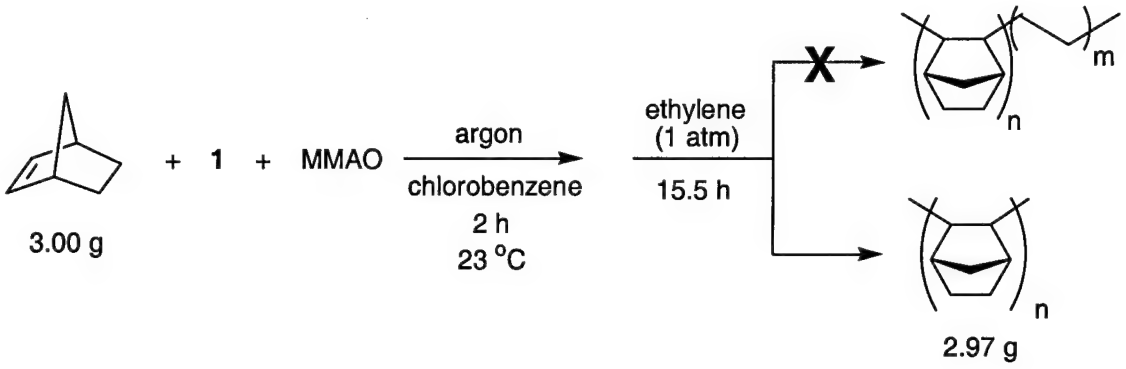

Conclusions

Nickel(II) complexes bearing electron-deficient α-diimine ligands were found to be efficient catalysts for the polymerization of 1-hexene and propylene. The effects of monomer concentration and reaction temperature on the polymer microstructure are consistent with existing data from similar catalyst systems. Several conclusions may be made from these studies:

(1) Asymmetric substitution of the ortho aryl substituents on the diimine ligand leads to more chain-straightened polymers due to a relative increase in the preference for 2,1-insertions. The types of branches, as well as branching frequency, is sensitive to the nature of the ligand ortho aryl substituents.

(2) Previously observed trends in the effects of monomer concentration and reaction temperature on the polymerization of α-olefins were seen in these reactions. Increasing the monomer concentration raises the polymer branching frequency and overall turnover frequency, while raising the reaction temperature lowers the polymer branching frequency and molecular weights, and increases the molecular weight distributions.

(3) Complexes bearing mono ortho-substituted aryl α-diimine ligands produce low molecular weight poly(α-olefin)s (M_n <500 to 2500) for which olefinic endgroups may be seen. Both ortho aryl positions must contain non-hydrogen substituents in order to obtain high molecular weights.

(4) The dependence of the turnover numbers on monomer concentration was observed. Although this effect could be due to a change in the turnover-limiting step in the proposed polymerization mechanism (rate-limiting agostic trapping versus migratory insertion), the likely explanation for this effect is the existence of an equilibrium between the alkyl olefin resting state species and agostic intermediates.

(5) These Ni(II) systems are efficient catalysts in the addition polymerization of norbornene. Attempts to copolymerize norbornene and ethylene were not successful.

Experimental Section

General Methods. All manipulations of air- and/or water-sensitive compounds were performed using standard high-vacuum or Schlenk techniques. Argon was purified by passage through columns of BASF R3-11 catalyst (Chemalog) and 4-Å molecular sieves. Solid organometallic compounds were transferred in an argon-filled Vacuum Atmospheres drybox. ^{1}H NMR spectra were recorded on Bruker Avance-500, -400, or -300 MHz spectrometers. Chemical shifts are reported relative to residual $CHCl_3$ (δ 7.24 for ^{1}H). ^{1}H NMR spectra of poly(1-hexene) were taken in $CDCl_3$ at 40 °C. High pressure polymerizations were performed in a Fisher-Porter bottle. Gel permeation chromatography (GPC) was performed at two different locations for each polymer sample. High temperature GPC was performed by DuPont (Wilmington, DE) in 1,2,4-trichlorobenzene at 135 °C using a Waters HPLC 150C equipped with Shodex columns. A calibration curve was established with polystyrene standards and universal calibration was applied using Mark-Houwink constants for polyethylene ($k = 4.34 \times 10^{-4}$; $\alpha = 0.724$). GPC analyses performed at UNC were run in tetrahydrofuran at 35 °C using a Waters Alliance HPLC equipped with Waters Styragel HR2, HR4,

and HR5 columns in series and a Waters 410 refractive index detector. The estimated molecular weights are reported relative to polystyrene standards.

Materials. Toluene was purified using procedures recently reported by Pangborn et. al.[42] Chlorobenzene (>99.9%, Aldrich) was degassed before use. Polymer-grade propylene (99.5 %) was purchased from National Specialty Gases and used without further purification. 1-Hexene (99+%, Aldrich) was distilled from sodium under argon before use. Norbornene was distilled from sodium under argon before use, and stored in the drybox. 6.4% and 6.68% Al solutions of modified methylaluminoxane (MMAO) in heptane (d = 0.73 g/mL) containing 23-27% isobutyl groups were purchased from Akzo Nobel. The α-diimine ligands and the nickel(II) bromide complexes **1-6** were prepared using the procedures described in Chapter 3. Nickel(II) bromide complexes **3** and **4** were prepared by Dr. Enrique Oñate.

General Procedure for 1-Hexene Polymerizations. A 100 mL round-bottom Schlenk flask was equipped with a magnetic stir bar, and then flame-dried under vacuum. The flask was filled with argon, followed by toluene and the appropriate volume of 1-hexene (total volume 45.0 mL). The MMAO cocatalyst (1.5 mL of a 6.68% Al in heptane solution) was added, and the mixture was stirred for 15 min at the reaction temperature. A suspension of the appropriate catalyst precursor (**1-6**, 1.00 X 10^{-5} mol in 3.5 mL toluene) was transferred via cannula to the reaction vessel. After the appropriate reaction period, the reaction solution was poured into a stirred solution of 5 vol % 6M HCl/MeOH (200 mL) to quench the reaction and precipitate the polymer. The polymer product was recovered and dried overnight in a vacuum oven at 60 °C. Branches per 1000 carbons were determined by ^{1}H NMR spectroscopy.

General Procedure for Propylene Polymerization at 1 Atm. A 100 mL round-bottom Schlenk flask was equipped with a magnetic stir bar, and flame-dried under vacuum. The flask was filled with propylene (1 atm, oil bubbler vent), then toluene (45.5 mL) and MMAO (1.5 mL of a 6.68% Al in

heptane solution) were added. The mixture was stirred for 15 min at the reaction temperature, then a suspension of the appropriate catalyst precursor (**1-6**, 1.00 X 10^{-5} mol in 3.0 mL toluene) was transferred via cannula to the reaction vessel. After a 60 min reaction period, the reaction solution was poured into a stirred solution of 5 vol % 6M HCl/MeOH (200 mL) to quench the reaction and precipitate the polymer. The polymer product was recovered and dried overnight in a vacuum oven at 60 °C. Branches per 1000 carbons were determined by ^{1}H NMR spectroscopy.

General Procedure for Propylene Polymerization at Pressures above 1 Atm. A dry Fisher-Porter bottle was charged with a magnetic stir bar, evacuated, then filled with propylene. Toluene (45.5 mL) and MMAO (1.5 mL of 6.68% Al in heptane solution) were added to the bottle via syringe. The reaction mixture was stirred under constant propylene pressure for 15 min at 22 °C. A suspension of the appropriate catalyst precursor (**1-6**, 1.00 X 10^{-5} mol in 3.0 mL toluene) was transferred via cannula to the reaction vessel. The bottle was then sealed and pressurized with propylene. After a 60 min reaction period, the reactor was depressurized, and the reaction solution was poured into a stirred solution of 5 vol % 6M HCl/MeOH (200 mL) to quench the reaction and precipitate the polymer. The polymer product was recovered and dried overnight in a vacuum oven at 60 °C. Branches per 1000 carbons were determined by ^{1}H NMR spectroscopy.

General Procedure for Norbornene Polymerizations. A 100 mL round-bottom flask was equipped with a magnetic stir bar, then flame-dried under vacuum. Norbornene (ca.. 3 g, 32 mmol) was added to the flask in the dry box. The appropriate solvent was added, followed by MMAO (2.5 mL of 6.42% Al in heptane solution). The solution was allowed to stir at 23 °C for 10 min. A suspension of the appropriate catalyst precursor (**1** or **2**, 1.00 X 10^{-5} mol in 3.5 mL toluene) was transferred via cannula to the reaction vessel. The solution immediately turned a dark maroon color, became very viscous after 10 min, and a noticeable exotherm persisted for ca. 30 min. The solution

remained homogeneous throughout the reaction period. After the appropriate reaction period, the reaction solution was added to a stirred solution of 5 vol % 6M HCl/MeOH (200 mL) drop-wise via pipet to quench the reaction and precipitate the polymer. The polymer immediately precipitated as a white solid. The polymer product was washed several times with MeOH, and was then dried overnight in a vacuum oven at 60 °C. The polynorbornene product was not soluble in THF, CH_2Cl_2, or $CHCl_3$, but small amounts are soluble in boiling C_6D_5Br. The ^1H NMR of the product is consistent with an addition polymer (no olefin groups).

References and Notes

(1) Natta, G.; Pino, P.; Corradini, P.; Danusso, F.; Mantica, E.; Mazzanti, G.; Moraglio, G. *J. Am. Chem. Soc.* **1955**, *77*, 1708-1710.

(2) Natta, G. *J. Poly. Sci.* **1959**, *34*, 531-549.

(3) Bochmann, M. *J. Chem. Soc., Dalton Trans.* **1996**, 255-270.

(4) Brintzinger, H. H.; Fischer, D.; Mülhaupt, R.; Rieger, B.; Waymouth, R. M. *Angew. Chem., Int. Ed. Engl.* **1995**, *34*, 1143-1170.

(5) Coates, G. W.; Waymouth, R. M. *Science* **1995**, *267*, 217-219.

(6) Ewen, J. A.; Jones, R. L.; Razavi, A.; Ferrara, J. D. *J. Am. Chem. Soc.* **1988**, *110*, 6255-6256.

(7) Kaminsky, W.; Külper, K.; Brintzinger, H. H.; Wild, F. R. W. P. *Angew. Chem., Int. Ed. Engl.* **1985**, *24*, 507-508.

(8) Ewen, J. A. *J. Am. Chem. Soc.* **1984**, *106*, 6355-6364.

(9) Small, B. L.; Brookhart, M. *Macromolecules* **1999**, *32*, 2120-2130.

(10) Ruchatz, D.; Fink, G. *Macromolecules* **1998**, *31*, 4669-4673.

(11) Ruchatz, D.; Fink, G. *Macromolecules* **1998**, *31*, 4674-4680.

(12) Rische, T.; Waddon, A. J.; Dickinson, L. C.; MacKnight, W. J. *Macromolecules* **1998**, *31*, 1871-1874.

(13) Cherdron, H.; Brekner, M.-J.; Osan, F. *Angew. Makromol. Chem.* **1994**, *223*, 121-133.

(14) Kaminsky, W.; Bark, A.; Arndt, M. *Makromol. Chem., Macromol. Symp.* **1991**, *47*, 83-93.

(15) Seehof, N.; Mehler, C.; Breunig, S.; Risse, W. *J. Mol. Catal.* **1992**, *76*, 219-228.

(16) Mehler, C.; Risse, W. *Macromolecules* **1992**, *25*, 4226-4228.

(17) Goodall, B. L.; McIntosh, L. H.; Rhodes, L. F. *Macromol. Symp.* **1995**, *89*, 421-432.

(18) Kaminsky, W.; Arndt, M. Polymerization, Oligomerization, and Copolymerization of Olefins. In *Applied Homogeneous Catalysis with Organometallic Compounds*; Cornils, B., Herrmann, W. A., Eds.; VCH: New York, 1996; Vol. 1, pp 220-236.

(19) Goodall, B. L.; Benedikt, G. M.; McIntosh, L. H.; Barnes, D. A. Process for Making Polymers Containing a Norbornene Repeating Unit by Addition Polymerization using an Organo(Nickel or Palladium) Complex. U.S. Patent 5,468,819, Nov. 21, 1995.

(20) Muthukumaru Pillai, S.; Ravindranathan, M.; Sivaram, S. *Chem. Rev.* **1986**, *86*, 353-399.

(21) Skupinska, J. *Chem. Rev.* **1991**, *91*, 613-648.

(22) Möhring, V. M.; Fink, G. *Angew. Chem., Int. Ed. Engl.* **1985**, *24*, 1001-1003.

(23) Keim, W.; Appel, R.; Storeck, A.; Krüger, C.; Goddard, R. *Angew. Chem., Int. Ed. Engl.* **1981**, *20*, 116-117.

(24) Johnson, L. K.; Killian, C. M.; Brookhart, M. *J. Am. Chem. Soc.* **1995**, *117*, 6414-6415.

(25) Killian, C. M.; Tempel, D. J.; Johnson, L. K.; Brookhart, M. *J. Am. Chem. Soc.* **1996**, *118*, 11664-11665.

(26) Johnson, L. K.; Mecking, S.; Brookhart, M. *J. Am. Chem. Soc.* **1996**, *118*, 267-268.

(27) Mecking, S.; Johnson, L. K.; Wang, L.; Brookhart, M. *J. Am. Chem. Soc.* **1998**, *120*, 888-899.

(28) Tempel, D. J.; Johnson, L. K.; Huff, R. L.; Brookhart, M. Manuscript in preparation.

(29) Tempel, D. J. Mechanistic Studies of Pd(II)- and Ni(II)-Catalyzed Olefin Polymerization. Ph.D. Dissertation, University of North Carolina at Chapel Hill, 1998.

(30) Killian, C. M. Ni(II)-Based Catalysts for the Polymerization and Copolymerization of Olefins: A New Generation of Polyolefins. Ph.D. Dissertation, University of North Carolina-Chapel Hill, 1996.

(31) MMAO contains 25% isobutyl groups. MMAO has improved shelf life with little difference in reactivity as compared to MAO.

(32) Recent experiments on the living polymerization of α-olefins with MAO-activated nickel dibromide catalyst precursors hint that incomplete activation is occurring. Comparison of number-average polymer molecular weights determined by gel permeation chromatography with calculated molecular weights show that the calculated values are lower than the measured weights.

(33) Gates, D. P.; Svejda, S. A.; Onate, E.; Killian, C. M.; Johnson, L. K.; White, P. S.; Brookhart, M. Manuscript in preparation.

(34) McLain, S. J.; McCord, E. F.; Johnson, L. K.; Ittel, S. D.; Nelson, L. T. J.; Arthur, S. D.; Halfhill, M. J.; Teasley, M. F.; Tempel, D. J.; Killian, C. M.; Brookhart, M. *Polym. Prepr., Am. Chem. Soc. Div. Polym. Chem.* **1997**, *38*, 772.

(35) Nelson, L. T. J.; McCord, E. F.; Johnson, L. K.; McLain, S. J.; Ittel, S. D.; Killian, C. M.; Brookhart, M. *Polym. Prepr., Am. Chem. Soc. Div. Polym. Chem.* **1997**, *38*, 133.

(36) Svejda, S. A.; Brookhart, M. *Organometallics* **1999**, *18*, 65-74.

(37) Mechanistic studies with well-defined nickel complexes have uncovered that the observed species present in solution during low-temperature propylene polymerizations is a β-agostic complex. The only species observed in the same experiments using ethylene as the monomer is the alkyl ethylene complex. See Chapter 6 for these results and further discussion.

(38) In experiments with nickel complexes bearing very bulky diimine ligands, this effect was also observed. At very high monomer concentrations, the turnover numbers level out. See ref 29.

(39) Abeywickrema, R.; Bennett, M. A.; Cavell, K. J.; Kony, M.; Masters, A. F.; Webb, A. G. *J. Chem. Soc., Dalton Trans.* **1993**, 59-68.

(40) Kissin, Y. V.; Beach, D. L. *J. Poly. Sci., Part A: Polym. Chem.* **1989**, *27*, 147-155.

(41) Since the branching frequency rises with increasing polymerization temperatures, the hydrodynamic radii of the more highly branched polymer chains will be decreased relative to more linear chains. This will result in an underestimation of the molecular weights of the polymers formed at higher temperatures. In addition, the relative error increases with polymer branching frequency. However, this effect is unlikely to be completely responsible for the observed decrease in polymer molecular weights at higher polymerization temperatures.

(42) Pangborn, A. B.; Giardello, M. A.; Grubbs, R. H.; Rosen, R. K.; Timmers, F. J. *Organometallics* **1996**, *15*, 1518-1520.

CHAPTER 6

Low-Temperature Spectroscopic Observation of Chain Growth and Migratory Insertion Barriers in Well-Defined Cationic (α-Diimine)Ni(II) Olefin Polymerization Catalysts

Introduction

Access to soluble, well-defined transition metal olefin polymerization catalysts has allowed detailed mechanistic studies of this important class of catalysts. While much attention has centered on early transition metal d^0 and lanthanide d^0f^n systems,[1-7] we have focused on developing single-site late metal catalysts. Our initial report[8] that Ni(II) and Pd(II) aryl-substituted α-diimine complexes bearing bulky ortho substituents were capable of polymerizing ethylene and α-olefins has stimulated extensive experimental[9-20] and theoretical[21-27] work on this class of catalysts employing α-diimines. The Pd(II)-α-diimine systems yield highly branched polyethylene under typical polymerization conditions, while the microstructure of polyethylene produced by the Ni(II) systems is highly dependent on monomer concentration, reaction temperature, and ligand structure.

Extensive NMR spectroscopic studies at low temperatures employing well-defined Pd(II) complexes[8,28] have established that: (1) the catalyst resting state is an alkyl olefin complex and consequently the chain growth is zero order in ethylene and dependent only on the rate of migratory insertion, (2) the barriers to migratory insertion measured at -30 °C are in the range of 16.9 to 17.6 kcal/mol and (3) the alkyl cation formed following insertion is a β-agostic complex and Pd can rapidly migrate along the chain via β-hydride elimination/reinsertion reactions without chain transfer.

This process is responsible for formation of branches in the polyethylene produced. These features are summarized in Scheme 6.1.

For use in polymerization reactions, analogous Ni-based cationic alkyl complexes are generated by activation of nickel dihalide complexes with methylaluminoxane (MAO). The difficulty in preparation and the high reactivity of well-defined cationic nickel alkyl complexes has to date precluded mechanistic studies similar to those reported for the palladium systems. This chapter describes the preparation of (α-diimine)Ni(CH_3)(solvent)$^+BAr'_4^-$ ($BAr'_4^- \equiv B(3,5\text{-}C_6H_3(CF_3)_2)_4^-$) salts and the utilization of these complexes to study the mechanistic details of the chain growth process which allows a quantitative comparison of the Ni and Pd systems.

Scheme 6.1. Mechanism of palladium-catalyzed ethylene polymerization.[8]

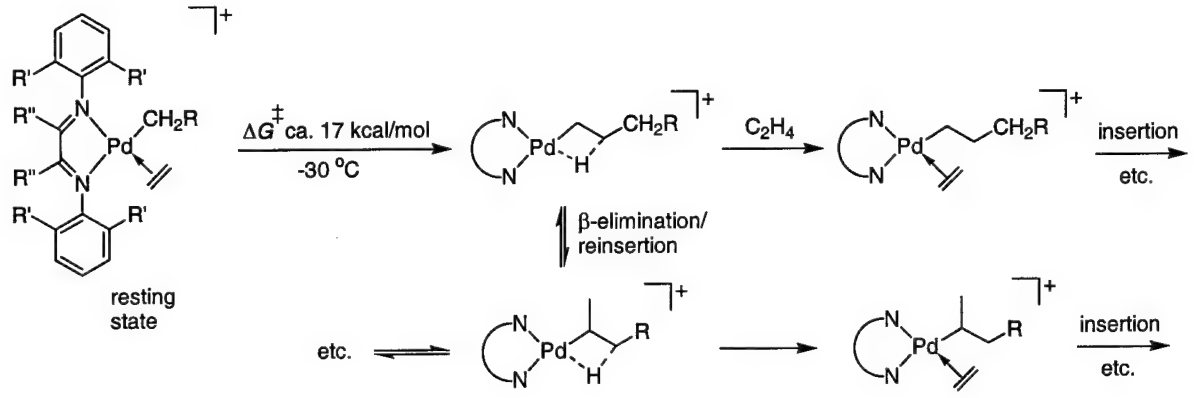

Results and Discussion

The (α-diimine)$NiMe_2$ complexes **2a,b** are the precursors to the cationic nickel methyl complexes. These dimethyl complexes are extremely air-sensitive, and are thermally unstable at room temperature.[29] Isolation of the clean complexes can be accomplished by rapid filtration through Florisil at -78 °C.[30] Protonation of dimethyl complexes **2a,b** with $[H^+(OEt_2)_2][BAr'_4^-]$ yields the cationic ether adducts **3** (Scheme 6.2). Rigorous exclusion of water is required to avoid the facile formation of aquo adducts **4**. Addition of stoichiometric amounts of water to CH_2Cl_2 solutions of ether adducts **3** at -78 °C results in quantitative conversion to the aquo adducts **4**. Complexes **3** and **4**

are thermally sensitive, and decompose in CD_2Cl_2 solutions and in the solid state at room temperature.

Scheme 6.2. Preparation of nickel dimethyl complexes **2**, ether adducts **3**, and water adducts **4**.

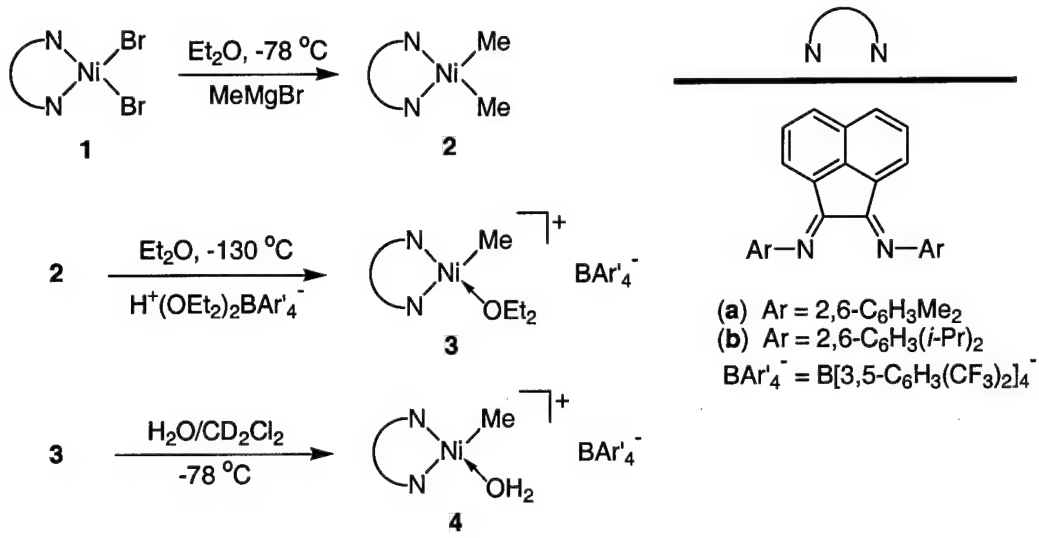

The kinetics of chain growth were monitored by generation of the nickel methyl ethylene complexes, **5a,b**, from the solvent adducts in $CDCl_2F$ and the sequence of migratory insertion reactions was followed by low-temperature ^1H NMR spectroscopy as the alkyl chain grew (Scheme 6.3). Clean generation of the methyl ethylene complex **5a** from **3a** is not straightforward due to the fact that migratory insertion of **5a** is competitive with associative displacement of ether by ethylene to form **5a**. Quantitative generation could be accomplished by treatment of **5a** with a large excess of C_2H_4 (20 equiv) at very low temperatures (-110 °C). Displacement requires ca. 3 hrs under these conditions. The first insertion of ethylene was monitored at -80 °C by measuring the clean first-order disappearance of the Ni-CH_3 singlet for **5a** (δ -0.53), and the first-order rate constant and activation barrier determined (Table 6.1). Subsequent ethylene insertions were followed by measuring the zero-order rate of ethylene consumption at -70 °C;[31] kinetic data is summarized in Table 6.1. The appearance and disappearance of methyl endgroups corresponding to the successive insertion products were clearly seen as triplets in the region between 0.4-0.9 ppm (Figure 6.1). The catalyst

resting state during chain growth is the alkyl olefin complex **7a**. No doublet resonances were observed in the region between 0-1 ppm at any time during the course of the chain-growth process, which would indicate the formation of methyl branches on the growing polymer chain through a competing chain isomerization process. The absence of any branching indicates that no chain isomerization is occurring under these conditions. Following complete consumption of ethylene, a complex containing an agostic hydrogen (δ -13.0, d, $^2J_{HH}$ = 16 Hz, Figure 6.2) is observed at -110 °C, but the exact structure of this species has not yet been determined.

Scheme 6.3. Ethylene chain growth kinetics.

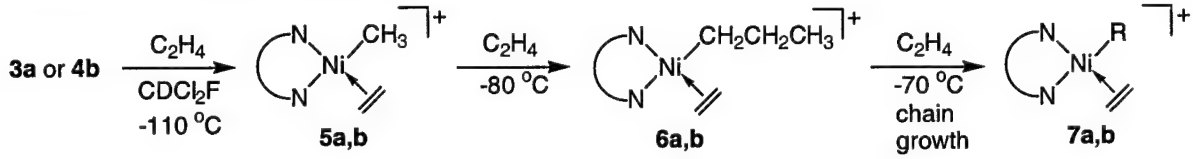

Table 6.1. Ethylene Migratory Insertion Barriers

	First Insertion		Subsequent Insertions	
Complex	k (temp)	$\Delta G^{\ddagger}$, kcal/mol	k (temp)	$\Delta G^{\ddagger}$, kcal/mol
5a	1.22 X 10^{-3} s^{-1} (-80.9 °C)	13.6	2.80 X 10^{-3} s^{-1} (-71.4 °C)	14.0
5b	3.08 X 10^{-4} s^{-1} (-92.9 °C)	13.3	1.03 X 10^{-3} s^{-1} (-83.0 °C)	13.5
8a	3.45 X 10^{-4} s^{-1} (-85.9 °C)	13.7	1.5 X 10^{-1} M^{-1} s^{-1} (-43.4 °C)	See text

Following migratory insertion of the final equivalent of ethylene, a β-agostic species will presumably be formed. Chain isomerization of this β-agostic species through a series of β-hydrogen elimination/olefin rotation/reinsertion cycles leads to many possible intermediate species, and all but one are consistent with the observed agostic doublet (shown in Figure 6.2). The possible isomerization products and the multiplicity of their corresponding agostic hydrogen resonances in ^{1}H NMR spectra are shown in Scheme 6.4. Since the experimentally observed agostic resonance is sharp, it is likely that only one of the species shown in Scheme 6.4 is actually present in solution.

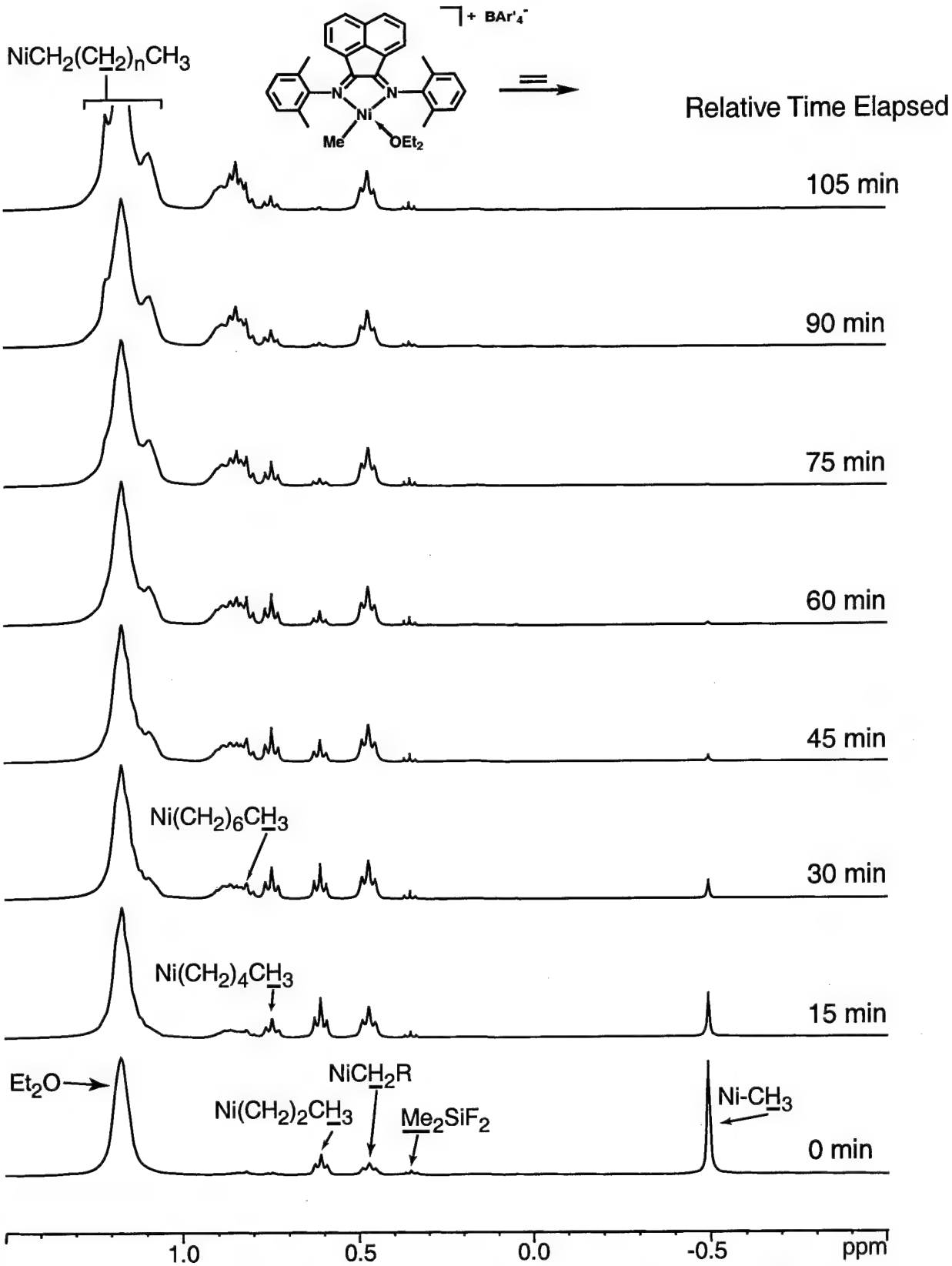

Figure 6.1. Polymer chain growth observed during ethylene insertion kinetic runs initiated by complex **3a**, 400 MHz.

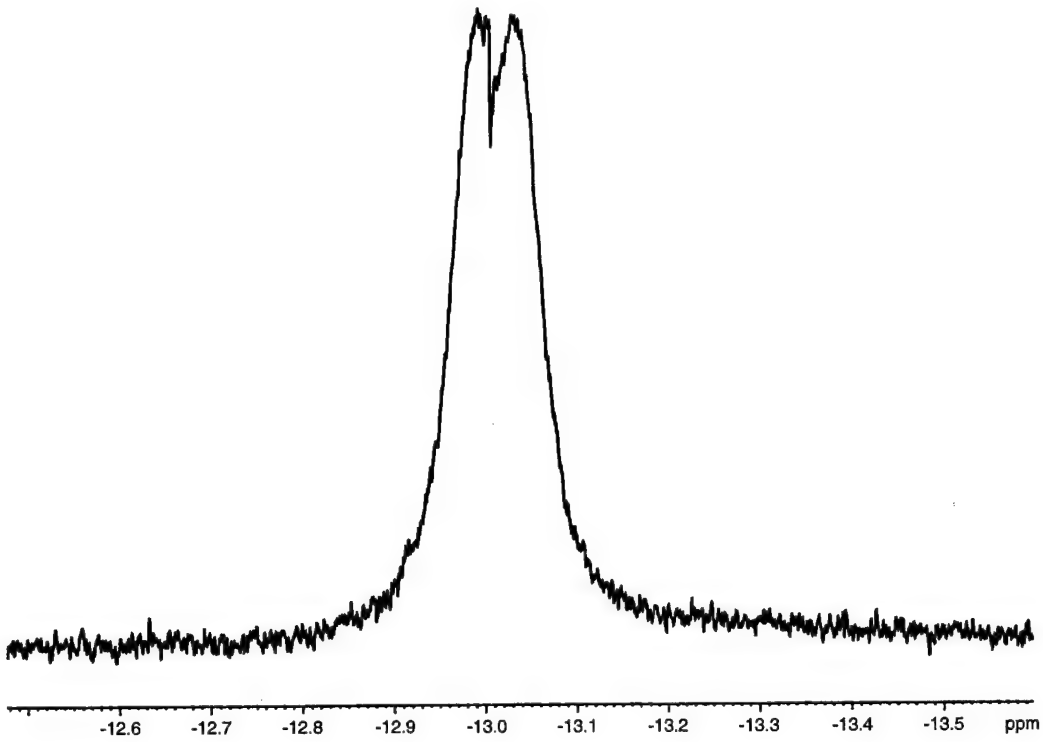

Figure 6.2. Agostic region of the ^{1}H NMR spectrum following complete ethylene consumption (20 eq) in an ethylene chain-growth kinetic experiment initiated by **5a** (-110 °C, $CDCl_2F$, 400 MHz).

Scheme 6.4. Possible β-agostic species following complete ethylene consumption.

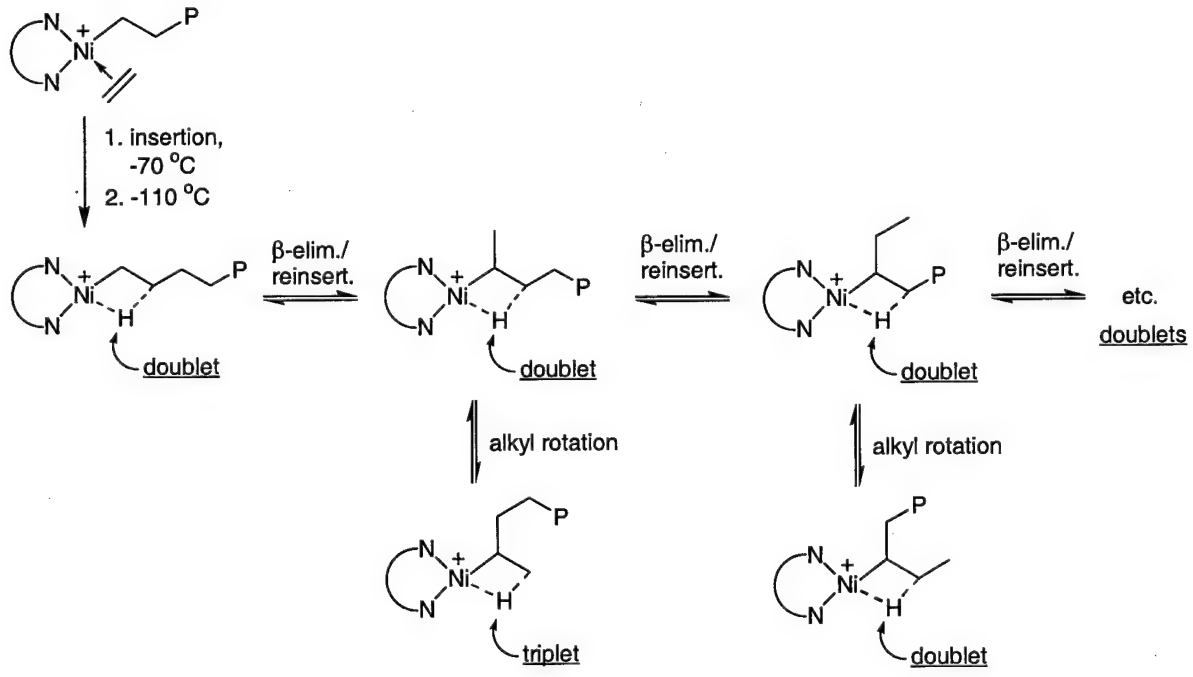

Kinetic measurements of chain growth using the sterically bulkier ether adduct **3b** proved difficult, as ether displacement to form **5b** was competitive with migratory insertion. Surprisingly, we found that water was rapidly and quantitatively displaced from **4b** by ethylene at -130 °C, yielding the desired methyl ethylene complex **5b**. Kinetic measurements of ethylene insertion in this bulkier complex were carried out as previously described, and the results are shown in Table 6.1.

Kinetic measurements of the migratory insertion of propylene were carried out using water adduct **4a** under the conditions shown in Scheme 6.5.[32] The first-order disappearance of methyl propylene complex **8a** was followed at -86 °C. In contrast to the ethylene kinetic studies, no alkyl olefin resting state complex was observed following the first insertion. Instead, an agostic resting state species was observed at -120 °C in $CDCl_2F$.[33,34] The reaction was warmed to -43 °C to measure the rate of subsequent propylene insertions. Pseudo first-order kinetics are observed in the initial phases of consumption of the remaining 19 equivalents of propylene from which a second-order rate constant can be calculated as 0.15 M^{-1} s^{-1} (-43 °C). Assuming that species **10** and the resting state **9** are in equilibrium, and that the $\Delta G^{\ddagger}$ for migratory insertion of **10a** is ca. 14 kcal/mol ($k_{insertion}$ estimated as 0.24 s^{-1}, -43 °C), the ratio of species **9** to **10** is ca. 2000 under these conditions (K_{eq} estimated as 0.0017 M^{-1}).

Scheme 6.5. Propylene chain growth kinetics.

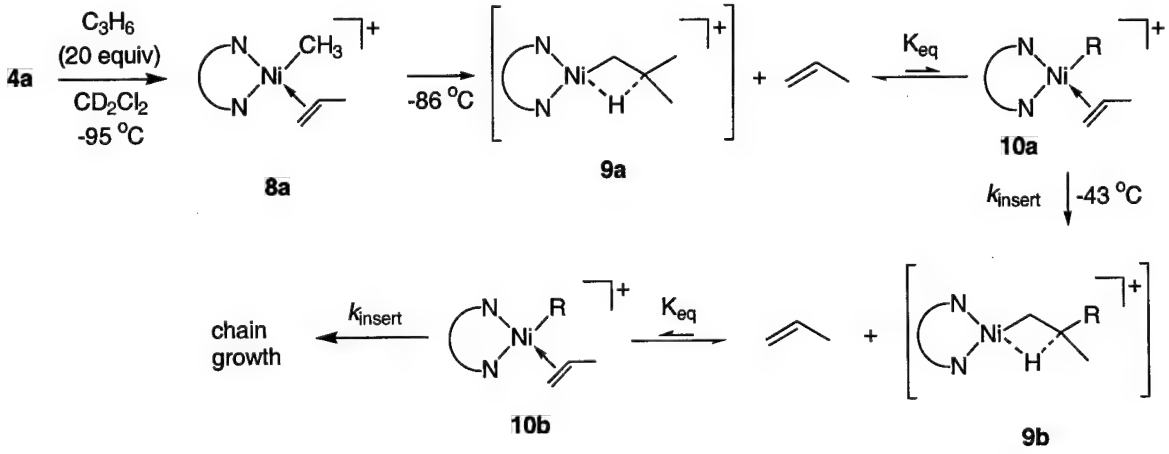

The results reported here now allow a detailed comparison of the Pd and Ni analogs and direct comparison of insertion barriers to theoretical calculations. The (diimine)Pd(C_2H_4)R^+ systems previously reported[8] exhibit barriers to insertion of ca. 17-18 kcal/mol; thus, the barriers for the Ni analogs are ca. 4-5 kcal/mol less. These barrier differences translate to differences in turnover frequencies of ca. 10^4 h^{-1} at 25 °C, consistent with observations.[8] Assuming a negligible $\Delta S^{\ddagger}$ of activation for migratory insertion,[35] the predicted TOF of **5b** is ca. 1700 s^{-1} at 35 °C and compares favorably[36] to an observed TOF of 800 s^{-1} for the catalyst generated by MAO activation in toluene.[37] As an additional comparison, it is interesting to contrast the $\Delta\Delta G^{\ddagger}$ of 5 kcal/mol for ethylene insertion for these Group 10 Ni and Pd complexes to the $\Delta\Delta G^{\ddagger}$ of 8 kcal/mol measured for the Group 9 Co and Rh complexes [Cp*M($P(OMe)_3$)(C_2H_4)$(Et)^+$][BF_4^-] (M = Co, Rh).[38] Theoretical calculations by Ziegler[23] estimate the insertion barrier in a complex very similar to **5b** to be 13.2 kcal/mol ($\Delta H^{\ddagger}$) which is in good agreement with the range of values observed here (Table 6.1). In addition, barriers to ethylene insertion are 0.3-0.5 kcal/mol lower for the complex bearing the bulkier 2,6-(diisopropyl)aryl-substituted diimine ligand. Theoretical calculations[21,23] suggest that increased steric bulk of the diimine ligand aryl substituents leads to an increase in the ground state energy of the resting state species relative to the migratory insertion transition state, and consequently lower migratory insertion barriers are expected with bulkier diimine substituents. Consistent with the observations for Pd systems, the barriers to insertion in the methyl ethylene complexes are quite similar to barriers for subsequent insertions. Also comparable to the Pd systems, the barrier to propylene insertion in the methyl propylene complex **8a** is similar to the insertion barrier in the methyl ethylene complex **5a**. The much lower TOFs observed for α-olefin polymerizations (as compared to ethylene) in the Ni systems are a consequence of the fact that after methyl migration the catalyst resting state is the agostic species and chain growth becomes first order in α-olefin, at least at low α-olefin concentrations.[39]

Conclusions

In summary, the successful preparation of these well-defined nickel complexes has opened the door to mechanistic studies of these systems. Activation barriers for the olefin chain-growth process have been determined, and a dependence of the catalyst resting state on the olefin monomer was observed. Mechanistic studies to uncover the details of the chain isomerization pathways in these nickel-catalyzed olefin polymerizations are currently in progress in the Brookhart group. Some initial results of these studies are described in Chapter 7.

Experimental Section

General Methods. All manipulations of air- and/or water-sensitive compounds were performed using standard high-vacuum or Schlenk techniques. Argon was purified by passage through columns of BASF R3-11 catalyst (Chemalog) and 4-Å molecular sieves. Solid organometallic compounds were transferred in an argon-filled Vacuum Atmospheres drybox. ^{1}H and ^{13}C NMR spectra were recorded on Bruker Avance 300, 400, or 500 MHz spectrometers. Chemical shifts are reported relative to residual $CHDCl_2$ (δ 5.32 for ^{1}H), $CHCl_2F$ (^{1}H: doublet centered at δ 7.47, J = 50 Hz), $CHClF_2$ (δ = 7.16 for ^{1}H), CD_2Cl_2 (δ 53.80 for ^{13}C), or residual $CDCl_3$ in $CDCl_2F$ solutions (δ 77.00 for ^{13}C). NMR probe temperatures were calibrated using an external anhydrous methanol sample.

Materials. Diethyl ether, pentane, and methylene chloride were purified using procedures recently reported by Pangborn et. al.[40] Polymer-grade ethylene and propylene were purchased from National Specialty Gases, and used without further purification. The α-diimine ligands (ArN=C(An)-C(An)=NAr, An,An = acenaphthyl = 1,8-naphth-diyl) and corresponding (α-diimine)nickel(II) bromide complexes were prepared according to modified literature procedures.[8,41-43] Nickel dimethyl complexes **2a,b** were prepared using a modified literature method;[43] see the following text for full details. $(DME)NiBr_2$[44] and $[H(OEt_2)_2]^+[BAr'_4]^-$ ($BAr'_4^- = B(3,5\text{-}C_6H_3(CF_3)_2)_4^-$)[45] were

prepared according to the literature procedures. Dichlorofluoromethane-*d* was prepared according to the literature,[46] and was purified by stirring over silica gel to remove silane byproducts,[47] dried over CaH_2, vacuum transferred, and degassed by repeated freeze-pump-thaw cycles. Acenaphthenequinone, 2,6-dimethylaniline, 2,6-diisopropylaniline, and MeMgBr were purchased from Aldrich Chemical Co. and used as received. $NaBAr'_4$ was purchased from Boulder Scientific.

Synthesis of Nickel Dimethyl Complexes

(ArN=C(An)-C(An)=NAr)NiMe$_2$ (Ar = 2,6-C$_6$H$_3$(Me)$_2$), 2a. A Schlenk flask was equipped with a magnetic stir bar and thoroughly flame-dried under vacuum. The flask was taken into the dry box and charged with (diimine)$NiBr_2$ **1a** (1.28 g, 2.11 mmol). The flask was sealed with a rubber septum which had been previously dried overnight at 100 °C. Teflon tape was placed around the outside septum-glass interface. Dry diethyl ether (50 mL) and *p*-dioxane (0.30 mL, 3.5 mmol) were added to the flask via syringe. The resulting red-brown slurry was stirred at room temperature for 15 min, then cooled to -78 °C under argon. After 15 min, MeMgBr (1.40 mL of a 3.0 M Et_2O solution, 4.22 mmol) was slowly added dropwise. The syringe hole in the septum was immediately covered with grease, and the flask was isolated from the argon line. The reaction slurry soon changed to a very dark purple color. After 2.5 h, the stirring was ceased and the reaction mixture allowed to settle for 10 min. A jacketed filter frit was charged with Florisil (2 cm wide by 1 cm deep column), attached to a Schlenk flask, and the entire assembly was flame-dried under vacuum. Upon cooling, the filter frit assembly was backfilled with argon, and the Florisil column and Schlenk flask were cooled to -78 °C. Dry diethyl ether (10 mL) was added to the top of the Florisil column, the receiver flask vented to an argon-purged oil bubbler, and the reaction mixture was quickly transferred to the filter frit using a 12-gauge cannula. The entire solution was forced through the Florisil as fast as possible under argon head pressure.[48] The filtered solution was filtered a second time through a filter cannula into another flame-dried Schlenk flask cooled to -78 °C. Following the second filtration, a greased glass stopper

was rapidly inserted into the flask, and the flask was immediately evacuated. The solvent was removed under vacuum at ca. -40 °C. The flask was quickly taken into the dry box, and the dark solid purple product was recovered (131 mg, 13%). The product is stable when stored below -15 °C in the dry box, but decomposes slowly at room temperature. CD_2Cl_2 solutions of the product decompose in minutes at room temperature. The product is extremely air-sensitive, and decomposes immediately upon exposure to oxygen. The ^{1}H NMR spectrum of **2a** is shown in Figure 6.3. ^{1}H NMR (CD_2Cl_2, -50 °C, 300 MHz) δ 8.19 (d, J = 8.2 Hz, 2H, An H_p), 7.42-7.26 (m, 6H, Ar*H*), 7.18 (dd, J = 8.2, 7.3 Hz, 2H, An H_m), 6.63 (d, J = 7.1 Hz, 2H, An H_o), 2.27 (s, 12H, ArCH_3), 0.67 (s, 6H, NiCH_3). ^{13}C NMR (CD_2Cl_2, -80 °C, 300 MHz) δ 163.6 (N=*C*-*C*=N), 147.2, 139.3, 132.1, 130.4, 129.6, 128.5, 127.9, 127.2, 125.6, 120.1, 17.8 (ArCH_3), -7.2 (NiCH_3).

(ArN=C(An)-C(An)=NAr)NiMe$_2$ (Ar = 2,6-C$_6$H$_3$(*i*-Pr)$_2$), 2b. This compound was synthesized using the procedure described above, except no *p*-dioxane was used;[49] 1.00 g (1.39 mmol) of (diimine)$NiBr_2$ complex **1b** and 0.93 mL of a 3.0 M solution of MeMgBr in Et_2O (2.78 mmol) were used as starting materials. The product was carefully isolated as described above (481 mg, 59% yield). The product is a dark purple solid and is stable when stored below -15 °C in the dry box, but decomposes in 2 days at room temperature. CD_2Cl_2 solutions of the product are stable indefinitely at -80 °C, but these same solutions decompose in about an hour at room temperature. The product is extremely air-sensitive, and decomposes immediately upon exposure to oxygen. ^{1}H NMR (CD_2Cl_2, -80 °C, 300 MHz) δ 8.16 (d, J = 8.2 Hz, 2H, An H_p), 7.58-7.44 (m, 6H, Ar*H*), 7.16 (virtual t, 2H, An H_m), 6.50 (d, J = 7.2 Hz, 2H, An H_o), 3.34 (m, 4H, C*H*MeMe'), 1.34 (d, J = 6.6 Hz, 12H, CH*Me*Me'), 0.75 (d, J = 6.7 Hz, 12H, CHMe*Me'*), 0.62 (s, 6H, NiCH_3). ^{13}C NMR (CD_2Cl_2, -80 °C, 75 MHz) δ 164.1 (N=*C*-*C*=N), 144.6, 138.8, 132.3, 130.7, 129.3, 127.1, 126.3, 124.3, 123.4, 121.0, 28.2 (*C*HMeMe'), 23.5 (CH*Me*Me'), 23.0 (CHMe*Me'*), -6.7 (NiCH_3).

Synthesis of Ether Adducts

$[(ArN=C(An)-C(An)=NAr)Ni(Me)(OEt_2)]^+[BAr'_4]^-$ (Ar = 2,6-$C_6H_3(Me)_2$), 3a. Two small Schlenk tubes were equipped with stir bars, fitted with rubber septa that had been dried in a glassware oven overnight, and were then flame-dried and taken into a dry box. The nickel dimethyl complex **2a** (107 mg, 0.22 mmol) was added to one tube, and $[H(OEt_2)_2]^+[BAr'_4]^-$ (227 mg, 0.22 mmol) was added to the other. The tubes were sealed, placed on a Schlenk line and cooled to -78 °C. After 5 min, 15 mL dry Et_2O was slowly added to each tube at -78 °C. The solutions were stirred to fully dissolve the solids, and then cooled to -130 °C (pentane/liquid N_2 slurry). The solution of the nickel dimethyl complex was quickly added to the stirred solution of the oxonium acid via cannula. The holes in the septum were covered with grease. The reaction mixture was allowed to warm to -78 °C over 30 min, then was allowed to stir at -78 °C for 2 h. No appreciable color change was observed over the reaction period. The rubber septum was quickly replaced with a lightly greased glass stopper, and the flask was immediately evacuated. The ether solvent was removed under vacuum at -35 °C. Upon removal of the solvent, the flask was quickly taken into the dry box, and the violet solid product recovered (263 mg, 85% recovery). The product is stable indefinitely when stored in the dry box below -15 °C, but decomposes in the solid state at room temperature over 2 days. The ^{1}H NMR spectrum of **3a** is shown in Figure 6.4. ^{1}H NMR ($CDCl_2F$, -120 °C, 400 MHz) δ 8.04 (overlapping d, 2H, An H_p and H_p'), 7.80 (s, 8H, BAr'_4), 7.51-7.26 (m, 12H, Ar*H*), 6.74 (d, J = 7.1 Hz, 1H, An H_o), 6.29 (d, J = 7.1 Hz, 1H, An H_o'), 3.58 (br, 2H, bound $(CH_3CH_2)_2O$), 3.28 (br, 2H, bound $(CH_3CH_2)_2O$), 2.48 (s, 6H, ArCH_3), 2.38 (s, 6H, Ar'CH_3), 1.22 (br, bound $(CH_3CH_2)_2O$), -0.17 (s, 3H, NiCH_3). ^{13}C NMR ($CDCl_2F$, -80 °C, 100 MHz) δ 173.1 and 167.3 (N=*C*-*C*'=N), 161.7 (q, $^1J_{CB}$ = 49.7 Hz, BAr'_4 C_{ipso}), 146.0, 142.4, 142.2, 134.6 (BAr'_4 C_o), 132.4, 132.3, 131.2, 129.3, 129.25 (q, $^2J_{CF}$ = 28.3 Hz, BAr'_4 C_m), 128.87, 128.85, 128.54, 128.48, 128.38, 128.26, 128.1, 127.9, 124.9, 124.8,

124.48, 124.41 (q, $^1J_{CF}$ = 272 Hz, *C*F_3), 117.5 (BAr'$_4$ C_p), 69.4 (bound $(CH_3CH_2)_2O$), 18.0 and 17.9 (Ar*C*H_3 and Ar'*C*H_3), 14.0 (bound $(CH_3CH_2)_2O$), -3.7 (Ni*C*H_3).

[(ArN=C(An)-C(An)=NAr)Ni(Me)(OEt$_2$)]$^+$[BAr'$_4$]$^-$ (Ar = 2,6-C$_6$H$_3$(*i*-Pr)$_2$), 3b. This compound was synthesized using the procedure described above; 130 mg (0.22 mmol) of nickel dimethyl complex **2b** and $[H(OEt_2)_2]^+[BAr'_4]^-$ (227 mg, 0.22 mmol) were used as starting materials. The product was carefully isolated as described above (288 mg, 87% recovered yield). The product is a violet solid and is stable when stored below -15 °C in the dry box, but decomposes in 2 days at room temperature. CD_2Cl_2 solutions of the product are stable indefinitely at -80 °C. The product is extremely air-sensitive, and decomposes immediately upon exposure to oxygen. ^{1}H NMR ($CDCl_2F/CDClF_2$ (1:1), -80 °C, 400 MHz): δ 8.02 (d, *J* = 8.4 Hz, 1H, An H_p), 7.99 (d, *J* = 8.6 Hz, 1H, An H_p'), 7.83 (s, 8H, BAr'$_4$), 7.56 (s, 4H, BAr'$_4$), 7.53-7.38 (m, 8H, ArH), 6.68 (d, *J* = 7.3 Hz, 1H, An H_o), 6.27 (d, *J* = 7.3 Hz, 1H, An H_o), 3.80 (m, 2H, C*H*MeMe'), 3.55 (m, bound $(CH_3CH_2)_2O$), 3.33 (m, 2H, C'*H*MeMe'), 1.29 (t, *J* = 6.6 Hz, 6H, bound $(CH_3CH_2)_2O$), 1.50 (br d, *J* = 4.6 Hz, 12H), 0.96 (d, *J* = 6.3 Hz, 6H), and 0.91 (d, *J* = 6.6 Hz, 6H, CH*MeMe'* and C'H*MeMe'*), 0.06 (s, 3H, NiCH_3). ^{13}C NMR (CD_2Cl_2, -80 °C, 100 MHz) δ 172.3 and 167.1 (N=*C*-*C*'=N), 161.2 (q, $^1J_{CB}$ = 49.7 Hz, BAr'$_4$ C_{ipso}), 145.1, 139.6, 139.2, 138.9, 138.4, 134.0 (BAr'$_4$ C_o), 131.8, 131.6, 130.7, 128.0 (q, $^2J_{CF}$ = 27.7 Hz, BAr'$_4$ C_m; three ligand Ar peaks obscured by this quartet), 125.0, 124.8, 124.6 (2C), 124.4, 124.3, 124.2, 123.8 (q, $^1J_{CF}$ = 273 Hz, *C*F_3), 117.0 (BAr'$_4$ C_p), 69.8 (bound $(CH_3CH_2)_2O$), 29.2 and 28.7 (*C*HMeMe' and *C*'HMeMe'), 24.6, 23.9, 23.12, and 23.07 (CH*MeMe'*, C'H*MeMe'*), 13.2 (bound $(CH_3CH_2)_2O$), -3.6 (Ni*C*H_3).

Water Adducts

Water adducts **4a,b** can be quantitatively prepared from the corresponding ether adducts **3a,b** through addition of 1 mol equivalent of degassed H_2O in CH_2Cl_2 to cooled CH_2Cl_2 solutions (-80 °C) of the ether adducts **3a,b**. When CD_2Cl_2 solutions of **4a,b** are warmed to 0 °C or above, CH_4 is observed by ^1H NMR, and a sparingly-soluble species with a ^1H NMR spectrum consistent with a μ-OH-bridged dimer is observed. The bridging OH signal appears at -7.4 ppm (CD_2Cl_2, 20 °C) when a CD_2Cl_2 solution of **4b** is allowed to stand at room temperature for 1 h.

[(ArN=C(An)-C(An)=NAr)Ni(Me)(OH_2)]$^+$[BAr'$_4$]$^-$ (Ar = 2,6-$C_6H_3(Me)_2$), 4a. ^1H NMR (CD_2Cl_2, -80 °C, 400 MHz) δ 8.09 (overlapping d, 2H, An H_p and H_p'), 7.71 (s, 8H, BAr'$_4$), 7.50 (s, 4H, BAr'$_4$), 7.45-7.20 (m, 8H, Ar*H*), 6.74 (d, *J* = 6.8 Hz, 1H, An H_o), 6.32 (d, *J* = 6.8 Hz, 1H, An H_o'), 3.83 (br s, 2H, bound H_2O), 2.43 (s, 6H, ArCH_3), 2.30 (s, 6H, Ar'CH_3), -0.09 (s, 3H, Ni-CH_3). See Figure 6.5 for the ^1H NMR spectrum of **4a**.

[(ArN=C(An)-C(An)=NAr)Ni(Me)(OH_2)]$^+$[BAr'$_4$]$^-$ (Ar = 2,6-C_6H_3(*i*-Pr)$_2$), 4b. ^1H NMR (CD_2Cl_2, -80 °C, 400 MHz) δ 8.06 (virtual t, 2H, An H_p and H_p'), 7.71 (s, 8H, BAr'$_4$), 7.50 (s, 4H, BAr'$_4$), 7.45-7.36 (m, 8H, Ar*H*), 6.75 (d, *J* = 7.0 Hz, 1H, An H_o), 6.29 (d, *J* = 7.1 Hz, 1H, An H_o'), 3.81 (br s, 2H, bound H_2O), 3.43 (m, 4H, C*H*MeMe' and C'*H*MeMe'), 1.48 (d, *J* = 5.6 Hz, 6H), 1.39 (d, *J* = 5.3 Hz, 6H), 0.99 (d, *J* = 5.6 Hz, 6H), and 0.83 (d, *J* = 5.6 Hz, 6H, CH*MeMe'*, C'H*MeMe'*), 0.04 (s, 3H, NiCH_3). ^{13}C NMR (CD_2Cl_2, -80 °C, 100 MHz) δ 171.3 and 167.4 (N=*C*-*C*'=N), 161.2 (q, $^1J_{CB}$ = 49.7 Hz, BAr'$_4$ C_{ipso}), 145.4, 139.7, 139.04, 139.02, 137.4, 134.0 (BAr'$_4$ C_o), 131.7, 131.4, 130.8, 129.0, 128.9, 128.6, 128.4, 128.0 (q, $^2J_{CF}$ = 27.5 Hz, BAr'$_4$ C_m), 125.0, 124.8, 124.6, 124.4, 124.3, 124.0, 123.8 (q, $^1J_{CF}$ = 272 Hz, *C*F_3), 117.0 (BAr'$_4$ C_p), 28.8 and 28.6 (*C*HMeMe' and

C'HMeMe'), 23.6, 23.0, 22.9, and 22.8 (CH*MeMe'*, C'H*MeMe'*), -1.8 ($NiCH_3$). See Figure 6.6 for the ^1H NMR spectrum of **4b**.

Olefin Insertion Kinetics

General Procedure for Kinetic Experiments. Approximately 10 μmol of the appropriate ether adduct $[(ArN=C(An)-C(An)=NAr)Ni(Me)(L)]^+[BAr'_4]^-$ was added to a high-grade NMR tube (Wilmad 528PP or 535PP) in the dry box. The tube was capped with a rubber septum and the top wrapped with Parafilm. The tube was cooled to -130 °C (liquid N_2/pentane slurry) and ~700 μL $CDCl_2F$ was added via a 22-gauge cannula. The tube was wrapped with more Parafilm, and shaken to dissolve the salt. A proton NMR spectrum was then acquired at -130 °C. The appropriate olefin was then added to the NMR tube via gastight syringe at -130 °C (using an 18-inch, 22 gauge needle inserted to the bottom of the NMR tube), and the tube quickly replaced into the cooled NMR probe. Following acquisition of another proton NMR spectrum at -130 °C, the probe was warmed to the appropriate temperature, and spectra acquired over 5 min intervals. Concentrations of all species in solution were calculated using the BAr'_4^- peaks as internal standards.

Kinetics of Ethylene Migratory Insertion of Complex 5a

Diethyl ether displacement by ethylene: An NMR tube containing **3a** (15.0 mg, 1.07×10^{-5} mol) and ethylene (5.00 mL at 25 °C, 2.0×10^{-4} mol) was prepared and placed into the NMR probe as described above. The sample was warmed to -110 °C, and diethyl ether was completely displaced by ethylene over 2 h. The pseudo first-order plot of this data is shown in Figure 6.9. The observed pseudo first-order rate constant for ether displacement at -110 °C: $k_{obs,3a} = 4.07 \times 10^{-4}\ s^{-1}$. The

second-order rate constant for ether displacement by ethylene at -110 °C is 1.42 X 10^{-3} L mol^{-1} s^{-1}. The resulting methyl ethylene complex **5a** was characterized by ^{1}H NMR spectroscopy:

[(ArN=C(An)-C(An)=NAr)Ni(Me)(C_2H_4)]$^+$[BAr'$_4$]$^-$ (Ar = 2,6-C_6H_3(Me)$_2$), 5a. ^{1}H NMR ($CDCl_2F$, -110 °C, 400 MHz) δ 8.09 (d, J = 8.3 Hz, 1H, An H_p), 8.04 (d, J = 8.3 Hz, 1H, An H_p'), 7.79 (s, 8H, BAr'$_4$), 7.52-7.24 (m, 12H, Ar*H*), 6.54 (overlapping d, 2H, An H_o and H_o'), 5.0-4.0 (very broad, bound C_2H_4), 2.35 (s, 6H, ArCH_3), 2.27 (s, 6H, Ar'CH_3), -0.53 (s, 3H, NiCH_3). The ^{1}H NMR spectrum of **5a** is shown in Figure 6.7.

Kinetics of the first ethylene migratory insertion: Methyl ethylene complex **5a** was warmed to -80 °C, and the first-order disappearance of the Ni-Me integral was monitored until it completely disappeared (2 h). The first-order plot of this data is shown in Figure 6.10. The first-order rate constant for the first migratory insertion of ethylene in **5a**: k_{5a} = 1.22 X 10^{-3} s^{-1}, $\Delta G^{\ddagger}$ = 13.6 kcal/mol. Subsequent insertions occur slowly at -80 °C relative to the first insertion. The resulting alkyl olefin species **7a** was characterized by ^{1}H NMR spectroscopy:

[(ArN=C(An)-C(An)=NAr)Ni(R)(C_2H_4)]$^+$[BAr'$_4$]$^-$ (Ar = 2,6-C_6H_3(Me)$_2$), 7a. ^{1}H NMR ($CDCl_2F$, -80 °C, 400 MHz) δ 8.09 (d, J = 8.3 Hz, 1H, An H_p), 8.05 (d, J = 8.3 Hz, 1H, An H_p'), 7.77 (s, 8H, BAr'$_4$), 7.55-7.26 (m, 12H, Ar*H*), 6.75 (d, J = 7.6 Hz, 1H, An H_o), 6.68 (d, J = 7.3 Hz, 1H, An H_o'), 4.6-3.8 (very broad, 4H, bound C_2H_4), 2.37 (s, 6H, ArCH_3), 2.27 (s, 6H, Ar'CH_3), 1.21 (br s, CH_2's), 0.93-0.78 (m, CH_3 end groups), 0.47 (t, J = 7.3 Hz, 2H, NiCH_2R). The ^{1}H NMR spectrum of **7a** is shown in Figure 6.8.

Kinetics of subsequent ethylene insertions: The alkyl olefin complex **7a** was warmed to -70 °C, and the zero-order disappearance of the free ethylene integral was monitored until it completely

disappeared (90 min). The zero-order plot of this data is shown in Figure 6.10. The zero-order rate constant for ethylene disappearance: $k'_{5a} = 2.80 \times 10^{-3}$ s^{-1}, $\Delta G^{\ddagger} = 14.0$ kcal/mol. Following complete ethylene consumption, a β-agostic species is observed at -110 °C (agostic H: -13.0 ppm).

Kinetics of Ethylene Migratory Insertion of Complex 5b

Water displacement by ethylene: An NMR tube was charged with methyl ether complex **3b** (14.8 mg, 9.78×10^{-6} mol) in the dry box. The tube was sealed, cooled to -78 °C, and ~700 μL of $CDCl_2F/CDClF_2$ (1:1) was added via cannula. The tube was cooled to -130 °C, and a solution of degassed H_2O (~0.5 μL) in 200 μL CD_2Cl_2 was added via syringe. After 2 h at -60 °C, ether adduct **3b** was cleanly converted to water adduct **4b**. The sample was cooled to -130 °C, and ethylene (5.00 mL at 25 °C, 2.0×10^{-4} mol) was added. Quantitative conversion of water adduct **4b** to the methyl ethylene complex **5b** was observed by ^{1}H NMR spectroscopy.

[(ArN=C(An)-C(An)=NAr)Ni(Me)(C_2H_4)]$^+$[BAr'$_4$]$^-$ (Ar = 2,6-C_6H_3(*i*-Pr)$_2$), 5b. ^{1}H NMR ($CDCl_2F/CDClF_2$ (1:1), -90 °C, 500 MHz) δ 8.04 (d, J = 7.4 Hz, 1H, H_p), 7.99 (d, J = 7.9 Hz, 1H, H_p'), 7.80 (s, 8H, BAr'$_4$), 7.54 (s, 4H, BAr'$_4$), 7.50-7.41 (m, 8H, Ar*H*), 6.46 (d, J = 6.6 Hz, 1H, H_o), 6.39 (d, J = 6.9 Hz, 1H, H_o'), 5.2-4.2 (very br, 4H, bound C_2H_4), 3.37 (m, 2H, C*H*MeMe'), 3.18 (m, 2H, C'*H*MeMe'), 1.48 (d, J = 5.0 Hz, 6H), 1.44 (d, J = 5.8 Hz, 6H), 0.96 (d, J = 5.6 Hz, 6H), and 0.85 (d, J = 5.2 Hz, 6H, CH*MeMe'*, C'H*MeMe'*), -0.35 (s, 3H, NiCH_3).

Kinetics of the first ethylene migratory insertion: Methyl ethylene complex **5b** was warmed to -92.9 °C, and the first-order disappearance of the Ni-Me integral was monitored until it completely disappeared (3 h). The first-order rate constant for the first migratory insertion of ethylene in **5b**: k_{5b}

= 3.08 X 10^{-4} s^{-1}, $\Delta G^{\ddagger}$ = 13.3 kcal/mol. Subsequent insertions are slow at this temperature. The resulting alkyl olefin species **7b** was characterized by ^{1}H NMR spectroscopy:

[(ArN=C(An)-C(An)=NAr)Ni(R)(C_2H_4)]$^+$[BAr'$_4$]$^-$ (Ar = 2,6-C_6H_3(*i*-Pr)$_2$), 7b. ^{1}H NMR ($CDCl_2F/CDClF_2$ (1:1), -80 °C, 500 MHz) δ 8.04 (virtual t, 2H, An H_p and H_p'), 7.79 (s, 8H, BAr'$_4$), 7.59-7.42 (m, 8H, Ar*H*), 7.53 (s, 4H, BAr'$_4$), 6.57 (d, *J* = 6.7 Hz, 1H, An H_o), 6.52 (d, *J* = 6.6 Hz, 1H, An H_o'), 5.2-4.2 (very br, 4H, bound C_2H_4), 3.33 (m, 2H, C*H*MeMe'), 3.13 (m, 2H, C'*H*MeMe'), 1.42 (d, *J* = 4.4 Hz, 6H), 1.34 (d, *J* = 4.0 Hz, 6H), 1.22 (br s, R chain CH_2's), 0.91 (overlapping doublets, apparent *J* = 6.0 Hz, 12H), 0.85 (t, *J* = 6.3 Hz, 3H, Ni$(CH_2)_n$CH_3 end group).

Kinetics of subsequent ethylene insertions: The alkyl olefin complex **7b** was warmed to -82.9 °C, and the zero-order disappearance of the free ethylene integral was monitored. The zero-order rate constant for ethylene disappearance: k'_{5b} = 1.03 X 10^{-3} s^{-1}, $\Delta G^{\ddagger}$ = 13.5 kcal/mol.

Kinetics of Propylene Insertion in Complex 8a

Water displacement by ethylene: An NMR tube was charged with methyl ether complex **3a** (14.0 mg, 1.00 X 10^{-5} mol) in the dry box. The tube was sealed, cooled to -78 °C, and 500 μL of CD_2Cl_2 was added via syringe. A solution of degassed H_2O (~0.5 μL) in 250 μL CD_2Cl_2 was then added to the sample via syringe at -80 °C. Ether adduct **3a** was cleanly converted to water adduct **4a** as observed by ^{1}H NMR. Propylene (5.00 mL at 25 °C, 2.0 X 10^{-4} mol) was then added at -80 °C. Quantitative conversion of water adduct **4a** to the methyl propylene complex **8a** (9:1 mixture of rotamers) was observed by ^{1}H NMR spectroscopy.

[(ArN=C(An)-C(An)=NAr)Ni(Me)(CH_2=$CHCH_3$)]$^+$[BAr_4']$^-$ (Ar = 2,6-$C_6H_3(Me)_2$), 8a. ^{1}H NMR (CD_2Cl_2, -85.9 °C, 500 MHz, major rotamer) δ 8.13 (d, J = 8.1 Hz, 1H, An H_p), 8.09 (d, J = 8.1 Hz, 1H, An H_p'), 7.71 (s, 8H, BAr'_4), 7.49 (s, 4H, BAr'_4), 7.37-7.23 (m, 8H, Ar*H*), 6.49 (d, J = 7.6 Hz, 1H, An H_o), 6.46 (d, J = 7.3 Hz, 1H, An H_o'), 5.42 (m, 1H, bound CH_2=C*H*CH_3), 4.42-4.16 (m, 2H, bound C*H*$_2$=$CHCH_3$), 2.43, 2.33, 2.20, 2.16 (all s, 3H each, ArC*H*$_3$'s), -0.59 (s, 3H); CH_2=$CHCH_3$ obscured by Et_2O. The Ni-C*H*$_3$ resonance for the minor rotamer appears as a singlet at δ -0.54.

Kinetics of the first propylene migratory insertion: The rate of ethylene migratory insertion in **8a** was monitored by following the disappearance of the Ni-Me integral at -85.9 °C. The first-order rate constant for the first migratory insertion of propylene in **8a**: k_{8a} = 3.45 X 10^{-4} s^{-1}, $\Delta G^{\ddagger}$ = 13.7 kcal/mol.

Kinetics of subsequent propylene migratory insertions: Following completion of the first insertion, the sample was warmed to -43.4 °C, and the disappearance of propylene was monitored. No alkyl olefin species was observed. Pseudo first-order kinetics are observed in the initial phases of consumption of the remaining 19 equivalents of propylene; the observed rate constant extracted from this data is k_{obs} = 4.10 X 10^{-4} s^{-1}. The second-order rate constant is calculated as 0.15 M^{-1} s^{-1}. The catalyst resting state observed was an agostic species.

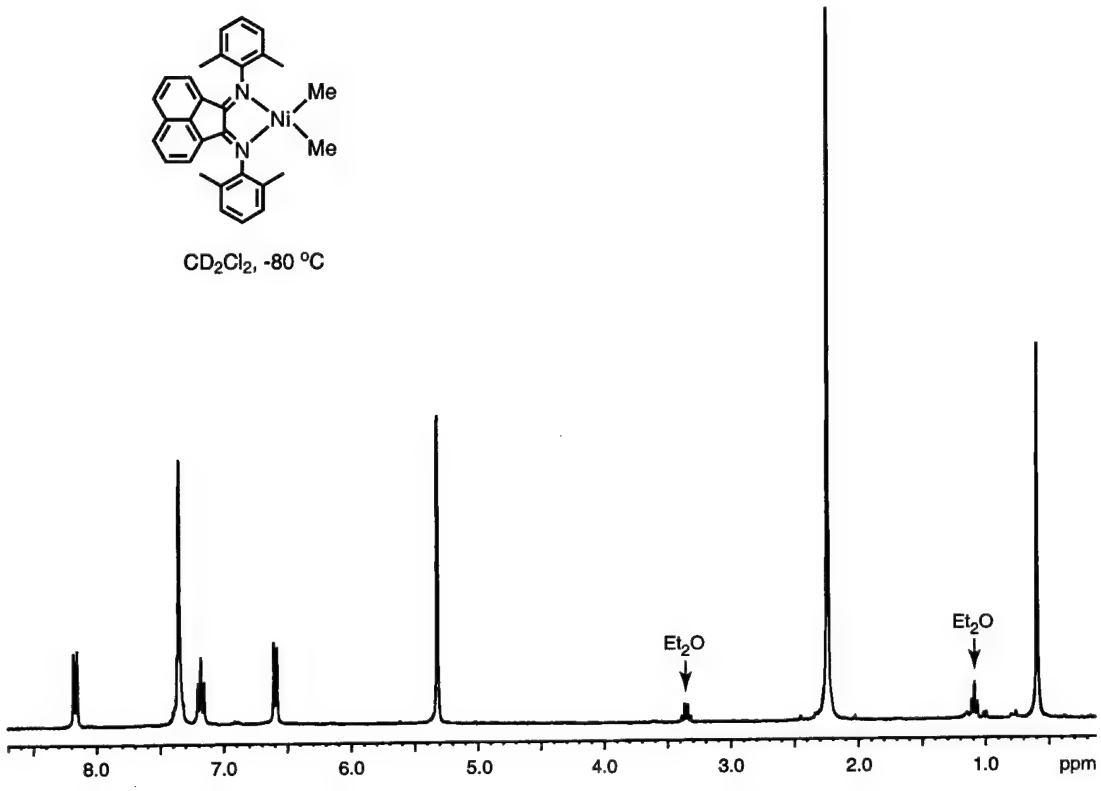

Figure 6.3. ^{1}H NMR spectrum of complex **2a**, CD_2Cl_2, -80 °C, 300 MHz.

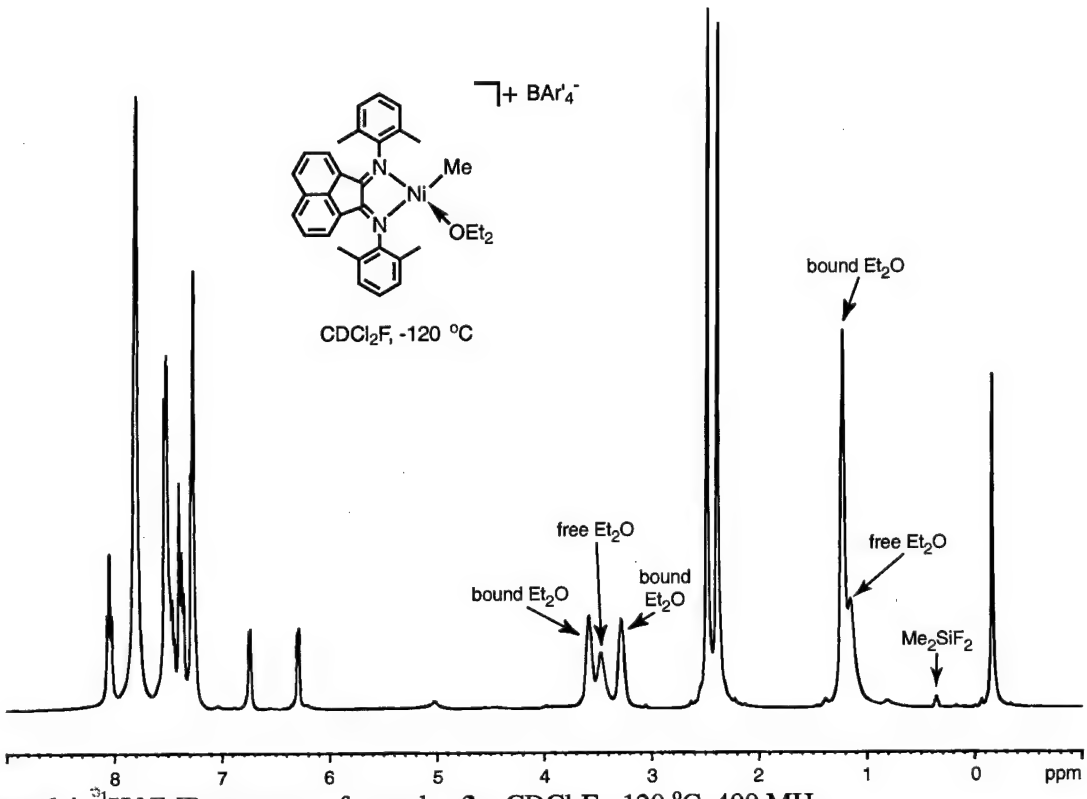

Figure 6.4. ^{1}H NMR spectrum of complex **3a**, $CDCl_2F$, -120 °C, 400 MHz.

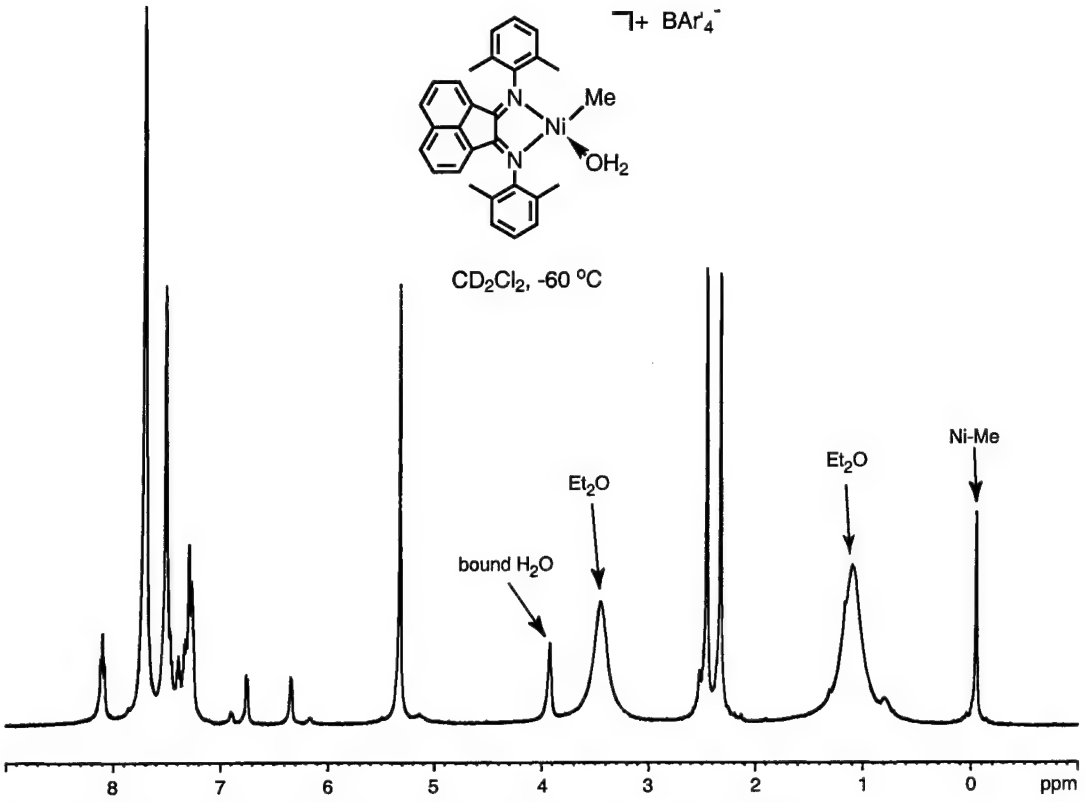

Figure 6.5. ^{1}H NMR spectrum of complex **4a**, CD_2Cl_2, -60 °C, 500 MHz.

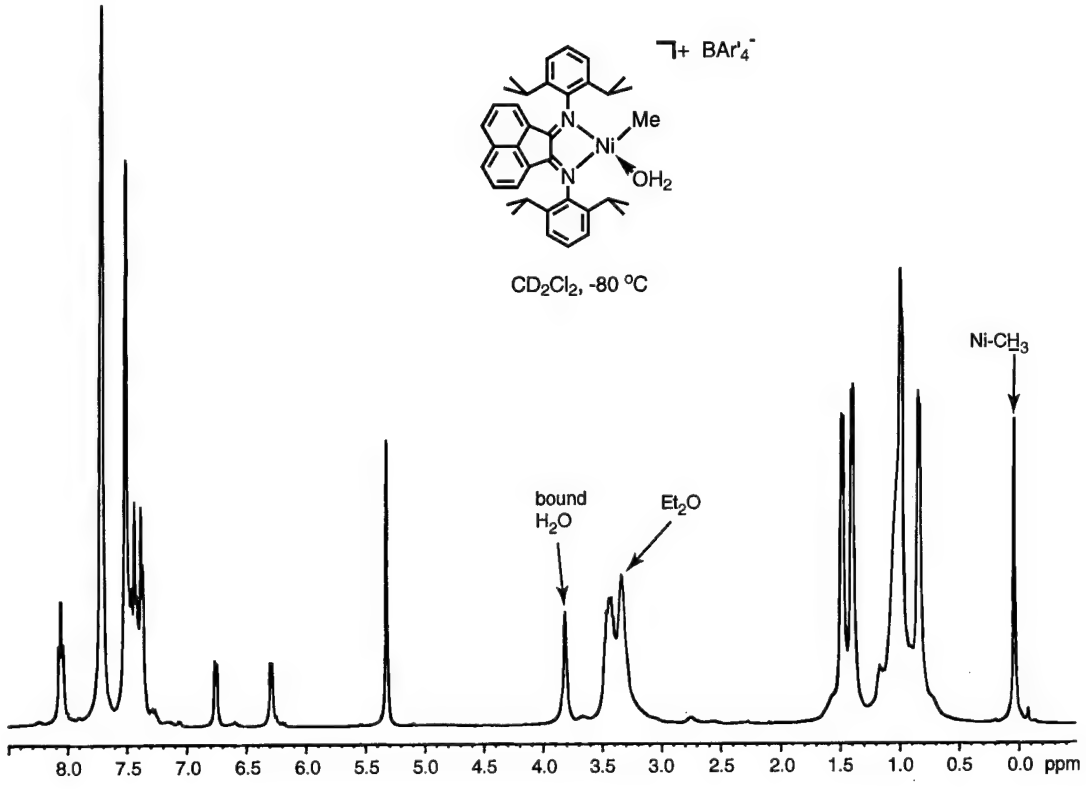

Figure 6.6. ^{1}H NMR spectrum of complex **4b**, CD_2Cl_2, -80 °C, 400 MHz.

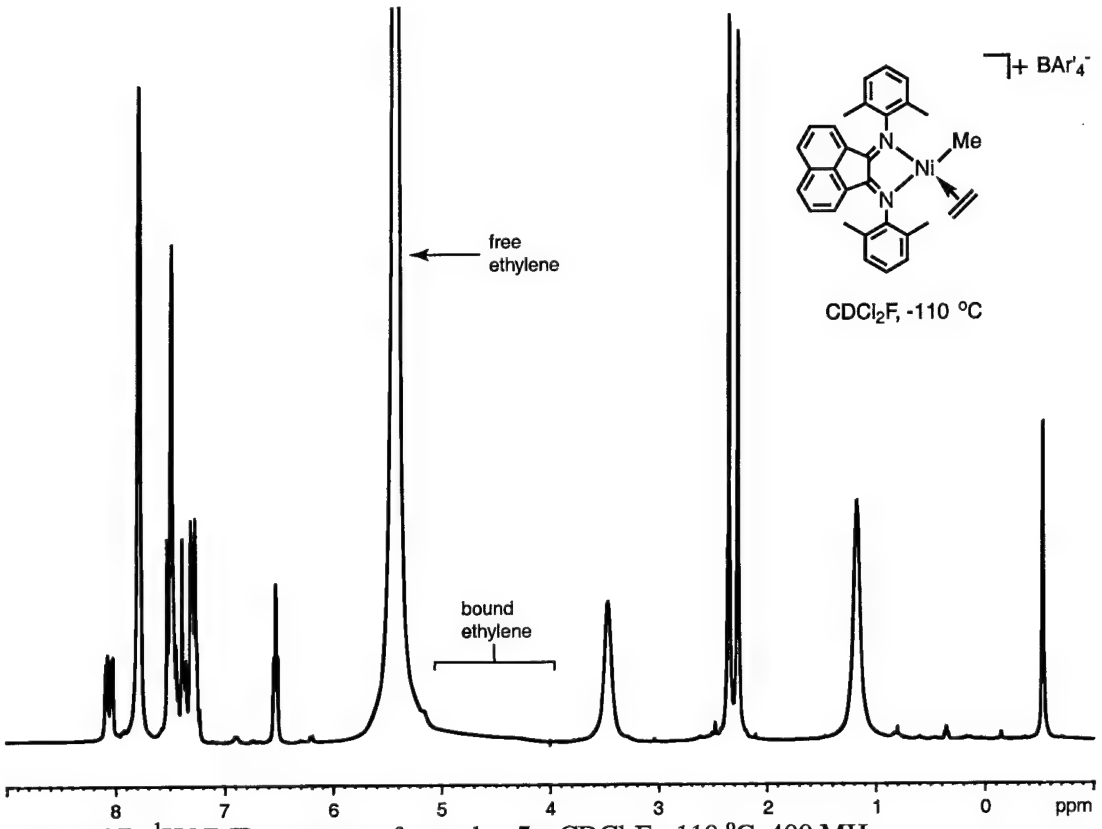

Figure 6.7. ^{1}H NMR spectrum of complex **5a**, $CDCl_2F$, -110 °C, 400 MHz.

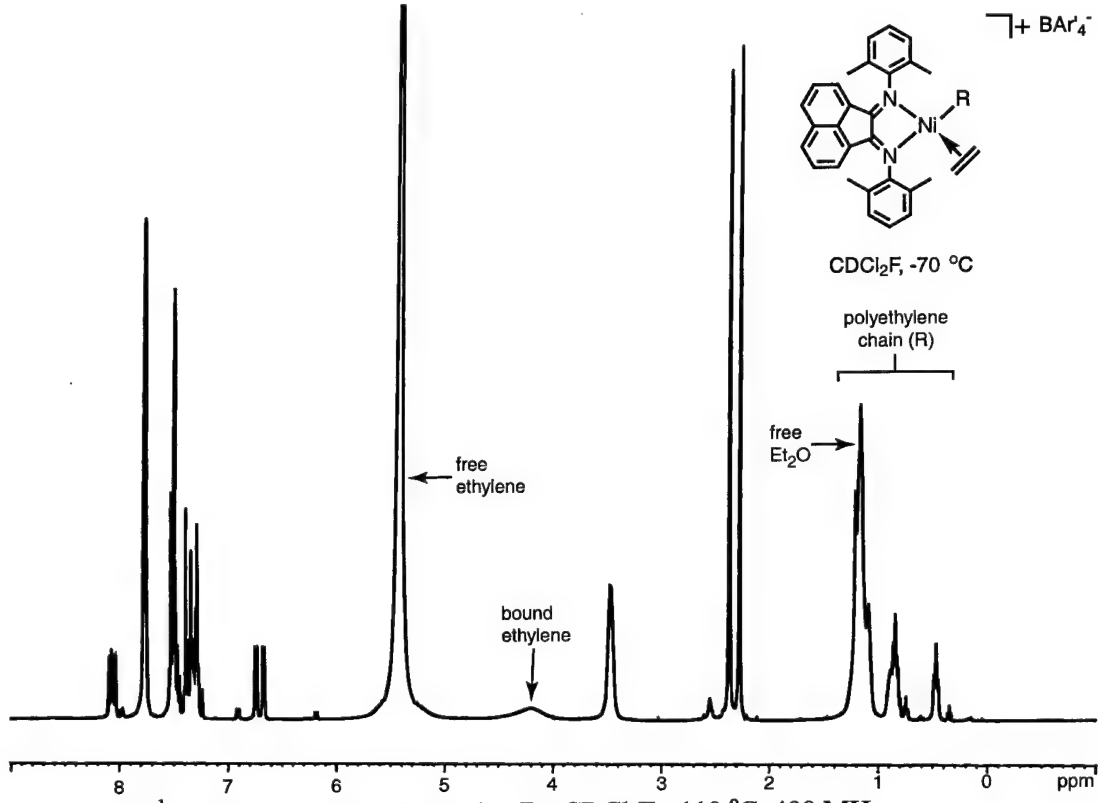

Figure 6.8. ^{1}H NMR spectrum of complex **7a**, $CDCl_2F$, -110 °C, 400 MHz.

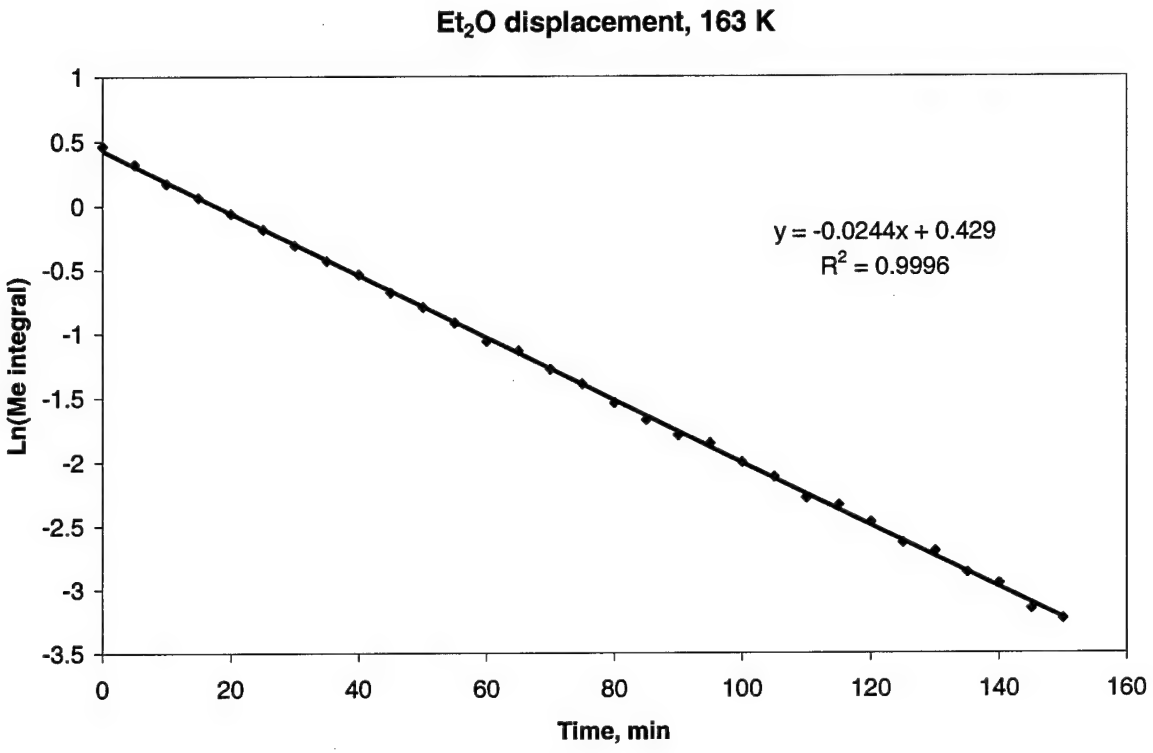

Figure 6.9. Pseudo first-order plot of ether displacement by ethylene for complex **3a**.

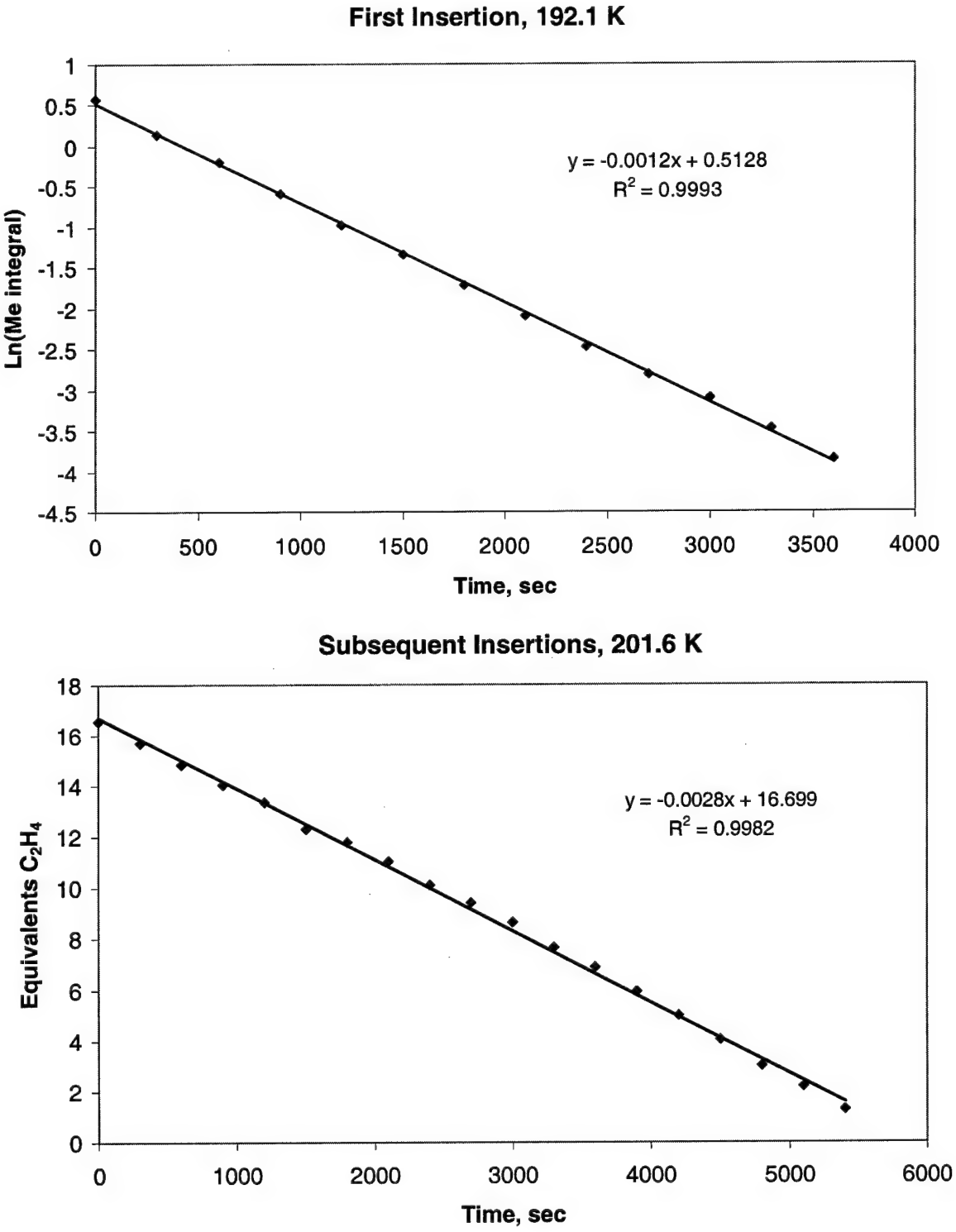

Figure 6.10. Representative plots for the determination of ethylene migratory insertion rates for complex **3a**; first-order insertion of ethylene in **5a** (top), and zero-order subsequent insertions of ethylene (bottom).

References and Notes

(1) Bochmann, M. *J. Chem. Soc., Dalton Trans.* **1996**, 255-270.

(2) Kaminsky, W.; Arndt, M. Polymerization, Oligomerization, and Copolymerization of Olefins. In *Applied Homogeneous Catalysis with Organometallic Compounds*; Cornils, B., Herrmann, W. A., Eds.; VCH: New York, 1996; Vol. 1, pp 220-236.

(3) Brintzinger, H. H.; Fischer, D.; Mülhaupt, R.; Rieger, B.; Waymouth, R. M. *Angew. Chem., Int. Ed. Engl.* **1995**, *34*, 1143-1170.

(4) Coates, G. W.; Waymouth, R. M. *Science* **1995**, *267*, 217-219.

(5) Yang, X.; Stern, C. L.; Marks, T. J. *J. Am. Chem. Soc.* **1994**, *116*, 10015-10031.

(6) Coughlin, E. B.; Bercaw, J. E. *J. Am. Chem. Soc.* **1992**, *114*, 7606-7607.

(7) Crowther, D. J.; Baenziger, N. C.; Jordan, R. F. *J. Am. Chem. Soc.* **1991**, *113*, 1455-1457.

(8) Johnson, L. K.; Killian, C. M.; Brookhart, M. *J. Am. Chem. Soc.* **1995**, *117*, 6414-6415.

(9) Galland, G. B.; de Souza, R. F.; Mauler, R. S.; Nunes, F. F. *Macromolecules* **1999**, *32*, 1620-1625.

(10) Schleis, T.; Spaniol, T. P.; Okuda, J.; Heinemann, J.; Mülhaupt, R. *J. Organomet. Chem.* **1998**, *569*, 159-167.

(11) Yang, K.; Lachicotte, R. J.; Eisenberg, R. *Organometallics* **1998**, *17*, 5102-5113.

(12) Ganis, P.; Orabona, I.; Ruffo, F.; Vitagliano, A. *Organometallics* **1998**, *17*, 2646-2650.

(13) Pellecchia, C.; Zambelli, A.; Mazzeo, M.; Pappalardo, D. *J. Mol Catal.* **1998**, *128*, 229-237.

(14) Zeng, X.; Zetterberg, K. *Macromol. Chem. Phys.* **1998**, *199*, 2677-2681.

(15) Carfagna, C.; Formica, M.; Gatti, G.; Musco, A.; Pierleoni, A. *Chem. Commun.* **1998**, 1113-1114.

(16) Fusto, M.; Giordano, F.; Orabona, I.; Ruffo, F.; Panunzi, A. *Organometallics* **1997**, *16*, 5981-5987.

(17) Yang, K.; Lachicotte, R. J.; Eisenberg, R. *Organometallics* **1997**, *16*, 5234-5243.

(18) Pappalardo, D.; Mazzeo, M.; Pellecchia, C. *Macromol. Rapid Commun.* **1997**, *18*, 1017-1023.

(19) Pellecchia, C.; Zambelli, A.; Oliva, L.; Pappalardo, D. *Macromolecules* **1996**, *29*, 6990-6993.

(20) Pellecchia, C.; Zambelli, A. *Macromol. Rapid Commun.* **1996**, *17*, 333-338.

(21) Froese, R. D. J.; Musaev, D. G.; Morokuma, K. *J. Am. Chem. Soc.* **1998**, *120*, 1581-1587.

(22) Musaev, D. G.; Froese, R. D. J.; Morokuma, K. *Organometallics* **1998**, *17*, 1850-1860.

(23) Deng, L.; Woo, T. K.; Cavallo, L.; Margl, P. M.; Ziegler, T. *J. Am. Chem. Soc.* **1997**, *119*, 6177-6186.

(24) Musaev, D. G.; Froese, R. D. J.; Svensson, M.; Morokuma, K. *J. Am. Chem. Soc.* **1997**, *119*, 367-374.

(25) Musaev, D. G.; Svensson, M.; Morokuma, K.; Stromberg, S.; Zetterberg, K.; Siegbahn, P. E. M. *Organometallics* **1997**, *16*, 1933-1945.

(26) Deng, L.; Margl, P. M.; Ziegler, T. *J. Am. Chem. Soc.* **1997**, *119*, 1094-1100.

(27) Musaev, D. G.; Froese, R. D. J.; Morokuma, K. *New J. Chem.* **1997**, *21*, 1269-1282.

(28) Tempel, D. J.; Brookhart, M. *Organometallics* **1998**, *17*, 2290-2296.

(29) Solutions of **2** in CD_2Cl_2 eliminate ethane readily at temperatures above 0 °C. In the solid state, these complexes decompose at room temperature over 2 days.

(30) The nickel dimethyl complexes were prepared using a procedure similar to that reported by Svoboda and tom Dieck: Svoboda, M.; tom Dieck, H. *J. Organomet. Chem.* **1980**, *191*, 321-328. See the Experimental Section for full experimental details.

(31) In monitoring chain growth of **5a** by ^1H NMR spectroscopy, specific resonance assignments can be made for (diimine)Ni$(C_2H_4)(CH_2)_n$ CH_3^+: n=2 (first insertion product), n=4 (second insertion) and n=6 (third insertion). See Figure 6.1 for illustrated spectra.

(32) Water adduct **4a** was used instead of ether adduct **3a** because ether displacement by propylene is competitive with olefin migratory insertion, whereas formation of methyl propylene complex **8a** from **4a** is quantitative and rapid at -80 °C.

(33) A β-agostic resting state in the addition polymerization of cyclopentene using very similar Ni and Pd diimine complexes has also been reported: McLain, S. J.; Feldman, J.; McCord, E. F.; Gardner, K. H.; Teasley, M. F.; Coughlin, E. B.; Sweetman, K. J.; Johnson, L. K.; Brookhart, M. *Macromolecules* **1998**, *31*, 6705-6707.

(34) Species **9** are dynamic and the structures of the isomer or isomers present have not been determined. Structure **9a** is written as shown based on previous reports; see refs 13, 19, and 20.

(35) A $\Delta S^{\ddagger}$ of -11.2 eu was measured for a similar Pd complex: see ref 8, Supporting Information.

(36) The two complexes being compared were measured in different solvents ($CDCl_2F$ vs. toluene) and had different counterions. In addition, it is likely that less than quantitative activation of all nickel sites by MMAO is occurring.

(37) Gates, D. P.; Svejda, S. A.; Brookhart, M. Unpublished results.

(38) Brookhart, M.; Volpe, A. F.; Lincoln, D. M.; Horvath, I. T.; Millar, J. M. *J. Am. Chem. Soc.* **1990**, *112*, 5634-5636.

(39) Killian, C. M. Ni(II)-Based Catalysts for the Polymerization and Copolymerization of Olefins: A New Generation of Polyolefins. Ph.D. Dissertation, University of North Carolina-Chapel Hill, 1996.

(40) Pangborn, A. B.; Giardello, M. A.; Grubbs, R. H.; Rosen, R. K.; Timmers, F. J. *Organometallics* **1996**, *15*, 1518-1520.

(41) van Asselt, R.; Elsevier, C. J.; Smeets, W. J. J.; Spek, A. L.; Benedix, R. *Recl. Trav. Chim. Pays-Bas* **1994**, *113*, 88-98.

(42) tom Dieck, H.; Svoboda, M.; Grieser, T. *Naturforsch* **1981**, *36b*, 823-832.

(43) Svoboda, M.; tom Dieck, H. *J. Organomet. Chem.* **1980**, *191*, 321-328.

(44) Ward, L. G. L. *Inorg. Syn.* **1971**, *13*, 154-164.

(45) Brookhart, M.; Grant, B.; Volpe, A. F. *Organometallics* **1992**, *11*, 3920-3922.

(46) Siegel, J. S.; Anet, F. A. *J. Org. Chem.* **1988**, *53*, 2629-2630.

(47) A small amount of Me_2SiF_2 was occasionally observed as a byproduct of the fluorination reaction. Formation of this product can be suppressed through minimal use of silicone grease on glass joints used in the preparation of $CDCl_2F$.

(48) Use of alumina or silica as the solid support for this purification step results in considerable decomposition of the nickel dimethyl product.

(49) Addition of sub-stoichiometric amounts of *p*-dioxane to the reaction aids in complexing the magnesium salts and thus facilitates more efficient filtration, but yields of the nickel dimethyl complexes decrease dramatically.

CHAPTER 7

Synthesis and Reactivity of Cationic (α-Diimine)Ni(II) β-Agostic Complexes and Related Derivatives

Introduction

The microstructure of polyethylene produced by nickel(II)- and palladium(II)-diimine catalysts varies from strictly linear to highly branched, while the microstructures of poly(α-olefins) produced by these same catalyst systems are characterized by fewer branches than are expected from 1,2-monomer enchainment (chain-straightening).[1] The degree of branching in the polyethylene depends on a number of factors: the metal, the steric bulk of the diimine ligand, and the reaction conditions. Polyethylenes produced by palladium(II)-diimine catalysts are highly branched (e.g. >70 methyls/1000 carbons) regardless of ligand structure or reaction conditions. In contrast, the branching in polyethylene produced by nickel(II)-diimine catalysts is quite variable. Polymerizations run at low temperatures, high ethylene concentrations, and employment of nickel complexes bearing relatively nonbulky diimine ligands yield strictly linear polyethylene, while higher temperatures, low ethylene concentrations, and use of nickel complexes bearing sterically demanding diimine ligands result in highly branched polyethylene.[1-3] In the case of nickel-catalyzed polymerization of α-olefins, the degree of chain-straightening observed in the resulting poly(α-olefin)s is strongly affected by diimine ligand symmetry and reaction conditions. Palladium catalysts generally produce more chain-straightened poly(α-olefin) products than their nickel analogs, but unlike the nickel systems, the degree of branching seen in poly(α-olefin)s produced by the palladium complexes is relatively independent of ligand structure and reaction conditions.[4]

Mechanistic studies of ethylene polymerizations catalyzed by both nickel(II)- and palladium(II)-diimine complexes have led to the proposed polymerization mechanism shown in Scheme 7.1.[1,4-6] Following initiation, the mechanism is characterized by chain propagation, chain isomerization, and chain transfer steps. To date, the chain propagation step is the best-studied portion of the overall mechanism. Low-temperature NMR studies of ethylene polymerization have established the catalyst resting state for both metals as the alkyl ethylene complexes, implying rate-limiting migratory ethylene insertion. Activation barriers to ethylene insertion have been measured for both palladium and nickel complexes. As discussed in the previous chapter, the activation barriers to ethylene insertion in the chain propagation step are 4-5 kcal/mol lower for the nickel complexes as compared to their palladium congeners.

Scheme 7.1. Proposed mechanism of olefin polymerization.

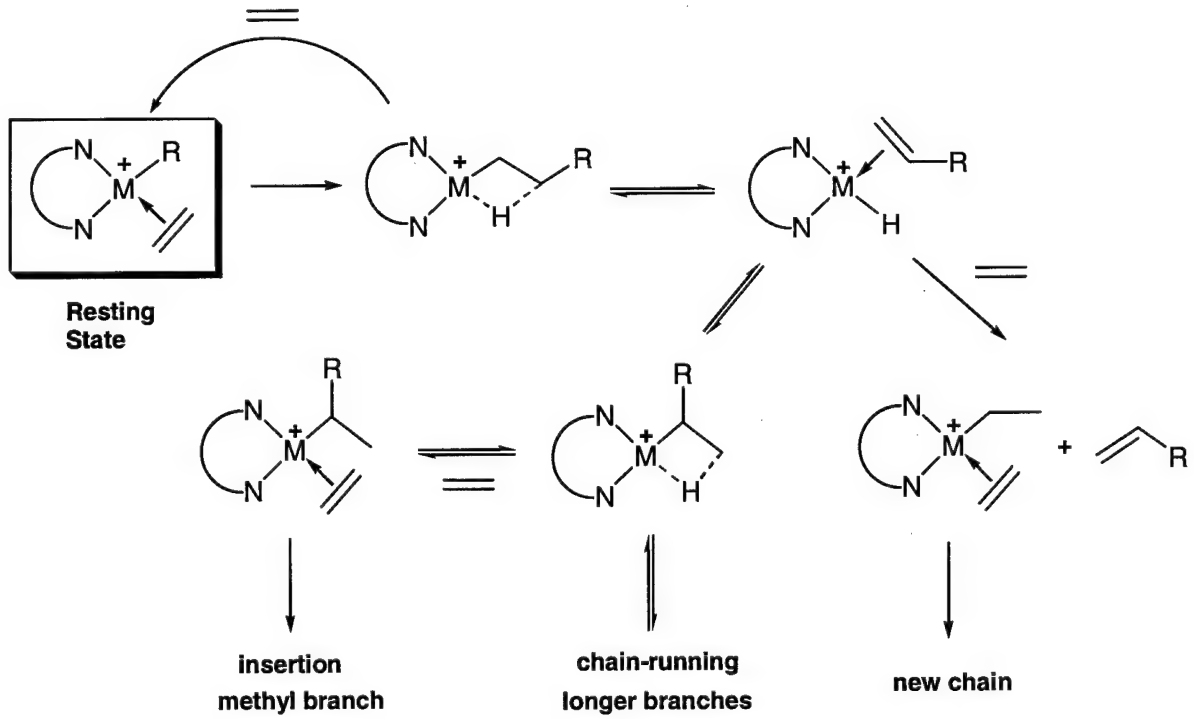

Mechanistic studies of the chain isomerization process have focused on (α-diimine)Pd(II) β-agostic complexes. Low-temperature NMR studies of these (α-diimine)Pd(II) β-agostic complexes have established that the activation barriers to chain propagation are ca. 17-18 kcal/mol, and are

significantly higher than the activation barriers to chain isomerization.[4,5] The proposed mechanism of chain isomerization in these Pd complexes is shown in Scheme 7.2. According to this mechanism, alkyl chain isomerization can occur following the loss of ethylene from the alkyl ethylene resting state.[7] The barrier to interconversion of the resulting β-agostic species is quite low (<11 kcal/mol), and the rate of the interconversion is much faster than the rate of trapping of the β-agostic species by ethylene. Therefore, chain isomerization occurs rapidly even from the catalyst resting state, which explains both the highly branched polyethylenes produced by the (α-diimine)palladium systems as well as the independence of the degree of polymer branching on ethylene pressure demonstrated by palladium catalysts.

Scheme 7.2. Isomerization equilibria in (α-diimine)Pd complexes.

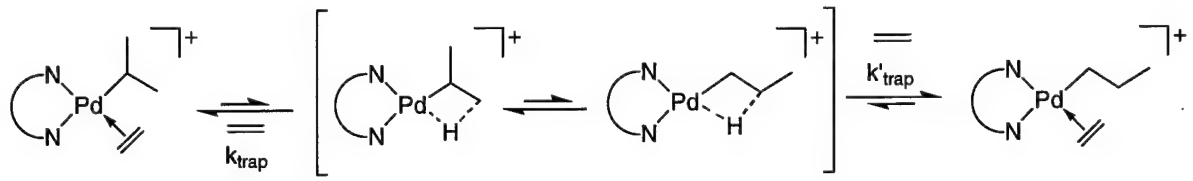

Thus far, the mechanism of chain growth and chain isomerization has been studied in some detail for the palladium systems. In contrast, difficult synthesis and manipulation of well-defined (α-diimine)nickel(II) complexes has hindered mechanistic investigations of these systems. In Chapter 6, the synthesis of well-defined (α-diimine)nickel(II) complexes and mechanistic studies of olefin chain growth processes in these nickel complexes were described. In this chapter, a preliminary account of our studies of cationic (α-diimine)Ni(II) β-agostic complexes is presented. Some implications of these studies concerning the mechanism of chain isomerization during (α-diimine)nickel(II)-catalyzed olefin polymerizations are discussed. Further studies in this area are currently in progress in the Brookhart group.

Results and Discussion

A. Synthesis and Reactivity of (α-Diimine)Ni(II) β-Agostic *n*-Propyl and Isopropyl Complexes. Recent work in our laboratory with (α-diimine)Pd(II) β-agostic complexes has established that chain isomerization occurs rapidly relative to chain propagation.[4,5] In these experiments, palladium β-agostic complex **1** was prepared and isolated on a preparative scale using the conditions shown in Scheme 7.3. Since the barrier to ethylene insertion is relatively high in these palladium complexes, the clean, quantitative formation of the methyl ethylene complex shown in Scheme 7.3 is straightforward. Excess monomer can be easily purged from the solution with argon. Migratory insertion of ethylene occurs when the solution is warmed to 0 °C. The isopropyl β-agostic complex **1** is the observed reaction product, which presumably forms following rapid isomerization of the initially formed *n*-propyl β-agostic complex. When the solution is cooled to -110 °C, the agostic hydrogen of complex **1** is clearly observed.

Scheme 7.3. Synthesis of Pd β-agostic isopropyl complexes.[4,5]

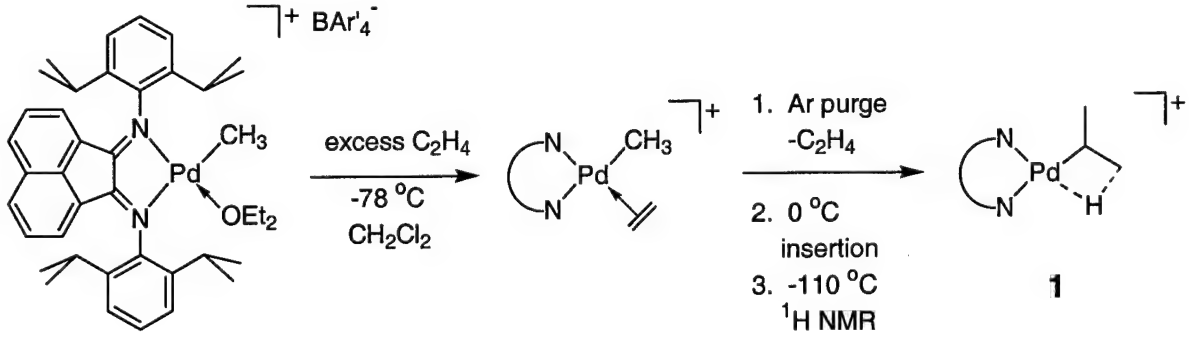

Attempts to form β-agostic nickel complexes through insertion of one equivalent of ethylene in nickel methyl ethylene complexes were unsuccessful (Scheme 7.4). The addition of one equivalent of ethylene to ether adduct **2** at -110 °C led to very slow formation of methyl ethylene complex **3**. Even at -110 °C, multiple insertions of ethylene occurred prior to complete ether displacement, resulting in a complex mixture of the starting ether adduct, the desired methyl ethylene compound **3**, and various insertion products. Use of a large excess of ethylene to hasten the formation of the methyl ethylene

complex **3** from ether adduct **2**, followed by an argon purge to remove the excess ethylene, also failed. Multiple insertions of ethylene again occurred, possibly due to slight warming of the solution by the argon purge gas. The sterically bulkier diisopropyl ether adduct **4** (Scheme 7.5) was anticipated to undergo more facile ether displacement by ethylene to form methyl ethylene complex **3**. The conditions used to attempt the synthesis of **4** are shown in Scheme 7.5. Unfortunately, numerous attempts to prepare **4** failed to yield the desired product; this compound appears to be unstable, even at -78 °C.

Scheme 7.4. Attempted synthesis of Ni β-agostic complexes through a single insertion of ethylene.

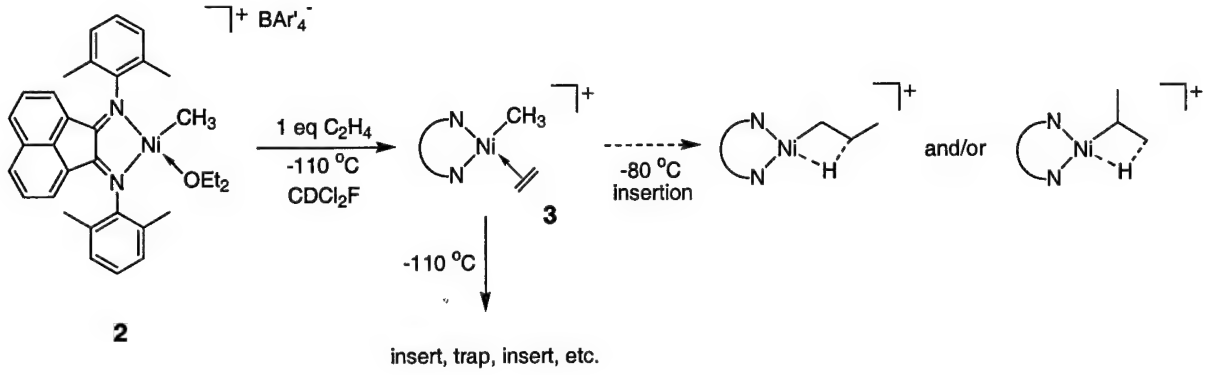

Scheme 7.5. Attempted synthesis of diisopropyl ether adduct **4**.

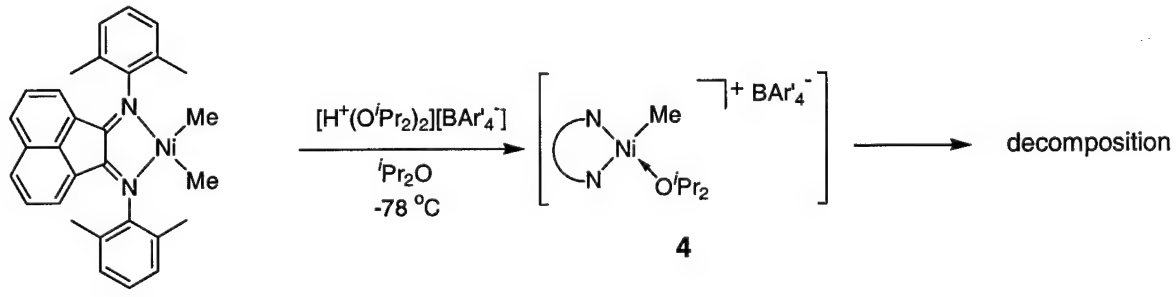

An alternative route to the desired β-agostic nickel complexes based upon protonolysis of an (α-diimine)$NiPr_2$ complex with $[H(OEt_2)_2]^+[BAr'_4]^-$ was attempted and was found to be successful. Alkylation of (α-diimine)$NiBr_2$ complex **5** with two equivalents of *n*-propylmagnesium chloride in diethyl ether at -78 °C produced the corresponding (α-diimine)$NiPr_2$ complex **6** (Scheme 7.6). Use of

ethylmagnesium chloride in this synthesis produces the corresponding (α-diimine)$NiEt_2$ complex **7** (Scheme 7.6). Diethyl ether solutions of either complex are very dark midnight blue in color, while the complexes are dark purple in the solid state. The solids appear to be stable indefinitely when stored at temperatures below -15 °C in a drybox, but are thermally sensitive in solution. Both complexes undergo reductive elimination to yield hexane or butane, respectively, when their CD_2Cl_2 solutions are warmed above -20 °C. Complexes **6** and **7** are extremely air-sensitive, and immediately decompose to form unknown products (black in color) when exposed to the air. Reactions of the nickel diethyl complex **7** will be discussed later in this chapter.

Scheme 7.6. Synthesis of nickel di-*n*-propyl complex **6** and nickel diethyl complex **7**.

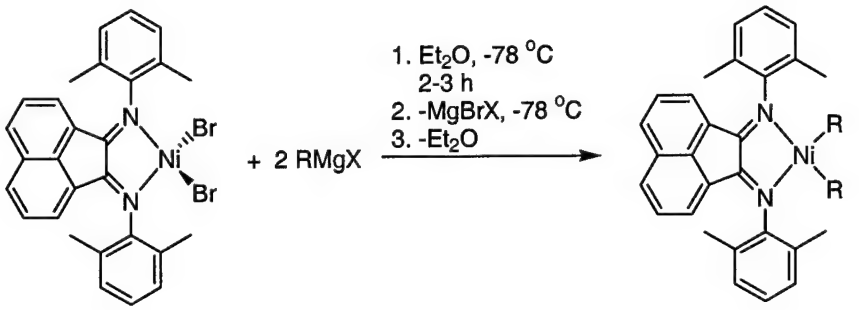

5

6 R = *n*-propyl
7 R = ethyl

Protonolysis of nickel dipropyl complex **6** with one equivalent of $[H(OEt_2)_2]^+[BAr'_4]^-$ in diethyl ether at approximately -100 °C yields propane and a mixture of two β-agostic species (Scheme 7.7). The mixture consists of a 20:1 ratio of β-agostic isopropyl complex ***i*-8**:β-agostic *n*-propyl complex ***n*-8**. The *n*-propyl complex ***n*-8** is presumably the initial product formed immediately following the loss of propane after protonation of **6**. Complex ***n*-8** then isomerizes to the β-agostic isopropyl complex ***i*-8**. The structure of the β-agostic isopropyl complex ***i*-8** was confirmed by low-temperature NMR experiments (^1H and ^1H-^1H COSY) obtained in $CDCl_2F$ at -130 °C. The proton NMR resonance of the β-agostic hydrogen of ***i*-8** is observed as a triplet (δ -12.5, $^2J_{HH}$ = 19 Hz), while the β-agostic hydrogen of the *n*-propyl complex ***n*-8** appears as a doublet (δ -13.0, $^2J_{HH}$ = 19 Hz) (see Figure 7.5

following the Experimental Section for the ^{1}H NMR spectrum of the agostic region). The other two hydrogens on the agostic methyl group (complex ***i*-8**) are chemically inequivalent, and appear as broad multiplets at 0.26 and 0.11 ppm. The nonagostic methyl group resonance appears as a broad singlet at -0.09 ppm. The resonance due to the isopropyl methine hydrogen (δ 2.00) is a complex multiplet at temperatures below -120 °C, but appears as a septet at temperatures above -80 °C.

Scheme 7.7. Synthesis of Ni β-agostic complexes ***i*-8/*n*-8** via protonolysis of nickel dipropyl complex **6**.

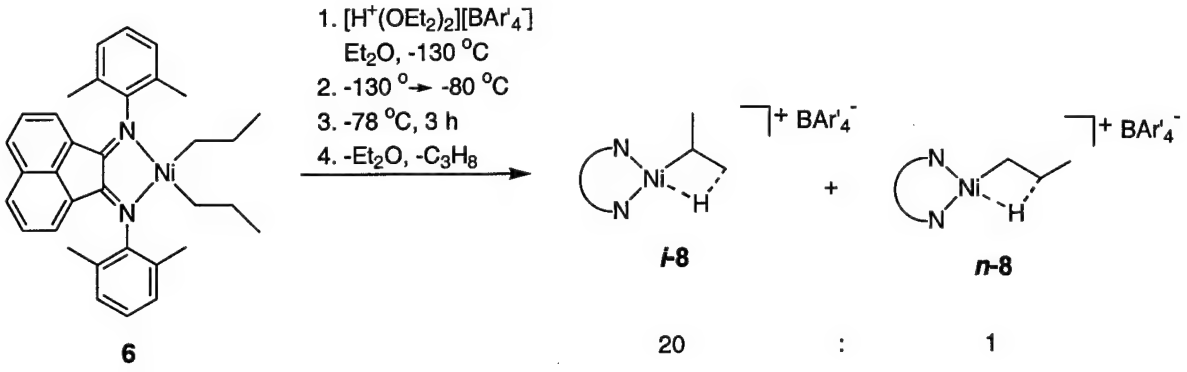

Variable-temperature ^{1}H NMR studies reveal that three distinct dynamic processes occur in complex ***i*-8**: in-place methyl rotation, isopropyl methyl exchange, and methyl/methine hydrogen exchange. These processes are shown in Scheme 7.8. Two of these processes, in-place methyl rotation and isopropyl methyl exchange, are relatively low-energy processes as compared to methyl/methine hydrogen exchange. As previously mentioned, at temperatures below -120 °C, the proton NMR resonance of the β-agostic hydrogen of complex ***i*-8** is observed as a triplet. At higher temperatures this signal quickly broadens, as do the agostic and non-agostic isopropyl methyl resonances. This dynamic behavior is indicative of facile hydrogen exchange through an in-place rotation of the agostic methyl group, along with exchange of the agostic methyl group with the free methyl group via rotation of the isopropyl group about the Ni-C bond (Scheme 7.8).[8] Over the temperature range of -140 to -40 °C, the isopropyl methine resonance displays no discernable line broadening. At -30 °C this resonance begins to broaden. These observations indicate that the barrier

to exchange of the isopropyl methine hydrogen with the isopropyl methyl hydrogens (interconversion of ***i*-8** and ***i*-8'**) is considerably higher than the barriers to in-place methyl rotation and isopropyl methyl exchange. The overall dynamic behavior exhibited by this agostic nickel complex is qualitatively very similar to that reported for the analogous, well-studied β-agostic isopropyl palladium complex.[8]

Scheme 7.8. Dynamic processes demonstrated by β-agostic isopropyl complex ***i*-8**.

<u>In-Place Methyl Rotation</u>

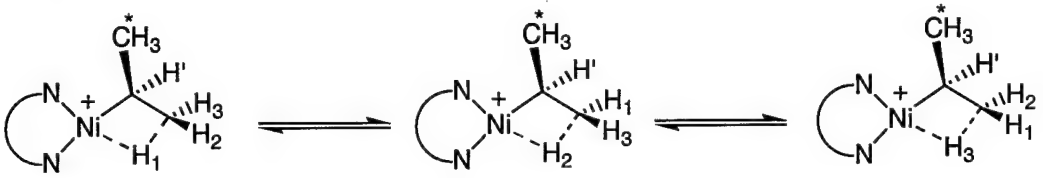

***i*-8**

<u>Isopropyl Methyl Exchange</u>

<u>Methyl/Methine Exchange</u>

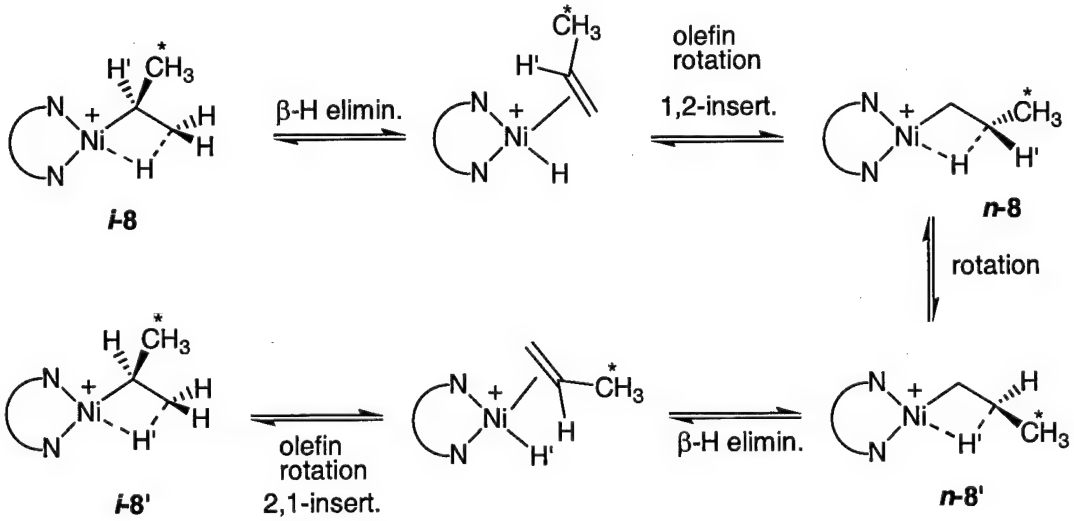

***i*-8'** ***n*-8** ***n*-8'**

When ca. 7 equivalents of diethyl ether relative to complex ***i*-8** are present in a $CDCl_2F$ NMR solution, new resonances in the proton NMR spectrum are observed. At -130 °C, previously unobserved peaks appear at 6.28 ppm (br), 3.95 ppm (br m) and 0.24 ppm (d, J = 6.7 Hz). These signals are consistent with a diethyl ether adduct. The resonance appearing at 6.28 ppm is likely due to the acenaphthene backbone *ortho* hydrogens, the resonance at 3.95 ppm is likely a methylene resonance of bound diethyl ether, and the doublet at 0.24 ppm is consistent with the isopropyl methyl group (eq 7.1). The equilibrium shown in eq 7.1 lies in favor of the β-agostic isopropyl complex ***i*-8** as no diethyl ether adduct is observed when only 1 equivalent of free ether is present. With 7 equivalents of diethyl ether present, a roughly 1:1 ratio of the β-agostic isopropyl complex:diethyl ether adduct is observed.

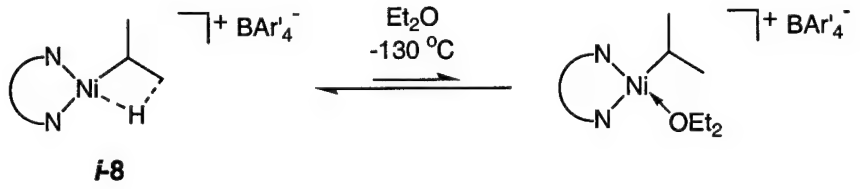

***i*-8** (7.1)

The addition of ethylene at -130 °C to the mixture of β-agostic complexes ***i*-8** and ***n*-8** produced following protonolysis of nickel dipropyl complex **6** results in trapping of the agostic complexes as their corresponding alkyl ethylene complexes ***i*-9** and ***n*-9** (Scheme 7.9). The structure of each complex was confirmed by low-temperature ^1H NMR and ^1H-^1H COSY NMR spectroscopy. Key ^1H NMR resonances for ***i*-9** ($CDCl_2F/CDClF_2$, -130 °C) include bound ethylene signals at 3.96 and 3.53 ppm (d, J = 14 Hz, 2H each), the isopropyl methine resonance at 1.47 ppm (m, 1H), and the isopropyl methyl resonance at 0.40 ppm(br s, 6H). Diagnostic resonances for ***n*-9** ($CDCl_2F/CDClF_2$, -100 °C) include the bound ethylene resonance at 4.19 ppm (br s, 4H), and the *n*-propyl group resonances at 1.22 ppm (m, 2H, $NiCH_2C\underline{H}_2CH_3$), 0.61 ppm (t, J = 6.9 Hz, 3H, $NiCH_2CH_2C\underline{H}_3$), and 0.48 ppm (t, J = 7.5 Hz, 2H, $NiC\underline{H}_2CH_2CH_3$). At -130 °C, no insertion of ethylene into the Ni-alkyl bond of either complex is observed. Studies of similar Pd alkyl ethylene complexes have established that an

equilibrium exists between Pd *n*-propyl ethylene and Pd isopropyl ethylene complexes.[4,5] The existence and nature of such an equilibrium between ***i*-9** and ***n*-9** has not yet been established, but these studies are currently in progress.

Scheme 7.9. Trapping of β-agostic species ***i*-9/*n*-9** with ethylene at -130 °C.

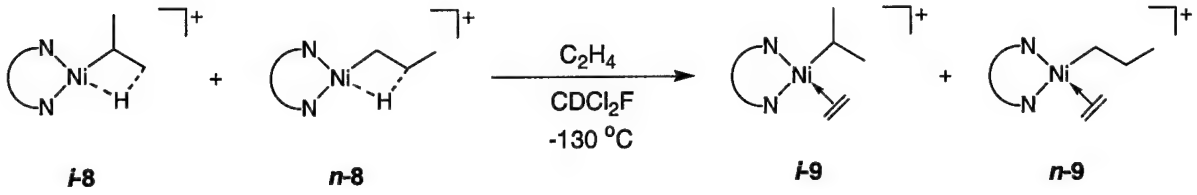

When the protonolysis of nickel dipropyl complex **6** with one equivalent of $[H(OEt_2)_2]^+[BAr'_4]^-$ is carried out in the presence of ethylene at -130 °C, the *n*-propyl ethylene complex ***n*-9** is the only product observed (Scheme 7.10). This result supports the initial formation of an *n*-propyl species immediately following protonolysis, presumably the β-agostic *n*-propyl complex ***n*-8**. In the absence of a trapping ligand such as ethylene, the β-agostic *n*-propyl complex ***n*-8** isomerizes to the β-agostic isopropyl complex ***i*-8**. In the presence of ethylene, the initially formed β-agostic *n*-propyl complex ***n*-8** is trapped by ethylene, forming ***n*-9**. No isomerization of ***n*-9** to ***i*-9** is observed at temperatures between -130 °C and -90 °C. However, ethylene insertion does occur at -90 °C, and subsequent chain growth is observed.

Scheme 7.10. Protonolysis of **6** in the presence of 5 eq C_2H_4 at -130 °C, and subsequent reactivity of *n*-propyl ethylene complex ***n*-9**.

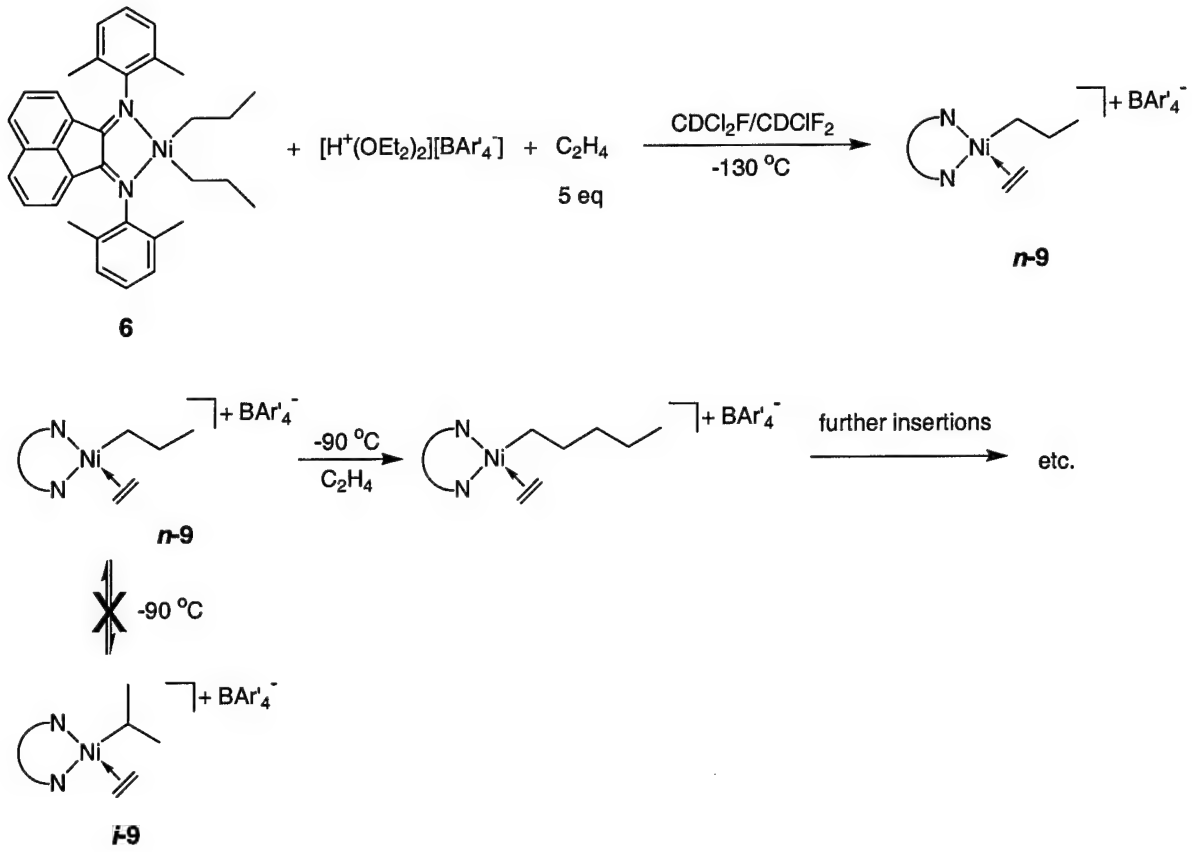

At temperatures above -90 °C, migratory insertion of ethylene in complex ***i*-9** is observed (Scheme 7.11). As the isopropyl methyl ^{1}H NMR resonance disappears (δ 0.39, d, J = 5.9 Hz, -80 °C), a new peak appears (δ 0.64, d, J = 6.1 Hz, -80 °C), which is consistent with the isopropyl methyl groups of the single insertion product **10** (Scheme 7.11). The rate of this migratory insertion of ethylene into the Ni-2° alkyl bond has not been measured, but qualitatively, it is on the order of the rate previously determined for migratory ethylene insertion into Ni-1° alkyl bonds for this complex (Chapter 6). It is important to note that some isomerization of ***i*-9** to ***n*-9** prior to the initial ethylene insertion cannot be ruled out by ^{1}H NMR due to overlapping signals of these isomers and their insertion products. However, the appearance of the previously unobserved doublet at 0.64 ppm with the coincidental

disappearance of the isopropyl methyl doublet in ***i*-9** strongly suggests that migratory insertion of ethylene into the Ni-2° alkyl bond of ***i*-9** is occurring much faster than isomerization of ***i*-9** to ***n*-9**.

Scheme 7.11. Ethylene insertion into the Ni-isopropyl bond of complex ***i*-9**.

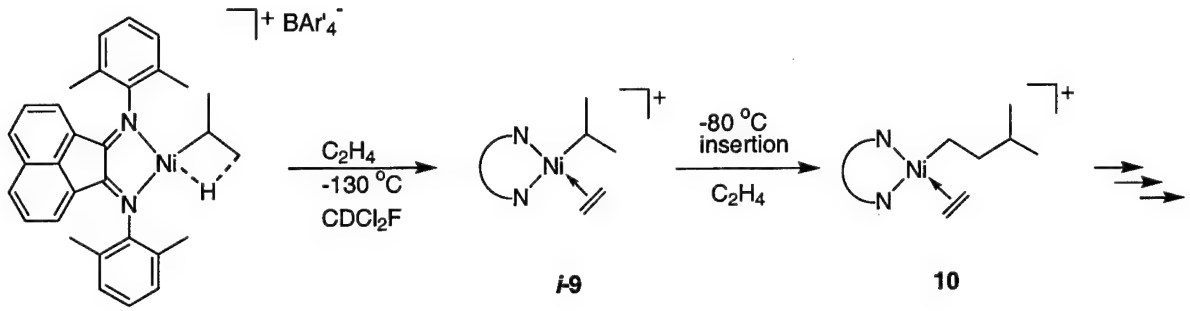

***i*-8** ***i*-9** **10**

The results of this experiment provide some insight into the differences between the nickel-based and palladium-based diimine complexes in terms of their alkyl chain-isomerization behavior. In the case of the palladium complexes, it has been established that the rate of chain isomerization is rapid relative to chain propagation (migratory olefin insertion), and furthermore, chain isomerization can occur from the alkyl ethylene catalyst resting state.[4,5] The height of the activation barriers for the basic mechanistic steps in palladium-catalyzed ethylene polymerization therefore increase in the order of $\Delta G^{\ddagger}_{\text{chain isomerization}} < \Delta G^{\ddagger}_{\text{chain propagation}} < \Delta G^{\ddagger}_{\text{chain transfer}}$. In contrast to the palladium complexes, the activation barriers to migratory ethylene insertion in the nickel complexes have been predicted by theory to be ca. 3 kcal/mol *lower* than the chain isomerization activation barriers.[9] If this is indeed the case, the barriers for the basic mechanistic steps in the nickel systems increase in the order of $\Delta G^{\ddagger}_{\text{chain propagation}} < \Delta G^{\ddagger}_{\text{chain isomerization}} < \Delta G^{\ddagger}_{\text{chain transfer}}$. According to this mechanistic scheme, chain isomerization in the nickel systems would likely take place only prior to trapping of agostic intermediates by ethylene, since the lowest energy process leading out of the alkyl ethylene resting state is migratory insertion of ethylene. If the agostic trapping barriers (by ethylene) are lower than the chain isomerization barriers, then the concentration of ethylene should have an effect on the degree of chain isomerization in the polymer product. Therefore, as the ethylene concentration is

increased, the rate at which the agostic intermediates are trapped should increase, and consequently chain isomerization would be inhibited. The end result would be less chain isomerization with increasing ethylene pressure, and this is consistent with experimental observations.

In addition to the effect of ethylene concentration on the degree of branching, the steric bulk of the *ortho*-aryl substituents on the diimine ligands also affects the degree of chain isomerization in nickel-catalyzed ethylene polymerizations.[1,3] According to theory,[9] these bulky *ortho*-aryl substituents serve to impede coordination of ethylene to the nickel center. As a result, the agostic species formed following migratory ethylene insertion is longer-lived, and more chain isomerization can take place. This theoretical conclusion is at least consistent with current data, but experimental proof in the form of observed chain-isomerization behavior of complexes containing bulkier diimine ligands is not yet available.

B. (α-Diimine)Ni(II) β-Agostic Ethyl Complexes. The dynamics of the β-agostic isopropyl complex ***i*-8** discussed above shed some light on basic processes that occur during chain isomerization reactions of (α-diimine)Ni complexes. The anticipated dynamic behavior of the similar β-agostic ethyl complex **11** would provide additional insight into the mechanism of chain isomerization, and may also be a useful species in the study of the chain transfer mechanism. It should be noted that the dynamics of ethyl β-agostic phosphine complexes of nickel, palladium, platinum have been studied by Spencer et. al.[10,11] In this section, some preliminary work on the synthesis of **11** is described.

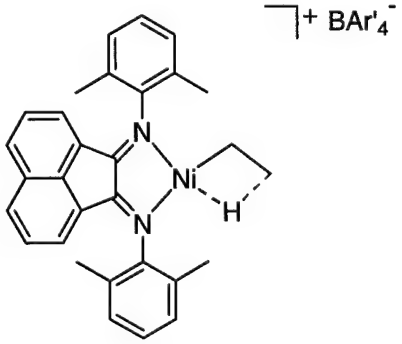

11

As mentioned in the previous section, protonolysis of nickel dipropyl complex **6** with $[H(OEt_2)_2]^+[BAr'_4]^-$ (Scheme 7.7) proved to be a convenient synthetic route to the β-agostic isopropyl complex ***i*-8**. Using the same strategy, protonolysis of nickel diethyl complex **7** with $[H(OEt_2)_2]^+[BAr'_4]^-$ was considered the best starting point for the synthesis of β-agostic ethyl complex **11**. The synthesis of **7** was described in the previous section, and is shown in Scheme 7.6. The combination of **7** and $[H(OEt_2)_2]^+[BAr'_4]^-$ at -130 °C in $CDCl_2F$ resulted in no immediate reaction as determined by ^1H NMR (Scheme 7.12). The sample was slowly warmed in 10 °C increments, and no appreciable protonation was observed until the temperature reached -90 °C. At -90 °C, the resonances of nickel diethyl complex **7** slowly disappeared, and at least two new nickel complexes were observed. The major compound present in this solution appeared to be the nickel ethyl diethyl ether adduct **12**. A ^1H-^1H COSY NMR spectrum taken at -100 °C indicated that the ethyl resonances for complex **12** appear at 1.23 (m) and -0.21 ppm (t). No agostic resonance was observed (-12 to -14 ppm), but the ^1H-^1H COSY NMR spectrum revealed resonances that are consistent with the β-agostic ethyl complex **11**. A correlation between two broad resonances at 1.92 and 1.56 ppm (tentatively NiCHH') with a multiplet at 0.18 ppm (agostic methyl) was observed, and these signals are consistent with **11**. A more definitive identification of diethyl ether coordination to a similar cationic palladium ethyl species has recently been obtained.[12]

Scheme 7.12. Protonation of nickel diethyl complex **7** with $[H(OEt_2)_2]^+[BAr'_4]^-$.

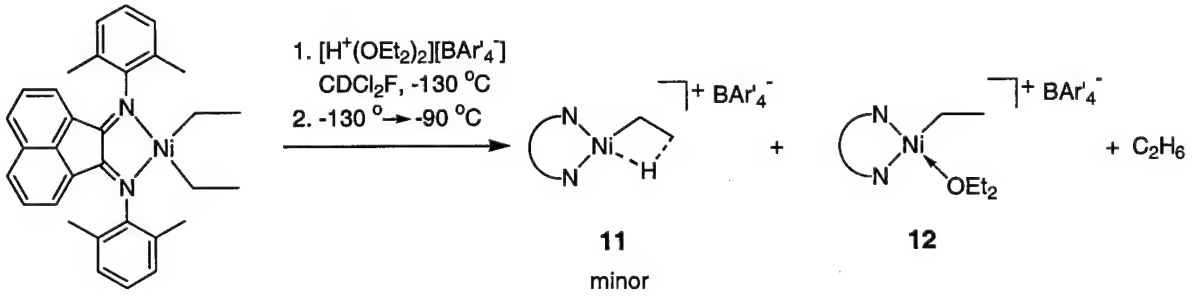

7 **11** minor **12**

Recent work with palladium analogs of **11** have revealed that diethyl ether competes with the agostic hydrogen for the vacant metal coordination site. However, substitution of diethyl ether with sterically bulkier diisopropyl ether resulted in clean formation of the palladium β-agostic ethyl complex, with no evidence for a palladium ethyl diisopropyl ether complex.[12] Using this same approach, formation of the ether adduct can also be suppressed in the nickel systems. Substitution of $[H(OEt_2)_2]^+[BAr'_4]^-$ with $[H(O^iPr_2)_2]^+[BAr'_4]^-$ under the synthetic conditions shown in Scheme 7.12 results in the formation of **11** as the major reaction product. The agostic hydrogen for complex **11** appears at -13.7 ppm (br t, $J \approx 20$ Hz, $CDCl_2F$, -130 °C) in the ^1H NMR spectrum. Some of the diethyl ether adduct **12** was also observed. Complete removal of diethyl ether from complex **7** has proven difficult due to the extreme thermal sensitivity of **7**. Therefore, the diethyl ether adduct **12** presumably forms as a consequence of this residual diethyl ether competing with the agostic hydrogen for the vacant coordination site. The combination of diethyl ether-free **7** with $[H(O^iPr_2)_2]^+[BAr'_4]^-$, or the employment of bulkier isopropyl *o*-aryl substituents on the diimine ligand are anticipated to favor formation of the desired β-agostic ethyl complexes free of the ether adducts.

C. Chelate Complexes from Insertion of Methyl Acrylate. A further example of the difference between the reactivity of the nickel and palladium α-diimine complexes is illustrated by their relative behavior towards insertion and isomerization of methyl acrylate. The palladium complexes have been found to copolymerize nonpolar monomers such as ethylene or propylene with polar monomers such as methyl acrylate or methyl vinyl ketone. In contrast, under the same copolymerization conditions, the nickel complexes are strongly inhibited by the polar comonomer. A detailed mechanistic picture of these copolymerizations using the palladium complexes has been developed.[13,14] Some significant conclusions from the studies of the reaction of methyl acrylate with palladium ether adducts are summarized in Scheme 7.13 and include the following: (1) insertion of methyl acrylate is highly regioselective (>95%) for 2,1-insertion into the Pd-Me bond, producing a

four-membered chelate, (2) this migratory insertion proceeds at very low temperatures (-80 °C), with a lower insertion barrier than is observed for ethylene and α-olefins, (3) the four-membered chelate rearranges to a five-membered chelate at -60 °C, which in turn isomerizes to the six-membered chelate at -20 °C, and (4) the carbonyl oxygen binds strongly to the metal, and displacement of the carbonyl oxygen by an olefin is the turnover-limiting step in copolymerizations of ethylene and methyl acrylate. The difficulty in preparing the analogous well-defined nickel ether adducts has been discussed at length in Chapter 6, and consequently, not much is known about the behavior of these nickel diimine complexes toward polar monomers. The development of synthetic procedures for making these well-defined nickel complexes has led to the opportunity to study their reactivity with polar monomers, and some initial results are presented below.

Scheme 7.13. Reaction of well-defined Pd(II) complexes with methyl acrylate.[13,14]

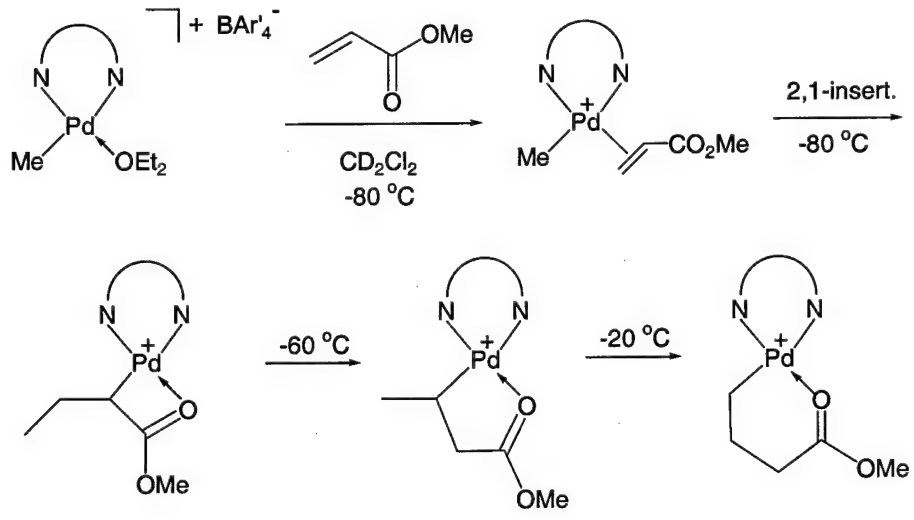

The reaction of methyl acrylate with the well-defined nickel ether adduct **2** was studied by ^{1}H NMR, and a summary of the results is shown in Scheme 7.14. Diethyl ether was displaced by methyl acrylate at -80 °C, but no migratory insertion took place at this temperature. The mode by which methyl acrylate binds to the metal is not clear from the ^{1}H or ^{1}H-^{1}H COSY NMR spectra. The diimine ligand, Ni-Me, and methyl acrylate resonances are all shifted from their starting locations, but

assignment to either the olefin complex **13** or the κ-O carbonyl complex **14** (Scheme 7.14) was ambiguous. After standing for 11 h at -80 °C, no migratory insertion was observed. This was somewhat surprising given the low barriers to migratory insertion of ethylene and propylene into the Ni-Me bond of this complex (Chapter 6). Upon warming to -40 °C, migratory insertion to form the four-membered chelate **15** was observed. The migratory insertion reaction is highly regioselective for 2,1-insertion; no 1,2-insertion product was seen. Greater than 95% insertion takes place over 30 min. The ^{1}H NMR spectrum of the four-membered chelate **15** is characterized by resonances at 3.23 ppm (m, 1H, NiC<u>H</u>), 0.76 and -0.57 ppm (m, m, 1H each, C<u>H</u>H'), and 0.69 ppm (t, J = 7.0 Hz, 3H, C<u>H</u>$_3$).

Scheme 7.14. Reaction of **2** with methyl acrylate.

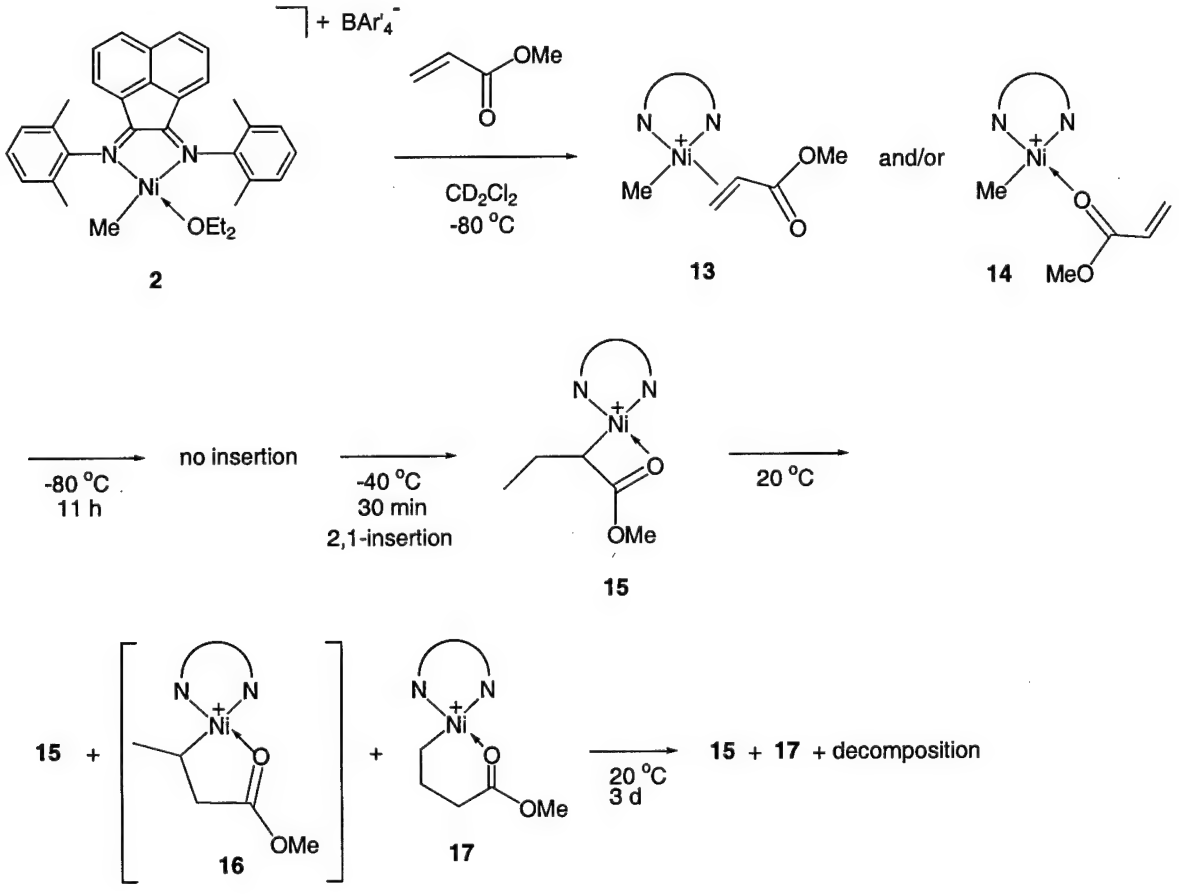

After standing for 10 h at -40 °C, no isomerization of **15** was observed. Upon warming to room temperature, the four-membered chelate **15** slowly began to isomerize to the 6-membered chelate **17**.

The formation of the five-membered chelate **16** could not be confirmed by this experiment. However, if **16** is formed, it appears that it rapidly isomerizes to **17**, since **17** is the major product observed throughout the isomerization of **15**. Some ^{1}H NMR resonances could be assigned to **17**, but the complete assignment could not be made. The resonances assigned to **17** are found at 3.64 ppm (s, $OC\underline{H}_3$), 2.23 ppm (t, J = 7.5 Hz, $C(O)C\underline{H}_2$), 1.60 (m, $CH_2C\underline{H}_2CH_2$), 0.92 (t, J = 7.3 Hz, $NiC\underline{H}_2$).[15] After standing at room temperature for 3 days, substantial decomposition was observed, but significant amounts of **15** and **17** remained in solution. The solution remained red and homogeneous throughout this reaction sequence, and no sign of a precipitate was observed. The stability of these acrylate chelate complexes in CD_2Cl_2 at room temperature for such long periods is encouraging, as it may be possible to use them as well-defined initiators for aluminum alkyl-free polymerization reactions.

A proposed mechanism for the isomerization of the 4-membered chelate complex **15** is shown in Scheme 7.15. The mechanism simply consists of a series of β-hydrogen elimination steps, followed by olefin rotation and reinsertion. The high temperatures required for isomerization to take place (relative to analogous Pd complexes, Scheme 7.13) is a key difference between the Ni and the Pd complexes. Two likely explanations exist for this difference: (1) the chelating O carbonyl atom binds more strongly to Ni than to Pd, and/or (2) the barriers to isomerization (e.g. β-hydrogen elimination/rotation/reinsertion) are higher in the nickel complexes. The experimental data seems to indicate that the first explanation is valid, but the relatively high temperatures involved in these experiments make conclusions about the second difficult.

Scheme 7.15. Proposed chelate isomerization mechanism.

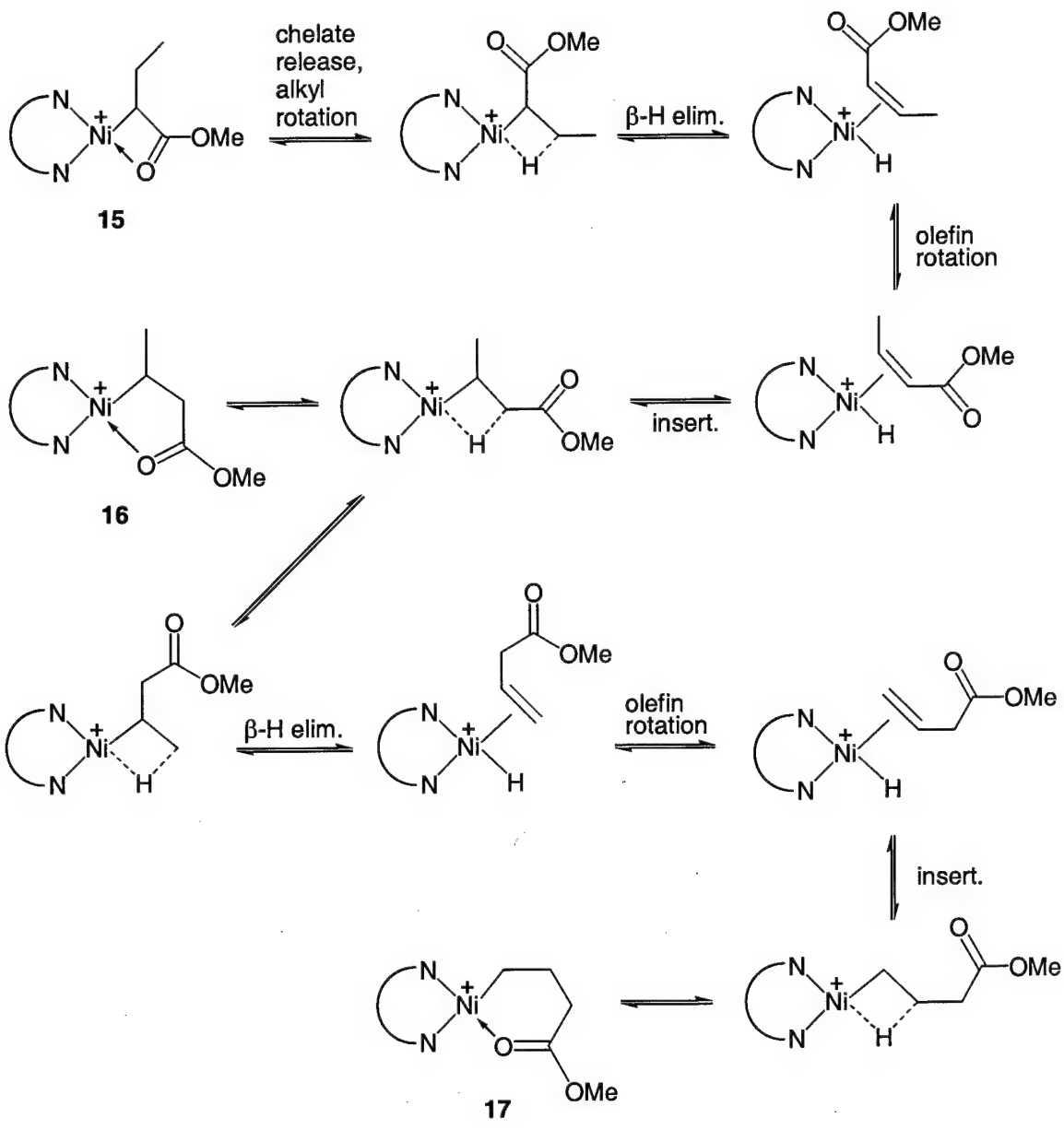

The relatively high temperature required for migratory insertion of methyl acrylate to form **15** may reflect the additional energy required to break a strong Ni-O interaction in the proposed κ-O carbonyl acrylate adduct **14** to form the olefin adduct **13**. The sum of these observations tend to indicate that a stronger interaction between Ni and the chelating O atom relative to the Pd chelate complexes is

responsible for the differences in isomerization behavior between chelate complexes of the two metals.

Conclusions

The development of synthetic procedures for producing (α-diimine)Ni(II) β-agostic complexes has created the opportunity to study the detailed mechanism of alkyl chain isomerization (chain-running) that occurs during nickel-catalyzed olefin polymerization reactions. Protonolysis of an (α-diimine)$NiPr_2$ complex results in the formation of an *isopropyl* agostic species, indicating the isomerization of the *n*-propyl chain is facile in the absence of a trapping monomer. The same protonolysis reaction run in the presence of a trapping ligand (ethylene) results in the formation of the *n*-propyl ethylene complex. Preliminary experiments with cationic nickel isopropyl and *n*-propyl ethylene complexes show that qualitatively, migratory insertion of ethylene into both 1°- and 2°-carbon bonds is much faster than alkyl chain isomerization. The important conclusion from these experiments is that chain isomerization in the nickel systems likely occurs prior to ethylene coordination.

Methyl acrylate was found to displace diethyl ether from nickel ether adducts at low temperature. Methyl acrylate undergoes a regioselective 2,1-migratory insertion into the nickel-methyl bond to form a 4-membered chelate. In contrast to analogous palladium acrylate chelate complexes, isomerization of the nickel acrylate chelates only occurs slowly, even at room temperature. When compared to the nickel ether adducts, the chelate complexes are considerably more stable. This stability may make nickel acrylate chelate complexes good candidates as initiators for cocatalyst-free olefin polymerization reactions.

Experimental Section

General Methods. All manipulations of air- and/or water-sensitive compounds were performed using standard high-vacuum or Schlenk techniques. Argon was purified by passage through columns of BASF R3-11 catalyst (Chemalog) and 4-Å molecular sieves. Solid organometallic compounds were transferred in an argon-filled Vacuum Atmospheres drybox. ^{1}H and ^{13}C NMR spectra were recorded on Bruker Avance 300, 400, or 500 MHz spectrometers. Chemical shifts are reported relative to residual $CHDCl_2$ (δ 5.32 for ^{1}H), $CHCl_2F$ (^{1}H: doublet centered at δ 7.47, J = 50 Hz), $CHClF_2$ (δ = 7.16 for ^{1}H), CD_2Cl_2 (δ 53.80 for ^{13}C), or residual $CDCl_3$ in $CDCl_2F$ solutions (δ 77.00 for ^{13}C).

Materials. Diethyl ether, pentane, and methylene chloride were purified using procedures recently reported by Pangborn et. al.[16] Polymer-grade ethylene and propylene were purchased from National Specialty Gases, and used without further purification. The α-diimine ligands (ArN=C(An)-C(An)=NAr, An,An = acenaphthyl = 1,8-naphth-diyl) and corresponding (α-diimine)nickel(II) bromide complexes were prepared according to modified literature procedures.[1,17-19] Nickel methyl ether adduct **2** was prepared as described in Chapter 6. $(DME)NiBr_2$[20] and $[H(OEt_2)_2]^+[BAr'_4]^-$ ($BAr'_4^- = B(3,5\text{-}C_6H_3(CF_3)_2)_4^-$)[21] were prepared according to the literature procedures. Diisopropyl ether was distilled from potassium/benzophenone ketyl under argon. Dichlorofluoromethane-*d* was prepared according to the literature,[22] and was purified by stirring over silica gel to remove silane byproducts,[23] dried over CaH_2, vacuum transferred, and degassed by repeated freeze-pump-thaw cycles. Acenaphthenequinone, 2,6-dimethylaniline, 2,6-diisopropylaniline, and PrMgCl were purchased from Aldrich Chemical Co. and used as received. Diisopropyl ether was purchased from Aldrich and distilled from sodium under argon before use. $NaBAr'_4$ was purchased from Boulder Scientific.

Synthesis of Nickel Dialkyl Complexes

(ArN=C(An)-C(An)=NAr)Ni($CH_2CH_2CH_3$)$_2$ (Ar = 2,6-$C_6H_3(Me)_2$), 6. A Schlenk flask was equipped with a magnetic stir bar and thoroughly flame-dried under vacuum. The flask was taken into the drybox and charged with (diimine)$NiBr_2$ **5** (1.00 g, 1.65 mmol). The flask was sealed with a rubber septum which had been previously dried overnight at 100 °C. Teflon tape was placed around the outside septum-glass interface. Dry diethyl ether (30 mL) was added to the flask via syringe. The resulting red-brown slurry was stirred at room temperature for 15 min, then cooled to -78 °C under argon. After 15 min, PrMgCl (1.65 mL of a 2.0 M Et_2O solution, 3.30 mmol) was slowly added dropwise. The reaction slurry immediately changed to a very dark blue color. The syringe hole in the septum was immediately covered with grease, and the flask was isolated from the argon line. After 3 h at -78 °C, the stirring was ceased and the reaction mixture allowed to settle for 10 min. A jacketed filter frit was charged with Florisil (2 cm wide by 1 cm deep column), attached to a Schlenk flask, and the entire assembly was flame-dried under vacuum. Upon cooling, the filter frit assembly was backfilled with argon, and the Florisil column and Schlenk flask were cooled to -78 °C. Dry diethyl ether (10 mL) was added to the top of the Florisil column, the receiver flask vented to an argon-purged oil bubbler, and the reaction mixture was quickly transferred to the filter frit using a 12-gauge cannula. It is critical to transfer the solution as fast as possible; reductive elimination of hexane occurs if the solution warms appreciably in the cannula. The entire solution was forced through the Florisil as fast as possible under argon head pressure. The filtered solution was filtered a second time through a filter cannula (2 pieces of very fine filter paper) into another flame-dried Schlenk flask cooled to -78 °C. The cannula was kept as cool as possible with dry ice to avoid product decomposition. Following the second filtration, a greased glass stopper was rapidly inserted into the flask, and the flask was immediately evacuated. The solvent was removed under vacuum at ca. -40 °C. The flask was quickly taken into the drybox, and the dark solid purple product was recovered (610 mg, 69%). This manipulation of the product was performed at room temperature, but as quickly

as practical. The product is stable when stored below -15 °C in the drybox, but decomposes within an hour at room temperature. CD_2Cl_2 solutions of the product decompose in minutes at room temperature, turning from the characteristic blue color of the desired nickel dipropyl complex to a purple color. The structure of the complex(es) formed at this point are unknown. Exposure of the purple solution to air results in the immediate formation of a black heterogeneous solution. In addition, the isolated nickel dipropyl complex is extremely air-sensitive, and decomposes immediately upon exposure to oxygen, forming a black solid. The product was contaminated with a small amount of *n*-hexane, presumably formed from reductive elimination from the nickel dipropyl complex during collection of the product; product composition was determined to be 92 mol % of the nickel dipropyl complex **6** and 8 mol % hexane. The product was characterized by low-temperature ^{1}H NMR (Figure 7.1), ^{13}C NMR, ^{1}H-^{1}H COSY, and ^{13}C DEPT NMR experiments. ^{1}H NMR (CD_2Cl_2, -80 °C, 300 MHz) δ 8.31 (d, J = 8.3 Hz, 2H, An H_p), 7.47-7.37 (m, 6H, Ar*H*), 7.06 (apparent t (overlapping doublets), 2H, An H_m), 6.65 (d, J = 7.1 Hz, 2H, An H_o), 2.30 (br t, 4H, NiCH_2), 2.22 (s, 12H, ArCH_3), 0.53 (br s, 10H, coincidental overlap of $NiCH_2CH_2CH_2CH_3$ and $NiCH_2CH_2CH_2CH_3$). ^{13}C NMR (CD_2Cl_2, -80 °C, 100 MHz) δ 162.7 (N=*C*-*C*=N), 149.2, 136.7, 133.4, 133.2, 130.1, 127.84, 127.78, 125.9, 125.4, 118.7, 23.3 ($NiCH_2$ or $NiCH_2CH_2$), 18.06 (ArCH_3), 18.01 ($NiCH_2CH_2CH_3$), 15.9 ($NiCH_2$ or $NiCH_2CH_2$).

(ArN=C(An)-C(An)=NAr)Ni(CH_2CH_3)$_2$ (Ar = 2,6-C_6H_3(Me)$_2$), 7. This compound was prepared using the same procedure described above for **6**. (Diimine)$NiBr_2$ **5** (1.00 g, 1.65 mmol) and EtMgCl (1.65 mL of a 2.0 M Et_2O solution, 3.30 mmol) were used as starting materials. Using the workup described above, 610 mg (69%) of the purple solid product was recovered. Et_2O and CH_2Cl_2 solutions of the product are dark blue in color. Solutions of the product decompose at temperatures above -20 °C, producing butane and unidentified products; the solution is purple and homogeneous. Exposure of the purple solution to air results in immediate decomposition to a black heterogeneous

solution. The product was characterized by low-temperature ^{1}H (Figure 7.2), ^{13}C, ^{1}H-^{1}H COSY, and ^{13}C DEPT NMR experiments. ^{1}H NMR (CD_2Cl_2, -80 °C, 400 MHz) δ 8.28 (d, J = 8.0 Hz, 2H, An H_p), 7.46-7.40 (m, 6H, Ar*H*), 7.07 (apparent t (overlapping doublets), 2H, An H_m), 6.59 (d, J = 7.0 Hz, 2H, An H_o), 2.23 (s, 12H, ArCH_3), 2.12 (q, J = 7.6 Hz, 4H, NiCH_2), 0.22 (t, J = 7.6 Hz, 6 H, $NiCH_2CH_3$). ^{13}C NMR (CD_2Cl_2, -80 °C, 100 MHz) δ 163.5 (N=*C*-*C*=N), 148.8, 136.9, 133.0, 132.9, 130.0, 127.9 (2 overlapping signals), 126.1, 125.5, 118.9, 18.0 (ArCH_3), 14.1 ($NiCH_2CH_3$), 6.4 (NiCH_2).

Synthesis of β-Agostic Isopropyl Complex *i*-8

[(ArN=C(An)-C(An)=NAr)Ni(CH(CH$_2$-μ-H)(CH$_3$))]$^+$[BAr$_4$']$^-$ (Ar = 2,6-C$_6$H$_3$Me$_2$), *i*-8. Two small Schlenk tubes were equipped with stir bars, fitted with rubber septa that had been dried in a glassware oven for 2 days, and were then flame-dried and taken into a drybox. The nickel dipropyl complex **6** (58 mg, 0.10 mmol effectively, see purity note in synthesis of **6**) was added to one tube, and $[H(OEt_2)_2]^+[BAr'_4]^-$ (101 mg, 0.10 mmol) was added to the other. The tubes were sealed, placed on a Schlenk line and cooled to -78 °C. After 5 min, 10 mL dry Et_2O was slowly added to each tube at -78 °C. The solutions were stirred to fully dissolve the solids (15 min), and then cooled to -130 °C (pentane/liquid N_2 slurry). The solution of the nickel dipropyl complex **6** was quickly added to the stirred solution of the oxonium acid via cannula. The holes in the septum were covered with grease. The reaction was initially the deep blue color of the nickel dipropyl complex. The reaction mixture was allowed to warm to -78 °C over 30 min, and slowly turned a darker midnight-blue color. The reaction was then was allowed to stir at -78 °C for 3 h. No apparent color change was observed over the 3 h reaction period at -78 °C. The rubber septum was quickly replaced with a lightly greased glass stopper, and the flask was immediately evacuated. The ether solvent was removed under vacuum at -50 °C. Upon removal of the solvent, the flask was quickly taken into the drybox, and a sticky blue-black solid product was recovered (95 mg). The product was characterized by low-

temperature ^{1}H NMR (Figure 7.3) and ^{1}H-^{1}H COSY NMR (Figure 7.4). The agostic region of the ^{1}H NMR region is shown in Figure 7.5. At -120 °C, the product appears to be a 20:1 mixture of the β-agostic isopropyl species ***i*-8**:β-agostic *n*-propyl species ***n*-8** (preliminary assignment). ^{1}H NMR ($CDCl_2F/CDClF_2$ (1:1), -130 °C, 400 MHz) δ 8.12 (apparent t (overlapping doublets), 2H, An H_p and H_p'), 7.85 (s, 8H, BAr_4'), 7.55-7.27 (m, 8H, Ar*H*), 7.53 (s, 4H, BAr_4'), 6.89 (d, J = 7.3 Hz, 1H, An H_o), 6.74 (d, J = 7.3 Hz, 1H, An H_o'), 2.43, 2.41, 2.37, 2.25 (all s, 3H each, ArCH_3, ArCH_3', ArCH_3", ArCH_3'"), 2.00 (m, 1H, NiC*H*), 0.26 (br m, 1H, C*H*H'(μ-H)), 0.11 (br m, 1H, CH*H*'(μ-H)), -0.09 (br s, 3H, CH_3), -12.49 (t, $^2J_{HH}$ = 19 Hz, 1H, μ-*H*). Proposed *n*-propyl β-agostic species ***n*-8**: δ -13.0 (d, $^2J_{HH}$ = 19 Hz).

Synthesis of Alkyl Olefin Complexes

[(ArN=C(An)-C(An)=NAr)NiCH(CH$_3$)$_2$)(C$_2$H$_4$)]$^+$[BAr$_4$']$^-$ (Ar = 2,6-C$_6$H$_3$Me$_2$), *i*-9. β-Agostic isopropyl complex ***i*-8** (~13 mg, 10 μmol) was placed in an NMR tube in the drybox. The tube was quickly capped with a rubber septum, wrapped with Parafilm, and cooled to -130 °C. A solution of $CDCl_2F/CDClF_2$ (1:1, ~700 μL) was added to the tube via cannula. Ethylene (0.5 mL, ca. 2 equiv) was added to the solution via gastight syringe at -130 °C. The tube was briefly agitated to dissolve the sample, and the resulting solution was red and homogenous. The sample was then transferred to a NMR probe precooled to -130 °C. The structure of ***i*-9** was confirmed by ^{1}H (Figure 7.6) and ^{1}H-^{1}H COSY NMR experiments. No agostic hydrogen resonances were observed at -130 °C. ^{1}H NMR ($CDCl_2F/CDClF_2$ (1:1), -130 °C, 500 MHz) δ 8.09 (apparent t (overlapping doublets), 2H, An H_p and H_p'), 7.83 (s, 8H, BAr_4'), 7.49 (s, 4H, BAr_4'), 7.51-7.30 (m, 8H, Ar*H*), 6.70 (apparent t (overlapping doublets), 2H, An H_o and H_o'), 3.96 (d, J = 14 Hz, 2H, bound C*H*H'=C*H*H'), 3.53 (d, J = 14 Hz, 2H, bound CH*H*'=CH*H*'), 2.28 (s, 6H, ArCH_3), 2.23 (s, 6H, ArCH_3'), 1.47 (m, 1H, Ni-C*H*), 0.40 (br s, 6H, CH(CH_3)$_2$).

[(ArN=C(An)-C(An)=NAr)Ni($CH_2CH_2CH_3$)(C_2H_4)]$^+$[BAr_4']$^-$ (Ar = 2,6-$C_6H_3Me_2$), *n*-9. Nickel dipropyl complex **6** (6.5 mg, 1.2 X 10^{-5} mol) and [$H(OEt_2)_2$]$^+$[BAr'_4]$^-$ (11.6 mg, 1.2 X 10^{-5} mol) were combined as solids in an NMR tube in the drybox. The tube was quickly sealed with a rubber septum, wrapped with Parafilm, and cooled to -130 °C. Ethylene (1.0 mL, ~4 eq) was added to the tube via gastight syringe. The tube was briefly immersed in liquid nitrogen, and a mixture of $CDCl_2F/CDClF_2$ (1:1) was added via cannula. Initially, a near-black solution was formed. The NMR tube was placed in the NMR probe, which had been precooled to -130 °C. The presence of the nickel *n*-propyl group was confirmed by low-temperature ^{1}H NMR (Figure 7.7) and ^{1}H-^{1}H COSY NMR. ^{1}H NMR ($CDCl_2F/CDClF_2$ (1:1), -100 °C, 500 MHz) δ 8.11 (d, J = 8.3 Hz, 1H, An H_p), 8.07 (d, J = 8.3 Hz, 1H, An H_p'), 7.84 (s, 8H, BAr_4'), 7.56 (s, 4H, BAr_4'), 7.54-7.29 (m, 8H, Ar*H*), 6.78 (d, J = 7.3 Hz, 1H, An H_o), 6.71 (d, J = 7.3 Hz, 1H, An H_o'), 5.47 (very br, free C_2H_4), 4.19 (br s, 4H, bound C_2H_4), 2.38 (s, 6H, ArCH_3), 2.29 (s, 6H, Ar'CH_3), 1.22 (m, 2H, $NiCH_2CH_2CH_3$), 0.61 (t, J = 6.9 Hz, 3H, $NiCH_2CH_2CH_3$), 0.48 (t, J = 7.5 Hz, 2H, $NiCH_2CH_2CH_3$). Propane, diethyl ether, and a small amount of residual [$H(OEt_2)_2$]$^+$[BAr'_4]$^-$ are also present in the sample. The sample was observed to be a red homogeneous solution upon removal from the NMR probe.

Synthesis of [H(O-*i*-Pr_2)$_2$]$^+$[BAr'_4]$^-$. Preparation of this compound has been reported in the literature;[24] however, no characterization of the product has yet been described. We prepared this oxonium acid using a procedure similar to that previously reported for the synthesis of [$H(OEt_2)_2$]$^+$[BAr'_4]$^-$.[21] $NaBAr'_4$ (2.5 g, 2.8 mmol) was added to a flame-dried Schlenk flask containing freshly activated 4 Å molecular sieves in the drybox. Freshly distilled diisopropyl ether (30 mL) was added to dissolve the salt. The solution was allowed to dry overnight. The solution was then transferred to a flame-dried Schlenk tube via a filter cannula. The solution was cooled to 0 °C, and HCl gas (prepared by slowly dripping conc. H_2SO_4 into NaCl) was bubbled through the solution for 15 min. The initially clear solution rapidly became cloudy as NaCl precipitated from solution.

The solution was then cooled to -78 °C, and Ar was purged through the solution for 1 h to remove excess HCl. The solution was then filtered through Celite at -78 °C using a vacuum-jacketed filter frit. The clear solution was then concentrated to 10 mL under vacuum, and 6 mL pentane was slowly added. The flask was then sealed and allowed to stand at -30 °C overnight to induce crystal growth. After 1 day of crystallization, the supernatant was removed via filter cannula while the mixture was kept at -78 °C. The white crystalline product was washed with cold pentane (3 mL), and the supernatant was again removed via filter cannula. The product was dried under vacuum at 20 °C for 15 min to yield 1.62 g (54%) of the white solid product. The product was characterized by low-temperature ^{1}H NMR (Figure 7.8) and ^{13}C NMR. The ^{1}H NMR spectrum of $[H(OEt_2)_2]^+[BAr'_4]^-$ is shown in Figure 7.9 for comparison. ^{1}H NMR (CD_2Cl_2, -80 °C, 300 MHz) δ 16.39 (quintet, J = 2.4 Hz, 1H, H^+), 7.71 (s, 8H, BAr'$_4$ H_o), 7.54 (s, 4H, BAr'$_4$ H_p), 4.35 (doublet of septets, J = 6.4, 2.4 Hz, 4H, C*H*(CH$_3$)$_2$), 1.33 (d, J = 6.4 Hz, 24H, CH(C*H*$_3$)$_2$); ^{13}C NMR (CD_2Cl_2, -80 °C, 75 MHz) δ 162.1 (q, $^1J_{CB}$ = 49.0 Hz, BAr'$_4$ C_{ipso}), 134.9 (BAr$_4$' C_o), 128.9 (q, $^2J_{CF}$ = 31.6 Hz, BAr'$_4$ C_m), 124.7 (q, $^1J_{CF}$ = 273 Hz, *C*F$_3$), 117.8 (BAr'$_4$ C_p), 77.4 (*C*H(CH$_3$)$_2$), 22.2 (CH(*C*H$_3$)$_2$).

Synthesis of Acrylate Chelate Complex 15.

[(ArN=C(An)-C(An)=NAr)Ni(CH(CH$_2$CH$_3$)C(O)OCH$_3$)]$^+$[BAr$_4$']$^-$ (Ar = 2,6-C$_6$H$_3$Me$_2$), 15. Nickel ether adduct **2** (19 mg, 1.4 X 10^{-5} mol) was placed in an NMR tube in the drybox. The tube was sealed with a rubber septum, wrapped with Parafilm, and cooled to -78 °C. CD_2Cl_2 (~700 μL) was slowly added to the NMR tube via syringe. The tube was briefly shaken to dissolve the sample. Methyl acrylate (1.2 mg (1.2 μL), 3 X 10^{-5} mol) was added to the NMR tube via syringe at -78 °C. The sample was placed into a precooled NMR probe (-80 °C). At this temperature, methyl acrylate displaces bound diethyl ether from ether adduct **2**, but the mode of binding for methyl acrylate to the metal center is not obvious by proton NMR (e.g. binding of the carbonyl (η^1 or η^2) vs. binding of the alkene). Migratory insertion of methyl acrylate occurred at -40 °C. The product was characterized by

^{1}H (Figure 7.10), ^{13}C, and ^{1}H-^{1}H COSY NMR experiments as the 4-membered chelate **15**. ^{1}H NMR (CD_2Cl_2, -40 °C, 400 MHz) δ 8.14 (overlapping doublets, 2H, An H_p and H_p'), 7.71 (s, 8H, BAr_4'), 7.56-7.19 (m, 8H, Ar*H*), 7.51 (s, 4H, BAr_4'), 6.88 (d, J = 7.2 Hz, 1H, An H_o), 6.57 (d, J = 7.2 Hz, 1H, An H_o'), 3.64 (s, 3H, OCH_3), 3.23 (m, 1H, NiC*H*), 2.53 (s, 6H, $ArCH_3$, $ArCH_3$'), 2.50 (s, 3H, $ArCH_3$''), 2.24 (s, 3H, $ArCH_3$'''), 0.76 (m, 1H, C*H*H'), 0.69 (t, J = 7.0 Hz, 3H, CH_3), -0.57 (m, 1H, CH*H*'). ^{13}C NMR (CD_2Cl_2, -60 °C, 126 MHz) δ 175.2, 173.6, 169.9, 161.4 (q, $^1J_{CB}$ = 49.6 Hz, BAr'_4 C_{ipso}), 147.5, 142.1, 141.7, 134.3 (BAr'_4 C_o), 132.82, 132.77, 130.7, 129.3-127.9 (complex multiplet), 125.2, 124.0 (q, $^1J_{CF}$ = 273 Hz, BAr'_4 CF_3), 123.6, 123.3, 117.2 (BAr'_4 C_p), 34.7, 18.14 ($ArCH_3$), 18.01 ($ArCH_3$'), 17.96 ($ArCH_3$''), 17.62 ($ArCH_3$'''), 15.5, 11.1; OCH_3 obscured by CD_2Cl_2 resonance.

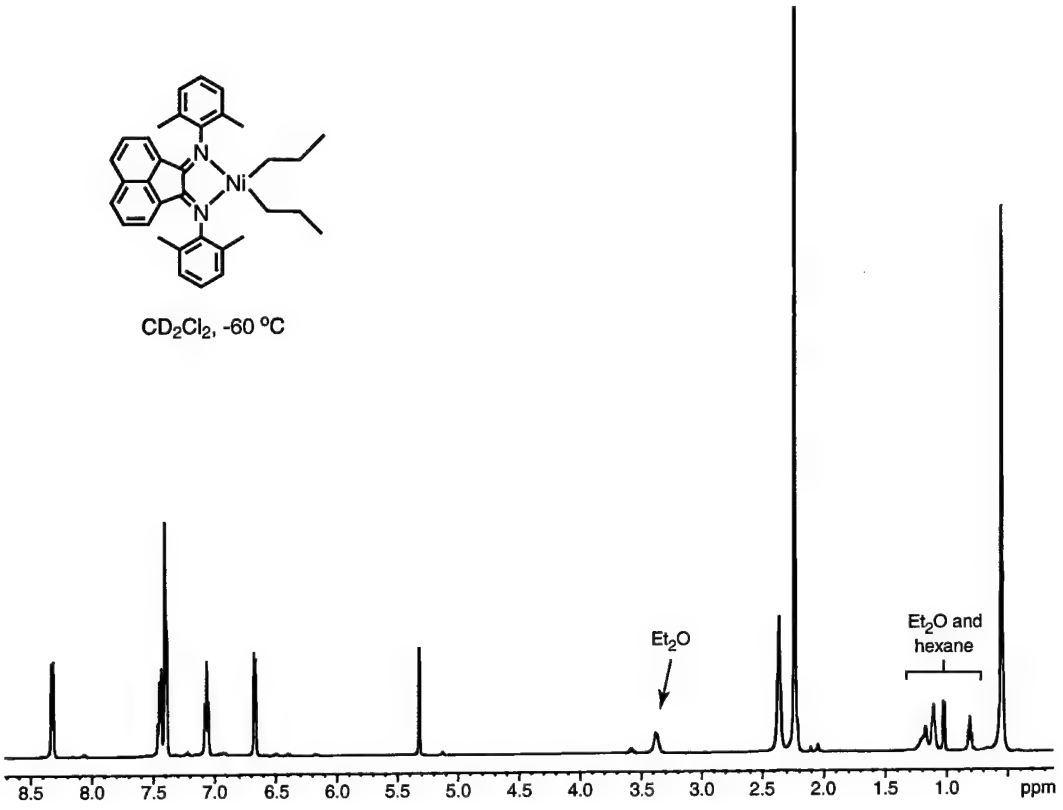

Figure 7.1. ^{1}H NMR spectrum of complex **6**, CD_2Cl_2, -60 °C, 500 MHz.

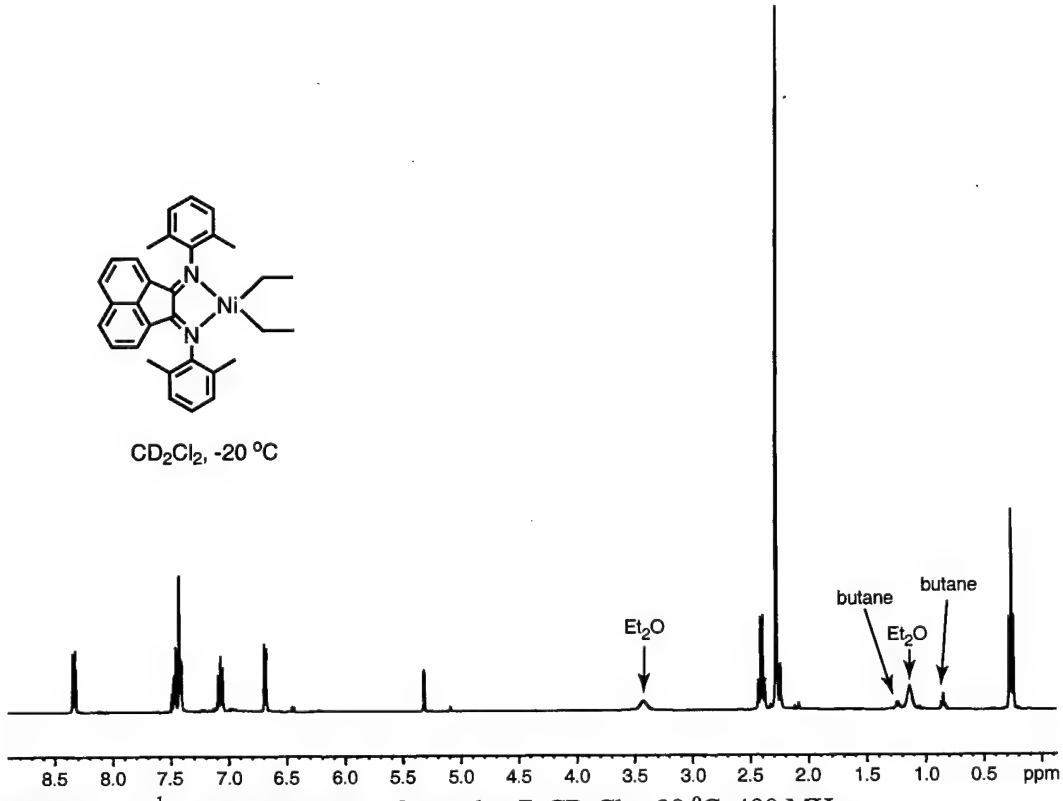

Figure 7.2. ^{1}H NMR spectrum of complex **7**, CD_2Cl_2, -20 °C, 400 MHz.

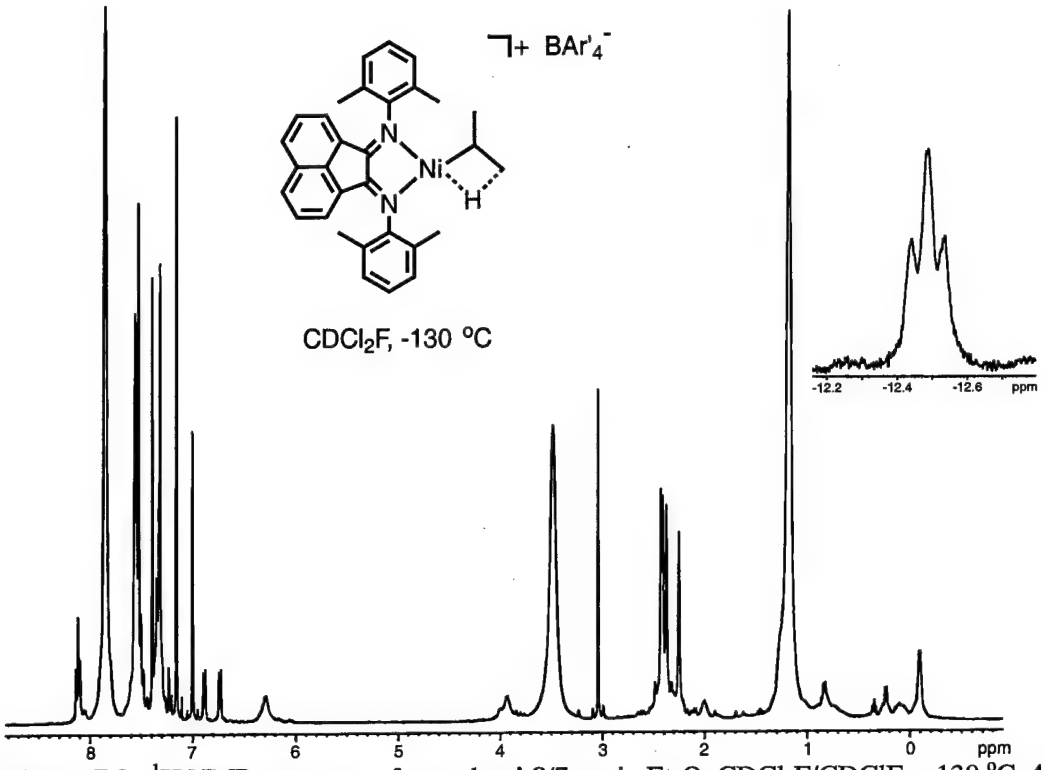

Figure 7.3. ^{1}H NMR spectrum of complex ***i*-8**/7 equiv Et_2O, $CDCl_2F/CDClF_2$, -130 °C, 400 MHz.

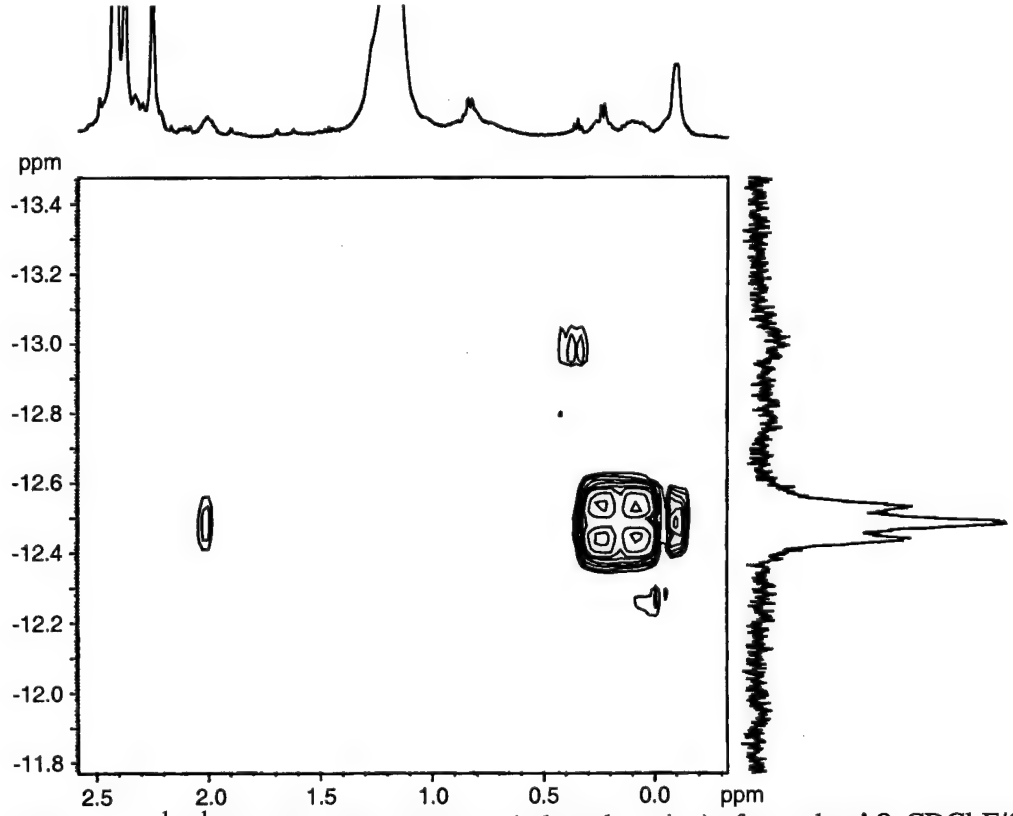

Figure 7.4. ^{1}H-^{1}H COSY NMR spectrum (selected portion) of complex ***i*-8**, $CDCl_2F/CDClF_2$, -130 °C, 400 MHz.

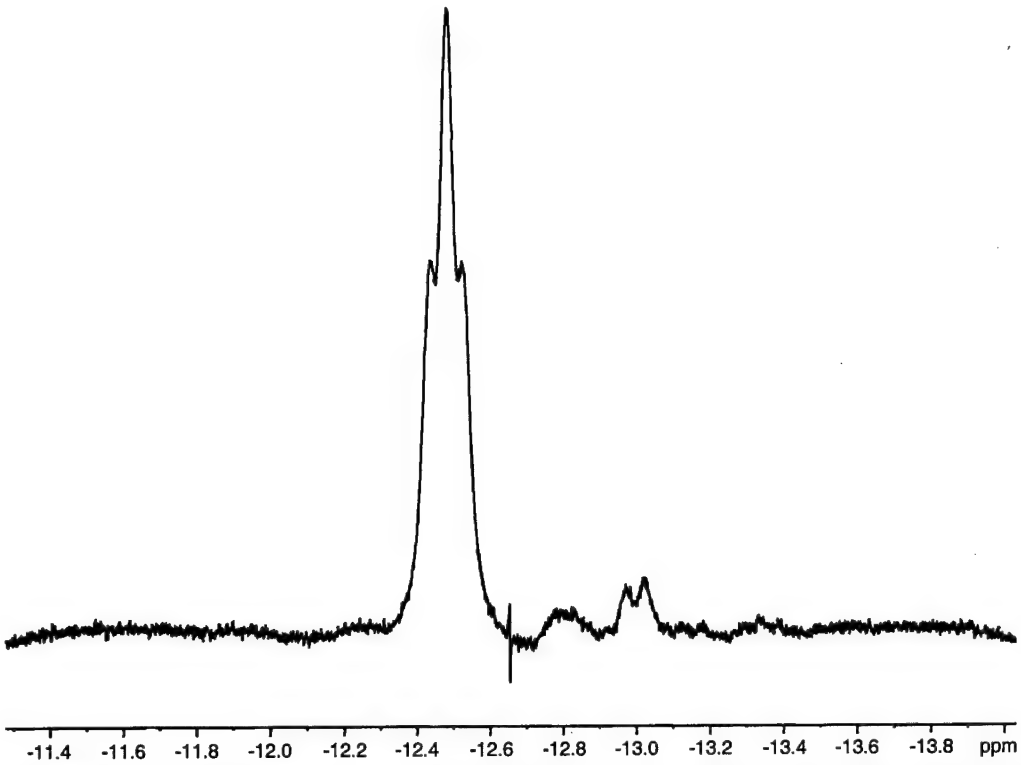

Figure 7.5. ^{1}H NMR spectrum ($CDCl_2F/CDClF_2$, -120 °C, 400 MHz) of the agostic region of the mixture of complexes ***i*-8** and ***n*-8** obtained following protonolysis of **6**.

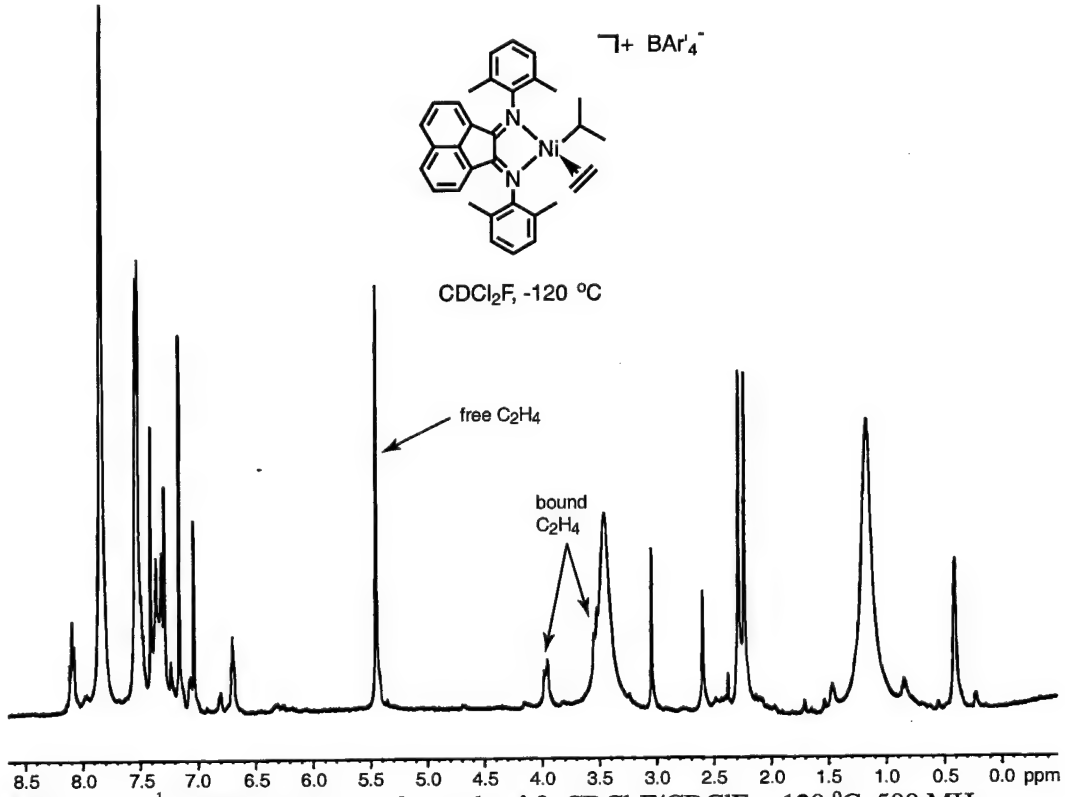

Figure 7.6. ^{1}H NMR spectrum of complex ***i*-9**, $CDCl_2F/CDClF_2$, -120 °C, 500 MHz.

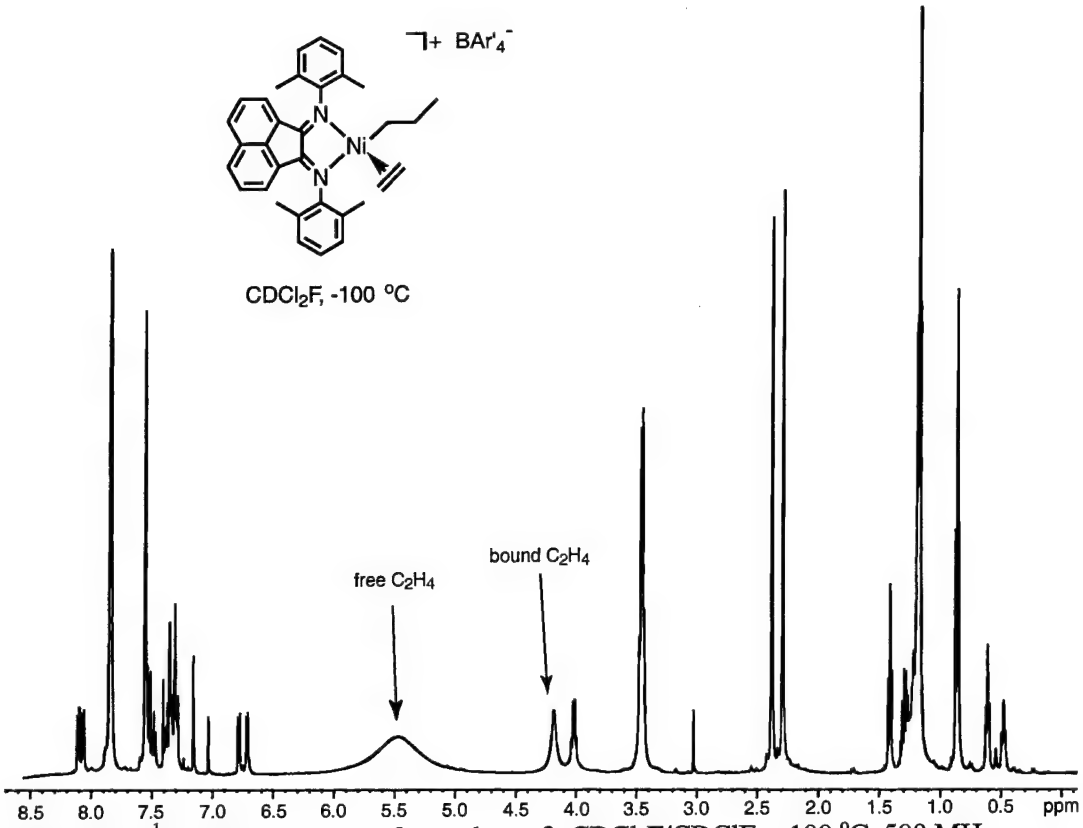

Figure 7.7. ^{1}H NMR spectrum of complex ***n*-9**, $CDCl_2F/CDClF_2$, -100 °C, 500 MHz.

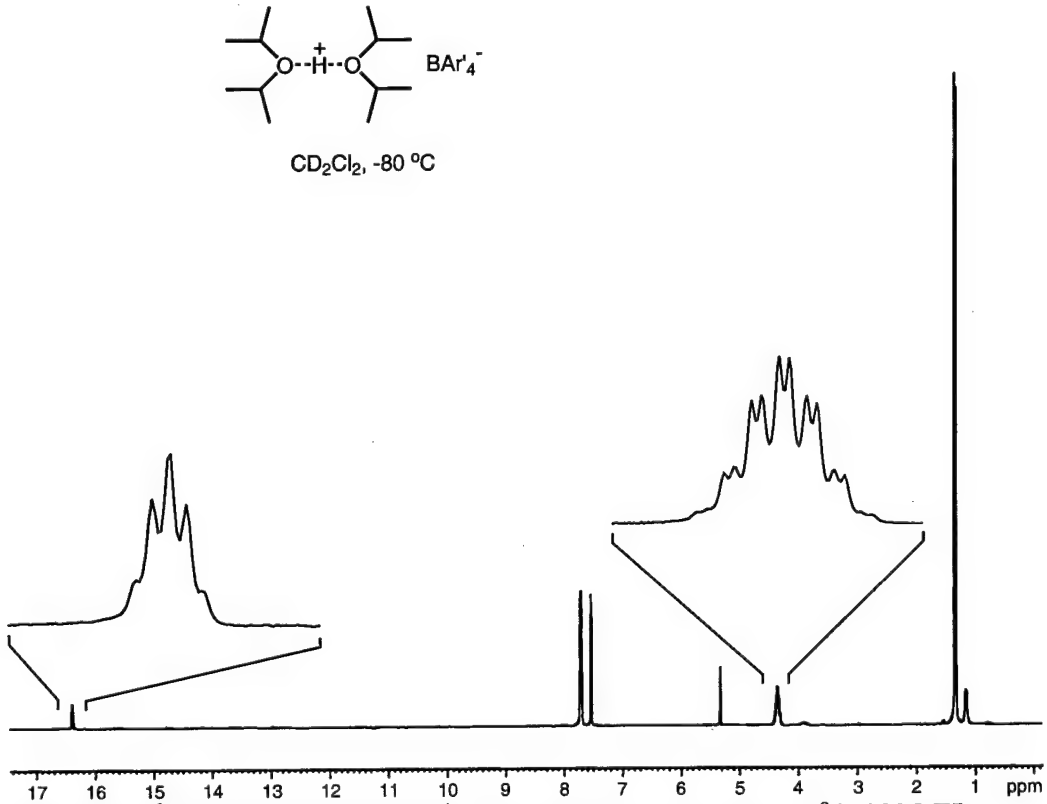

Figure 7.8. ^{1}H NMR spectrum of $[H^+(O\text{-}i\text{Pr}_2)_2][BAr'_4^-]$, CD_2Cl_2, -80 °C, 300 MHz.

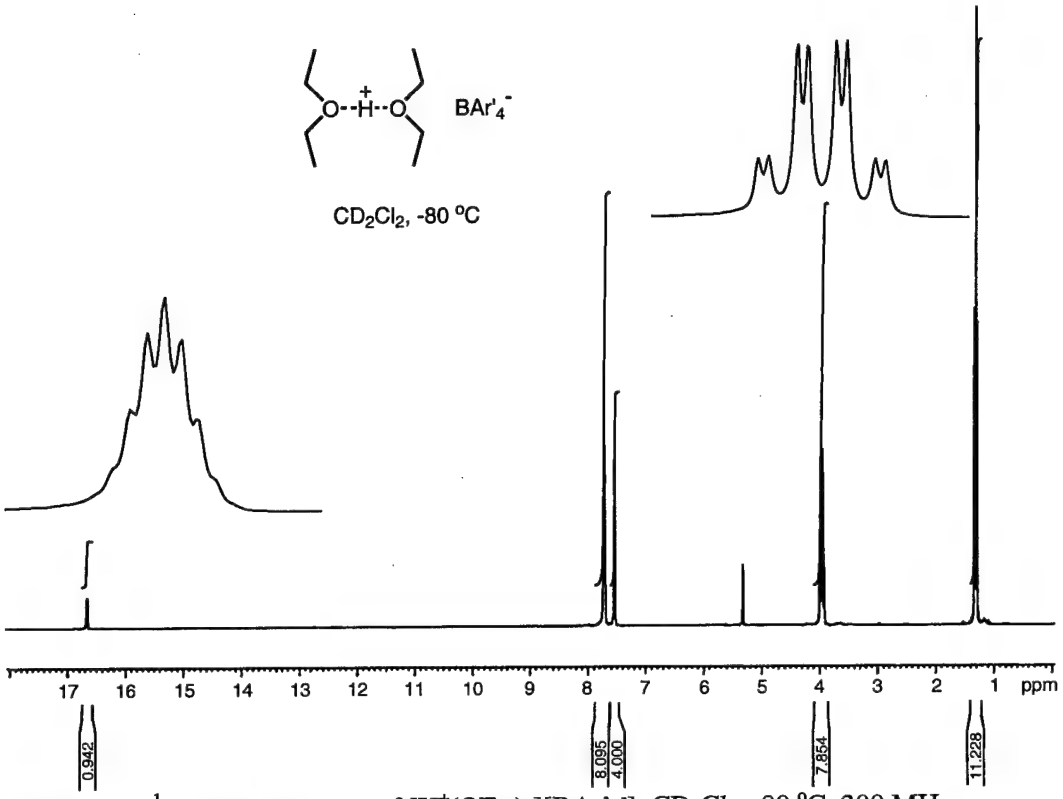

Figure 7.9. ^{1}H NMR spectrum of $[H^+(OEt_2)_2][BAr'_4^-]$, CD_2Cl_2, -80 °C, 300 MHz.

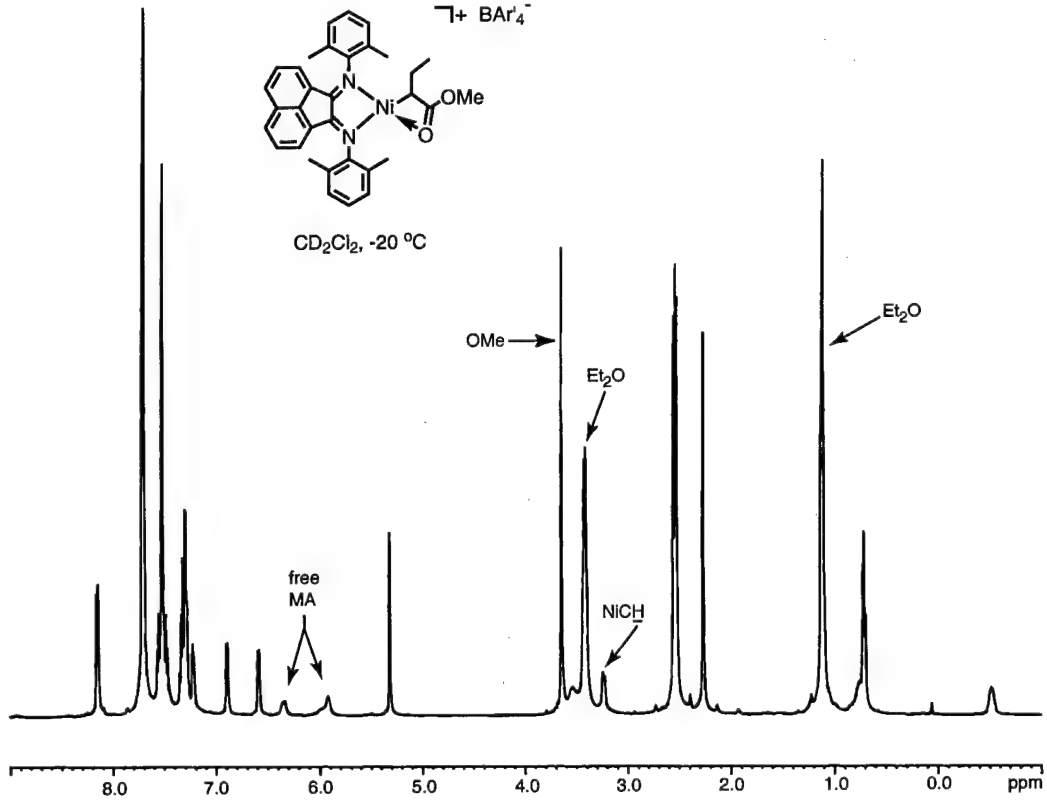

Figure 7.10. ^{1}H NMR spectrum of complex **15**, CD_2Cl_2, -20 °C, 500 MHz.

References and Notes

(1) Johnson, L. K.; Killian, C. M.; Brookhart, M. *J. Am. Chem. Soc.* **1995**, *117*, 6414-6415.

(2) Killian, C. M. Ni(II)-Based Catalysts for the Polymerization and Copolymerization of Olefins: A New Generation of Polyolefins. Ph.D. Dissertation, University of North Carolina-Chapel Hill, 1996.

(3) Gates, D. P.; Svejda, S. A.; Onate, E.; Killian, C. M.; Johnson, L. K.; White, P. S.; Brookhart, M. Manuscript in preparation.

(4) Tempel, D. J. Mechanistic Studies of Pd(II)- and Ni(II)-Catalyzed Olefin Polymerization. Ph.D. Dissertation, University of North Carolina at Chapel Hill, 1998.

(5) Tempel, D. J.; Johnson, L. K.; Huff, R. L.; Brookhart, M. Manuscript in preparation.

(6) Svejda, S. A.; Johnson, L. K.; Brookhart, M. *J. Am. Chem. Soc.*, communication submitted.

(7) Chain isomerization may also take place via this mechanism from the β-agostic species formed immediately following migratory insertion of ethylene.

(8) Tempel, D. J.; Brookhart, M. *Organometallics* **1998**, *17*, 2290-2296.

(9) Deng, L.; Woo, T. K.; Cavallo, L.; Margl, P. M.; Ziegler, T. *J. Am. Chem. Soc.* **1997**, *119*, 6177-6186.

(10) Conroy-Lewis, F. M.; Mole, L.; Redhouse, A. D.; Litster, S. A.; Spencer, J. L. *J. Chem. Soc., Chem. Commun.* **1991**, 1601-1603.

(11) Carr, N.; Mole, L.; Orpen, A. G.; Spencer, J. L. *J. Chem. Soc., Dalton Trans.* **1992**, 2653-2662.

(12) Huff, R. L.; Brookhart, M. Unpublished results.

(13) Johnson, L. K.; Mecking, S.; Brookhart, M. *J. Am. Chem. Soc.* **1996**, *118*, 267-268.

(14) Mecking, S.; Johnson, L. K.; Wang, L.; Brookhart, M. *J. Am. Chem. Soc.* **1998**, *120*, 888-899.

(15) These assignments are supported by a similar ^{1}H NMR experiment performed by Dr. Lynda Johnson. Johnson, L. K.; Brookhart, M. Unpublished results.

(16) Pangborn, A. B.; Giardello, M. A.; Grubbs, R. H.; Rosen, R. K.; Timmers, F. J. *Organometallics* **1996**, *15*, 1518-1520.

(17) van Asselt, R.; Elsevier, C. J.; Smeets, W. J. J.; Spek, A. L.; Benedix, R. *Recl. Trav. Chim. Pays-Bas* **1994**, *113*, 88-98.

(18) tom Dieck, H.; Svoboda, M.; Grieser, T. *Z. Naturforsch* **1981**, *36b*, 823-832.

(19) Svoboda, M.; tom Dieck, H. *J. Organomet. Chem.* **1980**, *191*, 321-328.

(20) Ward, L. G. L. *Inorg. Syn.* **1971**, *13*, 154-164.

(21) Brookhart, M.; Grant, B.; Volpe, A. F. *Organometallics* **1992**, *11*, 3920-3922.

(22) Siegel, J. S.; Anet, F. A. *J. Org. Chem.* **1988**, *53*, 2629-2630.

(23) A small amount of Me_2SiF_2 was occasionally observed as a byproduct of the fluorination reaction. Formation of this product can be suppressed through minimal use of silicone grease on glass joints used in the preparation of $CDCl_2F$.

(24) White, P. A.; Calabrese, J.; Theopold, K. H. *Organometallics* **1996**, *15*, 5473-5475.

ABSTRACT

STEVEN A. SVEJDA: Studies of Olefin Dimerization, Oligomerization, and Polymerization Catalyzed by Cationic (α-Diimine)Ni(II) Complexes
(Under the direction of Professor Maurice Brookhart)

The polymerization of olefins by transition metal catalysts is an area of tremendous commercial significance and academic interest. Over the past twenty years, substantial improvements have been made in the design and industrial employment of these catalysts, especially with the development of early transition-metal metallocenes. The development of cationic (α-diimine)nickel(II) and palladium(II) complexes which catalyze the polymerization of both ethylene and α-olefins to high polymers represents a major advance in the field of olefin polymerization catalysis. Through simple variations of the α-diimine ligand structure and reaction conditions, the polymer molecular weights, molecular weight distributions, and microstructures can be easily controlled. The work in this dissertation focuses on olefin dimerization, oligomerization, and polymerization reactions catalyzed by (α-diimine)Ni(II) complexes, with the general goal of gaining an increased understanding of the mechanism of olefin polymerization by these nickel systems.

This dissertation consists of seven chapters. Chapter One is a general introduction to late metal polymerization catalysts. Chapter Two is a study of the effects of monomer concentration, reaction temperature, aluminum cocatalyst, and electron-donating or -withdrawing diimine ligand substituents on the (α-diimine)Ni(II)-catalyzed oligomerization of ethylene and the dimerization of propylene.

Chapters Three, Four, and Five describe detailed investigations of the effects of reaction conditions and diimine ligand structure on the properties of polyethylene and poly(α-olefin)s produced by (α-diimine)Ni(II) complexes. The effects of these variables on catalyst productivities, polymer molecular weights, and microstructures are presented.

Chapters Six and Seven consist of low-temperature mechanistic studies of the chain growth and chain isomerization steps in (α-diimine)Ni-catalyzed olefin polymerizations.

Steven A. Svejda
Capt, USAF
1999
235 pages
Ph.D., Organic Chemistry
University of North Carolina at Chapel Hill, Chapel Hill, NC

Chapter 1 References

(1) Reisch, M. S. *Chem. Eng. News* **1997**, *75* (May 26), 14.
(2) Ziegler, K.; Holzkamp, E.; Briel, H.; Martin, H. *Angew. Chem.* **1955**, *67*, 541-547.
(3) Natta, G.; Pino, P.; Corradini, P.; Dannusso, F.; Mantica, E.; Mazzanti, G.; Moraglio, G. *J. Am. Chem. Soc.* **1955**, *77*, 1708-1710.
(4) Theopold, K. H. *Eur. J. Inorg. Chem.* **1998**, 15-24.
(5) McKnight, A. L.; Waymouth, R. M. *Chem. Rev.* **1998**, *98*, 2857-2868.
(6) Bochmann, M. *J. Chem. Soc., Dalton Trans.* **1996**, 255-270.
(7) Brintzinger, H. H.; Fischer, D.; Mülhaupt, R.; Rieger, B.; Waymouth, R. M. *Angew. Chem., Int. Ed. Engl.* **1995**, *34*, 1143-1170.
(8) Coates, G. W.; Waymouth, R. M. *Science* **1995**, *267*, 217-219.
(9) Yang, X.; Stern, C. L.; Marks, T. J. *J. Am. Chem. Soc.* **1994**, *116*, 10015-10031.
(10) Coughlin, E. B.; Bercaw, J. E. *J. Am. Chem. Soc.* **1992**, *114*, 7606-7607.
(11) Crowther, D. J.; Baenziger, N. C.; Jordan, R. F. *J. Am. Chem. Soc.* **1991**, *113*, 1455-1457.
(12) Ewen, J. A.; Jones, R. L.; Razavi, A.; Ferrara, J. D. *J. Am. Chem. Soc.* **1988**, *110*, 6255-6256.
(13) Kaminsky, W.; Külper, K.; Brintzinger, H. H.; Wild, F. R. W. P. *Angew. Chem., Int. Ed. Engl.* **1985**, *24*, 507-508.
(14) Ewen, J. A. *J. Am. Chem. Soc.* **1984**, *106*, 6355-6364.
(15) Kaminsky, W.; Miri, M.; Sinn, H.; Woldt, R. *Makromol. Chem., Rapid Commun.* **1983**, *4*, 417-421.
(16) Sinn, H.; Kaminsky, W. *Adv. Organomet. Chem.* **1980**, *18*, 99-149.
(17) Muthukumaru Pillai, S.; Ravindranathan, M.; Sivaram, S. *Chem. Rev.* **1986**, *86*, 353-399.
(18) Skupinska, J. *Chem. Rev.* **1991**, *91*, 613-648.
(19) Chauvin, Y.; Olivier, H. Dimerization and Codimerization. In *Applied Homogeneous Catalysis with Organometallic Compounds*; Cornils, B., Herrmann, W. A., Eds.; VCH Publishers: New York, 1996; Vol. 1, pp 258-268.
(20) Andrews, J. W. *Hydrocarbon Process.* **1982**, *61*, 110.
(21) Chauvin, Y.; Gaillard, J. F.; Quang, D. V.; Andrews, J. W. *Chem. Ind. (London)* **1974**, 375-378.
(22) Vogt, D. Oligomerization of Ethylene to Higher Linear α-Olefins. In *Applied Homogeneous Catalysis with Organometallic Compounds*; Cornils, B., Herrmann, W. A., Eds.; VCH Publishers: New York, 1996; Vol. 1, pp 245-258.
(23) Bonnet, M. C.; Dahan, F.; Ecke, A.; Keim, W.; Schulz, R.; Tkatchenko, I. *J. Chem. Soc., Chem. Commun.* **1994**, 615-616.
(24) Hirose, K.; Keim, W. *J. Mol. Catal.* **1992**, *73*, 271-276.
(25) Keim, W. *Angew. Chem., Int. Ed. Engl.* **1990**, *29*, 235-244.
(26) Müller, U.; Keim, W.; Krüger, C.; Betz, P. *Angew. Chem., Int. Ed. Engl.* **1989**, *28*, 1011-1013.
(27) Keim, W. *J. Mol. Catal.* **1989**, *52*, 19-25.
(28) Keim, W. *New J. Chem.* **1987**, *11*, 531-534.
(29) Keim, W.; Behr, A.; Gruber, B.; Hoffmann, B.; Kowaldt, F. H.; Kürschner, U.; Limbäcker, B.; Sistig, F. P. *Organometallics* **1986**, *5*, 2356-2359.
(30) Peuckert, M.; Keim, W. *Organometallics* **1983**, *2*, 594-597.
(31) Keim, W.; Hoffmann, B.; Lodewick, R.; Peuckert, M.; Schmitt, G. *J. Mol. Catal.* **1979**, *6*, 79-97.
(32) Keim, W.; Kowaldt, F. H.; Goddard, R.; Krüger, C. *Angew. Chem., Int. Ed. Engl.* **1978**, *17*, 466.
(33) Ostoja Starzewski, K. A.; Witte, J. *Angew. Chem., Int. Ed. Engl.* **1987**, *26*, 63-64.
(34) Ostoja Starzewski, K. A.; Witte, J. *Angew. Chem., Int. Ed. Engl.* **1985**, *24*, 599-601.
(35) Klabunde, U.; Ittel, S. D. *J. Mol. Catal.* **1987**, *41*, 123-134.
(36) Klabunde, U.; Mulhaupt, R.; Herskovitz, T.; Janowicz, A. H.; Calabrese, J.; Ittel, S. D. *J. Poly. Sci., Part A: Polym. Chem.* **1987**, *25*, 1989-2003.
(37) Möhring, V. M.; Fink, G. *Angew. Chem., Int. Ed. Engl.* **1985**, *24*, 1001-1003.

(38) Keim, W.; Appel, R.; Storeck, A.; Krüger, C.; Goddard, R. *Angew. Chem., Int. Ed. Engl.* **1981**, *20*, 116-117.
(39) Johnson, L. K.; Killian, C. M.; Brookhart, M. *J. Am. Chem. Soc.* **1995**, *117*, 6414-6415.
(40) Tempel, D. J. Mechanistic Studies of Pd(II)- and Ni(II)-Catalyzed Olefin Polymerization. Ph.D. Dissertation, University of North Carolina at Chapel Hill, 1998.
(41) Killian, C. M.; Tempel, D. J.; Johnson, L. K.; Brookhart, M. *J. Am. Chem. Soc.* **1996**, *118*, 11664-11665.
(42) Killian, C. M. Ni(II)-Based Catalysts for the Polymerization and Copolymerization of Olefins: A New Generation of Polyolefins. Ph.D. Dissertation, University of North Carolina-Chapel Hill, 1996.
(43) Gates, D. P.; Brookhart, M. Manuscript in preparation.
(44) Johnson, L. K.; Mecking, S.; Brookhart, M. *J. Am. Chem. Soc.* **1996**, *118*, 267-268.
(45) Mecking, S.; Johnson, L. K.; Wang, L.; Brookhart, M. *J. Am. Chem. Soc.* **1998**, *120*, 888-899.
(46) McLain, S. J.; Feldman, J.; McCord, E. F.; Gardner, K. H.; Teasley, M. F.; Coughlin, E. B.; Sweetman, K. J.; Johnson, L. K.; Brookhart, M. *Macromolecules* **1998**, *31*, 6705-6707.
(47) Killian, C. M.; Johnson, L. K.; Brookhart, M. *Organometallics* **1997**, *16*, 2005-2007.
(48) Tempel, D. J.; Brookhart, M. *Organometallics* **1998**, *17*, 2290-2296.
(49) Tempel, D. J.; Johnson, L. K.; Huff, R. L.; Brookhart, M. Manuscript in preparation.
(50) Svejda, S. A.; Brookhart, M. *Organometallics* **1999**, *18*, 65-74.

Chapter 2 References

(1) Keim, W.; Kowaldt, F. H.; Goddard, R.; Krüger, C. *Angew. Chem., Int. Ed. Engl.* **1978**, *17*, 466.
(2) Keim, W.; Hoffmann, B.; Lodewick, R.; Peuckert, M.; Schmitt, G. *J. Mol. Catal.* **1979**, *6*, 79-97.
(3) Peuckert, M.; Keim, W. *Organometallics* **1983**, *2*, 594-597.
(4) Keim, W. *Angew. Chem., Int. Ed. Engl.* **1990**, *29*, 235-244.
(5) Vogt, D. Oligomerization of Ethylene to Higher Linear α-Olefins. In *Applied Homogeneous Catalysis with Organometallic Compounds*; Cornils, B.; Herrmann, W. A., Eds.; VCH Publishers: New York, 1996; Vol. 1, pp 245-258.
(6) Chauvin, Y.; Olivier, H. Dimerization and Codimerization. In *Applied Homogeneous Catalysis with Organometallic Compounds*; Cornils, B.; Herrmann, W. A., Eds.; VCH Publishers: New York, 1996; Vol. 1, pp 258-268.
(7) Andrews, J. W. *Hydrocarbon Process.* **1982**, *61*, 110.
(8) Chauvin, Y.; Gaillard, J. F.; Quang, D. V.; Andrews, J. W. *Chem. Ind. (London)* **1974**, 375-378.
(9) Muthukumaru Pillai, S.; Ravindranathan, M.; Sivaram, S. *Chem. Rev.* **1986**, *86*, 353-399.
(10) Skupinska, J. *Chem. Rev.* **1991**, *91*, 613-648.
(11) Keim, W. *J. Mol. Catal.* **1989**, *52*, 19-25.
(12) Keim, W. *New J. Chem.* **1987**, *11*, 531-534.
(13) Keim, W.; Behr, A.; Gruber, B.; Hoffmann, B.; Kowaldt, F. H.; Kürschner, U.; Limbäcker, B.; Sistig, F. P. *Organometallics* **1986**, *5*, 2356-2359.
(14) Keim, W.; Behr, A.; Limbäcker, B.; Krüger, C. *Angew. Chem., Int. Ed. Engl.* **1983**, *22*, 503.
(15) Bonnet, M. C.; Dahan, F.; Ecke, A.; Keim, W.; Schulz, R.; Tkatchenko, I. *J. Chem. Soc., Chem. Commun.* **1994**, 615-616.
(16) Matt, D.; Huhn, M.; Fischer, J.; DeCian, A.; Kläui, W.; Tkatchenko, I.; Bonnet, M. C. *J. Chem. Soc., Dalton Trans.* **1993**, 1173-1178.
(17) Kissin, Y. V.; Beach, D. L. *J. Poly. Sci., Part A: Polym. Chem.* **1989**, *27*, 147-155.
(18) Strömberg, S.; Oksman, M.; Zhang, L.; Zetterberg, K. *Acta Chemica Scandinavica* **1995**, *49*, 689-695.
(19) Braunstein, P.; Pietsch, J.; Chauvin, Y.; Mercier, S.; Saussine, L.; DeCian, A.; Fischer, J. *J. Chem. Soc., Dalton Trans.* **1996**, 3571-3574.

(20) Desjardins, S. Y.; Cavell, K. J.; Jin, H.; Skelton, B. W.; White, A. H. *J. Organomet. Chem.* **1996**, *515*, 233-243.
(21) Ostoja Starzewski, K. A.; Witte, J. *Angew. Chem., Int. Ed. Engl.* **1985**, *24*, 599-601.
(22) Ostoja Starzewski, K. A.; Witte, J. *Angew. Chem., Int. Ed. Engl.* **1987**, *26*, 63-64.
(23) Klabunde, U.; Mulhaupt, R.; Herskovitz, T.; Janowicz, A. H.; Calabrese, J.; Ittel, S. D. *J. Poly. Sci., Part A: Polym. Chem.* **1987**, *25*, 1989-2003.
(24) Hirose, K.; Keim, W. *J. Mol. Catal.* **1992**, *73*, 271-276.
(25) Keim, W.; Schulz, R. P. *J. Mol. Catal.* **1994**, *92*, 21-33.
(26) Abeywickrema, R.; Bennett, M. A.; Cavell, K. J.; Kony, M.; Masters, A. F.; Webb, A. G. *J. Chem. Soc., Dalton Trans.* **1993**, 59-68.
(27) Brown, S. J.; Masters, A. F. *J. Organomet. Chem.* **1989**, *367*, 371-374.
(28) Cavell, K. J.; Masters, A. F. *Aust. J. Chem.* **1986**, *39*, 1129-1134.
(29) Brown, S. J.; Clutterbuck, L. M.; Masters, A. F.; Sachinidis, J. I.; Tregloan, P. A. *Applied Catalysis* **1989**, *48*, 1-11.
(30) Small, B. L.; Brookhart, M. *J. Am. Chem. Soc.* **1998**, *120*, 7143-7144.
(31) Johnson, L. K.; Killian, C. M.; Brookhart, M. *J. Am. Chem. Soc.* **1995**, *117*, 6414-6415.
(32) Brookhart, M. S.; Johnson, L. K.; Killian, C. M.; Arthur, S. D.; Feldman, J.; McCord, E. F.; McLain, S. J.; Kreutzer, K. A.; Bennett, A. M.; Coughlin, B. E.; Ittel, S. D.; Parthasarathy, A.; Tempel, D. J. *Pat. Appl.* WO 96/23010, **1996**.
(33) Killian, C. M.; Johnson, L. K.; Brookhart, M. *Organometallics* **1997**, *16*, 2005-2007.
(34) van Asselt, R.; Rijnberg, E.; Elsevier, C. J. *Organometallics* **1994**, *13*, 706-720.
(35) van Asselt, R.; Gielens, E. E. C. G.; Rülke, R. E.; Vrieze, K.; Elsevier, C. J. *J. Am. Chem. Soc.* **1994**, *116*, 977-985.
(36) van Asselt, R.; Elsevier, C. J.; Smeets, W. J. J.; Spek, A. L. *Inorg. Chem.* **1994**, *33*, 1521-1531.
(37) van Asselt, R.; Elsevier, C. J.; Smeets, W. J. J.; Spek, A. L.; Benedix, R. *Recl. Trav. Chim. Pays-Bas* **1994**, *113*, 88-98.
(38) van Asselt, R. Ph.D. Thesis, Universiteit van Amsterdam, Amsterdam, The Netherlands, 1993.
(39) tom Dieck, H.; Svoboda, M.; Grieser, T. *Naturforsch* **1981**, *36b*, 823-832.
(40) Svoboda, M.; tom Dieck, H. *J. Organomet. Chem.* **1980**, *191*, 321-328.
(41) MAO-IP is a new proprietary product sold by Akzo Nobel.
(42) Flory, P. J. *J. Am. Chem. Soc.* **1940**, *62*, 1561-1565.
(43) Schulz, G. V. *Z. Phys. Chem., Abt. B* **1935**, *30*, 379-398.
(44) Schulz, G. V. *Z. Phys. Chem., Abt. B* **1939**, *43*, 25-46.
(45) Henrici-Olivé, G.; Olivé, S. *Adv. Polym. Sci.* **1974**, *15*, 1-29.
(46) Tempel, D. J.; Brookhart, M. *Organometallics* **1998**, *17*, 2290-2296.
(47) McLain, S. J.; Feldman, J.; McCord, E. F.; Gardner, K. H.; Teasley, M. F.; Coughlin, E. B.; Sweetman, K. J.; Johnson, L. K.; Brookhart, M. *Polym. Mater. Sci. Eng.* **1997**, *76*, 20.
(48) McLain, S. J.; Feldman, J.; McCord, E. F.; Gardner, K. H.; Teasley, M. F.; Coughlin, E. B.; Sweetman, K. J.; Johnson, L. K.; Brookhart, M. *Macromolecules* **1998**, *31*, 6705-6707.
(49) Theoretical studies suggest such species do not lie in potential energy minima and are thus transition states for interconversion of agostic species.
(50) Musaev, D. G.; Froese, R. D. J.; Morokuma, K. *Organometallics* **1998**, *17*, 1850-1860.
(51) Deng, L.; Woo, T. K.; Cavallo, L.; Margl, P. M.; Ziegler, T. *J. Am. Chem. Soc.* **1997**, *119*, 6177-6186.
(52) Longo, P.; Oliva, L.; Grassi, A.; Pellecchia, C. *Makromol. Chem.* **1989**, *190*, 2357-2361.
(53) Further evidence of turnover frequency dependence on solvent polarity is that turnover frequencies decrease as the solvent is changed from chlorobenzene to toluene to a 1/1 mixture of toluene/pentane.
(54) Fogg, P. G. T.; Gerrard, W. *Solubility of Gases in Liquids*; John Wiley & Sons Ltd.: West Sussex, England, 1991.

(55) In addition to the mass flow data, reactions initiated with MAO-type cocatalysts are exothermic at the start of the reaction, while reactions initiated with Et_2AlCl exhibit maximum exotherms 10-20 min after the reaction start.
(56) Svejda, S. A.; Onate, E.; Gates, D. P.; Brookhart, M. Manuscript in preparation.
(57) Müller, U.; Keim, W.; Krüger, C.; Betz, P. *Angew. Chem., Int. Ed. Engl.* **1989**, *28*, 1011-1013.
(58) Collman, J. P.; Hegedus, L. S.; Norton, J. R.; Finke, R. G. *Principles and Applications of Organotransition Metal Complexes*; University Science Books: Mill Valley, CA, 1987, pp 578-596.
(59) Pangborn, A. B.; Giardello, M. A.; Grubbs, R. H.; Rosen, R. K.; Timmers, F. J. *Organometallics* **1996**, *15*, 1518-1520.

Chapter 3 References

(1) See for example: (a) Brintzinger, H. H.; Fischer, D.; Mülhaupt, R.; Rieger, B.; Waymouth, R. M. *Angew. Chem., Int. Ed. Engl.* **1995**, *34*, 1143; (b) McKnight, A. L.; Waymouth, R. M. *Chem. Rev.* **1998**, *98*, 2587; (c) Yang, X.; Stern, C. L.; Marks, T. J. *J. Am. Chem. Soc.* **1994**, *116*, 10015; (d) Britovsek, G. J. P.; Gibson, V. C.; Wass, D. F. *Angew. Chem., Int. Ed. Engl.* **1999**, *38*, 429; (e) Bochmann, M. *J. Chem. Soc., Dalton Trans.* **1996**, 255; (f) Fink, G.; Mülhaupt, R.; Brintzinger, H. H., Eds. *Ziegler Catalysts: Recent Scientific Innovations and Technological Improvement*; Springer-Verlag: Berlin, 1995.
(2) Schmidt, G. F.; Brookhart, M. *J. Am. Chem. Soc.* **1985**, *107*, 1443.
(3) Brookhart, M.; Volpe, A. F.; Lincoln, D. M.; Horvath, I. T.; Millar, J. M. *J. Am. Chem. Soc.* **1990**, *112*, 5634.
(4) Brookhart, M.; DeSimone, J. M.; Grant, B. E.; Tanner, M. J. *Macromolecules* **1995**, *28*, 5378.
(5) Wang, L.; Flood, T. C. *J. Am. Chem. Soc.* **1992**, *114*, 3169.
(6) Timonen, S.; Pakkanen, T. T.; Pakkanen, T. A. *J. Mol. Catal.* **1996**, *111*, 267.
(7) For early examples of Ni-catalyzed ethylene polymerization see: (a) Keim, W.; Appel, R.; Storeck, A.; Krüger, C.; Goddard, R. *Angew. Chem., Int. Ed. Engl.* **1981**, *20*, 116; (b) Klabunde, U.; Ittel, S. D. *J. Mol. Catal.* **1987**, *41*, 123; (c) Klabunde, U.; Mülhaupt, R.; Herskovitz, T.; Janowicz, A. H.; Calabrese, J.; Ittel, S. D. *J. Polym. Sci., Part A: Polym. Chem.* **1987**, *25*, 1989; (c) Ostoja Starzewski, K. A.; Witte, J. *Angew. Chem., Int. Ed. Engl.* **1987**, *26*, 63.
(8) Johnson, L. K.; Killian, C. M.; Brookhart, M. *J. Am. Chem. Soc.* **1995**, *117*, 6414. Following initial discoveries at UNC, collaborative efforts were initiated with the group at DuPont.
(9) (a) Johnson, L. K.; Killian, C. M.; Arthur, S. D.; Feldman, J.; McCord, E. F.; McLain, S. J.; Kreutzer, K. A.; Bennett, A. M. A.; Coughlin, E. B.; Ittel, S. D.; Parthasarathy, A.; Tempel, D. J.; Brookhart, M. S. WO 96/23010; (b) Brookhart, M. S.; Johnson, L. K.; Arthur, S. D.; Feldman, J.; Kreutzer, K. A.; Bennett, A. M. A.; Coughlin, E. B.; Ittel, S. D.; Parthasarathy, A.; Tempel, D. J. U.S. Patent 5 866 224, 1999; (c) Brookhart, M. S.; Johnson, L. K.; Killian, C. M.; Arthur, S. D.; Feldman, J.; McCord, E. F.; McLain, S. J.; Kreutzer, K. A.; Bennett, A. M. A.; Coughlin, E. B.; Ittel, S. D.; Parthasarathy, A.; Wang, L.; Yang, Z. U.S. Patent 5 866 663, 1999; (d) Brookhart, M. S.; Johnson, L. K.; Killian, C. M.; Arthur, S. D.; McCord, E. F.; McLain, S. J. U.S. Patent 5 891 963, 1999; (e) Brookhart, M. S.; Johnson, L. K.; Killian, C. M.; McCord, E. F.; McLain, S. J.; Kreutzer, K. A.; Ittel, S. D.; Tempel, D. J. U.S. Patent 5 880 241, 1999.
(10) Killian, C. M.; Tempel, D. J.; Johnson, L. K.; Brookhart, M. *J. Am. Chem. Soc.* **1996**, *118*, 11664.
(11) Killian, C. M.; Johnson, L. K.; Brookhart, M. *Organometallics* **1997**, *16*, 2005.
(12) Svejda, S. A.; Brookhart, M. *Organometallics* **1999**, *18*, 65.
(13) McLain, S. J.; Feldman, J.; McCord, E. F.; Gardner, K. H.; Teasley, M. F.; Coughlin, E. B.; Sweetman, K. J.; Johnson, L. K.; Brookhart, M. *Macromolecules* **1998**, *31*, 6705.
(14) Möhring, V. M.; Fink, G. *Angew. Chem., Int. Ed. Engl.* **1985**, *24*, 1001.

(15) Schubbe, R.; Angermund, K.; Fink, G.; Goddard, R. *Macromol. Chem. Phys.* **1995**, *196*, 467.
(16) Feldman, J.; McLain, S. J.; Parthasarathy, A.; Marshall, J.; Calabrese, J. C.; Arthur, S. D. *Organometallics* **1997**, *16*, 1514.
(17) Schleis, T.; Spaniol, T. P.; Okuda, J.; Heinemann, J.; Mülhaupt, R. *J. Organomet. Chem.* **1998**, *569*, 159.
(18) Wang, C.; Friedrich, S.; Younkin, T. R.; Li, R. T.; Grubbs, R. H.; Bansleben, D. A.; Day, M. W. *Organometallics* **1998**, *17*, 3149.
(19) Pellecchia, C.; Zambelli, A. *Macromol. Rapid Commun.* **1996**, *17*, 333.
(20) Pappalardo, D.; Mazzeo, M.; Pellecchia, C. *Macromol. Rapid Commun.* **1997**, *18*, 1017.
(21) Pellecchia, C.; Zambelli, A.; Mazzeo, M.; Pappalardo, D. *J. Mol Catal.* **1998**, *128*, 229.
(22) Galland, G. B.; de Souza, R. F.; Mauler, R. S.; Nunes, F. F. *Macromolecules* **1999**, *32*, 1620.
(23) Zeng, X.; Zetterberg, K. *Macromol. Chem. Phys.* **1998**, *199*, 2677.
(24) Kim, J. S.; Pawlow, J. H.; Wojcinski, L. M.; Murtuza, S.; Kacker, S.; Sen, A. *J. Am. Chem. Soc.* **1998**, *120*, 1932.
(25) Johnson, L. K.; Mecking, S.; Brookhart, M. *J. Am. Chem. Soc.* **1996**, *118*, 267.
(26) Mecking, S.; Johnson, L. K.; Wang, L.; Brookhart, M. *J. Am. Chem. Soc.* **1998**, *120*, 888.
(27) Small, B. L.; Brookhart, M.; Bennett, A. M. A. *J. Am. Chem. Soc.* **1998**, *120*, 4049.
(28) Britovsek, G. J. P.; Gibson, V. C.; Kimberly, B. S.; Maddox, P. J.; McTavish, S. J.; Solan, G. A.; White, A. J. P.; Williams, D. J. *Chem. Commun.* **1998**, 849.
(29) (a) Small, B. L.; Brookhart, M. *Macromolecules* **1999**, *32*, 2120; (b) Pellecchia, C.; Mazzeo, M.; Pappalardo, D. *Macromol. Rapid Commun.* **1998**, *19*, 651.
(30) Tempel, D. J.; Brookhart, M. *Organometallics* **1998**, *17*, 2290.
(31) Svejda, S. A.; Johnson, L. K.; Brookhart, M. *J. Am. Chem. Soc.*, manuscript submitted for publication.
(32) ^{13}C NMR spectroscopic and light scattering studies have shown that the polyethylene produced with (α-diimine)palladium(II) catalysts is hyperbranched. See reference 9, and Guan, Z.; Cotts, P. M.; McCord, E. F.; McLain, S. J. *Science*, **1999**, *283*, 2059.
(33) Deng, L.; Margl, P. M.; Ziegler, T. *J. Am. Chem. Soc.* **1997**, *119*, 1094.
(34) Deng, L.; Woo, T. K.; Cavallo, L.; Margl, P. M.; Ziegler, T. *J. Am. Chem. Soc.* **1997**, *119*, 6177.
(35) Musaev, D. G.; Froese, R. D. J.; Morokuma, K. *Organometallics* **1998**, *17*, 1850.
(36) Froese, R. D. J.; Musaev, D. G.; Morokuma, K. *J. Am. Chem. Soc.* **1998**, *120*, 1581.
(37) van Asselt, R.; Elsevier, C. J.; Smeets, W. J. J.; Spek, A. L.; Benedix, R. *Recl. Trav. Chim. Pays-Bas* **1994**, *113*, 88.
(38) tom Dieck, H.; Svoboda, M.; Grieser, T. *Z. Naturforsch* **1981**, *36b*, 823.
(39) Due to the high activity of these catalysts, even under conditions of high dilution and low catalyst loadings, the consumption of monomer is very rapid and the catalyst rapidly becomes starved for monomer.
(40) It is also possible that the 2,6-disubstituted aryl groups undergo slow rotation in solution, however, on the timescale of the polymerization reactions, it is likely that these groups are fixed either in the C_2 or C_S conformations.
(41) Turnover frequencies given assume complete catalyst activation. Recent results suggest the initial reaction with methylaluminoxane may produce some inactive nickel materials: Gates, D. P.; Brookhart, M. Unpublished results.
(42) Killian, C. M. Ni(II)-Based Catalysts for the Polymerization and Copolymerization of Olefins: A New Generation of Polyolefins. Ph.D. Dissertation, University of North Carolina-Chapel Hill, 1996.
(43) The branching numbers determined by ^1H NMR give no information about the types of branches (i.e. methyl, ethyl, propyl). A series of multidimensional NMR experiments conducted by E. F. McCord on polyethylene produced from nickel diimine catalysts indicate the frequency of branching to be Me>Et>Pr>Bu, etc. See reference 9.

(44) Activation of an ortho C-H bond in a (DAD)$NiBr_2$ compound [DAD = glyoxalbis(diisopropylmethylimine)] has been observed in reactions with bulky *o*-tolylmagnesium bromide. See tom Dieck, H.; Svoboda, M. *Chem. Ber.* **1976**, *109*, 1657. We have also observed an intramolecular C-H activation in (2,6-diisopropyl)phenyl substituted [(α-diimine)Pd(Me)(OEt_2)]$^+$ complexes in solution (Johnson, L. K.; Tempel, D. J.; Brookhart, M. Unpublished results.
(45) Doak, K. W. In *Encyclopedia of Polymer Science and Engineering*, Revd. Ed.; Mark, H. F.; Kroschwitz, J. I., Eds.; Wiley-Interscience: New York, 1986; Vol. 6, see p. 410.
(46) Hoffman, J. D.; Williams, G.; Passaglia, E. *J. Polymer Sci.: Part C* **1966**, *14*, 173.
(47) Popli, R.; Glotin, M.; Mandelkern, L.; Benson, R. S. *J. Polymer Sci.: Polymer Phys.* **1984**, *22*, 407.
(48) Alberola, N.; Cavaille, J. Y.; Perez, J. *Eur. Polym. J.* **1992**, *28*, 935.
(49) Pangborn, A. B.; Giardello, M. A.; Grubbs, R. H.; Rosen, R. K.; Timmers, F. J. *Organometallics* **1996**, *15*, 1518.
(50) Svoboda, M.; tom Dieck, H. *J. Organomet. Chem.* **1980**, *191*, 321.
(51) Chen, Q. Y.; Li, Z. T. *J. Org. Chem.* **1993**, *58*, 2599.
(52) Chupp, J. P.; Balthazor, T. M.; Miller, M. J.; Pozzo, M. J. *J. Org. Chem.* **1984**, *49*, 4711.
(53) Gabe, E. J.; LePage, Y.; Charland, J. P.; Lee, F. L.; White, P. S. *J. Appl. Cryst.* **1989**, *22*, 284.

Chapter 4 References

(1) van Koten, G.; Vrieze, K. *Adv. Organomet. Chem.* **1982**, *21*, 151-239.
(2) Klein, R. A.; Hartl, F.; Elsevier, C. J. *Organometallics* **1997**, *16*, 1284-1291.
(3) van Asselt, R.; Elsevier, C. J.; Amatore, C.; Jutand, A. *Organometallics* **1997**, *16*, 317-328.
(4) Groen, J. H.; Delis, J. G. P.; van Leeuwen, W. N. M.; Vrieze, K. *Organometallics* **1997**, *16*, 68-77.
(5) Groen, J. H.; Elsevier, C. J.; Vrieze, K.; Smeets, W. J. J.; Spek, A. L. *Organometallics* **1996**, *15*, 3445-3455.
(6) van Asselt, R.; Gielens, E. E. C. G.; Rülke, R. E.; Vrieze, K.; Elsevier, C. J. *J. Am. Chem. Soc.* **1994**, *116*, 977-985.
(7) van Asselt, R.; Rijnberg, E.; Elsevier, C. J. *Organometallics* **1994**, *13*, 706-720.
(8) van Asselt, R.; Elsevier, C. J.; Smeets, W. J. J.; Spek, A. L. *Inorg. Chem.* **1994**, *33*, 1521-1531.
(9) van Asselt, R.; Gielens, E. E. C. G.; Rülke, R. E.; Elsevier, C. J. *J. Chem. Soc., Chem. Commun.* **1993**, 1203-1205.
(10) Yang, K.; Lachicotte, R. J.; Eisenberg, R. *Organometallics* **1998**, *17*, 5102-5113.
(11) Yang, K.; Lachicotte, R. J.; Eisenberg, R. *Organometallics* **1997**, *16*, 5234-5243.
(12) Ganis, P.; Orabona, I.; Ruffo, F.; Vitagliano, A. *Organometallics* **1998**, *17*, 2646-2650.
(13) Fusto, M.; Giordano, F.; Orabona, I.; Ruffo, F.; Panunzi, A. *Organometallics* **1997**, *16*, 5981-5987.
(14) Carfagna, C.; Formica, M.; Gatti, G.; Musco, A.; Pierleoni, A. *Chem. Commun.* **1998**, 1113-1114.
(15) Johnson, L. K.; Killian, C. M.; Brookhart, M. *J. Am. Chem. Soc.* **1995**, *117*, 6414-6415.
(16) Svejda, S. A.; Brookhart, M. *Organometallics* **1999**, *18*, 65-74.
(17) Tempel, D. J.; Brookhart, M. *Organometallics* **1998**, *17*, 2290-2296.
(18) Mecking, S.; Johnson, L. K.; Wang, L.; Brookhart, M. *J. Am. Chem. Soc.* **1998**, *120*, 888-899.
(19) LaPointe, A. M.; Brookhart, M. *Organometallics* **1998**, *17*, 1530-1537.
(20) Killian, C. M.; Johnson, L. K.; Brookhart, M. *Organometallics* **1997**, *16*, 2005-2007.
(21) Killian, C. M.; Tempel, D. J.; Johnson, L. K.; Brookhart, M. *J. Am. Chem. Soc.* **1996**, *118*, 11664-11665.

(22) Johnson, L. K.; Mecking, S.; Brookhart, M. *J. Am. Chem. Soc.* **1996**, *118*, 267-268.
(23) Galland, G. B.; de Souza, R. F.; Mauler, R. S.; Nunes, F. F. *Macromolecules* **1999**, *32*, 1620-1625.
(24) McLain, S. J.; Feldman, J.; McCord, E. F.; Gardner, K. H.; Teasley, M. F.; Coughlin, E. B.; Sweetman, K. J.; Johnson, L. K.; Brookhart, M. *Macromolecules* **1998**, *31*, 6705-6707.
(25) Pellecchia, C.; Zambelli, A.; Mazzeo, M.; Pappalardo, D. *J. Mol Catal.* **1998**, *128*, 229-237.
(26) Schleis, T.; Spaniol, T. P.; Okuda, J.; Heinemann, J.; Mülhaupt, R. *J. Organomet. Chem.* **1998**, *569*, 159-167.
(27) Zeng, X.; Zetterberg, K. *Macromol. Chem. Phys.* **1998**, *199*, 2677-2681.
(28) Feldman, J.; McLain, S. J.; Parthasarathy, A.; Marshall, J.; Calabrese, J. C.; Arthur, S. D. *Organometallics* **1997**, *16*, 1514-1516.
(29) Pappalardo, D.; Mazzeo, M.; Pellecchia, C. *Macromol. Rapid Commun.* **1997**, *18*, 1017-1023.
(30) Pellecchia, C.; Zambelli, A.; Oliva, L.; Pappalardo, D. *Macromolecules* **1996**, *29*, 6990-6993.
(31) Pellecchia, C.; Zambelli, A. *Macromol. Rapid Commun.* **1996**, *17*, 333-338.
(32) Deng, L.; Woo, T. K.; Cavallo, L.; Margl, P. M.; Ziegler, T. *J. Am. Chem. Soc.* **1997**, *119*, 6177-6186.
(33) Deng, L.; Margl, P. M.; Ziegler, T. *J. Am. Chem. Soc.* **1997**, *119*, 1094-1100.
(34) Froese, R. D. J.; Musaev, D. G.; Morokuma, K. *J. Am. Chem. Soc.* **1998**, *120*, 1581-1587.
(35) Musaev, D. G.; Froese, R. D. J.; Morokuma, K. *Organometallics* **1998**, *17*, 1850-1860.
(36) Musaev, D. G.; Froese, R. D. J.; Svensson, M.; Morokuma, K. *J. Am. Chem. Soc.* **1997**, *119*, 367-374.
(37) Musaev, D. G.; Svensson, M.; Morokuma, K.; Stromberg, S.; Zetterberg, K.; Siegbahn, P. E. M. *Organometallics* **1997**, *16*, 1933-1945.
(38) Musaev, D. G.; Froese, R. D. J.; Morokuma, K. *New J. Chem.* **1997**, *21*, 1269-1282.
(39) van Asselt, R.; Elsevier, C. J.; Smeets, W. J. J.; Spek, A. L.; Benedix, R. *Recl. Trav. Chim. Pays-Bas* **1994**, *113*, 88-98.
(40) Ma, M. S.; Angelici, R. J.; Powell, D.; Jacobson, R. A. *Inorg. Chem.* **1980**, *19*, 3121-3128.
(41) Ma, M. S.; Angelici, R. J. *Inorg. Chem.* **1980**, *19*, 924-927.
(42) Ma, M. S.; Angelici, R. J. *Inorg. Chem.* **1980**, *19*, 363-370.
(43) Nakamura, A.; Konishi, A.; Otsuka, S. *J. Chem. Soc., Dalton Trans.* **1979**, 488-495.
(44) Ma, M. S.; Angelici, R. J.; Powell, D.; Jacobson, R. A. *J. Am. Chem. Soc.* **1978**, *100*, 7068-7069.
(45) Tempel, D. J. Mechanistic Studies of Pd(II)- and Ni(II)-Catalyzed Olefin Polymerization. Ph.D. Dissertation, University of North Carolina at Chapel Hill, 1998.
(46) The mechanism through which the (*E*,*E*)/(*E*,*Z*) interconversion takes place in these diimines is not known, but two possible pathways are via pyramidal inversion at the nitrogen atom, or by a 180° rotation about the C=N bond. This latter process would of course necessitate breaking the π-bond, so this bond would have to be weak in order for this rotation to take place.
(47) This spectrum was only acquired once with one mixing time. Experimentation with the mixing time may yield useful results.
(48) Pangborn, A. B.; Giardello, M. A.; Grubbs, R. H.; Rosen, R. K.; Timmers, F. J. *Organometallics* **1996**, *15*, 1518-1520.
(49) Rülke, R. E.; Ernsting, J. M.; Spek, A. L.; Elsevier, C. J.; van Leeuwen, P. W. N. M.; Vrieze, K. *Inorg. Chem.* **1993**, *32*, 5769-5778.

Chapter 5 References

(1) Natta, G.; Pino, P.; Corradini, P.; Danusso, F.; Mantica, E.; Mazzanti, G.; Moraglio, G. *J. Am. Chem. Soc.* **1955**, *77*, 1708-1710.
(2) Natta, G. *J. Poly. Sci.* **1959**, *34*, 531-549.

(3) Bochmann, M. *J. Chem. Soc., Dalton Trans.* **1996**, 255-270.
(4) Brintzinger, H. H.; Fischer, D.; Mülhaupt, R.; Rieger, B.; Waymouth, R. M. *Angew. Chem., Int. Ed. Engl.* **1995**, *34*, 1143-1170.
(5) Coates, G. W.; Waymouth, R. M. *Science* **1995**, *267*, 217-219.
(6) Ewen, J. A.; Jones, R. L.; Razavi, A.; Ferrara, J. D. *J. Am. Chem. Soc.* **1988**, *110*, 6255-6256.
(7) Kaminsky, W.; Külper, K.; Brintzinger, H. H.; Wild, F. R. W. P. *Angew. Chem., Int. Ed. Engl.* **1985**, *24*, 507-508.
(8) Ewen, J. A. *J. Am. Chem. Soc.* **1984**, *106*, 6355-6364.
(9) Small, B. L.; Brookhart, M. *Macromolecules* **1999**, *32*, 2120-2130.
(10) Ruchatz, D.; Fink, G. *Macromolecules* **1998**, *31*, 4669-4673.
(11) Ruchatz, D.; Fink, G. *Macromolecules* **1998**, *31*, 4674-4680.
(12) Rische, T.; Waddon, A. J.; Dickinson, L. C.; MacKnight, W. J. *Macromolecules* **1998**, *31*, 1871-1874.
(13) Cherdron, H.; Brekner, M.-J.; Osan, F. *Angew. Makromol. Chem.* **1994**, *223*, 121-133.
(14) Kaminsky, W.; Bark, A.; Arndt, M. *Makromol. Chem., Macromol. Symp.* **1991**, *47*, 83-93.
(15) Seehof, N.; Mehler, C.; Breunig, S.; Risse, W. *J. Mol. Catal.* **1992**, *76*, 219-228.
(16) Mehler, C.; Risse, W. *Macromolecules* **1992**, *25*, 4226-4228.
(17) Goodall, B. L.; McIntosh, L. H.; Rhodes, L. F. *Macromol. Symp.* **1995**, *89*, 421-432.
(18) Kaminsky, W.; Arndt, M. Polymerization, Oligomerization, and Copolymerization of Olefins. In *Applied Homogeneous Catalysis with Organometallic Compounds*; Cornils, B., Herrmann, W. A., Eds.; VCH: New York, 1996; Vol. 1, pp 220-236.
(19) Goodall, B. L.; Benedikt, G. M.; McIntosh, L. H.; Barnes, D. A. Process for Making Polymers Containing a Norbornene Repeating Unit by Addition Polymerization using an Organo(Nickel or Palladium) Complex. U.S. Patent 5,468,819, Nov. 21, 1995.
(20) Muthukumaru Pillai, S.; Ravindranathan, M.; Sivaram, S. *Chem. Rev.* **1986**, *86*, 353-399.
(21) Skupinska, J. *Chem. Rev.* **1991**, *91*, 613-648.
(22) Möhring, V. M.; Fink, G. *Angew. Chem., Int. Ed. Engl.* **1985**, *24*, 1001-1003.
(23) Keim, W.; Appel, R.; Storeck, A.; Krüger, C.; Goddard, R. *Angew. Chem., Int. Ed. Engl.* **1981**, *20*, 116-117.
(24) Johnson, L. K.; Killian, C. M.; Brookhart, M. *J. Am. Chem. Soc.* **1995**, *117*, 6414-6415.
(25) Killian, C. M.; Tempel, D. J.; Johnson, L. K.; Brookhart, M. *J. Am. Chem. Soc.* **1996**, *118*, 11664-11665.
(26) Johnson, L. K.; Mecking, S.; Brookhart, M. *J. Am. Chem. Soc.* **1996**, *118*, 267-268.
(27) Mecking, S.; Johnson, L. K.; Wang, L.; Brookhart, M. *J. Am. Chem. Soc.* **1998**, *120*, 888-899.
(28) Tempel, D. J.; Johnson, L. K.; Huff, R. L.; Brookhart, M. Manuscript in preparation.
(29) Tempel, D. J. Mechanistic Studies of Pd(II)- and Ni(II)-Catalyzed Olefin Polymerization. Ph.D. Dissertation, University of North Carolina at Chapel Hill, 1998.
(30) Killian, C. M. Ni(II)-Based Catalysts for the Polymerization and Copolymerization of Olefins: A New Generation of Polyolefins. Ph.D. Dissertation, University of North Carolina-Chapel Hill, 1996.
(31) MMAO contains 25% isobutyl groups. MMAO has improved shelf life with little difference in reactivity as compared to MAO.
(32) Recent experiments on the living polymerization of α-olefins with MAO-activated nickel dibromide catalyst precursors hint that incomplete activation is occurring. Comparison of number-average polymer molecular weights determined by gel permeation chromatography with calculated molecular weights show that the calculated values are lower than the measured weights.
(33) Gates, D. P.; Svejda, S. A.; Onate, E.; Killian, C. M.; Johnson, L. K.; White, P. S.; Brookhart, M. Manuscript in preparation.

(34) McLain, S. J.; McCord, E. F.; Johnson, L. K.; Ittel, S. D.; Nelson, L. T. J.; Arthur, S. D.; Halfhill, M. J.; Teasley, M. F.; Tempel, D. J.; Killian, C. M.; Brookhart, M. *Polym. Prepr., Am. Chem. Soc. Div. Polym. Chem.* **1997**, *38*, 772.
(35) Nelson, L. T. J.; McCord, E. F.; Johnson, L. K.; McLain, S. J.; Ittel, S. D.; Killian, C. M.; Brookhart, M. *Polym. Prepr., Am. Chem. Soc. Div. Polym. Chem.* **1997**, *38*, 133.
(36) Svejda, S. A.; Brookhart, M. *Organometallics* **1999**, *18*, 65-74.
(37) Mechanistic studies with well-defined nickel complexes have uncovered that the observed species present in solution during low-temperature propylene polymerizations is a β-agostic complex. The only species observed in the same experiments using ethylene as the monomer is the alkyl ethylene complex. See Chapter 6 for these results and further discussion.
(38) In experiments with nickel complexes bearing very bulky diimine ligands, this effect was also observed. At very high monomer concentrations, the turnover numbers level out. See ref 29.
(39) Abeywickrema, R.; Bennett, M. A.; Cavell, K. J.; Kony, M.; Masters, A. F.; Webb, A. G. *J. Chem. Soc., Dalton Trans.* **1993**, 59-68.
(40) Kissin, Y. V.; Beach, D. L. *J. Poly. Sci., Part A: Polym. Chem.* **1989**, *27*, 147-155.
(41) Since the branching frequency rises with increasing polymerization temperatures, the hydrodynamic radii of the more highly branched polymer chains will be decreased relative to more linear chains. This will result in an underestimation of the molecular weights of the polymers formed at higher temperatures. In addition, the relative error increases with polymer branching frequency. However, this effect is unlikely to be completely responsible for the observed decrease in polymer molecular weights at higher polymerization temperatures.
(42) Pangborn, A. B.; Giardello, M. A.; Grubbs, R. H.; Rosen, R. K.; Timmers, F. J. *Organometallics* **1996**, *15*, 1518-1520.

Chapter 6 References

(1) Bochmann, M. *J. Chem. Soc., Dalton Trans.* **1996**, 255-270.
(2) Kaminsky, W.; Arndt, M. Polymerization, Oligomerization, and Copolymerization of Olefins. In *Applied Homogeneous Catalysis with Organometallic Compounds*; Cornils, B., Herrmann, W. A., Eds.; VCH: New York, 1996; Vol. 1, pp 220-236.
(3) Brintzinger, H. H.; Fischer, D.; Mülhaupt, R.; Rieger, B.; Waymouth, R. M. *Angew. Chem., Int. Ed. Engl.* **1995**, *34*, 1143-1170.
(4) Coates, G. W.; Waymouth, R. M. *Science* **1995**, *267*, 217-219.
(5) Yang, X.; Stern, C. L.; Marks, T. J. *J. Am. Chem. Soc.* **1994**, *116*, 10015-10031.
(6) Coughlin, E. B.; Bercaw, J. E. *J. Am. Chem. Soc.* **1992**, *114*, 7606-7607.
(7) Crowther, D. J.; Baenziger, N. C.; Jordan, R. F. *J. Am. Chem. Soc.* **1991**, *113*, 1455-1457.
(8) Johnson, L. K.; Killian, C. M.; Brookhart, M. *J. Am. Chem. Soc.* **1995**, *117*, 6414-6415.
(9) Galland, G. B.; de Souza, R. F.; Mauler, R. S.; Nunes, F. F. *Macromolecules* **1999**, *32*, 1620-1625.
(10) Schleis, T.; Spaniol, T. P.; Okuda, J.; Heinemann, J.; Mülhaupt, R. *J. Organomet. Chem.* **1998**, *569*, 159-167.
(11) Yang, K.; Lachicotte, R. J.; Eisenberg, R. *Organometallics* **1998**, *17*, 5102-5113.
(12) Ganis, P.; Orabona, I.; Ruffo, F.; Vitagliano, A. *Organometallics* **1998**, *17*, 2646-2650.
(13) Pellecchia, C.; Zambelli, A.; Mazzeo, M.; Pappalardo, D. *J. Mol Catal.* **1998**, *128*, 229-237.
(14) Zeng, X.; Zetterberg, K. *Macromol. Chem. Phys.* **1998**, *199*, 2677-2681.
(15) Carfagna, C.; Formica, M.; Gatti, G.; Musco, A.; Pierleoni, A. *Chem. Commun.* **1998**, 1113-1114.
(16) Fusto, M.; Giordano, F.; Orabona, I.; Ruffo, F.; Panunzi, A. *Organometallics* **1997**, *16*, 5981-5987.

(17) Yang, K.; Lachicotte, R. J.; Eisenberg, R. *Organometallics* **1997**, *16*, 5234-5243.
(18) Pappalardo, D.; Mazzeo, M.; Pellecchia, C. *Macromol. Rapid Commun.* **1997**, *18*, 1017-1023.
(19) Pellecchia, C.; Zambelli, A.; Oliva, L.; Pappalardo, D. *Macromolecules* **1996**, *29*, 6990-6993.
(20) Pellecchia, C.; Zambelli, A. *Macromol. Rapid Commun.* **1996**, *17*, 333-338.
(21) Froese, R. D. J.; Musaev, D. G.; Morokuma, K. *J. Am. Chem. Soc.* **1998**, *120*, 1581-1587.
(22) Musaev, D. G.; Froese, R. D. J.; Morokuma, K. *Organometallics* **1998**, *17*, 1850-1860.
(23) Deng, L.; Woo, T. K.; Cavallo, L.; Margl, P. M.; Ziegler, T. *J. Am. Chem. Soc.* **1997**, *119*, 6177-6186.
(24) Musaev, D. G.; Froese, R. D. J.; Svensson, M.; Morokuma, K. *J. Am. Chem. Soc.* **1997**, *119*, 367-374.
(25) Musaev, D. G.; Svensson, M.; Morokuma, K.; Stromberg, S.; Zetterberg, K.; Siegbahn, P. E. M. *Organometallics* **1997**, *16*, 1933-1945.
(26) Deng, L.; Margl, P. M.; Ziegler, T. *J. Am. Chem. Soc.* **1997**, *119*, 1094-1100.
(27) Musaev, D. G.; Froese, R. D. J.; Morokuma, K. *New J. Chem.* **1997**, *21*, 1269-1282.
(28) Tempel, D. J.; Brookhart, M. *Organometallics* **1998**, *17*, 2290-2296.
(29) Solutions of **2** in CD_2Cl_2 eliminate ethane readily at temperatures above 0 °C. In the solid state, these complexes decompose at room temperature over 2 days.
(30) The nickel dimethyl complexes were prepared using a procedure similar to that reported by Svoboda and tom Dieck: Svoboda, M.; tom Dieck, H. *J. Organomet. Chem.* **1980**, *191*, 321-328. See the Experimental Section for full experimental details.
(31) In monitoring chain growth of **5a** by ^{1}H NMR spectroscopy, specific resonance assignments can be made for (diimine)Ni$(C_2H_4)(CH_2)_n CH_3^+$: n=2 (first insertion product), n=4 (second insertion) and n=6 (third insertion). See Figure 6.1 for illustrated spectra.
(32) Water adduct **4a** was used instead of ether adduct **3a** because ether displacement by propylene is competitive with olefin migratory insertion, whereas formation of methyl propylene complex **8a** from **4a** is quantitative and rapid at -80 °C.
(33) A β-agostic resting state in the addition polymerization of cyclopentene using very similar Ni and Pd diimine complexes has also been reported: McLain, S. J.; Feldman, J.; McCord, E. F.; Gardner, K. H.; Teasley, M. F.; Coughlin, E. B.; Sweetman, K. J.; Johnson, L. K.; Brookhart, M. *Macromolecules* **1998**, *31*, 6705-6707.
(34) Species **9** are dynamic and the structures of the isomer or isomers present have not been determined. Structure **9a** is written as shown based on previous reports; see refs 13, 19, and 20.
(35) A $\Delta S^{\ddagger}$ of -11.2 eu was measured for a similar Pd complex: see ref 8, Supporting Information.
(36) The two complexes being compared were measured in different solvents ($CDCl_2F$ vs. toluene) and had different counterions. In addition, it is likely that less than quantitative activation of all nickel sites by MMAO is occurring.
(37) Gates, D. P.; Svejda, S. A.; Brookhart, M. Unpublished results.
(38) Brookhart, M.; Volpe, A. F.; Lincoln, D. M.; Horvath, I. T.; Millar, J. M. *J. Am. Chem. Soc.* **1990**, *112*, 5634-5636.
(39) Killian, C. M. Ni(II)-Based Catalysts for the Polymerization and Copolymerization of Olefins: A New Generation of Polyolefins. Ph.D. Dissertation, University of North Carolina-Chapel Hill, 1996.
(40) Pangborn, A. B.; Giardello, M. A.; Grubbs, R. H.; Rosen, R. K.; Timmers, F. J. *Organometallics* **1996**, *15*, 1518-1520.
(41) van Asselt, R.; Elsevier, C. J.; Smeets, W. J. J.; Spek, A. L.; Benedix, R. *Recl. Trav. Chim. Pays-Bas* **1994**, *113*, 88-98.
(42) tom Dieck, H.; Svoboda, M.; Grieser, T. *Naturforsch* **1981**, *36b*, 823-832.
(43) Svoboda, M.; tom Dieck, H. *J. Organomet. Chem.* **1980**, *191*, 321-328.
(44) Ward, L. G. L. *Inorg. Syn.* **1971**, *13*, 154-164.
(45) Brookhart, M.; Grant, B.; Volpe, A. F. *Organometallics* **1992**, *11*, 3920-3922.

(46) Siegel, J. S.; Anet, F. A. *J. Org. Chem.* **1988**, *53*, 2629-2630.
(47) A small amount of Me_2SiF_2 was occasionally observed as a byproduct of the fluorination reaction. Formation of this product can be suppressed through minimal use of silicone grease on glass joints used in the preparation of $CDCl_2F$.
(48) Use of alumina or silica as the solid support for this purification step results in considerable decomposition of the nickel dimethyl product.
(49) Addition of sub-stoichiometric amounts of *p*-dioxane to the reaction aids in complexing the magnesium salts and thus facilitates more efficient filtration, but yields of the nickel dimethyl complexes decrease dramatically.

Chapter 7 References

(1) Johnson, L. K.; Killian, C. M.; Brookhart, M. *J. Am. Chem. Soc.* **1995**, *117*, 6414-6415.
(2) Killian, C. M. Ni(II)-Based Catalysts for the Polymerization and Copolymerization of Olefins: A New Generation of Polyolefins. Ph.D. Dissertation, University of North Carolina-Chapel Hill, 1996.
(3) Gates, D. P.; Svejda, S. A.; Onate, E.; Killian, C. M.; Johnson, L. K.; White, P. S.; Brookhart, M. Manuscript in preparation.
(4) Tempel, D. J. Mechanistic Studies of Pd(II)- and Ni(II)-Catalyzed Olefin Polymerization. Ph.D. Dissertation, University of North Carolina at Chapel Hill, 1998.
(5) Tempel, D. J.; Johnson, L. K.; Huff, R. L.; Brookhart, M. Manuscript in preparation.
(6) Svejda, S. A.; Johnson, L. K.; Brookhart, M. *J. Am. Chem. Soc.*, communication submitted.
(7) Chain isomerization may also take place via this mechanism from the β-agostic species formed immediately following migratory insertion of ethylene.
(8) Tempel, D. J.; Brookhart, M. *Organometallics* **1998**, *17*, 2290-2296.
(9) Deng, L.; Woo, T. K.; Cavallo, L.; Margl, P. M.; Ziegler, T. *J. Am. Chem. Soc.* **1997**, *119*, 6177-6186.
(10) Conroy-Lewis, F. M.; Mole, L.; Redhouse, A. D.; Litster, S. A.; Spencer, J. L. *J. Chem. Soc., Chem. Commun.* **1991**, 1601-1603.
(11) Carr, N.; Mole, L.; Orpen, A. G.; Spencer, J. L. *J. Chem. Soc., Dalton Trans.* **1992**, 2653-2662.
(12) Huff, R. L.; Brookhart, M. Unpublished results.
(13) Johnson, L. K.; Mecking, S.; Brookhart, M. *J. Am. Chem. Soc.* **1996**, *118*, 267-268.
(14) Mecking, S.; Johnson, L. K.; Wang, L.; Brookhart, M. *J. Am. Chem. Soc.* **1998**, *120*, 888-899.
(15) These assignments are supported by a similar ^1H NMR experiment performed by Dr. Lynda Johnson. Johnson, L. K.; Brookhart, M. Unpublished results.
(16) Pangborn, A. B.; Giardello, M. A.; Grubbs, R. H.; Rosen, R. K.; Timmers, F. J. *Organometallics* **1996**, *15*, 1518-1520.
(17) van Asselt, R.; Elsevier, C. J.; Smeets, W. J. J.; Spek, A. L.; Benedix, R. *Recl. Trav. Chim. Pays-Bas* **1994**, *113*, 88-98.
(18) tom Dieck, H.; Svoboda, M.; Grieser, T. Z. *Naturforsch* **1981**, *36b*, 823-832.
(19) Svoboda, M.; tom Dieck, H. *J. Organomet. Chem.* **1980**, *191*, 321-328.
(20) Ward, L. G. L. *Inorg. Syn.* **1971**, *13*, 154-164.
(21) Brookhart, M.; Grant, B.; Volpe, A. F. *Organometallics* **1992**, *11*, 3920-3922.
(22) Siegel, J. S.; Anet, F. A. *J. Org. Chem.* **1988**, *53*, 2629-2630.
(23) A small amount of Me_2SiF_2 was occasionally observed as a byproduct of the fluorination reaction. Formation of this product can be suppressed through minimal use of silicone grease on glass joints used in the preparation of $CDCl_2F$.
(24) White, P. A.; Calabrese, J.; Theopold, K. H. *Organometallics* **1996**, *15*, 5473-5475.